UNIVERSIDADE DE SÃO PAULO
FACULDADE DE ZOOTECNIA E ENGENHARIA DE ALIMENTOS

CHRISTIAN GAUSS

Tratamento preservativo e modificação química do bambu para fins estruturais

Preservative treatment and chemical modification of bamboo for structural purposes

Pirassununga
2020

CHRISTIAN GAUSS

Tratamento preservativo e modificação química do bambu para fins estruturais

Preservative treatment and chemical modification of bamboo for structural purposes

Versão Corrigida

Tese apresentada à Faculdade de Zootecnia e Engenharia de Alimentos da Universidade de São Paulo, como parte dos requisitos para a obtenção do Título de Doutor em Engenharia e Ciência dos Materiais.

Área de Concentração: Desenvolvimento, Caracterização, e Aplicação de Materiais voltados à Agroindústria.

Orientador: Prof. Dr. Holmer Savastano Junior.

Pirassununga

2020

Ficha catalográfica elaborada pelo
Serviço de Biblioteca e Informação, FZEA/USP,
com os dados fornecidos pelo(a) autor(a)

Gauss, Christian
G274t Tratamento preservativo e modificação química do bambu para fins estruturais / Christian Gauss ; orientador Holmer Savastano Junior. -- Pirassununga, 2020.
333 f.

Tese (Doutorado - Programa de Pós-Graduação em Engenharia e Ciência de Materiais) -- Faculdade de Zootecnia e Engenharia de Alimentos, Universidade de São Paulo.

1. Bambu. 2. Tratamento preservativo. 3. Desempenho mecânico. 4. Propriedades físicas. 5. Qualidade. I. Savastano Junior, Holmer , orient. II. Título.

ACKNOWLEDGEMENTS

This work would not be conceived without the moral support and trust of my family. Special thanks to my mother, Fatima, my father, Rudolf, and my brother David, who always believed in my efforts to become the person who I am nowadays.

Thanks for the financial support from FAPESP (Processes 2016/26022-9 and 2018/18571-8) and CAPES that provided me with all the necessary means for the development of this work. These resources were possible because of all the taxpayers from São Paulo state and Brazil. Thank you for giving me this responsibility.

Special thanks to my advisor, Prof. Holmer Savastano Junior, for the guidance, support, and belief in my work even in moments of doubt and confusion. I really appreciate all the opportunities for learning and personal development available under his guidance. This thesis was made possible by his trust and advice during all my doctorate. I am also deeply thankful for Prof. Kent A. Harries, who received me with open arms during my internship at the University of Pittsburgh and guided me through important parts of this doctorate thesis. I am also grateful for his confidence in my capabilities and for driving me for the next stage of my professional path.

To my beloved friends, Laura, Bruno, Leonardo, and Paulo that somehow gave me spiritual strength and perseverance to materialize this thesis and helped me seeing the world from different perspectives.

To all my friends who have been part of my daily life during my journey through my doctorate (without importance order), Adriana, Gonzalo, Carlos, Carol, Leticia, G. Barbirato, Rafael, G. Carmello, Viviane, Loïc, Matheus, Erika, Valdemir, Ronaldo, Patrícia, Maria Júlia, Alda, and many others who passed through the lab. Special thanks to Marzieh Kadivar for her important help, contribution to my work, and valuable conversations about bamboo.

The laboratory of Construction and Ambience and other departments of the USP-FZEA campus will be recorded in my memory for all the support provided. The help of all the technicians, Zaqueu, Diego, Mariana, Josiane, Leonardo, and Rodrigo are deeply acknowledged. Thanks to Ricardo Pereira and Sergio Brazolin for the fungi decay tests developed at IPT, São Paulo, and for the rich conversations about this important topic. I am also deeply thankful for all the help provided by students and staff from the University of Pittsburgh, Scooter, Yusuf, Chase, Chelsea and Abdullah.

To Celina Llerena, Prof. Antônio L. Beraldo, and Prof. Khosrow Ghavami for introducing me to the bamboo world and for encouraging my curiosity.

Lastly, I would like to thank all the engineers, researchers, enthusiasts, and readers interested in the wonderful and world-changing material: bamboo.

Criamos nosso próprio caminho, com atenção no presente, ouvidos no passado e olhos no futuro.

C. Gauss

RESUMO

GAUSS, C. **Tratamento preservativo e modificação química do bambu para fins estruturais**. 2020. 333 p. Tese de Doutorado – Faculdade de Zootecnia e Engenharia de Alimentos, Universidade de São Paulo, Pirassununga, 2020.

Os materiais à base de bambu estão na caixa de ferramentas de práticas sustentáveis e têm um alto potencial para o desenvolvimento e a expansão de novos produtos na indústria da construção. Embora inúmeras vantagens sejam atribuídas ao bambu, existem vários problemas relacionados ao seu uso que devem ser resolvidos e mitigados. Sem tratamento adequado, os materiais de bambu não resistem a uma longa vida útil. Os procedimentos de tratamento são bem conhecidos, para os quais diversos métodos e soluções preservativas podem ser utilizados, dependendo da aplicação final, logística, condição do material e acessibilidade. No entanto, informações básicas sobre o tratamento químico do bambu em termos de tratabilidade, controle de qualidade e o efeito nas propriedades físico-mecânicas e o desenvolvimento de soluções menos perigosas são tópicos pouco explorados. Portanto, esta tese de doutorado foi dividida em duas partes/objetivos principais: avaliação de tratamentos convencionais para bambu e o uso de métodos de preservação alternativos baseados em modificação química e polimerização in-situ. Na primeira parte, preservativos convencionais foram aplicados no tratamento dos bambus *Dendrocalamus. asper* e *Phyllostachys edulis* e analisados sob o ponto de vista de aspectos de qualidade. Métodos analíticos para avaliação da tratabilidade, como penetração e retenção, foram utilizados para o bambu tratado com octaborato de sódio tetrahidratado (OST) e cromato de cobre cromatado (CCB). Testes mecânicos, físicos e químicos foram amplamente utilizados para caracterizar amostras tratadas e os efeitos dos preservativos nas propriedades mecânicas foram investigados. Adicionalmente, o bambu roliço foi objeto de caracterização mecânica detalhada por meio de análise de deformação por correlação de imagem digital. Os resultados obtidos resultaram em recomendações para futuras normas para ensaios de bambu e na observação do efeito local do nó em compressão, cisalhamento, tração e flexão. Ademais, os tratamentos investigados não mostraram efeitos prejudiciais sobre as propriedades mecânicas, especialmente o tratamento com OST, que resulta em uma melhora na resistência do bambu. Diretrizes para tratamento pelo método de imersão usando OST também foram apresentadas como uma proposta para melhorar a qualidade da produção do bambu tratado. Na segunda parte

desta tese, seguindo o objetivo de melhorar as propriedades gerais do bambu, foram testados tratamentos alternativos à base de ácido cítrico e tanino em combinação com compostos de boro. Amostras quimicamente modificadas com ácido cítrico apresentaram considerável melhora na estabilidade dimensional e diminuição da absorção de água como consequência de um processo de esterificação. No entanto, a modificação aumentou a fragilidade do bambu, reduzindo especialmente a resistência à flexão. O uso de tanino/hexamina/boro polimerizado apresentou resultados positivos nas propriedades gerais do bambu, aumentando as resistências à compressão e à tração na flexão e a resistência à degradação por fungos mesmo após a lixiviação. Embora o OST tenha sido eficaz para melhorar a resistência à decomposição de fungos, a lixiviação severa diminuiu completamente sua atividade fungicida. Contudo, por meio de análises termogravimétricas, as amostras tratadas com boro exibiram melhor estabilidade térmica. Em geral, o bambu é um material fascinante. No entanto, embora seja possível obter um tratamento satisfatório, é mais difícil de ser tratado e caracterizado do que a madeira. Para superar esses problemas, são necessárias mais pesquisas em métodos de caracterização e tratamento para melhor entendimento e uso desse abundante e versátil material.

Palavras chave: Ácido cítrico, Avaliação da qualidade, Boro, Caracterização mecânica, *Dendrocalamus asper*, *Phyllostachys edulis*, Tanino

ABSTRACT

GAUSS, C. **Preservative treatment and chemical modification of bamboo for structural purposes**. 2020. 333 p. Tese de Doutorado – Faculdade de Zootecnia e Engenharia de Alimentos, Universidade de São Paulo, Pirassununga, 2020.

Bamboo-based materials are in the toolbox of sustainable practices and have a high potential for the development and expansion of new products in the construction industry. Although uncountable advantages are attributed to bamboo, there are several problems related to its use that must be solved and mitigated. Without proper treatment, bamboo materials cannot withstand a long service life. The treatment procedures are already well-known, in which different methods and preservative solutions can be used depending on the final application, logistics, material condition, and affordability. Yet, necessary information about the chemical treatment of bamboo in terms of treatability, quality control, and the effect on physical-mechanical properties, and the development of less hazardous solutions are topics not adequately explored. Therefore, this doctorate thesis was divided into two major parts/objectives: assessment of conventional bamboo treatments and evaluation of alternative preservation methods based on chemical modification and in-situ polymerization. In the first part, conventional preservatives were applied for *Dendrocalamus. asper* and *Phyllostachys edulis* bamboo treatment and analysed in the quality aspects point of view. Analytical methods for treatability evaluation, such as penetration and retention, were used for disodium octaborate tetrahydrate (DOT) and chromate copper borate (CCB) treated bamboo. Mechanical, physical, and chemical tests were extensively used to characterize treated samples, and the effects of the preservatives on mechanical properties were investigated. Additionally, full-culm bamboo was object of detailed mechanical characterization through digital image correlation strain analysis. The obtained results led in recommendations for future standards for bamboo testing and the observation of the local effect of the node on compression, shear, tension, and bending. Besides, the investigated treatments did not show detrimental effects on the mechanical properties, yet DOT treatment causes an improvement in bamboo strength. Guidelines for treatment by the immersion method using DOT are also proposed to ensure the production quality of treated bamboo. In the second part of this thesis, pursuing the objective to improve the overall properties

of bamboo, alternative treatment formulations based on citric acid and tannin in combination with boron compounds were tested. Samples chemically modified with citric acid presented considerable improvement on dimensional stability and decrease of water absorption as the consequence of an esterification process. However, the modification increased bamboo brittleness, reducing especially tension and bending strengths. The use of polymerized tannin/hexamine/boron had positive outcomes on the overall properties of bamboo, increasing the compression and bending strengths and the fungi degradation resistance even after leaching. Moreover, although DOT was effective in improving fungi decay resistance, severe leaching completely decreased its fungicide activity. Through thermogravimetric analyses, boron treated samples exhibited better thermal stability. In general, bamboo is a fascinating material. Nevertheless, although satisfactory treatment can be achieved, it is more difficult to be treated and characterised than wood. To overcome these problems, more research in characterization and treatment methods are necessary for better understanding and use of this abundant and versatile material.

Keywords: Boron, Citric acid, *Dendrocalamus asper*, Mechanical characterization, *Phyllostachys edulis*, Quality assessment, Tannin

.

FIGURE LIST

TABLE LIST

LIST OF PUBLICATIONS RELATED TO THE DOCTORATE THESIS

Published papers in peer-reviewed journals:

GAUSS, C.; KADIVAR, M.; SAVASTANO JR, H. Effect of disodium octaborate tetrahydrate on the mechanical properties of *Dendrocalamus asper* bamboo treated by vacuum/pressure method. Journal of Wood Science, v. 65, n. 27, 2019.

GAUSS, C.; SAVASTANO JR, H.; HARRIES, K. A. Use of ISO 22157 mechanical test methods and the characterisation of Brazilian *P. edulis* bamboo. Construction and Building Materials, v. 228, p. 116728, 2019.

GAUSS, C.; HARRIES, K. A.; KADIVAR, M.; AKINBADE, Y. A.; SAVASTANO JR, H.; Quality assessment and mechanical characterization of preservative-treated Moso bamboo (*P. edulis*). European Journal of Wood and Wood Products, v. 78, p. 257-270, 2020.

Papers submitted/under submission for publication:

GAUSS, C.; KADIVAR, M.; PEREIRA, R.; SAVASTANO JR, H. Assessment of *Dendrocalamus asper* bamboo treated with tannin-boron preservatives. Manuscript submitted to Construction and Building Materials, 2020.

GAUSS, C.; KADIVAR, M.; HARRIES, K.; SAVASTANO JR, H. Chemical modification of *Dendrocalamus asper* bamboo with citric acid: effects on the physical-chemical, mechanical and thermal properties. Manuscript submitted to Journal of Cleaner Production (under revision), 2020.

Participation in events:

GAUSS, C.; SAVASTANO JR, H. The influence of disodium octaborate tetrahydrate on the mechanical properties of *Dendrocalamus asper* bamboo. In: V Simpósio Internacional del Bambu y la Guadua, Bogota, 2017. Abstract - Poster presentation.

GAUSS, C.; DOMINGUEZ, A. L. S.; SAVASTANO JR., H. Alternatives for bamboo treatment and chemical modification. In: 1st Brazilian-German Workshop on Composite Products From Alternative Lignocellulosic Resources, Pirassununga, 2018. Abstract – Oral presentation.

GAUSS, C.; DOMINGUEZ, A. L. S.; SAVASTANO JR., H. Dimensional stability and water absorption of *D. asper* bamboo treated with citric acid and boron salts. In: 3o Congresso Luso-Brasileiro Materiais de Construção Sustentáveis, Coimbra, 2018. Full paper – Oral presentation.

Other publications and collaborations related to bamboo during doctorate research:

MAGALHAES, T.; SANTOS, V.; GAUSS, C.; SAVASTANO JUNIOR, H. Conventional and microwave-assisted thermal treatment of *Dendrocalamus asper* bamboo In: International Conference on Bio-Based Building Materials, Clermont Ferrand, 2017.

SCHMIDT, G., GAUSS, C. Workshop Report: BRALECOMP - 1st Brazilian-German Workshop on Composite Products from Alternative Lignocellulosic Resources. University of Hamburg, 2018

GAUSS, C.; ARAUJO, V. De; GAVA, M.; CORTEZ-BARBOSA, J.; SAVASTANO JR, H. Bamboo particleboards: recent developments. Pesquisa Agropecuária Tropical, v. 49, p. 1–9, 2019.

HARRIES, K. A.; MORRILL, P.; GAUSS, C.; FLOWER, C.; AKINBADE, Y.; TRUJILLO, D. Screw withdrawal capacity of full-culm *P. edulis* bamboo. Construction and Building Materials, v. 216, p. 531–541, 2019.

KADIVAR, M.; GAUSS, C.; MÁRMOL, G.; SÁ, A. D; FIORONI, C.; GHAVAMI, K.; SAVASTANO JR, H. The influence of the initial moisture content on densification process of *D. asper* bamboo: Physical-chemical and bending characterization. Construction and Building Materials, v. 229, p. 116896, 2019.

KADIVAR, M.; GAUSS, C., CHARCA, S., GHAVAMI, K., SAVASTANO JR, H. Physical Properties of Thermo-Hydro-Mechanically (THM) Flattened and Densified Bamboo (Moso and *Dendrocalamus Asper*). In: XVIII Brazil MRS Meeting - Proceedings, Balneário Camboriú, 2019.

KADIVAR, M.; GAUSS, C.; MARMOL, G.; FIORONI, C.; SÁ, A. D.; SAVASTANO JR, H. Evaluation of an optimized bamboo sandwich panel using layers of two different bamboo functional elements. In: XVIII Brazil MRS Meeting - Proceedings, Balneário Camboriú, 2019.

TABLE OF CONTENTS

1. CHAPTER 1 - Introduction

1.1. Contextualization and motivation

The scientific consensus on anthropogenic global warming is consolidated within a range of 90-100%, which brings our attention to direct solutions and not discussions whether this change is happening or not (COOK et al., 2016). The construction sector was responsible for 5.7 billion tons of CO_2 emissions globally in 2009, which represents 23% of the total CO_2 emissions related to global economic activities. Interestingly, 94% of the construction emissions are indirect, e.g. hard coal, natural gas, and non-energy use. Emerging countries are the main contributors to the construction global emissions, mainly related to new infrastructure and housing projects, with rising numbers in the last years (HUANG et al., 2018). In this context, many researchers have been studying the application of natural and local resources as building materials to mitigate carbon emissions and reduce production costs, such as the use of bamboo in its natural form or as an engineered material, products based on agro-industrial wastes, and inorganic based composites reinforced with vegetable fibres (GHAVAMI; TOLEDO FILHO; BARBOSA, 1999; PAPADOPOULOS et al., 2004; GHAVAMI, 2005; MATTONE, 2005; ESPELHO; BERALDO, 2008; DE ARAÚJO et al., 2011; FIORELLI et al., 2012; HARRIES; SHARMA; RICHARD, 2012; ALMEIDA et al., 2013; SHARMA; HARRIES; GHAVAMI, 2013; SHARMA et al., 2014, 2015a; CORREIA et al., 2015; YU et al., 2015). Although significant efforts have been made to develop and improve new sustainable products based on non-conventional materials, it is necessary to obtain more experimental data in relation to their physical-chemical and mechanical properties for improved safety and predictability in applications for the built environment.

Bamboo is an example of natural abundancy that presents an enviable versatility in relation to other manmade materials. Bamboo is a fast-growing plant of the Poaceae family (subfamily Bambusoideae) with around 1450 species that is part of the cultural and ecological landscape of many countries in Asia, America and Africa (CLARK; LONDOÑO; RUIZ-SANCHEZ, 2015; GOH; YAP; TONG, 2019). It also works as an efficient carbon sink, storing approximately 5.7 kg of CO_2 per kg of dry biomass above the ground (VOGTLÄNDER; VAN DER VELDEN; VAN DER LUGT, 2014; VAN DER LUGT et al., 2015).

Bamboo forests are mainly found in the southern hemisphere, widely distributed in Asia (67%), Americas (30%) and Africa (3%), in regions with tropical, subtropical and temperate climate zones (HUANG; SUN; MUSSO, 2017a). Brazil presents great potential for the use of bamboo as an engineering material due to the favourable weather for its cultivation and for the possibility of industrialization. In Brazil, there are around 232 species of bamboo, corresponding to 89% of all the gender and 65% of all the bamboo species in America (FILGUEIRAS; GONÇALVES, 2004; PEREIRA, 2012). However, exotic species such as *Dendrocalamus asper*, *Phyllostachys aurea*, *Phyllostachys edulis*, *Bambusa vulgaris*, *Bambusa tuldoides*, and *Guadua angustifolia* are widely found and well adapted in national territory and, according to the International Network for Bamboo and Rattan (INBAR), those species have great potential for applications in industry, recovery of degraded land and for civil construction (RAO et al., 1998).

In its natural state, bamboo can be used as an excellent structural element. It is characterized by its excellent specific mechanical strength in comparison with traditional building materials such as steel, cement, and wood (GHAVAMI, 1992). Bamboo buildings have demonstrated great seismic resistance, as observed in the maintenance of structural integrity of several houses built with bamboo in Colombia and India after the occurrence of earthquakes (SHARMA, 2010). The various species available provide a great range of sizes and strengths. Entire structures can be built with bamboo in its natural shape, using manual tools and demanding less labour due to its weight. However, without a suitable treatment, bamboo is prone to biological degradation in a short period, reducing its use as a structural material (JANSSEN, 2000).

Conventional wood treatment solutions used in Brazil have good performance but are generally based on heavy metals and other toxic elements, such as CCA (chromated copper arsenate), pentachlorophenol and others. The use of boron compounds for the preservative treatment of bamboo and wood, specifically disodium octaborate tetrahydrate (DOT), has been widely applied instead of other toxic preservatives. Boron compounds are some of the most effective and versatile preservatives solutions used nowadays since they combine the properties of broad-spectrum efficacy, low mammalian toxicity, and flammability retardant properties. Nevertheless, its use presents restrictions for the treated material because of the excessive leaching of boron in the presence of water and therefore, makes it unsuitable to use it for exterior

and non-protected applications (HIDALDO-LÓPES, 2003; FREEMAN; MCINTYRE; JACKSON, 2009; CALDEIRA, 2010).

Solutions to mitigate the boron leaching of wood have been investigated for the development of new solutions for wood treatment. CCA has limited use in several countries, depending on the application. CCB (chromated copper borate) was developed as an alternative to CCA, substituting arsenic by a boron source, reducing the toxicity to humans and the environment (VIDAL et al., 2015). However, heavy metals are still used in its composition and the disposal of treated wood/bamboo continues to be a problem (CALDEIRA, 2010).

Other alternatives without relying on toxic products and processes have been under development for the last decades. Tannin extract associated with boric acid and the cross-link agent hexamethylenetetramine (hexamine) has shown interesting results in terms of biodegradation of wood even after leaching process (PIZZI; BAECKER, 1996; THEVENON; TONDI; PIZZI, 2009; TONDI et al., 2012a). In Brazil, tannin is a commercial product and normally extracted from *Acacia mearnsii* bark using hot water and sodium salts (SILVEIRA et al., 2017). Other methods using furfuryl alcohol and dimethyloldihydroxyethyleneurea (DMDHEU) have also shown good results in combination with boron compounds (HILL, 2006; LI et al., 2015b; GÉRARDIN, 2016).

The chemical modification has also been investigated and applied in industrial scale to improve the durability and applicability of wood. Acetylated wood process, for example, uses an acetylation reaction with acetic anhydride for wood stabilization, increasing hydrophobicity, and improving dimensional stability and resistance against biological degradation. This process makes the modified wood materials appropriate for exposed applications (HILL, 2006; ROWELL, 2012). As in the acetylation, esterification processes using citric acid as the main solution can chemically modify wood or other lignocellulosic materials. Citric acid has been recently used as a binder of particle boards and for the esterification of hydroxyl groups from wood after thermal treatment (DESPOT; HASAN; JUG, 2008; ŠEFC et al., 2009a; ROMAINOR et al., 2014; WIDYORINI et al., 2014; ESSOUA et al., 2016). This treatment presentd interesting results in relation to the effectiveness of wood chemical modification and presents the advantage of being a low-cost product and widely available. The chemical modification with citric acid can result in a considerable decrease in water absorption, swelling,

and rotten fungi decay (DESPOT; HASAN; JUG, 2008; ŠEFC et al., 2009a, 2012; FENG et al., 2014).

Wood and bamboo preservation can be seen as a way to enhance carbon storage in products. By using bamboo in its natural form associated with the preservation process, it is possible to obtain a high quantity of stored carbon in the form of building materials. In relation to preservation, the longest the time of service of material after treatment, the better will be its capacity as a carbon "sponge" (LEPAGE; DE SALIS; GUEDES, 2017). An efficient preservative treatment may satisfy several criteria in order to be considered a treatment able for use in built environments, especially as a structural element. The following criteria are considered for the development and application of the preservative solutions that are proposed in this doctorate work:

- Protection against fungi and xylophagous insects;
- Low or no influence on the mechanical properties;
- Low toxicity and environmental impact;
- Accessible cost;
- Raw-materials available in the market.

Tannin extract based on *Acacia mearnsii* bark is produced on a large scale by the company Tanac®, in the Rio Grande do Sul state, Brazil, mainly for use in leather tanning and production of wood adhesive. Citric acid is widely available at a low price due to its great production and use in the food industry. Therefore, bamboo or wood-based products treated with the association of tannin with DOT or citric acid with DOT could comply with the criteria mentioned above.

Bamboo presents all the necessary characteristics in terms of energy efficiency, specific mechanical strength, and versatility to be used in civil construction. However, its use is still discrete in relation to its true potential, especially due to the availability of bamboo in the Brazilian market (few plantations with commercial purposes). Additionally, its use is limited by the lack of standards about its production chain, inadequate machinery for processing and low quantity of experimental data related to preservative treatment and its effects on the mechanical-physical properties and degradation. These are aspects of high relevance in structural applications, making bamboo uncompetitive in comparison with other materials already available and consolidated in national and international markets.

As original aspects of this doctorate work, combined analyses for the evaluation of conventional preservative treatments and the use of new treatment systems are explored. The thesis is focused on the study of bamboo chemical modification during the treatment process, the evaluation of boron leaching in the presence of water, the effect of the proposed treatments on the mechanical and physical properties as well as the corresponding fungi degradation resistance. This work also gives light into practices and methods for quality control that should be used in commercial treatment plants working with bamboo. Bibliographic research performed in several international and national journals database, and also in the available abstracts from the International Research Group on Wood Protection (IRG-WP), showed the lack of information regarding standardization and quality assessment of treated bamboo and no reported papers about the use of novel treatments using citric acid or tannin extracts.

1.2. General objectives

This doctorate work has two main general objectives:

- To evaluate the treatability and corresponding mechanical, physical and chemical properties of full-culm bamboo submitted to conventional treatment procedures and assess pilot-scale treatment in terms of quality control. Target: **Set of characterization methods suitable for quality control of treated bamboo.**

- To investigate the physical-mechanical and chemical properties, fungi decay resistance and thermal stability of bamboo samples after treatment with alternative preservative solutions based on citric acid and tannin extract and their combination with disodium octaborate tetrahydrate (DOT). Target: **Improvement of overall bamboo performance.**

1.2.1. Specific objectives

This work aims specifically to:

- Investigate the effect of different preservatives on the mechanical properties of bamboo and evaluate its strain behaviour by digital image correlation analysis;

- Explore and apply methods for preservative treatments evaluation for quality control and organize guidelines for bamboo treatment;

- Understand the underlying mechanisms involved in the chemical modification of bamboo with citric acid;

- Assess the effect of treatments based on citric acid and its combination with disodium octaborate tetrahydrate on dimensional and thermal stability and on the fungi degradation resistance of bamboo;

- Analyse the leachability of boron-based formulations for bamboo treatment;

- Use tannin-based preservatives in combination with disodium octaborate tetrahydrate for bamboo treatment and evaluate the resulting changes by physical and thermal characterizations, and fungi decay tests;

1.3. Thesis structure

This thesis is divided into 5 chapters. Each chapter, described hereunder, is independent. Chapters 3 and 4 are presented in the format of fully published/submitted or under submission papers. Results still not organized for publication are also included at the end of those chapters, as additional and complementary information.

Chapter 1: This chapter brings the contextualization, motivation, and objectives of this work, followed by the thesis organization and structure.

Chapter 2: This chapter presents a literature review focused on the applications and properties of the bamboo material and presents discussions of the conventional and on-going development of treatment methods/technologies for bamboo/wood.

Chapter 3: This chapter presents an assessment of conventional treatment using disodium octaborate tetrahydrate (DOT) and chromated copper borate (CCB) of *P. edulis* and *D. Asper* bamboo. Treatments in lab and pilot scales were evaluated in terms of treatability, and effects on mechanical and physical properties. This Chapter has the main purpose of bringing technical

discussions about quality control of full culm bamboo as a structural material. Detailed information regarding mechanical testing methods assessed by Digital Image Correlation strain analysis is also presented.

Chapter 4: This chapter focuses on the development of alternative preservative treatments for bamboo. First, tannin extract in combination with DOT for an in-situ polymerization and reduction of boron leaching was investigated. This treatment process was evaluated using *D. asper* species through mechanical-physical characterization, thermal degradation, and fungi decay tests. Second, a chemical modification process using citric acid of *D. asper* bamboo as a novel alternative for ecological treatment was explored. This modification approach is investigated in detail through chemical, physical, mechanical, and thermal characterizations. Combined treatments with DOT were explored and compared with untreated bamboo samples.

Chapter 5: This chapter is dedicated to the final remarks and a summary of the main conclusions obtained throughout the development of this thesis. Future activities related to this area of research are advised.

2. CHAPTER 2 - Literature review

This chapter is dedicated to a concise literature review and theoretical background for the understanding of this doctorate thesis. More detailed information and recent advances of each topic explored in this work are reported in the corresponding chapters, which complements the information herein presented.

2.1. Research on bamboo

According to the Scopus database, a total of 18,355 documents related to the keyword "bamboo" since the 1940s are available, being 1,492 documents in 2019 alone. This trend is presented in Figure 2.1. Most of the publications are, in ascending order, from China (the double fold of the second position), United States, Japan, India, Taiwan, and Brazil. The interest on bamboo covers a wide range of subjects with most of the publications allocated to agriculture and biological sciences, engineering, materials science, and environmental science. Although the term bamboo is also used to describe some types of microstructures and in the field of humanities for historical background, there are around 5,230 publications in the fields of engineering and materials science, which are related to the scope of this work. Nevertheless, the main purpose of this Figure and the corresponding data is to bring attention to the increasing interest of the scientific community in bamboo research.

When the combined terms "bamboo" and "treatment" are included in the searching platform, a total of 2,638 documents are found, with the first one reported in 1952. The interest along the years has the same trend of the plot shown in Figure 2.1 and China followed by India, Japan, USA, and Brazil are the main countries with publications contribution. From all the documents, 705 publications are in the fields of materials science and engineering. Additionally, using the combined terms "bamboo" and "chemical modification" only 203 documents were found, with only 78 publications in the fields of materials science and engineering.

Figure 2.1 - Distribution of publications with the term “bamboo” from 1940 to 2020 and the corresponding areas of knowledge.

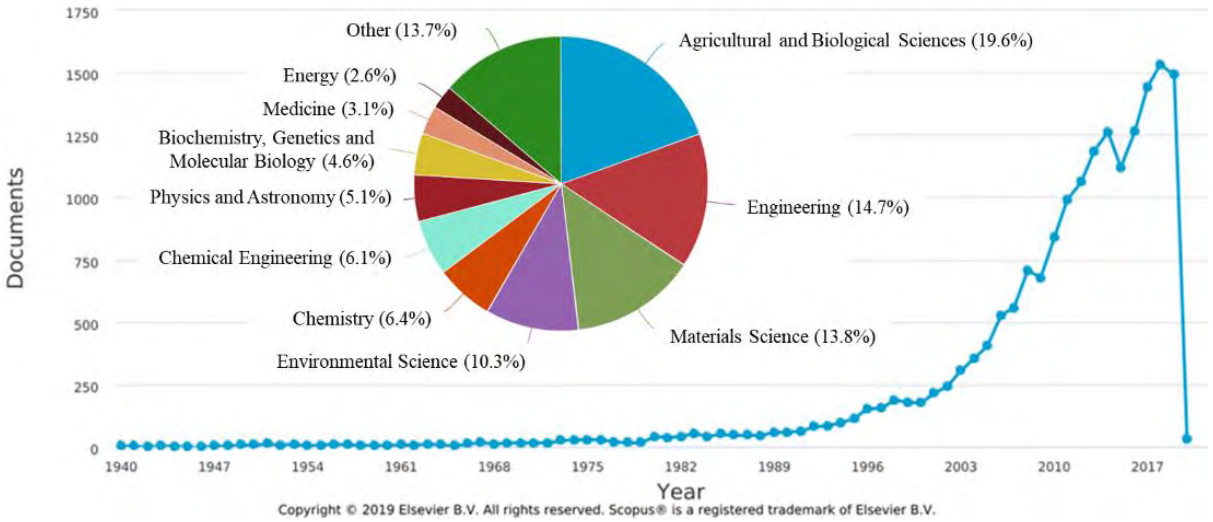

Source: Plots generated on Scopus® database platform (Elsevier B.V.)

2.2. The bamboo plant

Bamboo is a woody grass of the Poaceae family (subfamily Bambusoideae), order of Graminales, class of Monocotyledons and phylum of Spermayophyt (LIESE, 1998; CLARK; LONDOÑO; RUIZ-SANCHEZ, 2015). The bamboo forests are mainly found in the southern hemisphere, widely distributed in Asia (67%), Americas (30%) and Africa (3%), in regions with tropical, subtropical and temperate climate zones (HUANG; SUN; MUSSO, 2017a). The distribution of bamboo forests (planted and natural) and the corresponding climate classification is shown in Figure 2.2. The various bamboo species can also be classified as temperate woody bamboos, tropical woody bamboos (neotropical and paleotropical), and herbaceous bamboos, according to their evolutionary background (CLARK; LONDOÑO; RUIZ-SANCHEZ, 2015).

The area of bamboo available throughout the world, according to FAO (2010), is presented in Table 2.1. Although these numbers are estimates, we can have an overview of this resource availability and potential across the globe (KUEHL, 2015). In the work of Caravan et al. (2016), an interesting study was conducted on the quantification of bamboo species in 52 countries, which have been classified as native, introduced, or invasive species. The resulting data is presented in Figure 2.3. Brazil appears in the second position, after China, with the

highest amount of species, most of them native. In countries like Australia and the USA, most of the species have been introduced. One important aspect of this work is that it shows although some bamboo species can be invasive, the percentage of these species over the native and introduced ones is quite low. The main contribution to the migration of bamboo species across the continents is attributed to intentionally introduced species (CANAVAN et al., 2016).

Figure 2.2 - Distribution of bamboo forests and the corresponding climate classification.

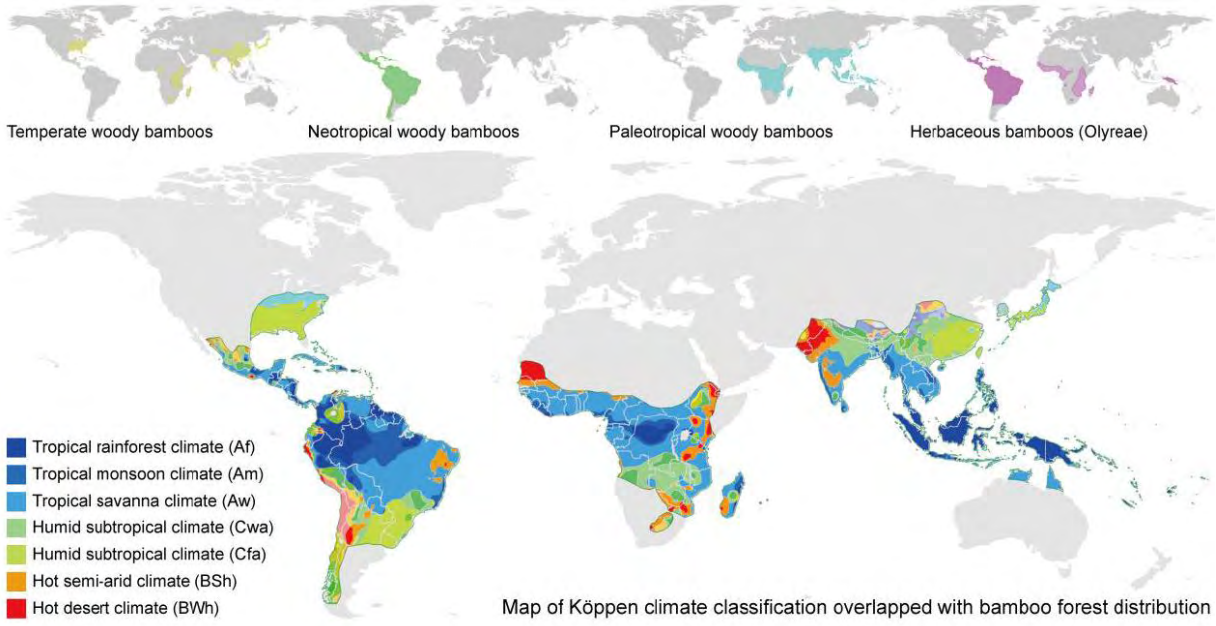

Source: (HUANG; SUN; MUSSO, 2017b).

Table 2.1 - Bamboo resources in the world according (FAO, 2010).

Region	Area of bamboo (1,000 ha)			
	1990	2000	2005	2010
Africa	3,688	3,656	3,640	3,627
Asia	15,412	16,311	16,943	17,360
Europe	n.s.	n.s.	n.s.	n.s.
North and Central America	37	37	37	39
Oceania	23	38	45	45
South America	10,399	10,399	10,399	10,399
World	29,560	30,442	31,065	31,470

n.s. not significant

Source: (KUEHL, 2015).

Figure 2.3 - Number of bamboo species in 52 countries and the classification in native, introduced and invasive species.

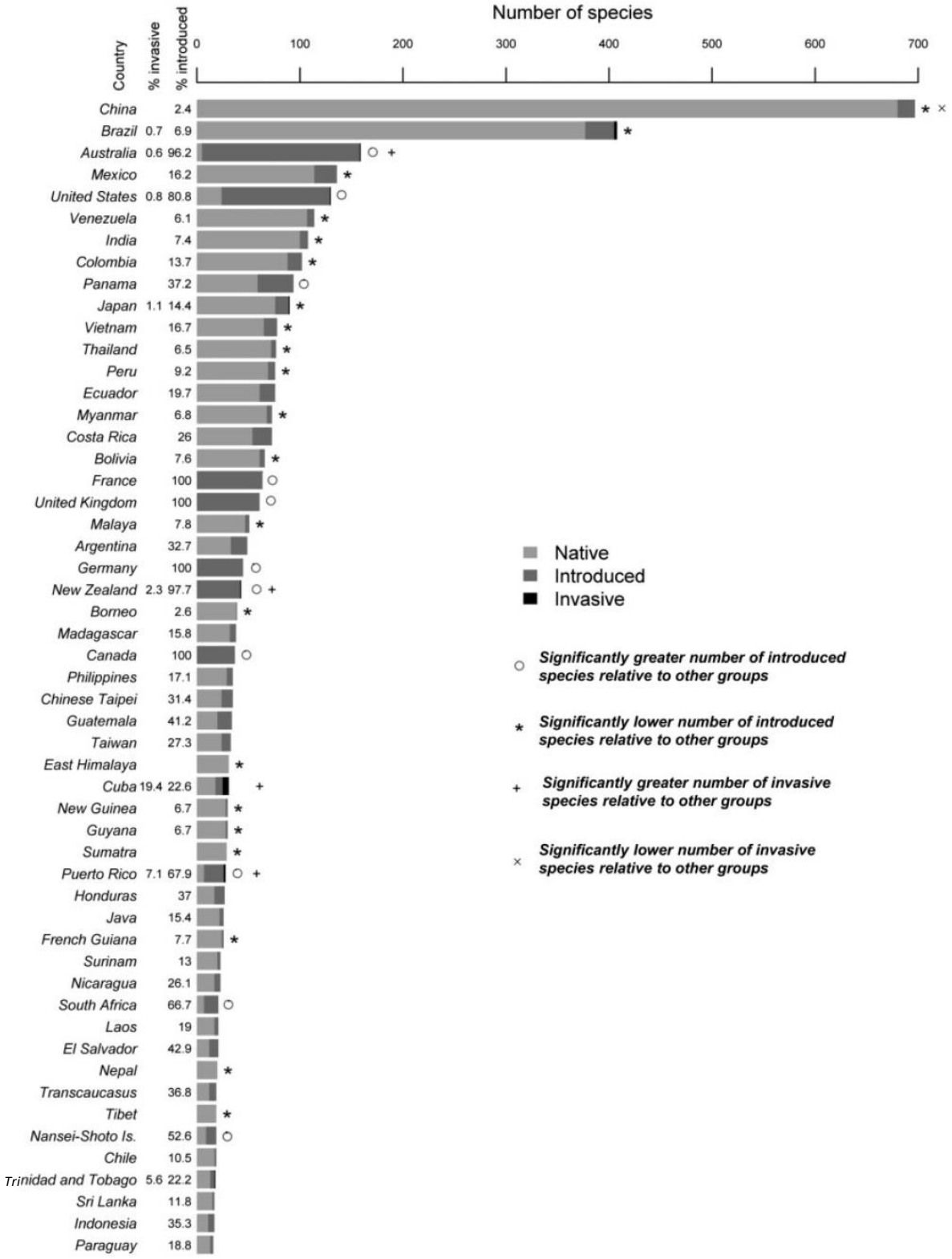

Source: (CANAVAN et al., 2016)

The various bamboo species can be classified in different types of root/rhizome system and growth behaviour: monopodial (running), sympodial (clumping) and amphipodial (running or clumping) (PEREIRA, 2012). A representation of the most used types, runner and clumping, and the nomenclature of the parts that compose the bamboo are shown in Figure 2.4 (SHARMA et al., 2014). Examples of clumping and runner bamboos, *Dendrocalamus asper* and *Phyllostachys edulis*, respectively, are presented in Figure 2.5. Basically, in clumping bamboos, the culms grow close to each other, forming a stabilized clump, and the runner bamboos have independent culms that spread through the land as conventional grass.

Bamboo can be divided into two major components, rhizome and culm (LIESE; TANG, 2015a). The underground part is the rhizome, which is the structural foundation of the culm. The rhizome, besides producing new shoots/culms, is responsible for the uptake, supply, transfer, and storage of water and nutrients (CHAOWANA; BARBU, 2017). The bamboo culm is the part above the ground, containing most of the woody material. The culm grows as a hollow cylinder composed of regions with aligned fibre bundles, the internodal spacing or internode, separated by solid transversal diaphragms, called nodes, with interwoven fibre bundles along with the wall thickness (GROSSER; LIESE, 1971).

It is well known that bamboo grows very fast, up to 30 m within a year, depending on the species. After growth completion, the culms lignify and gain strength until optimum mechanical properties, after 3-5 years. In this respect, there is no counterpart in the vegetal kingdom (LIESE; WEINER, 1996; PEREIRA, 2012).

Figure 2.4 - The bamboo plant and its different types and elements.

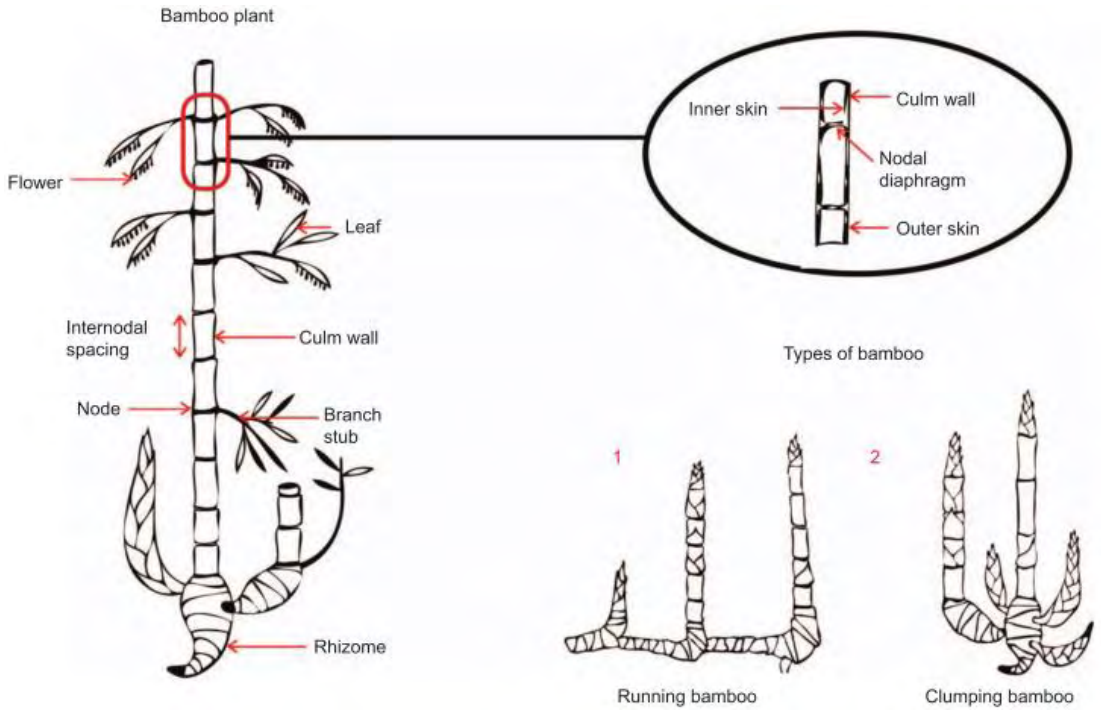

Source: (SHARMA et al., 2014).

Figure 2.5 - *D. asper* (clumping), on the left, and *P. edulis* (runner), on the right, in Brazil.

Source: Author's personal records.

Detailed information regarding the two species focused in this work (Figure 2.5) is presented below. The data has been extracted from the INBAR report for priority species, published in 1998 (RAO et al., 1998)**.** Both species are also widely found in Brazil, especially in the south and south-east regions.

"*Dendrocalamus asper* *(= Bambusa aspera, Gigantochloa aspera, Dendrocalamus f/age/lifer, Dendrocalamus merrillianus) Common name: Giant bamboo, Bamboo Betung. Common name in Brazil*[*]*: Bambu gigante, Bambu balde, Corote.*

This is a large bamboo with culms 20-30 m tall; lower nodes covered with a circle of rootlets; internodes 20-45 cm long with a diameter of 8-20 cm and with relatively thick walls (11-20 mm), but thinner towards the top of the plant; leaf 30 x 2.5 cm; inflorescence long, clustered pseudo spikelets, flowers sterile, fruits collected from hybrids. Vegetative propagation

- culm and branch cutting.

Distribution: Commonly planted in Thailand, Vietnam, Malaysia (Peninsular and East), Indonesia and the Philippines; commercially important in eastern parts of India; widely introduced elsewhere in tropical and subtropical botanic gardens, origin somewhere in south-east Asia.

Climate and soils: This species grows best in rich and heavy soils of the humid regions from the lowlands to 1500 m altitude, but it also grows well in semi-dry areas in Thailand, grows best with good drainage or sandy soil, tolerates -3°C.

Uses: Structural timber, strong, large, very good quality. General purpose, one of the most useful bamboos for heavy construction in rural communities. However, it is mainly used for building due to the strength of the culms which are relatively durable. It is also used in making good quality furniture, musical instruments, containers, chopsticks, household utensils and handicrafts. The young shoot is sweet and considered delicious; plantations for shoot production have been established in Thailand and other countries. Six cultivars recognized, Dasper, cv betung wulung, large black bamboo of Indonesia; cv Thai green, suitable for plantations as used in Thailand, cv Phai Tong Dam, less popular than Thai green, slightly black in colour.

Phyllostachys pubescens *(= P. heterocycla, var. pubescens, = Bambusa heterocycla, = P. edulis var. heterocycla (including P. bambusoides and P. eduliis) Common name: Moso. Common name in Brazil*: Mossô, Bambu gigante.*

Phyllostachys is a large temperate, monopodial genus with about 70 recognized species, various species are extensively cultivated in China because of their many uses and economic importance; there are many taxonomic uncertainties in the limitation of various species. P. pubescens is changed to P. heterocycla with distinct variety pubescens P. heterocycla var. pubescens). Culm green, smooth, culm sheath brownish yellow, shoots edible, culms used as timber, cultivated including following varieties: var castillonis, var. lacrima, var. mixta, var shoujhu yi. This is a medium to large monopodial bamboo with culms l0-20 m tall and a diameter of ca 18 cm. Culms are straight, strong and suitable for heavy construction. Vegetative propagation: Culm cutting, layering, marcotting.

Distribution: Native to China. Extensively cultivated, in different provinces of China, Japan, Korea and Vietnam. Introduced to many Botanical gardens.

Climate and soils: This is a temperate species complex, planted on rich soil, also found as natural pure stands, suitable for many soil types.

Uses: This species and different varieties are used as building material, for shoot production (especially in China), and for making agricultural and household implements, wood industry. Widely cultivated for shoots and timber in China, Japan and Korea."

*** Information added by the author.**

2.2.1. Harvesting and culm maturity

Bamboo can be utilised in a wide range of applications, e.g. construction sector, chemical, composites, chemicals, pharmaceuticals, and food, mainly using the culms. In civil construction, the culms are used in its natural form, or as engineered materials such as bamboo particleboards, bamboo scrimber, laminated bamboo lumber, plybamboo, oriented strand board (OSB) and others (SUMARDI; ONO; SUZUKI, 2007; ANWAR et al., 2011; BISWAS; BOSE; HOSSAIN, 2011; MAHDAVI; CLOUSTON; ARWADE, 2011; MALANIT; BARBU; FRÜHWALD, 2011; GAUSS et al., 2019).

The maturity of the bamboo culms is one very important aspect for the most part of products and applications, being utilised in all the applications mentioned above. Therefore, one small section of this chapter will be focused on this issue. The culm age is also an essential parameter for the management of a bamboo clump or bamboo forest.

Typically, the culms are considered mature when they are 3-5 years old. However, in terms of chemical and technological characterisation, the point of maturity is inconsistent (LIESE, 1985). The lack of growth rings in the culms makes it impossible to estimate their age, as it is usually performed in dicotyledonous plants. The size of the culms cannot also be used as a criterion since the culms begin their growth already with a definitive diameter (BANIK, 2015). Liese and Weiner (1996) investigated the culms age up to 12 years of the bamboo species *Phyllostachys viridiglaucescens*. They showed that there are anatomical changes during the maturation period and later years of the culm. These changes are observed as cell wall thickening of the fibres and depositions in vessels and sieve tubes (LIESE; WEINER, 1996).

Although it is difficult to determine the age of bamboo culms, several visual and other aspects can be used for age estimation in the field. Generally, 1-2 years-old culms are recognisable by their colour (intense greenish/blueish colour, depending on the species), the presence of culm sheath at the base, and sometimes, white powder on the internodes. The mature culms, after 3 years, present white spots, caused by fungi, and lichens along the culm length. If the culm appears to be dry and has whitish-grey nodes, it is then considered overmature (BANIK, 2015). These features can be observed in Figure 2.6, where Guadua angustifolia culms, planted in Brazil, with several ages are shown. The lack of culm sheaths and colour are the main attributes for age estimation in this case. Experienced workers can determine if a culm

is mature or not by the sound of the culm when struck with a machete. In a plantation field, although laborious, the best practice to control the culms age is to mark each culm to be harvested with the year of growth (by colour, numbers or other sorts of marking).

Bamboo plantations should always be managed to favour new culms production and facilitate harvesting operations. Additionally, it is interesting to mention that regular harvests, when adequately managed, increase carbon sequestration in bamboo forests. In Figure 2.7 a comparison between Moso bamboo (*P. edulis*) and Chinese fir tree in plantations with and without regular harvest clearly show this difference in terms of total carbon accumulation per hectare. Regular-harvest also contributes to higher productivity (KUEHL; LI; HENLEY, 2013).

Figure 2.6 - Example of culm age by visual inspection of a Guadua angustifolia from Brazil. a) culm with 1-year-old; b) culm with 2 years-old; c) mature culms between 3-5 years-old.

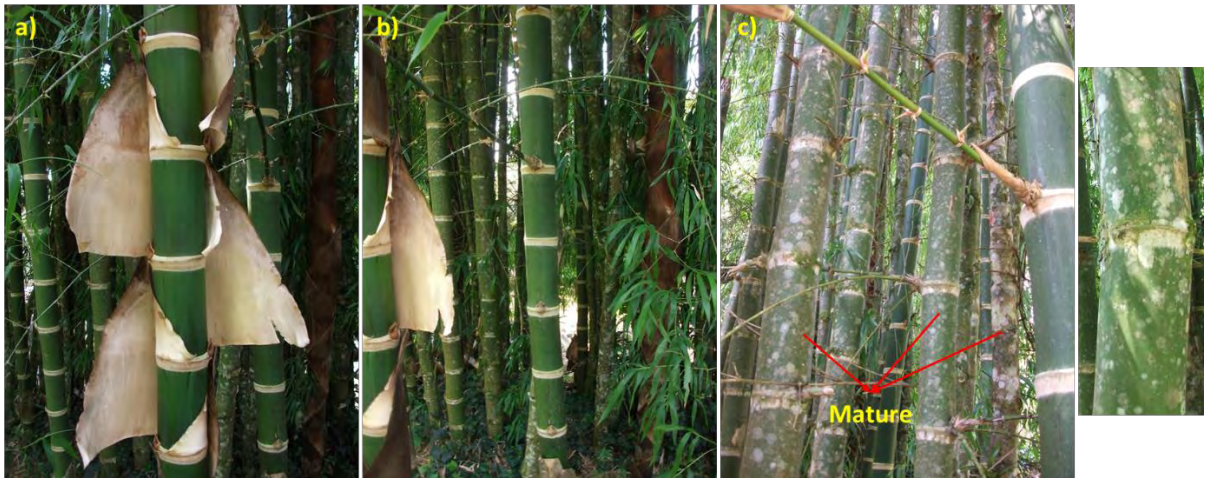

Source: Author's personal records.

Figure 2.7 - The effect of regular-harvest on total carbon accumulation in Moso bamboo and Chinese fir plantations.

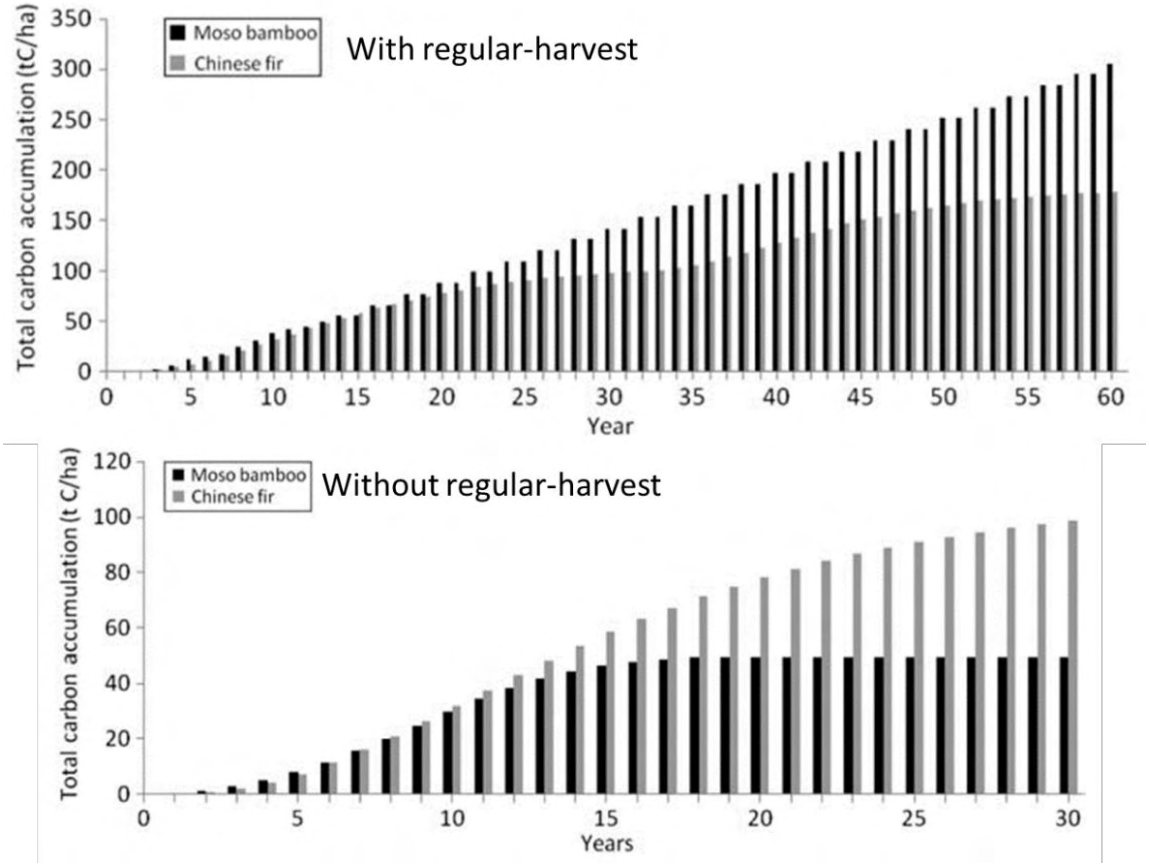

Source: (KUEHL; LI; HENLEY, 2013).

2.3. Structure and anatomy of bamboo

Bamboo culms achieve maturity in 3-5 years and are composed mainly of 50-80% of holocellulose (cellulose + hemicellulose), 30% of pentosan and 20-28% of lignin, depending on the species and culm age. Table 2.2 presents the chemical composition of some Asian bamboo species. The chemical composition also varies, although not significantly, depending on the region of the culm (bottom, middle or top) (LIESE, 1987; LIESE; TANG, 2015a).

Table 2.2 - Chemical composition of a few bamboo species in relation to the culm heights (top, middle, bottom).Data from (1) - (RATANOPHAT, 2004) and (2) - (LI et al., 2007)

Species	Culm portion	Holocellulose (%)	Lignin (%)	Ash (%)	Hot water extract (%)
Bambusa sp. (1)	Top	78.8	25.0	2.4	12.4
	Middle	80.8	25.1	1.8	10.6
	Bottom	78.5	25.9	1.4	11.3
Bambusa blumeana (1)	Top	81.9	27.6	4.9	8.6
	Middle	81.2	27.6	5.8	6.9
	Bottom	81.7	26.3	3.4	9.1
Dendrocalamus asper (1)	Top	80.5	27.5	1.8	8.6
	Middle	78.4	26.9	1.4	11.8
	Bottom	79.7	28.2	0.9	9.1
Dendrocalamus strictus (1)	Top	79.3	27.4	2.8	12.7
	Middle	77.7	27.8	1.1	12.8
	Bottom	77.9	28.0	2.1	11.6
Gigantochloa albociliata (1)	Top	79.6	23.4	1.5	8.9
	Middle	80.8	27.2	2.4	12.4
	Bottom	79.6	27.3	1.5	8.3
Phyllostachys pubescens (2)	Top	54.1	24.7	1.2	7.0
	Middle	53.6	24.5	1.2	8.5
	Bottom	54.4	24.0	1.1	9.3

Source: Adapted from (LIESE; TANG, 2015a)

The culm wall thickness, diameter and internode length change with the height position. Chaowana et al. (2017) investigated the macroscopic characteristics along the culm length of four bamboo species. From their results, it is possible to observe that the middle part of the culm is more homogenous (in terms of wall thickness, diameter, and internode length) than the bottom and upper parts. These differences in the structure of the culm consequently also cause changes in density, shrinkage, strength, and moisture content of the bamboo material (CHAOWANA; BARBU, 2017).

In terms of anatomy and microstructure, bamboo is composed by 40% of fibres, 50% of parenchyma cells and 10% of vessels, as shown in Figure 2.8 (LIESE, 1987; LIESE; TANG,

2015a). Additionally, because of the fibres distribution and variation of the thickness and diameter along the culm length, bamboo can be considered a natural composite of Functional Graded properties, naturally developed to withstand wind forces and harsh weather (NOGATA; TAKAHASHI, 1995; GHAVAMI; MARINHO, 2005; TAN et al., 2011). The fibre bundles are distributed along the wall thickness in a way that higher amounts of fibres are localized in the external layer, decreasing towards the inner layer, as shown in Figure 2.9 (GHAVAMI; RODRIGUES; PACIORNIK, 2003; GEROTO, 2014; AKINBADE et al., 2019). The density of fibre bundles also changes along with the culm height, with higher densities in the upper part of the culm. The variation of fibre density across the wall thickness is observed to be described by quadratic, linear, exponential, or power functions, depending on the species (AKINBADE et al., 2019).

Figure 2.8 - Details of the microstructure of the bamboo.

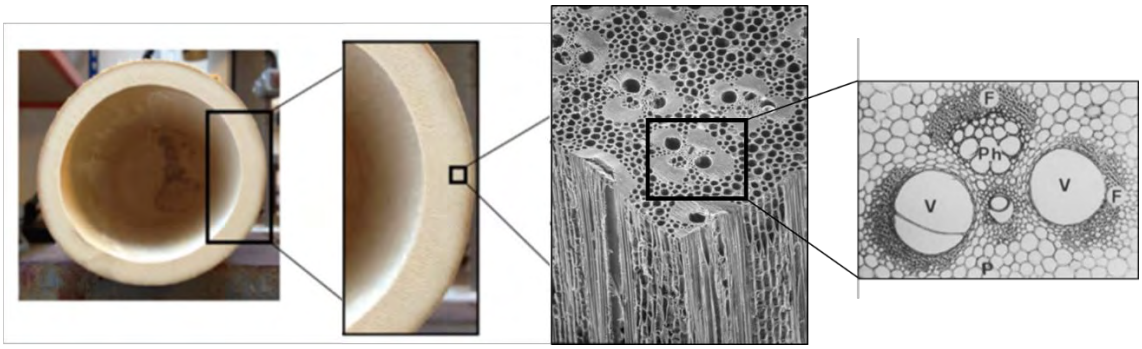

V= Vessel, F= fibre sheath, Ph= Phloem, P= Parenchyma

Source: Adapted from (SHARMA et al., 2015a), (LIESE, 1987), and (LIESE, 1998)

Figure 2.9 - Fibre volume fraction variation along the wall thickness of P. edulis bamboo.

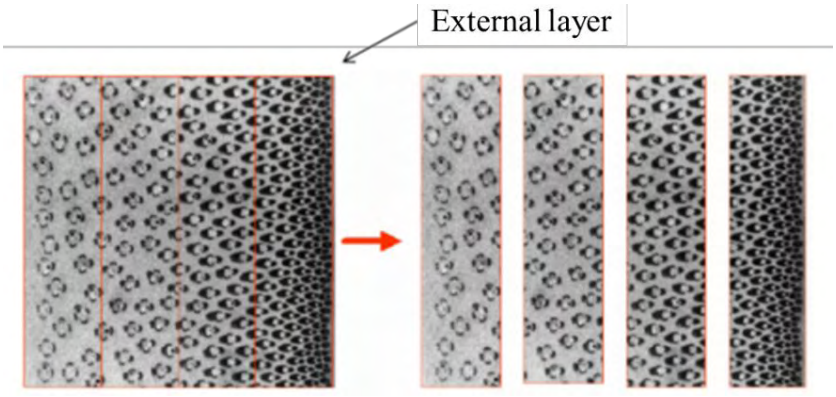

Source: Adapted from (GHAVAMI; RODRIGUES; PACIORNIK, 2003)

The overall performance of bamboo is dependent on its structure and components. It can be described as a unidirectional composite with a matrix (parenchyma) and a reinforcing phase (fibres). The parenchyma cells and the vascular bundles simultaneously contribute to the flexibility and stability of the culm. The shape of the parenchyma cells also changes across the culm wall thickness, being larger and longer towards the inner part. Parenchyma cells also play a crucial role in culms life. Starch particles are formed within the cell lumina and are mobilized before shoot formation (LIESE; TANG, 2015a). The bamboo fibres are the main responsible for the mechanical performance of bamboo. These fibres are present around the vascular bundles as sheaths, also called fibre bundle. The fibre bundles are composed of unitary fibres, with considerable variation of the length among different species (between 1.5 and 3.0 mm), which is longer than those of hardwood and softwood. The fibre length is correlated with fibre diameter, cell wall thickness and culm modulus of elasticity/strength. The vascular bundles are composed of two metaxylem vessels, fibres, and the phloem (see Figure 1.8). Their form and shape vary along the culm wall thickness and height and are species-dependent (LIESE; TANG, 2015a).

The nature of bamboo's microstructure also interferes in the penetration of preservative solutions, differing from the penetration mechanisms of wood. Culm age and species also present great influence in its durability and treatability (LIESE; WEINER, 1996; LIESE, 2004).

2.4. Bamboo Standards

Since bamboo is a natural material, there is a considerable variation of geometry and properties among species and even in the same clump. Additionally, connections complexity, low elastic modulus, shrinkage and swelling, the susceptibility of chemical and microorganisms attack are some of the problems that hinder the standardization of bamboo (HARRIES; SHARMA; RICHARD, 2012).

Although international standards for structural design and laboratory tests are available (e.g. ISO 22156:2004, ISO 22157:2019, IS 9096:2006, IS 1902:2006, and others), testing and designing with natural materials is still challenging (HARRIES et al., 2012; GHAVAMI, 1992). Several authors emphasize the main inconvenient for the mechanical properties determination is the lack of standardization of the tests, becoming more challenging the comparison of the results.

A summary of international bamboo standards available is shown in Table 2.3 (GATÓO et al., 2014). A complete review about the Colombian, Ecuadorian, Peruvian and ISO standards is presented in (MARÇAL, 2018).

In general, the standards complement each other and address structural design and physical-mechanical characterization. Specific standards for treatment were only found in India and Colombia, although other standards describe this subject briefly. Process variables and validation analyses for quality control are normally not discussed.

The main bamboo standard used in recent publications is the ISO 22157-1:2004, recently substituted by the ISO 22157:2019. In Brazil, new standards for structural design and mechanical tests have been recently elaborated based on part of the standards presented in Table 3, and now they are being assessed in a public consulting phase (Standard NBR 16828). In Chapter 3, detailed discussion about tests standardization is provided.

In Brazil, there are no existing standards related to harvesting, production and treatment of bamboo. However, these areas are fundamental for the development of bamboo production chain. In terms of treatment characterization, the standard ABNT NBR 6232:2013 for the characterization of treated wood can be used for penetration and retention analyses.

Table 2.3 – Present international Standards for bamboo use.

Country	Code	Standard
China	-	JG/T 199:2007 - Testing method for physical and mechanical properties of bamboo used in building
Colombia	Reglamento Colombiano de Construcción Sismoresistente – chapter G12 Estructuras de Guadua (Guadua structures)	NTC 5407:2006 - Uniones de Estructuras con Guadua angustifolia Kunth (Structural unions with Guadua angustifolia Kunth)
		NTC 5525:2007 - Métodos de Ensayo para Determinar las Propiedades Físicas y Mecánicas de la Guadua angustifolia Kunth (Methods and tests to determine the physical and mechanical properties of Guadua angustifolia Kunth)
		NTC 5301:2007 - Preservación y secado del culmo de Guadua angustifolia Kunth (Preservation and drying of Guadua angustifolia Kunth culm)
Ecuador	Norma Ecuatoriana de la Construcción – Estructuras de Guadúa (Guadua structures)	NEC-SE-GUADÚA:2017 – Estructuras de Guadúa (GaK) (Guadua structures)
India	National Building Code of India, section 3 Timber and bamboo: 3B	IS 6874:2008 - Method of tests for bamboo
		IS 15912:2012 - Structural design using bamboo – code of practice
		IS 1902:2006 - Preservation of bamboo and cane for non-structural proposes - code of practice
		IS 9096:2006 - Preservation of bamboo and cane for structural proposes - code of practice
Peru	Reglamento Nacional de Edificaciones, Section III	E100:2012 – Diseño y Construcción con Bambú (Design and Building with Bamboo)
International	-	ISO 22156:2004 - Bamboo – structural design
		ISO 22157:2019 - Bamboo – determination of physical and mechanical properties. Substitutes the former ISO 22157:2004 parts 1 and 2.

Source: Adapted from (GATÓO et al., 2014).

2.5. Mechanical properties of bamboo

Despite the considerable variability of the physical and mechanical properties of bamboo, its great potential is observed by analysing it from the materials selection point of view. Figure 2.9 shows the Ashby diagram of strength versus density of several classes of materials (composites, polymers, natural materials, ceramics, and metals). The properties of bamboo, tensile strength and density, were included as the green circle, marked in red (added by the author according to the properties presented in Table 2.4). The selection of a given material can be accomplished by combining its properties, maximizing and optimizing the performance of a structure through a merit index, which is used as guide-line for minimum mass design. For a glue-laminated bamboo beam loaded in bending, for example, the strength-limited design at minimum mass can be represented as $\left(\frac{\sigma_f^{\frac{1}{2}}}{\rho}\right)$, where σ_f is the tensile strength and ρ the density (WEGST; ASHBY, 2004). In an ideal situation, materials above the line shown in Figure 2.10 behave better in flexure than bamboo, while materials below this line are less effective (when the guide-line is positioned in a specific material). The efficiency and advantage of bamboo in relation to other materials are clearly observed.

In the work of Wegst and Ashby (2004), an interesting review of the efficiency of natural materials is presented. Figure 2.11 shows the Ashby diagram of strength versus density of several natural materials (mineral and organic). Even among natural materials, which have high efficiency, bamboo stands out as one of the most efficient considering tensile strength-limited design at minimum mass. Although many of these natural materials are not used for structural or functional applications, it brings our attention to the potential of bamboo as an efficient material suitable for multiple purposes.

Figure 2.10 - Strength/density Ashby diagram with different classes of materials. The bamboo properties were included by the author.

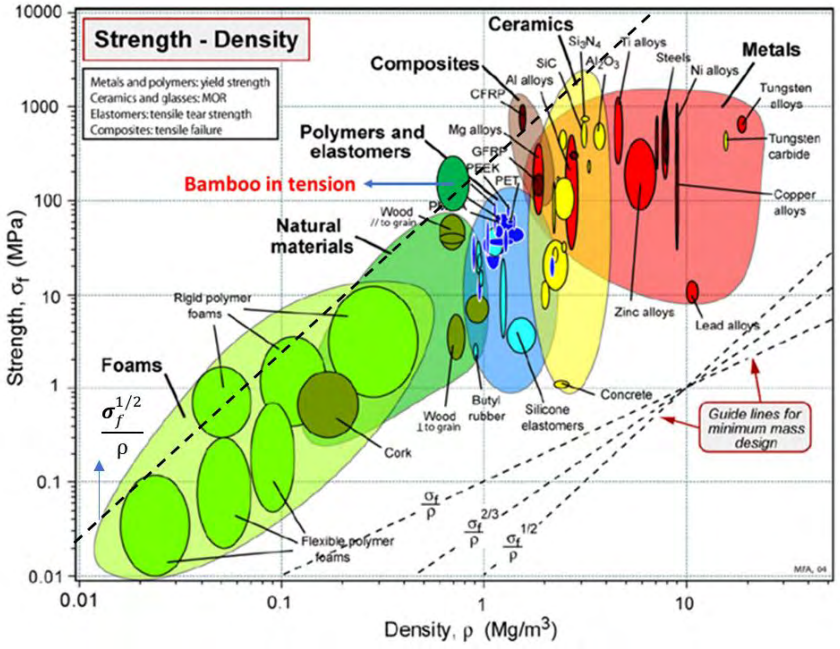

Source: Adapted from (GRANTA-DESIGN, 2010).

Figure 2.11 - Strength/density Ashby diagram with natural materials.

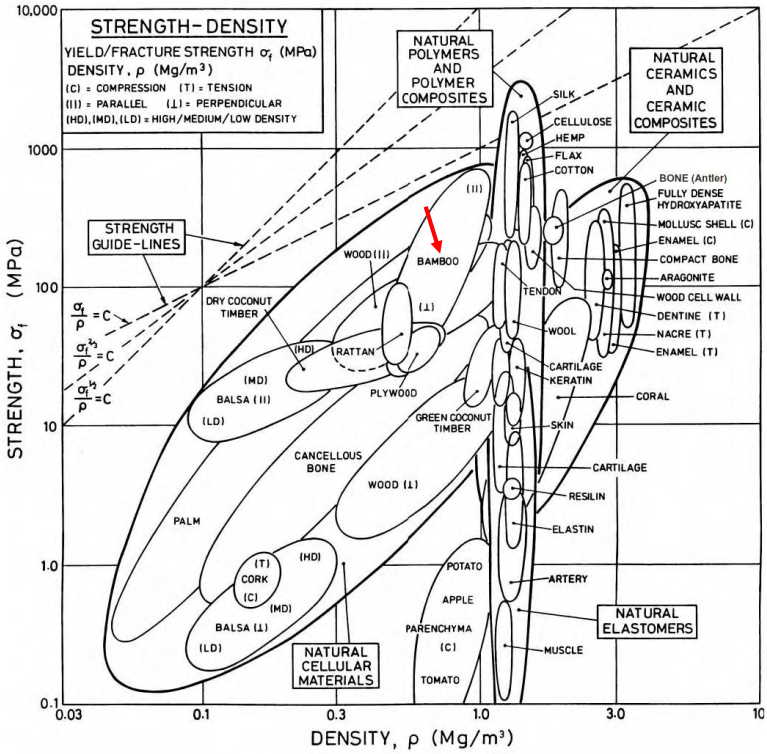

Source: (WEGST; ASHBY, 2004)

In terms of mechanical properties, the bamboo species *Dendrocalamus asper,* for example, widely found in Brazil, presents compression, tension, and bending strength of 30 to 60 MPa, 100 to 200 MPa and 80 to 150 MPa, respectively, depending on the presence or not of the node and the position along the culm length (PEREIRA, 2012). These mechanical properties are similar and sometimes superior to those of other species from *Dendrocalamus*, *Guadua* and *Bambusa* genera (GHAVAMI; MARINHO, 2005; GEROTO, 2014).

A review of recent papers regarding the mechanical properties of *P. edulis* and *D. asper* bamboo (species focused in this work) can be found in Table 2.4. As described in the former section, the use of different standards makes it more difficult to compare the study of different authors. However, it is possible to have a good overview of the variability of these two bamboo species in tension, compression, bending and shear behaviours. For the bending results, only results of small coupon tests are presented (reduced size specimens).

In addition to the different testing methods utilised in the different papers, the position of the samples along the culm length and thickness, moisture content, and average apparent density are also factors that have considerable influence on the mechanical properties of bamboo. It is important to mention that in many published papers not always the moisture content and density of the samples are presented, which greatly impact the comparison among the different works. Moreover, the modulus elasticity is not correctly measured in some papers, lacking correct instrumentation (extensometer or strain gauges) for the analyses. Nevertheless, although different methods were used, it is possible to obtain a range of strength/moduli considering these two species (without the influence of the node), which also brings light into the variation related to the testing methods; strengths of 77 - 326 MPa, 42.5 - 94.7 MPa, 52 - 258 MPa, 11.9 - 15.1 MPa in tension, compression, bending and shear respectively; elasticity modulus of 11.4 – 30.7 GPa, 7.8 – 21.2 GPa, 4.4 - 26.0 GPa in tension, compression and bending respectively.

Table 2.4 - Summary of *P. edulis* and *D. asper* mechanical properties.

Bamboo species	Description	Testing method	Apparent density (g/cm^3)	$f_{t,0}$ (MPa)	$E_{t,0}$ (GPa)	$f_{c,0}$ (MPa)	$E_{c,0}$ (GPa)	MOR (MPa)	MOE (GPa)	f_v (MPa)	Source
P. edulis (moso)	2-years old culms	ISO 22157:2004	0.54 - 0.67 (dry density)	272	11.4	42.5	21.2	-	-		[1]
P. edulis (moso)	4-years old and 6-year old culms (MC= 8-12 %	ISO 22157:2004	0.66 - 0.80 (MC=8-12%)	-	-	48.0 - 62.0	-	-	-	11.9 - 15.3	[2]
P. edulis (moso)	Between 3 and 6-years old culms (MC 4%)	Reduced size specimens: 1-6 x 5-20 x 100-160 mm	0.40 - 0.85	-	-	-	-	52 - 215	4.4 - 16.7	-	[3]
P. edulis (moso)	Mature culms - at least 3-years old. Averages of samples with MC= 5-30%	Compression = "INBAR Standard - 1998" L=2D Bending = Full-culm three-point bending (clear span of 1000 mm)	0.79 (dry density)	-	-	75.0	7.80	88	11.4	-	[4]
P. edulis (moso)	Unspecified age	ISO 22157:2019	0.90 (MC=12%)	-	-	48.1	-	-	-	15.1	[5]
D. giganteus	6-years old culm (bamboo strips across wall thickness)	ASTM D-3039 (Tensile) ASTM D-3410 (Compression)	0.69 - 0.98	194 - 326	17.6 - 30.7	67.3 - 94.7	-	-	-		[6]

Table 2.4 - Continued

Bamboo species	Description	Testing method	Apparent density (g/cm^3)	$f_{t,0}$ (MPa)	$E_{t,0}$ (GPa)	$f_{c,0}$ (MPa)	$E_{c,0}$ (GPa)	MOR (MPa)	MOE (GPa)	f_v (MPa)	Source
D. asper	5-years old culm (MC=12%)	Shear = 15 x 20 x 20 mm (bottom part); 7 x 12 x 15 mm (top part) Tensile = Dumbbell-shaped - 2 x 4 x 80 mm (gauge portion) Bending = 15 x 15 x 230 mm (bottom part); 7 x 7 x 160 (top part)	0.69 - 0.92 (MC=12%)	165 - 290 (without node) 73 - 145 (with node)	-	-	-	140-258 (without node) 95-147 (with node)	13.2-26.0 (without node) 12.5-24.8 (with node)	12.3-14.2 (without node) 11.9-13.1 (with node)	[7]
D. asper	Unspecified age (MC=16-18.5%)	ISO 22157:2004	-	201 - 233	-	53.1 - 73.6	-	-	-	-	[8]
D. asper	Unspecified age	ISO 22157:2004 3 x 10 x 110 mm (Bending Test)	-	77	-	53.9	-	191	11.3	-	[9]

Where: MC (Moisture content), $f_{t,0}$ (Tensile strength parallel to the fibres), $E_{t,0}$ (Tensile modulus of elasticity), $f_{c,0}$ (Compressive strength parallel to the fibres), $E_{c,0}$ (Compressive modulus of elasticity), MOR (Modulus of rupture in bending), MOE (Modulus of elasticity in bending), $f_{v,0}$ (Shear strength parallel to the fibres) [1] = (YE; FU, 2018)*; [2]* = (DENG et al., 2016)*; [3]* = (DIXON et al., 2015)*; [4]* = (CHUNG; YU, 2002); *[5]* = (AKINBADE et al., 2019)*; [6]* = (KRAUSE et al., 2016)*; [7]* = (SRIVARO; JAKRANOD, 2016)*; [8]* = (AWALLUDDIN et al., 2017)*; [9]* = (OUNJAIJOM; MANEE-INTA; PUNYACUM, 2017)*;*

Source: Author's authorship

2.6. Bamboo degradation

The durability of bamboo is also a problem addressed in academia and is of great importance for the expansion of bamboo usage. The lack of toxic constituents in bamboo makes it a ready food source for xylophagous organisms compromising its structural integrity and durability (KUMAR et al., 1994). Without proper treatment, bamboo is decomposed and has a durability of 4 to 6 years in covered places and up to 15 years in regions with a not very humid climate (JANSSEN, 2000). However, in a short time, a decrease in mechanical strength is already observed, especially if attacked by insects. Therefore, its use is only recommended after a preservative treatment process that can guarantee long term protection. Regardless of treatment, load-carrying (i.e. structural) bamboo should never be placed in direct contact with soil or water and should be protected, to the extent possible, from intermittent wetting. In such environments, bamboo demonstrates little durability (KAMINSKI et al., 2016; ISO 22156-2019).

The main destroying agent of bamboo in the tropics is the insect *Dinoderus minutus*, also called Powderpost beetle. Its presence is confirmed by the presence of fine powder and the appearance of small holes in the dry bamboo. The palatability of bamboo to the insect is related to the amount of starch inside the parenchyma (WATANABE; YANASE; FUJII, 2015). The decay of bamboo by this insect and other xylophagous organisms, such as rotting fungi and termites, can severely affect its structural integrity and consequently compromise the useful life of structures (TIBURTINO et al., 2015a; BERALDO, 2016). The destructive effect of this insect and rotting fungi can be seen in Figure 2.12. The *D. minutus* only attacks dry bamboo (usually in untreated bamboo storages) reproducing itself inside bamboo's structure. This insect lays its eggs into the metaxylem vessels and passes through the larval, pupa and adult phases, as represented in Figure 2.13 (GARCIA; MORRELL, 2009).

Figure 2.12 - *D. asper* bamboo severely attacked by a) *Dinoderus minutus* insect and b) fungi decay in exposed material.

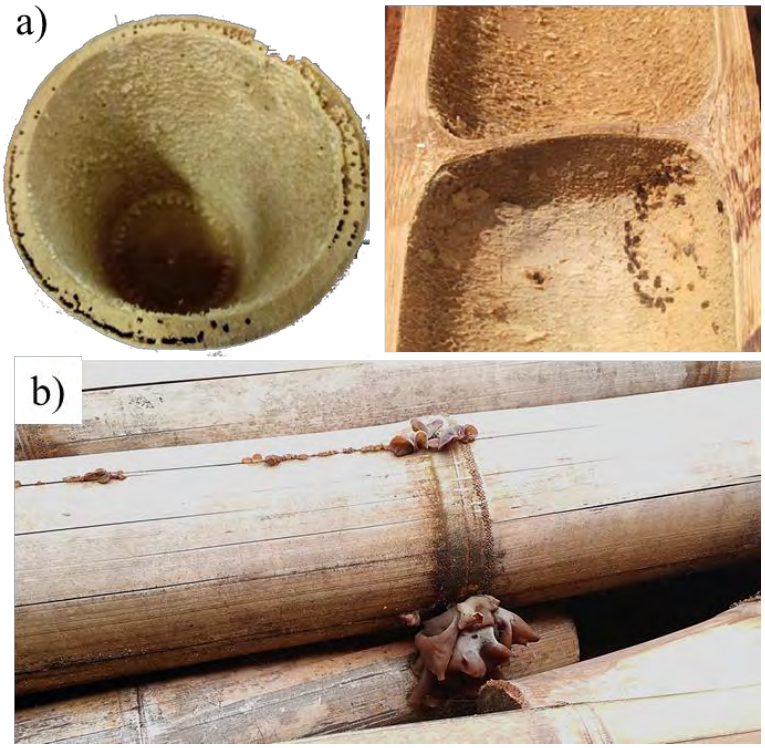

Source: Author's personal records

Figure 2.13 - The life stages of *D. minutus*. a) eggs deposited into a vessel, b) larval development, c) pupa, and d) adults.

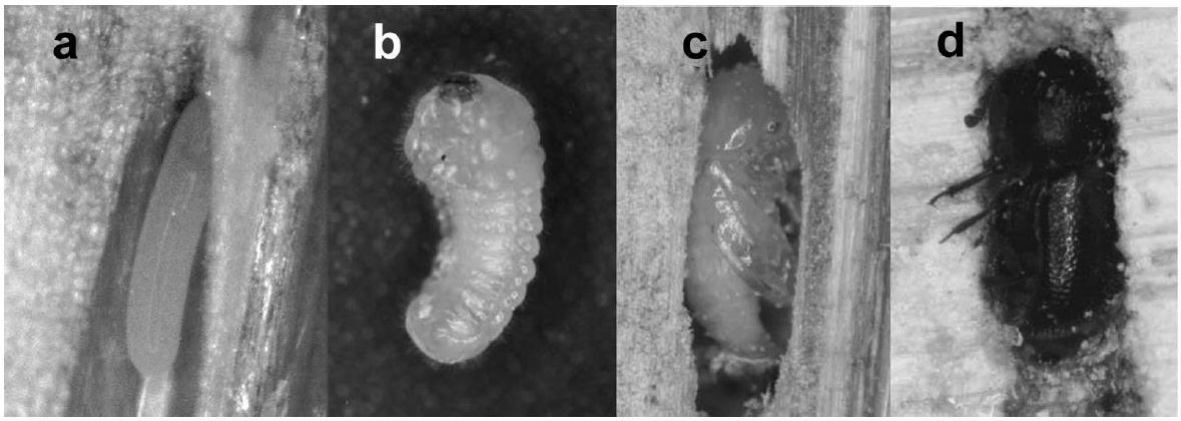

Source: (GARCIA; MORRELL, 2009)

Another important aspect to be investigated and of great relevance to the application of building materials is fire behaviour. Most flammability studies have been conducted with wood. Regarding bamboo, few works are reported: (SHARMA; CHARIAR; PRASAD, 2015); (SHARMA et al., 2015b); (MENA et al., 2012). With proper preservative treatment, the combustion resistance of wood or bamboo can be increased in the presence of a flame. Boron-based treatments, besides being effective against biological degradation, have the advantage of also acting as flame retardants (BAYSAL et al., 2007; LEVAN; JERROLD. E., 2007; CALDEIRA, 2010; TONDI et al., 2012b; SHARMA et al., 2015b).

Other sources of degradation may occur during the service life of bamboo. UV-light degradation and excessive moisture variation lead to chemical degradation, discolouration and cracks (ZHUANG et al., 2018), weakening its strength and increasing rotting fungi attack, as seen in Figure 2.11b (SCHMIDT et al., 2011).

Wei, Schmidt and Liese (2013a) evaluated five different bamboo species (*Bambusa maculata, Dendrocalamus asper, Gigantochloa atroviolacea, Guadua angustifolia, and Phyllostachys pubescens*) for degradation by different rotten fungi; brown-rot (cellulose degradation), white-rot (lignin and hemicellulose degradation), and soft-rot (cellulose degradation). The tests were conducted based on the European standards EN-350-1 (1996), EN 350-2 (1997), and EN113 (1996) for 16 weeks in a conditioned environment. Their results show that all the bamboo species presented considerable resistance to the brown-rot fungi *Coniophora puteana* and *Gloeophyllum trabeum*, white-rot fungi *Schizophyllum commune*, and soft-rot fungi *Paecilomyces variotti*, being classified as Class II (durable). However, the bamboo samples were classified as Class II and III (moderately durable) when decayed by the soft-rot fungi *Chaetomium globosum* and Class III and IV (slightly durable) when decayed by the white-rot fungi *Trametes versicolor* (WEI; SCHMIDT; LIESE, 2013). Suprapti (2011) also reported Classes between II (durable) and V (not durable) for five Indonesian bamboos decayed by different brown-rot, white-rot and soft-rot fungi (SUPRAPTI, 2010).

2.7. Conventional treatment of bamboo

2.7.1. Traditional and nonchemical methods

Traditional nonchemical treatment methods such as clump curing, water soaking and fire treatments provide increased bamboo durability (ESPELHO; BERALDO, 2008). Although the effect of these treatments is limited, they are advised in situations where handling of toxic materials and chemicals can be a problem, especially in rural areas (LIESE, 2004).

The moon phases are an important aspect for bamboo harvesting in popular beliefs. The durability of the bamboo culms is believed to be influenced by different moon phases, which may alter the amount of starch on the above the ground part of bamboo. Although difficult to test, some works prove that there is no considerable influence of the moon on bamboo durability. Other factors such as harvesting season and culm maturity are more important for the quality of the culm (SARLO, 2000; HIDALDO-LÓPES, 2003).

The clump curing method, also called "*avinagrado*" in South America, is a useful traditional method for bamboo treatment. In this method, bamboo culms are cut and left in an upright position with the branches and leaves, normally supported by the clump, on the top of a brick or stone. The culms are then left in this position for up to two weeks to let the bamboo to dry slowly and consume and ferment part of the available starch. The name *avinagrado (vinegared)* is used because of the strong sour smell that is released during curing (HIDALDO-LÓPES, 2003). This process reduces the attractivity of the bamboo by borers but causes no effect on the attack by termites and fungi (LIESE; TANG, 2015b).

Water-soaking or waterlogging is a traditional method in many Asian countries, especially in places where bamboo is harvested close to water streams (LIESE; TANG, 2015b). Fresh bamboo culms are immersed in stagnant or running water for 1-3 months to leach and ferment starch, carbohydrates and other water-soluble substances (KAUR et al., 2016). This process also improves the bamboo resistance against borers and fungi for some extent but still does not guarantee long term protection (LIESE; TANG, 2015b; KAUR et al., 2016).

Other methods such as fumigation (or smoke) and fire treatments are also commonly used to improve bamboo durability, especially for handicraft and furniture use. However, investigations point out that smoke treated bamboo has similar behaviour of water-treated materials, and are non-durable in the long term and under field conditions (KAUR et al., 2016).

2.7.2. Chemical treatment methods

Chemical treatments are the most used and efficient methods to protect wood and bamboo. In applications where long-term durability and safety are key issues, as for building applications, chemical treatments are mandatory. There are a broad range of possible chemicals available in the market and advised by wood/bamboo standards. Their use will depend on the application, toxicity, and treatment method.

Table 2.5 gives a list of possible compounds that can be used for bamboo (KAUR et al., 2016). Kumar et al. (1994) and the Indian standards IS 1902:2006 and IS 9096:2006 also recommend the use of these chemicals. These solutions can be classified in waterborne and oily preservatives c.

The waterborne types, such as chromated copper arsianate (CCA), chromated copper borate (CCB), and disodium octaborate tetrahydrate (DOT), are composed of inorganic or organic salts, or even oxides, that can be diluted in water and applied by pressure/diffusion and other methods (to be discussed below). These preservatives are effective, cheap and accessible, and are widely applied for bamboo treatment.

Waterborne preservatives can be further divided into fixing and non-fixing types. The fixing preservatives are resistant to leaching and are recommended for exposed conditions, in contact with the ground or underwater. CCA and CCB are the main fixing preservatives used nowadays. Upon treatment, there are chemical reactions forming complexes based on chromium that fix within the bamboo/wood structure. Although these chemicals increase the service life of bamboo and wood considerably, they are based on highly toxic chemicals and can cause environmental problems. The non-fixing preservatives are normally composed of leachable salts, such as boron-based (DOT, boric acid, borax) and zinc chloride/copper sulphate preservatives, and are recommended for applications where the material does not have direct contact to the ground or exposed to the weather. They can provide good penetration due to the high diffusion of ions after penetrating in the bamboo vessels.

Oily preservatives, composed of tar products such as creosote, have been extensively used in wood since ancient times. This preservative is exclusively used by pressure and hot and cold treatment methods. Although not usually used in commercial treated bamboo, it is very effective against a wide range of rotting fungi, insects and at high retention levels, provides

long-term durability. However, its use is restricted to exterior applications due to strong odour and toxicity (LIESE; TANG, 2015b).

Table 2.5 - Commercial preservatives used for wood/bamboo treatment. * CCB in an oxide composition is also available.

Compound	Formula	Average life	Advantages	Disadvantages
Disodium octaborate tetrahydrate (DOT)	$Na_2B_8O_{13}.4H_2O$	NA	Self-diffusing, effective against fungi, insects, and termites	Highly leachable, not suitable for outdoor application
CCA (copper, chromium, arsenic)	47.5% CrO_3, 18.5% CuO, and 34% As_2O_5	NA	Fixable, broad spectrum biocide	Contains harmful chromium and arsenic
Bis-tri-butyl tin oxide (TBTO)	$[(CH_3CH_2CH_2CH_2)_3Sn]_2O$	NA	Difficult to leach	Toxic
Creosote	By-product of coal manufacture	24.9 years	Good use of an otherwise undesirable product	Oil-soluble and expensive
Zinc chloride / Copper sulphate	$ZnCl_2$/ $CuSO_4$	NA	Hydroscopic, good fungicide, can retard fire as well	Not effective in outdoor applications, ineffective for termites and insects
Sodium pentachlorophenate	$C_6C_{l5}ONa$	15.9 years	Effective fungicide	Banned in many countries because of presence of PCP
CCB * (copper, chromium, boron)	$CuSO_4$:$K_2Cr_2O_7$:H_3BO_3 (3:4:1.5)	NA	Fungicide, insecticide	Low fixation, presence of chromium
Ammonical-Copper-Arsenate(ACA)	$CuSO_4$:As_2O_3 (3:1) in ammonia	NA	High fixation	Presence of arsenic makes it toxic
Bis-(N-cyclohexyl-diazeniumdioxide)-copper(Cu-HDO)	$C_{12}H_{22}N_4O_4Cu$	NA	Good fungicide, insecticide	Expensive, toxic to aquatic organisms
Copper Naphthenate	$2(C_{11}H_7O_2).Cu$	29.6 years	Effective against insects and fungi	Should be used with superficial treatment
3-Iodo-2-propynyl butylcarbamate-(IPBC)	$CH_3(CH_2)_3NHCO_2CH_2C{\equiv}Cl$	NA	Fungicide	Not an effective insecticide

Source (Table organization): (KAUR et al., 2016); Source (information): (LIESE; KUMAR, 2003; EVANS et al., 2007).

The methods for chemical treatment of bamboo can be classified in non-pressure and pressure methods. A complete description of all the possibilities for bamboo treatment is presented in (KUMAR et al., 1994; LIESE; TANG, 2015b).

The non-pressure treatments are recommended to be used with waterborne preservatives and can be applied by different methods as follow (commonly used ones):

- Sap displacement: Round freshly harvested poles (up to 3 m long) are immersed vertically (butt end) at least 25 cm in waterborne preservatives (Figure 2.14). The solution rises with the sap displacement. For good penetration, the poles should be turned over after 7 days and immersed for more 7 days. Although useful in some situations, this method is not used in commercial-scale production (KUMAR et al., 1994).

Figure 2.14 – Example of sap displacement treatment method of green bamboo.

Source: Unknown author.

- Diffusion/immersion/soaking: This is one of the most used methods for bamboo treatment in Asia and South America because of its simplicity and productivity. As-harvested bamboo poles with high moisture content (above 50%) are submerged in waterborne preservatives for 10-20 days to guarantee diffusion of the active ingredients. The immersion time, however, depends on the solutions concentrations, species and other factors, varying from 6 to 20 days, depending on the producer. Making holes near or through the nodes is necessary to guarantee total penetration and good retention levels. The main steps for the immersion treatment are presented in Figure 2.15. By increasing the temperature of the preservative solution, the diffusion rate can be increased. Chromium-based preservatives, however, precipitate upon heating and should be used at room temperatures. Dry bamboos can also be treated by this method (soaking), but the penetration is then predominantly by capillarity, although diffusion process still occurs (KUMAR et al., 1994; LIESE; TANG, 2015b).

Figure 2.15 – Procedure used for bamboo treatment by the immersion method. a) Perforation of the nodes; b) cleaning of bamboo culms; c) treatment tank with submerged culms.

(A) **(B)** **(C)**

Source: (MARÇAL, 2018).

- Vertical soak diffusion: This method, also called the Vietnamese method, works in the same way of the diffusion/soaking process. First, the diaphragms of the nodes of fresh bamboo poles are ruptured along the length (leaving the last node without breaking). Then, the poles are stand in an upright position, and the inner part of the bamboo is filled with a waterborne solution (around 10% depending on the preservative), working as a reservoir for the diffusion process

(Figure 2.16). Boron-preservatives are commonly used for this method (LIESE, 2004; LIESE; TANG, 2015b).

Figure 2.16 – Illustration of the setup used for the vertical soak diffusion method.

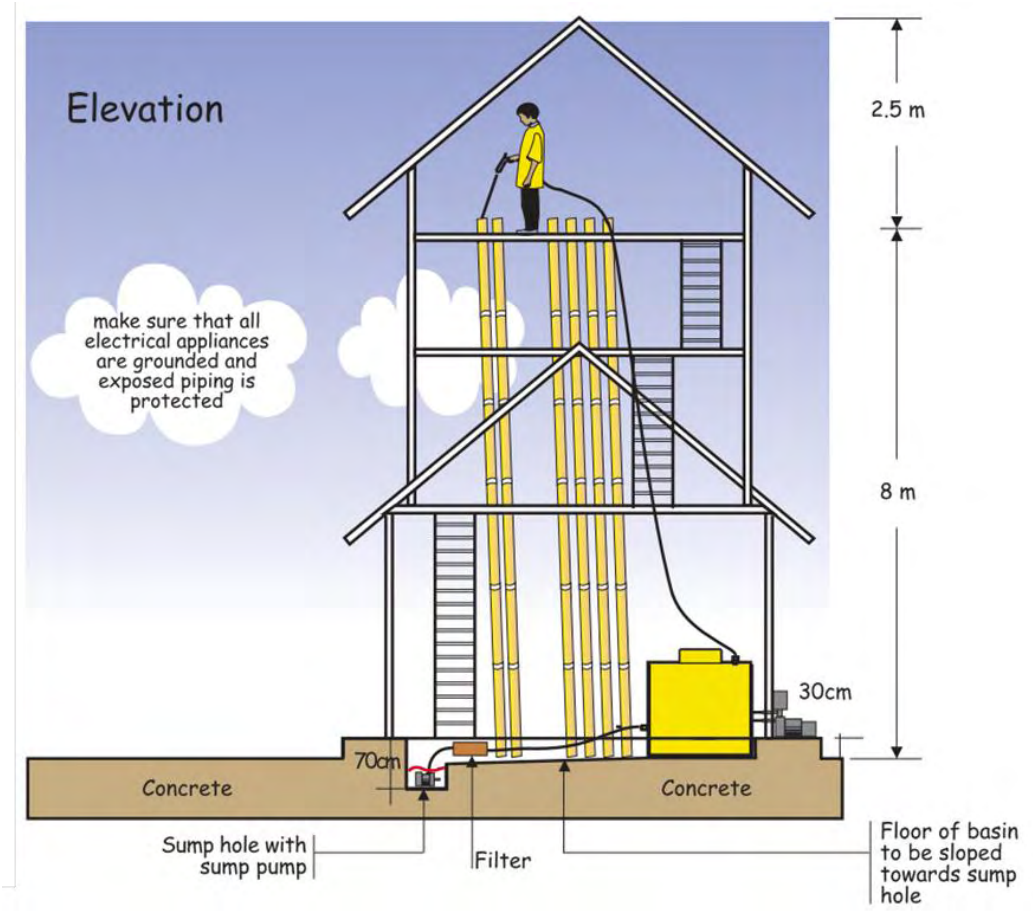

Source: (EBF, 2003)

Pressure methods can be an alternative when productivity is a key issue. Although costly equipment is necessary, these methods are effective and are the main treatment method for wood. Basically, two processes can be used for bamboo:

- Modified Boucherie process: Unlike other pressure methods, the Boucherie process requires the use of freshly cut bamboo. In this method, the preservative solution is pressurized in a container (by using a manual air pump or compressed air) and using hoses and hydraulic connections, the solution is pushed into the butt end of the pole (Figure 2.17). Using pressures

of up to 2 kg/cm^2, it takes 30-60 min, depending on the pole length, for the solution start dripping on the other end of the pole. The use of freshly cut bamboo is a critical aspect of this method. In the first hours after cutting, the permeability of the bamboo vessels starts to decrease considerably and affect the preservative penetration. Although it is a reliable and efficient method, it is labour intensive, and the wide range of bamboo sizes can be a problem for the necessary connections (KUMAR et al., 1994; LIESE, 2004).

Figure 2.17 – a) Sap replacement of green bamboo by the modified Boucherie method. b) Preservative solution dripping from the culm end.

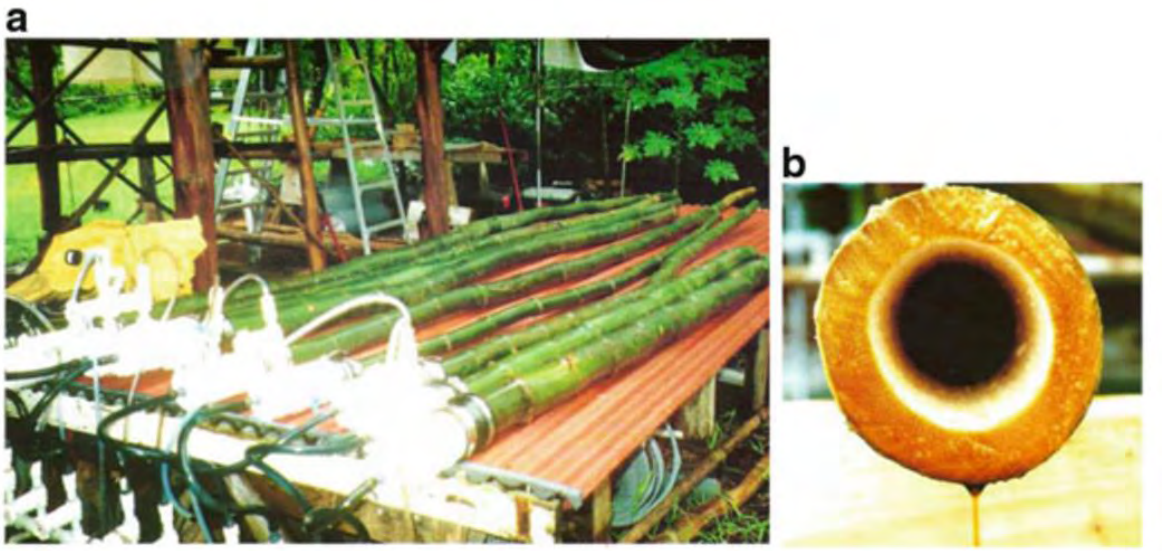

Source: (LIESE; TANG, 2015b)

- Vacuum/pressure treatment: For this method, air-dried half split or bamboo poles (moisture content below 30%) are necessary. Similar procedure used for wood can be applied for bamboo. In the full-cell process, the material to be treated is allocated in a pressure vessel and submitted to three processing stages (Figure 2.18). First, vacuum is applied to remove the air from bamboo/wood cavities, leaving available space for the preservatives. Then the preservative solution is pumped into the pressure vessel, and a positive pressure is applied. After the pressure phase, the solution is pumped back to a storage tank, and a final vacuum phase is applied to remove excess solution within the bamboo/wood structure. When round bamboo poles are treated, holes close to the nodes or throughout the pole length are necessary to prevent collapse

(due to vacuum and pressure) and increase solution absorption. Oily and waterborne preservatives can be used in this method. For bamboo, an initial vacuum of 500-600 mmHg for 30 min, pressure of 10-12 kgf/cm² for 60-90 min. and final vacuum of 500-600 mmHg for 10-15 min. are recommended, in the case of CCA and CCB preservatives (most commonly used in the full-cell process). However, treatment parameters depend on bamboo species, preservative type and concentration should be defined whenever necessary (LEPAGE, 2008; LIESE; TANG, 2015b; LEPAGE; DE SALIS; GUEDES, 2017).

Figure 2.18 – Pressure vessel used for vacuum/pressure treatment of dry bamboo.

Source: Unknown author.

Although there are available documents recommending retention levels according to the application of treated bamboo (Indian Standards IS 1902:2006 and IS 9096:2006), there is a lack of reliable information regarding experimental results of bamboo treatment procedures. After extensive research on the open literature, few papers were found addressing results of retention levels of treated bamboo. Table 2.6 gives a summary of these papers. Only works that used chemical analysis for retention calculation were considered.

Several factors may affect treatability: species, position in relation to the culm height, active ingredients, treatment method, and moisture content. From the results of Table 2.6, it is possible to observe a wide range of retention values. In general, pressure methods provide greater retention values. However, in comparison to wood, bamboo can be more difficult to absorb preservative solutions using the same commercial full-cell process (LEE; CHEN; TAINTER, 2001). Interestingly, higher retention values are normally reported on the top part of the bamboo culm, followed by the middle and bottom parts. Although the bottom part of bamboo present lower density, and hence higher porosity, there are proportionally more metaxylem vessels (with a higher amount of fibre bundles surrounding them) in the top part of the bamboo culm (WAHAB et al., 2015). Another important aspect is that the vacuum/pressure methods in general present higher retention levels than other passive methods, such as immersion and sap displacement. The retention levels are directly dependent on the solution concentration and sensitive to the pressure and time used for treatment (KIM; TANG; LIESE, 2011).

Table 2.6 - Summary with treatment methods, preservatives and corresponding retention values from the literature.

Source	Bamboo species	Treatment method	Active ingredient (a.i)	Retention of a.i. (kg/m^3)	Obser vation
[1]	*T. siamensis*	Full-cell process: vaccum (670 mmHg for 30 min) + pressure (2.5-8.5 bar for 60-120 min) + final vaccum (650 mmHg for 15 min)	6% BB - Borax/Boric acid (1.5:1) 6% CCB (salt composition)	BB: 3.7 - 15.5 CCB: 3.9 - 17.5	Samples of the middle and bottom parts of the culms were tested in two different moisture content range (30-40% and 15-20%)
	B. stenostachya			BB: 3.1 - 13.8 CCB: 3.5 - 15.9	
	D. asper			BB: 2.7 - 11.9 CCB: 3.4 - 14.4	
[2]	*D. giganteus*	Immersion/soaking for 5-15 days	1% CCB 3% CCB (oxide based)	1%: 0.60 - 1.43 3%: 0.63 - 1.72	No information regarding moisture content and positions of the samples.
	B. vulgaris			1%: 0.68 - 2.20 3%: 1.93 - 10.80	
	D. giganteus	Modified boucherie (pressure of 0.7 MPa)	1% CCB 3% CCB (oxide based)	1%: 0.28 3%: 1.40	
	B. vulgaris			1%: 0.84 3%: 2.14	
[3]	*B. vulgaris*	Full-cell process: vaccum (600 mmHg for 30 min) + pressure (12 kg/cm^2 for 120 min) + final vaccum (600 mmHg for 30 min)	2-4% ACQ - Amoniacal copper-quaternary 2-4% BB 2-4% CCA	ACQ: 4.33 - 10.74 BB: 4.2 - 10.58 CCA: 4.87 - 14.54	Samples from the bottom, middle and top parts of culms with 2 and 4 years old
[4]	*D. giganteus*	Sap displacement for 5-15 days	1% CCB 3% CCB (oxide based)	1%: 0.81 - 3.20 3%: 1.48-19.44	Culms with unbroken and broken nodes were tested
	B. vulgaris			1%: 1.00 - 5.64 3%: 4.21 - 10.52	
[5]	*P. edulis*	Full-cell process - commercial (no treatment schedule provided)	CCA-4 (target of 4.0 kg/m^3) CCA-6.4 (target of 6.4 kg/m^3)	4: 0.88 6.4: 1.49	Splitted bamboo was used. As reference southern pine had rententions of 4: 4.61 and 6.4: 7.12 kg/m^3

- Only chemical analyses for the retention were considered [1] = (KIM; TANG; LIESE, 2011); [2] = (TIBURTINO et al., 2015b); [3] = (WAHAB et al., 2015); [4] = (TIBURTINO et al., 2016); [5] = (LEE; CHEN; TAINTER, 2001)

Source: Author's authorship

The usual treatments used in Brazil for structural and nonstructural wood are based on commercial solutions of CCA and CCB applied under pressure (VIDAL et al., 2015). However, although effective, they present high toxicity due to the presence of chromium and/or arsenic salts, which represents environmental and health risks to the workers involved in its production, use and disposal. The use of low-cost, water-soluble, and low mammalian toxicity compounds such as boron-based salts (DOT, boric acid and borax) is an interesting and advised alternative for the treatment of bamboo and wood (CALDEIRA, 2010).

Bamboo treated with boric acid and borax solutions may exhibit degradation resistance compatible with CCB treated bamboo in some specific applications (ESPELHO, 2007; ESPELHO; BERALDO, 2008). Boron-based salts are commonly used in agriculture as foliar fertilizers and being properly conditioned and diluted do not impact their disposal. Without the presence of a fixative, however, boron salts can be leached if exposed to external adversities or in contact with the ground (OBANDA; SHUPE; BARNES, 2008; FREEMAN; MCINTYRE; JACKSON, 2009). Therefore, although not limiting the use of bamboo in structural applications, it is necessary a waterproof coating when used in exposed conditions and, more importantly, protect the bamboo by the design of the building, as a famous Colombian phrase "*buen sombrero y buenas botas*" ("good hat and good boots", meaning a long eave and high columns).

2.8. Alternative chemical treatments for wood and bamboo

Organic compounds such as natural extracts and pyroligneous acid may also be used to promote increased durability of wood/bamboo, but few studies are reported evaluating the effectiveness of these treatments (MATSUOKA, 2011; GONZÁLEZ-LAREDO et al., 2015). Organic acids associated with inorganic salts have also been used to protect bamboo against fungi degradation showing promising results (TANG; SCHMIDT; LIESE, 2012).

Other treatments based on chemical modification were also developed for wood to improve resistance to biological degradation, dimensional stability and hydrophobicity (ROWELL, 2007; SANDBERG; KUTNAR; MANTANIS, 2017). The in-situ polymerization of organic networks within wood/bamboo structure has also been explored to improve degradation resistance and physical-mechanical properties (THÉVENON; TONDI; PIZZI, 2010; ORTIZ, 2015; GÉRARDIN, 2016).

The chemical modification is based on the addition of organic chemicals to hydroxyl groups of the wood components. The bulking of the cell walls and the reduction of available hydroxyl groups reduce the moisture uptake, water absorption considerably and increase dimensional stability. The reaction of wood with chemicals such as anhydrides, isocyanates, carboxylic acids, acid chlorides, and others can result in anti-swelling efficiencies (ASE) of up to 75% (reduction of swelling in comparison to untreated wood) at weight gains between 20-30% after the modification (IBACH, 2010). The chemically modified wood also presents improved resistance to decay fungi, termites, and marine organisms (SANDBERG; KUTNAR; MANTANIS, 2017). Wood acetylation, for example, has been known for many years and is already an industrial-scale process for the production of acetylated wood (HOMAN; JORISSEN, 2004; GÉRARDIN, 2016). In this process, acetic anhydride is used to substitute the wood hydroxyl groups by carbonyl groups through an industrial closed system reaction, as shown in Figure 2.19.

Figure 2.19 - Acetylation process of wood using acetic anhydride.

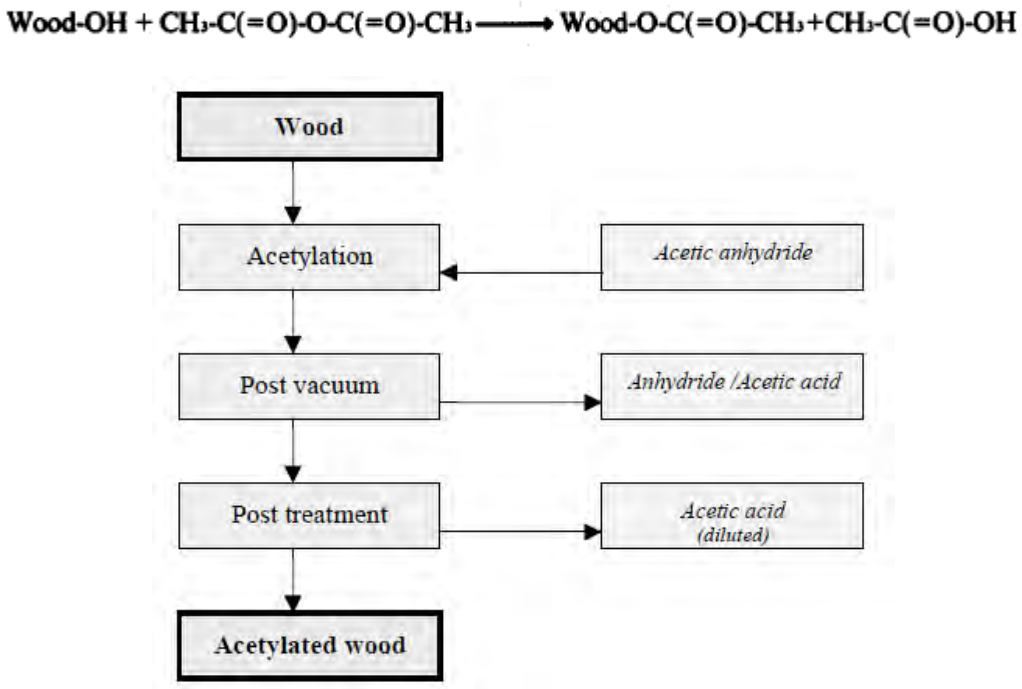

Source: (HOMAN; JORISSEN, 2004)

As in the acetylation process, an esterification process using citric acid as the main solution can chemically modify the wood or other lignocellulosic materials. Citric acid has been used as a binder of particle boards and for the esterification of hydroxyl groups from wood after thermal treatment between 100 ºC and 140ºC, as shown in the reaction of Figure 2.20 (DESPOT; HASAN; JUG, 2008; ŠEFC et al., 2009a; ROMAINOR et al., 2014; WIDYORINI et al., 2014; ESSOUA et al., 2016). This treatment presented interesting results in relation to the effectiveness in the wood chemical modification and had the advantage of relying on low cost and widely available products. The chemical modification with citric acid can result in a considerable decrease of water absorption, swelling and can be used for protection against rotten fungi (DESPOT; HASAN; JUG, 2008; ŠEFC et al., 2009a, 2012). Additionally, according to Feng and collaborators, it was possible to observe that it is not necessary the use of the catalyst sodium hypophosphite for the reaction between wood and citric acid (FENG et al., 2014).

Figure 2.20 - Esterification reaction of cellulose with citric acid.

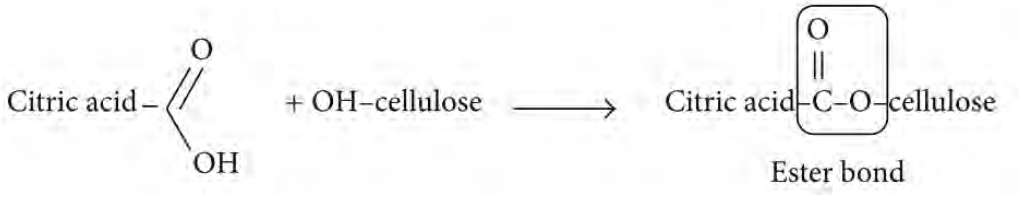

Source: (ROMAINOR et al., 2014).

The use of boron compounds for wood treatment has been widely used for use in situations without direct contact with soil and for indoor environments mainly in the US and Europe, where the use of CCA and other toxic products is prohibited in some applications. However, due to the limited application in outdoor environments and consequent boron leaching, several efforts have been made to develop solutions for the fixation of boron in wood, such as surface treatments, heat treatments, the use of organo borates, chemical modification, in situ polymerization among others (OBANDA; SHUPE; BARNES, 2008). Literature about boron fixation for bamboo treatment is scarce or inexistent. However, research with wood shows that the polymerization of tannin-based solutions in combination with boric acid, for example, results in decreased boron leaching, besides decreasing the flammability and improving degradation resistance of wood (THEVENON; TONDI; PIZZI, 2009; TONDI et al., 2012b).

Tannins are very abundant compounds found in most part of the biomass. These compounds, naturally biosynthesized by plants, are primarily concentrated in tree barks for protection against external adversities. Tannins have a complex chemical structure, composed of heterogeneous polyphenolic molecules with molar weights from 300 g/mol in simple phenolic compounds to over 3000 g/mol in highly polymerized structures (BRAGHIROLI et al., 2019). The condensed tannins (polymerized tannin) are hydroxylated aromatic polymers composed of flavonoid monomers units and are natural preservatives and anti-fungal agents (LAKS et al., 1988). The flavonoid units found in most parts of tannins, prorobinetinidin, prodelphinidin, profisetinidin, and procyanadin are presented in Figure 2.21. Tannin extracts are extensively used for wood adhesives and are industrially produced from various tree sources: Acacia (wattle or mimosa bark extract), Pinus (bark extract), Schinopsis (quebracho wood extract), Tsuga (hemlock bark extract), and Rhus (sumach extract) species (PIZZI, 2006).

Figure 2.21 - Flavanoid units found in condensed tannins.

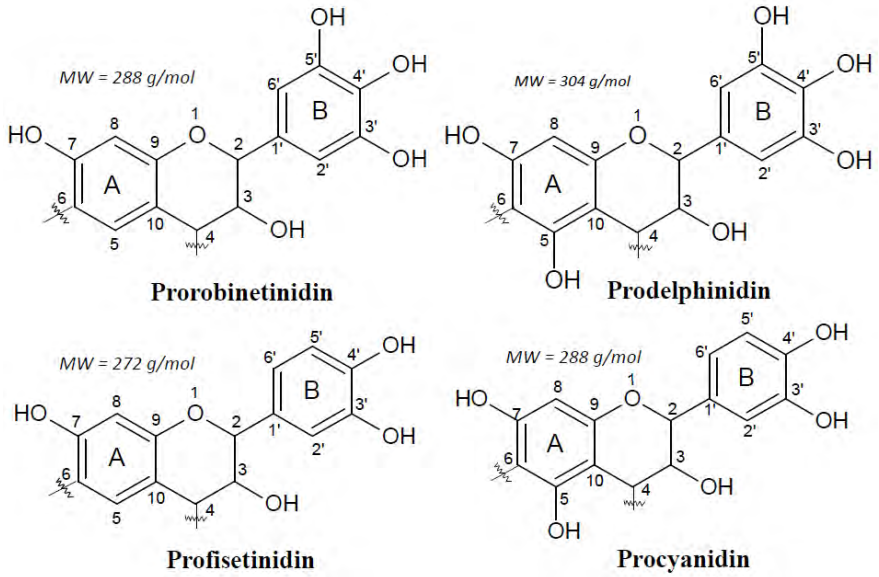

Source: (BRAGHIROLI et al., 2019)

The use of cross-linking agents, such as formalin and hexamine, in combination with tannin extracts, can produce stable polymerized products. These types of formulations have a wide range of applications, especially as wood adhesives, decreasing the use of oil-based resins and, in the case of hexamine-based formulations, considerably reducing formaldehyde emissions (PIZZI, 2006). These systems can also be used for wood treatment. This procedure is based on impregnating the wood with a tannin-hexamine extract solution with the addition of boric acid as a source of boron. Tannin in combination with hexamine polymerizes in situ in wood through thermal activation, mobilizing the available hydroxyl groups. In the work of Thévenon et al., 2010, wood treated by this method met the requirements of EN113 (degradation in tropical conditions). According to Pizzi (1996), tannin can also undergo a polycondensation process in the presence of wood and boric acid and thus does not require a curing agent such as hexamine, making the treatment process simpler and less expensive, in which can be useful in some situations (PIZZI; BAECKER, 1996). One of the great advantages of using this treatment system is the availability and price of tannin extract, which can be easily found on a commercial scale, especially in Brazil.

3. CHAPTER 3 – Assessment of conventionally treated bamboo

In this Chapter, the treatability behaviour and detailed mechanical characterization of bamboo treated with DOT and CCB were explored. This chapter was divided into three main parts for better clarity and understanding of the results.

First, some considerations about the use of DOT, its chemical composition and its effect on the mechanical properties of *D. asper* bamboo was explored. Second, comments and a description of bamboo treatment through the immersion method was assessed, showing methods for the evaluation of treatability of bamboo culms. Procedures commonly used for preservative-treated wood are still not used for bamboo quality control, and therefore, this part is dedicated to the application of these methods for bamboo evaluation. A small production batch of DOT-treated *P. edulis* bamboo poles was quality assessed and compared to CCB-treated bamboo poles in terms of mechanical performance. Finally, additional analyses related to the mechanical characterization of *P. edulis* bamboo using DIC method and considerations regarding the use of ISO 22157 Standard were scrutinized. Additional results and considerations about treatment by the immersion method are presented at the end of this chapter as useful and complementary information.

The following published/submitted papers are related to this Chapter:

GAUSS, C.; KADIVAR, M.; SAVASTANO JR, H. Effect of disodium octaborate tetrahydrate on the mechanical properties of *Dendrocalamus asper* bamboo treated by vacuum/pressure method. Journal of Wood Science, v. 65, n. 27, 2019.

GAUSS, C.; SAVASTANO, H.; HARRIES, K. A. Use of ISO 22157 mechanical test methods and the characterisation of Brazilian *P. edulis* bamboo. Construction and Building Materials, v. 228, p. 116728, 2019.

GAUSS, C.; HARRIES, K. A.; KADIVAR, M.; AKINBADE, Y. A.; SAVASTANO, H.; Quality assessment and mechanical characterization of preservative-treated Moso bamboo (*P. edulis*). European Journal of Wood and Wood Products, v. 78, p. 257-270, 2020.

3.1. Effect of disodium octaborate tetrahydrate on the mechanical properties of *Dendrocalamus asper* bamboo treated by vacuum/pressure method

3.1.1. Introduction

Developing and using low embodied carbon building materials and services, at the life cycle perspective, is identified as one of the main pivotal opportunities to reduce the carbon emissions of the construction sector (HUANG et al., 2018). The construction industry requires heavy investment and produces intensive pollutions (YAN et al., 2017), and accounts for around 36% of worldwide CO_2 emissions (CHAU et al., 2012). Bio-based construction materials have the advantage of being not only renewable but also having a significant contribution to carbon sequestration during their growth (VOGTLÄNDER; VAN DER VELDEN; VAN DER LUGT, 2014; YUEN; FUNG; ZIEGLER, 2017), as well as carbon storage during their use phase (ESCAMILLA; HABERT, 2014).

Life cycle assessment studies of bamboo based-construction materials clearly showed the potential of bamboo for use in the construction sector (VOGTLÄNDER; VAN DER LUGT; BREZET, 2010; YU; TAN; RUAN, 2011; CHANG et al., 2018; ESCAMILLA et al., 2018). In these studies, transportation is an important issue to a product such as bamboo culm which has a high volume per mass. There is a large environmental impact of transferring such raw materials from its origin to site of construction and this, therefore, makes the use of local materials (local bamboo species) indisputable in the industrial and construction sectors.

The excellent physical and mechanical properties of bamboo have led to its empirical use in construction and have attracted the attention of several researchers to start the process of rediscovering bamboo recently (CORREAL, 2016). Even for modern buildings, bamboo has been widely employed to fabricate mechanical elements and structures (GUO et al., 2013; SHARMA et al., 2015a).

However, bamboo properties are directly related to the species, age, moisture content, soil, harvest season, culm geometry among other factors (GHAVAMI; MARINHO, 2005). The mechanical strength of *D. asper*, a species which has been used in this research, in compression, tension and bending is reported to be 53 to 95 MPa, 73 to 326 MPa and 95 to 258 MPa,

respectively, depending on the presence or not of the node and the position in relation to the culm height (KRAUSE et al., 2016; SRIVARO; JAKRANOD, 2016; AWALLUDDIN et al., 2017; CHAOWANA; BARBU, 2017; OUNJAIJOM; MANEE-INTA; PUNYACUM, 2017).

These mechanical properties are medium to higher than those of other species of *Dendrocalamus* genera, *Guadua* and *Bambusa* (GHAVAMI, 2005; GEROTO, 2014). Along with mechanical strength adequate to the requirements of different applications, a building material should have an acceptable lifespan. The durability of untreated bamboo varies based on the species, age, and conservation actions taken, and it is strongly related to the bamboo chemical composition (GHAVAMI, 2008; LIESE; TANG, 2015b; CHAOWANA; BARBU, 2017). In an open environment, and in the contact with soil, bamboo is estimated to last 1 to 3 years; 4 to 6 years if undercover and free from soil contact (JANSSEN, 2000; JAYANETTI; FOLLETT, 2008). Only under very favourable use conditions such as internal framing, is untreated bamboo estimated to last around 15 years (CORREAL, 2016) which is not sufficient as a construction material.

The powderpost beetle (*Dinoderus minutus*) which is the main destructive agent of bamboo (WATANABE; YANASE; FUJII, 2015), and other xylophagous organisms, such as decay fungi and termites, can seriously affect its structural integrity and consequently compromise the service life of the resulting structures or constructive systems (JAYANETTI; FOLLETT, 2008; TIBURTINO et al., 2015a). Additionally, flammability, the volume variation due to water absorption and the susceptibility to chemical degradation are other problems that hinder their use in some applications (HARRIES; SHARMA; RICHARD, 2012; XU et al., 2018). Therefore, an adequate preservative treatment of bamboo is necessary so that it can be safely used as a structural element. There are several treating methods to improve the durability and preserve bamboo materials; but some methods which use thermal and natural products like vegetable oils (palm, sunflower, or soybean) have been proved to decrease the mechanical properties of bamboo (WAHAB et al., 2005; SULAIMAN et al., 2006; LI et al., 2015a). Wahab et al. (2005) studied tropical bamboo treated in palm oil at 140, 180, and 220 °C, during 30, 60, and 90 min. The results showed that the treatment decreased the mechanical properties (bending, compressive, and shear strengths). When the treatment duration increases, the mechanical strengths could decrease by 15-58% from the initial strength, depending on each treatment procedure and each mechanical property (BUI; GRILLET; TRAN, 2017). On the other hand,

some treatments lead to colour changes (NGUYEN et al., 2012; LEE et al., 2018a) which is an undesirable effect (BUI; GRILLET; TRAN, 2017).

Since ancient times, chemical methods have been used for wood and bamboo preservation and whilst nonchemical methods have also been used, the chemical methods are considered as more appropriate for bamboo preservation in large-scale building projects (CORREAL, 2016). There are a lot of chemical materials that have been used to preserve wood and bamboo against water, insect and fungal attack and as a fire retardant. However, the use of some chemical preservatives is ambivalent. For example, conventional wood treatment solutions used in Brazil have good performance but are normally based on heavy metals and other toxic elements, such as CCA (Chromated Copper Arsenate) and pentachlorophenol in which have an impact on animals and plants.

Among the various substances and their mixtures that have been suggested, investigated, and commercialized, the use of low-cost soluble salts, such as boron-based salts specifically disodium octaborate tetrahydrate (DOT), boric acid and borax, are interesting alternatives for the treatment of bamboo and wood (CALDEIRA, 2010; KIM; TANG; LIESE, 2011; LIESE; TANG, 2015b; TIBURTINO et al., 2015a). Boron compounds are some of the most effective and versatile preservatives solutions used nowadays since they combine the broad-spectrum efficacy, low mammalian toxicity, odourless, colourless and fire-retardant properties (TONDI et al., 2012a; DONMEZ CAVDAR; MENGELOĞLU; KARAKUS, 2015; JIT KAUR, 2018; ZHOU et al., 2018). The preservation method with boron compounds can be even a way to improve the quality of bamboo, increasing the tensile strength in comparison with bamboo without preservatives (PRININDYA; ARDIANSYAH, 2014; SULAEMAN et al., 2017).

Bamboo requires essential preservation treatment before its utilization as a structural material to ensure the durability of a building. Although chemical treatment is considered a commonly used treatment procedure in the construction industry, it might damage the material mechanically. Therefore, the influence of chemical treatments in the mechanical properties of those building materials must be known. It is worth mentioning that most parts of the structural projects using bamboo in Latin America and Asia use boron compounds (boric acid, borax or DOT) as the main preservative and therefore, studies about treatability, mechanical performance and durability are necessary. In spite of the high use of DOT, which is an active component in Bora-Care® and is an available popular commercial preservative, to the best of our knowledge,

there has been no prior comprehensive study on the effect of this type of treatment on bamboo with regard to the mechanical performance.

The objectives of this work were to determine the retention of DOT for treated bamboo and evaluate the effects of DOT treatment on mechanical properties assessed by non-destructive test by excitation pulse, three-point static bending, and axial compression tests.

3.1.2. Materials and methods

3.1.2.1. Materials and sample preparation

The *D. asper* bamboo species has been used for this study due to its availability and easy access in several tropical regions. Bamboo culms were harvested at the experimental field in the University of São Paulo campus at Pirassununga, Brazil (21°58'53.5"S 47°26'03.3"W). The referred collection area is located at an altitude of 630 m above the sea level, with an annual average rainfall of 1363 mm and tropical climate with well-defined seasons (rainy summer and dry winter).

Mature culms (more than three years old) were collected and conditioned in a protected environment for drying until reaching constant moisture content. Tangentially oriented strips, approximately 250 mm long and 20 mm wide, were then cut from the inner region between nodes, also called internodes. Since the samples have been taken from the same or adjacent internodes, a possible influence of the variation of the mechanical properties along the culm in the effect of each treatment was minimized. Then the samples were sanded to obtain dimensional uniformity in width and thickness.

The physical properties of the samples, moisture content (MC) and the apparent density (ρ), before treating with DOT are shown in Table 3.1. Internodes (Int) of two different culms have been used for this study. Int A in the table stands for the samples taken from the middle part of a bamboo culm with the external diameter of approximately 11 cm and Int B, taken from the bottom part of a bamboo culm with approximately 16 cm external diameter.

Table 3.1 - Apparent density (ρ) and moisture content (MC) of the bamboo samples used for treatment (COV in parentheses).

Internode	ρ (g/cm^3)	MC (%)
Int A	0.69 (0.04)	8.3 (0.01)
Int B	0.77 (0.03)	8.7 (0.02)

Source: (GAUSS; KADIVAR; SAVASTANO JR, 2019)

3.1.2.2. Treatment procedures

A combination of boric acid and disodium borate decahydrate was used in the ratio of 1: 1.54 by mass for the formation of DOT, ($Na_2B_8O_{13}.4H_2O$) according to the stoichiometric reaction:

$$Na_2B_4O_7.10H_2O + 4H_3BO_3 \rightarrow Na_2B_8O_{13}.4H_2O + 12H_2O$$

Boric acid and disodium borate decahydrate of analytical grade were used. Then aqueous solutions of the preservatives with concentrations of 5% and 8 % (wt/wt%) were prepared using distilled water for the impregnation procedure. These concentrations were selected based on recommendations of bamboo treatment manuals of the International Network of Bamboo and Rattan (INBAR) (with concentrations between 5-10 %), Indian Standard of preservation of bamboo for structural purposes, IS 9096:2006, (concentration of 4 and 5 %) and other related papers (LIESE, 2004; LIESE; TANG, 2015b). Additionally, those are concentrations normally used in bamboo treatment plants around Colombia and Brazil.

The obtained solutions were applied through a vacuum/pressure steel chamber with a diameter of 150 mm and 270 mm height. This method was adopted to guarantee the penetration of the boron compounds in the samples. Prior to treatment, the samples were oven-dried at 60 ± 5 ºC until constant weight.

First, the specimens were placed in the empty chamber under an initial vacuum (-650 mmHg) for 15 min to withdraw air from the chamber and from the bamboo structure. Thereafter, the solution was injected into the chamber (about 8 L was required for total immersion of the

samples) and the same vacuum was maintained for an additional 1 h. Then, a pressure of approximately 3103 mmHg (60 psi) was applied into the chamber and held constant for 1h. After this step, the solution was drained, and the samples were taken out from the chamber and left in room temperature for 48 h and then dried at (100 ± 2) ºC for 48 h. After the drying process, the samples were conditioned in a climatic chamber at 25 ºC and 70% RH prior to mechanical testing.

3.1.2.3. Retention and boron penetration

Retention is usually expressed as weight of chemical per unit volume of wood (pounds per cubic foot or kilograms per cubic meter) or on the weight of chemical to the weight of wood basis (wt/wt%). The weights of the specimens were measured before and shortly after the treatment to determine the absorption of the treatment solution and then the theoretical retention was calculated using Equation 3.1, as per AWPA E10:2016 Standard.

$$R(\mathrm{kg/m^3}) = \frac{Ab \times C_w}{V} \times 10 \qquad \text{Eq. 3.1}$$

Where,

R: DOT retention (kg/m^3)

Ab: Mass of the absorbed solution after treatment (g)

Cw - Concentration of the preservative solution (wt/wt) (%)

V - Sample volume (cm^3)

The penetration analysis was also performed on samples treated with the boron compounds according to Brazilian Standard ABNT NBR 6232:2013 (Penetration and retention of preservatives in pressure treated wood) and Indian Standard IS 1902:2006 (Preservation of bamboo and cane for non-structural purposes) to observe the presence of boron. Across-sectional area of (10 × 20) mm^2 from samples extracted from the central region of the treated prismatic specimens was reacted with two different etching solutions. Solution 1 is composed of curcumin (earth turmeric) and ethyl alcohol (10% wt/vol alcohol) and solution 2 composed of a saturated salicylic acid alcoholic solution (13 g to 100 mL solution) and 20 mL of concentrated hydrochloric acid. First, solution 1 is applied and when dried, solution 2 is used.

The observation of red colour indicates the presence of boron. Except for turmeric, all reagents used are analytical grade.

3.1.2.4. Mechanical Tests

Samples originated from Int A and Int B were used for the mechanical characterization, with a total of 8 specimens per treatment condition: Reference, Water Treated, DOT 5% Solution, DOT 8% Solution). Each sample was subjected to the three tests performed in this work (excitation pulse, three-point bending and axial compression tests)

3.1.2.4.1. Excitation pulse non-destructive test

The dynamic elastic modulus was determined for each sample which was subsequently tested via static bending and in compression. The tests were performed in an excitation pulse testing machine Sonelastic®, as per recommendations of the ASTM E1876-15 Standard. The dynamic modulus of elasticity was determined in the longitudinal and flexural mode. Samples with nominal dimensions of 250 mm × 20 mm × thickness were used with a gap between the inferior supports of 0.552 × L.

3.1.2.4.2. Three-point bending test

After the determination of the dynamic elastic modulus by the impulse excitation technique, the same samples were subjected to a static three-point bending test using a universal testing machine EMIC model DL30000. The supported distance for each specimen was L = 160 mm and single point load F was applied at $L/2$. These dimensions are established in order to maintain a minimum length-to-depth ratio of 15 (according to the ASTM D1037 -12 Standard). The specimens were loaded continuously until failure at a loading rate of 5 mm/min and a deflectometer was used to record the deflection in the centre of the specimen. The modulus of rupture (MOR) and the modulus of elasticity (MOE) were then calculated according to Equations 3.2 and 3.3.

$$MOR\ (\text{MPa}) = \frac{3.F_r.D}{2.w.(t^2)} \qquad \text{Eq. 3.2}$$

$$MOE\ (\text{MPa}) = \frac{F_{LP}.(D^3)}{4.d.w.(t^3)} \qquad \text{Eq. 3.3}$$

Where,

F_r – Load at failure (N)

D – Distance between the supports (mm)

w – Width of the sample (mm)

t – Thickness of the sample (mm)

F_{LP} – Maximum load in the elastic region (N)

d – Deflection related to F_{LP} (mm)

3.1.2.4.3. Axial compression tests

Compression tests parallel to fibres were conducted in a Servohydraulic Test System MTS Landmark with a 15 kN load cell. Before the official axial compression tests, several tests were carried out to evaluate the applied methodology. First, the deformation difference between the inner and outer faces of the bamboo was evaluated. In samples extracted from the same specimens that were used in the bending tests, an extensometer was placed on the outer and the inner layers. It was found that due to the dimensions of the specimen, there was no significant difference between the different positions.

After the static bending test, two samples of approximate dimensions of 40 mm × width × thickness (width = thickness) per test piece were cut. The test was performed at a rate of 10 MPa/min, according to the recommendations of the Brazilian ABNT NBR 7190:1997 Standard (Wood Structures Project) and within the recommended testing time of ASTM D4761-13. First, a test specimen was used to determine the compressive strength, without the use of extensometer, calculated using the maximum load at failure. Then a second specimen (of the same sample used in bending) was used to determine the compressive modulus of elasticity. In this step, two loading cycles were performed between 20 and 50% of the compressive strength (determined previously), as shown in Figure 3.1. The elastic modulus was then calculated

through linearization of the second loading step. After the double-loading, the extensometer was withdrawn, and the test continued until failure of the specimen.

Figure 3.1 - Loading cycles used for determination of modulus of elasticity in the axial compression tests.

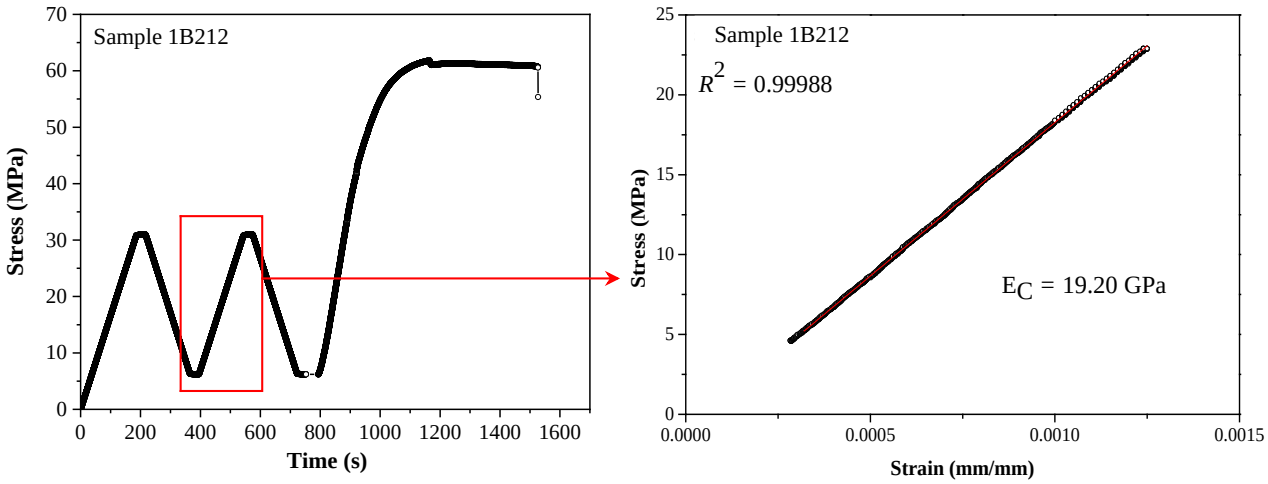

Source: (GAUSS; KADIVAR; SAVASTANO JR, 2019)

3.1.2.5. Statistical analysis

The averages of the results from each test are presented with the corresponding coefficient of variation (COV presented in parentheses). The differences between the treatment conditions on the mechanical properties were checked by a Tukey's test and analysis of variance (ANOVA) ($p < 0.05$) in case of a significant difference. For the statistical analysis normalized mechanical properties in relation to density (also called specific property) were used in order to better observe the effect of each treatment. All analyses were performed by the software MINITAB® Release 14 Statistical Software.

3.1.3. Results and discussion

3.1.3.1. Retention and boron penetration

Table 3.2 shows the analysed solution absorption values of each condition. Apparently, despite increasing the viscosity of the solution, the concentration of DOT did not significantly affect the absorption of the solution compared to water. However, it is noticed that the absorption is correlated with the density, as shown in Figure 3.2. This relationship is related to the number of pores since the solution uptake is strongly dependent on wood/bamboo permeability (LEE et al., 2018b).

Table 3.2 - Absorption of the solution after the treatment process in the vacuum/pressure vessel.

Absorption after impregnation, weight increase (%)			
Treatment	Int A	Int B	Overall
Water	67.6 (0.20)	57.9 (0.17)	61.6 (0.19)
5% DOT	73.1 (0.031)	61.3 (0.059)	65.7 (0.10)
8% DOT	65.7 (0.11)	55.4 (0.052)	58.8 (0.11)

Source: (GAUSS; KADIVAR; SAVASTANO JR, 2019)

Figure 3.2 - Relationship between solution absorption and the apparent density of bamboo samples.

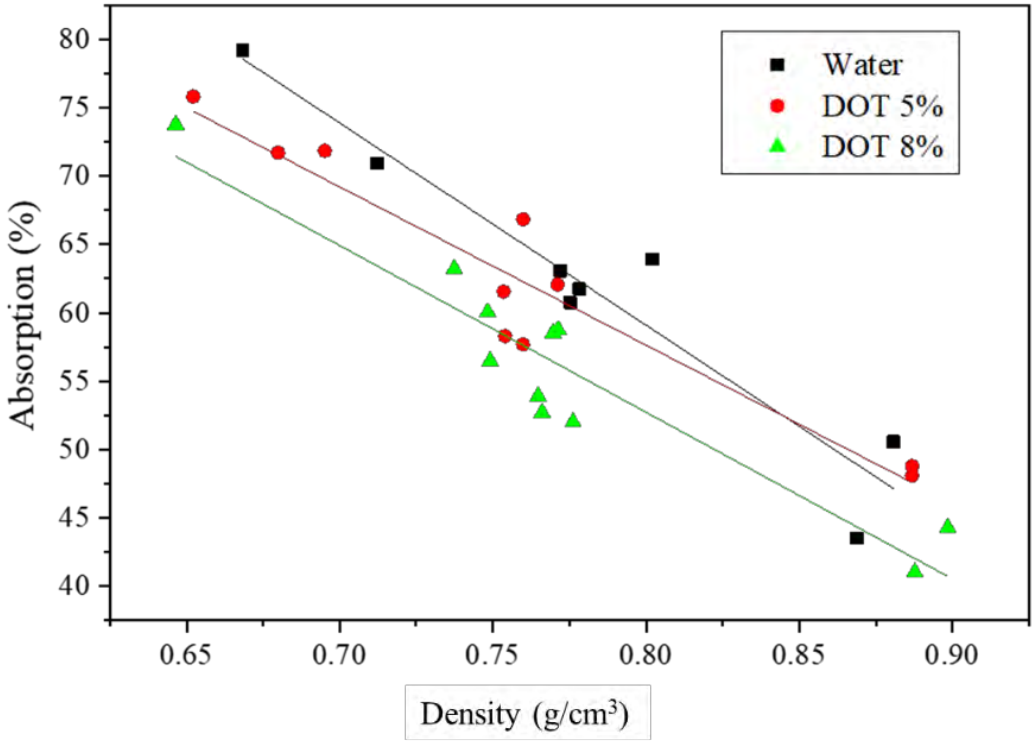

Source: (GAUSS; KADIVAR; SAVASTANO JR, 2019)

In general, the treatment involves placing an adequate amount of chemical to a depth that will achieve the desired degree of protection. Thus, most treatment standards address penetration or the depth to which the chemical penetrates and the retention, or the amount of chemicals deposited in a specific area of the wood (MORRELL, 2018).

The retention values calculated according to Equation 1 are presented in Table 3.3. It is worth mentioning that these theoretical values have been calculated considering the absorption of the treatment solution. The retention is presented as the equivalent of dried DOT per unit volume of bamboo. According to the stoichiometric reaction shown previously, for solutions based on boric acid and borax in the proportion of 1:1.54 (wt:wt), the resulting mass of DOT is 65.6% from the total mass of boric acid and borax. For the 5% solution, for example, the mass of the absorbed solution is multiplied by 0.328 to have the corresponding amount of formed DOT.

The results shown in Table 3 can also be represented as the retention of B_2O_3 per unit volume of bamboo. In the case of DOT, B_2O_3 represents 67.51% of its molecular weight, resulting in retentions of 9.98 kg/m^3 and 14.71 kg/m^3 for the 5% and 8% solutions respectively. These both results satisfy the desired B_2O_3 retention as recommended by American Wood Preservers' Association (2.7 kg/m^3) (CALDEIRA, 2010) and the Indian Standard IS401:2001 (5 kg/m^3) for indoor use application of wood. Although acceptable retention levels were obtained, compared to sapwood, the retention levels of bamboo are smaller mainly because of its anatomical structure. The bamboo used in this work has higher density then Scots pine (0.4-0.5 g/cm^3), for example, which limits the maximum amount of solution that can be absorbed by the material. In sapwood treatment, more than 100% of its weight can be absorbed. In bamboo, the outer layer part of the culm wall is protected by an epidermis as a waterproof seal. Additionally, there are no radial penetration pathways in bamboo, like the rays in wood. Especially in dry bamboo, the main path for penetration is the metaxylem vessels of the vascular bundles and the access to the parenchyma is difficult (LIESE, 2004; LIESE; TANG, 2015b; BAYSAL et al., 2016).

In Figure 3.3, photos obtained through a stereoscope show the total penetration of boron over the thickness of the treated samples (Fig. 3.3b). In Figure 3.3a, an image of a sample without treatment subjected to the test is presented for comparison. Both samples treated with 5% and 8% DOT solutions showed similar staining and total penetration.

Table 3.3 - Retention values of DOT calculated according to Equation 3.1.

Retention of DOT (kg/m^3)			
Treatment	Int A	Int B	Overall
5% DOT	15.28 (0.01)	14.35 (0.06)	14.79 (0.06)
8% DOT	22.93 (0.03)	20.65 (0.05)	21.79 (0.06)

Source: (GAUSS; KADIVAR; SAVASTANO JR, 2019)

Figure 3.3 - Analysis of penetration with solutions of curcumin and salicylic acid. In a) the solution was used in an untreated sample and in b) the treated sample.

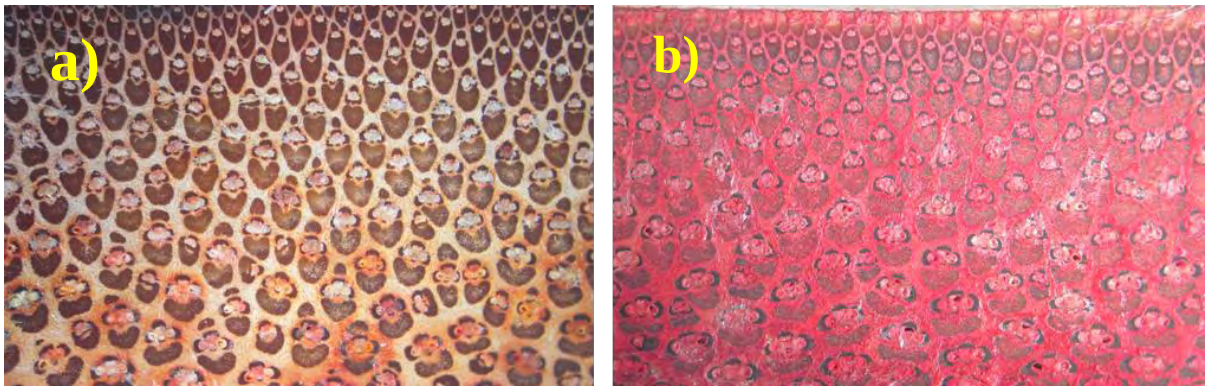

Source: (GAUSS; KADIVAR; SAVASTANO JR, 2019)

3.1.3.2. Mechanical characterization

3.1.3.2.1. Dynamic modulus of elasticity

Non-destructive testing (NDT) was used to evaluate the dynamic modulus of elasticity of treated and untreated bamboo samples. Since bamboo is a natural composite composed of aligned fibre bundles in the growth direction in a parenchyma matrix, it is expected an anisotropic behaviour. Therefore, the measurements were performed in flexural and longitudinal modes.

Figure 3.4 shows the relationship between the dynamic MOE and density of each sample. There is an almost linear correlation between the dynamic MOE and density of bamboo. This observation is correlated with the fact that higher density in bamboo means higher volume fraction of fibres within its structure. Dixon et al. (2015) found the same relationship between the MOE (obtained by static flexure tests) and the density of the bamboo species Moso, Tre Gai, and Guadua, with MOE varying between 10-40 GPa (DIXON et al., 2015).

Figure 3.4 - Correlation between dynamic MOE (flexural and longitudinal mode) and apparent density.

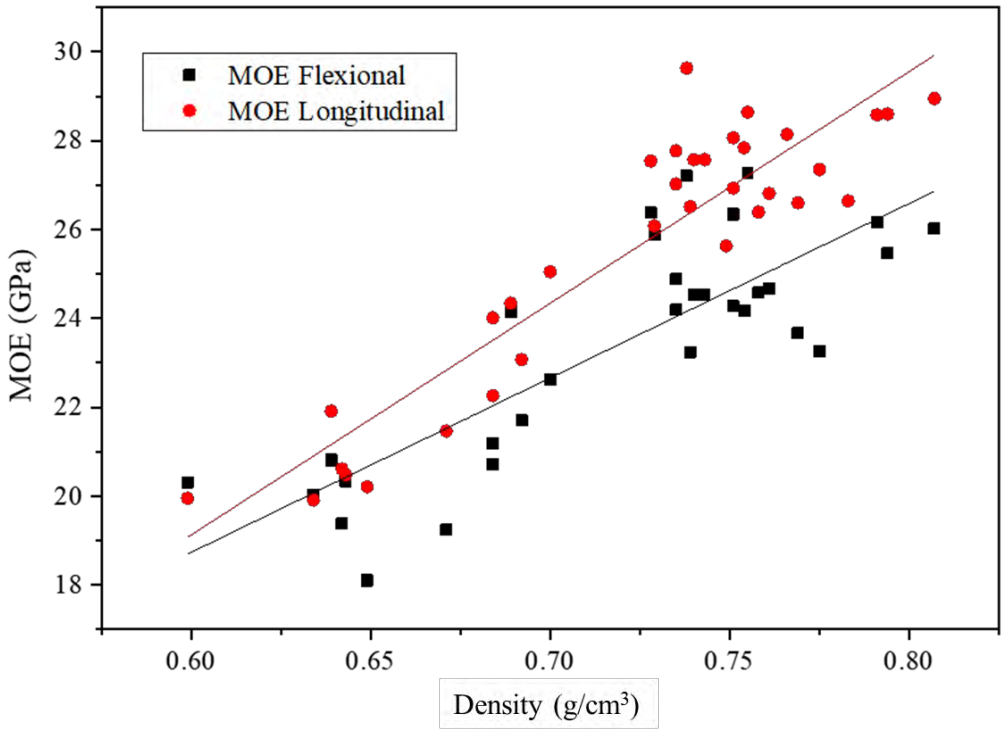

Source: (GAUSS; KADIVAR; SAVASTANO JR, 2019)

A summary of the achieved results for each treatment condition is shown in Table 3.4. Since there is a correlation of the dynamic MOE with density (Figure 3.4) and in order to better compare the effect of each treatment condition, the specific MOE was calculated for each specimen and an average for the 8 samples was obtained. It can be observed that even with high retention, there was no significant change ($p > 0.05$) in the dynamic MOE among the investigated conditions and the preservatives have no negative effect on bamboo samples in terms of MOE in both flexural and longitudinal direction. Although a slight increase was observed, 6.65% and 5.53% on the flexural MOE and 2.7% and 3.14% on the longitudinal MOE for the 5% and 8% DOT treated samples respectively, these results are statistically equivalent to the reference samples.

Table 3.4 - Summary of NDT-Excitation pulse measurements for determination of the dynamic MOE.

Treatment conditions		MC (%)	Flexural MOE (GPa)	Longitudinal MOE (GPa)
Reference	Int A	10.72	20.91 (0.03)	21.94 (0.06)
	Int B		24.57 (0.09)	27.99 (0.03)
	Overall Avg.		23.35 (0.07)	25.97 (0.12)
	Specific*		31.26 (0.04)[a]	34.67 (0.05)[a]
Water	Int A	9.37	21.44 (0.11)	22.29 (0.08)
	Int B		24.34 (0.19)	26.36 (0.04)
	Overall Avg.		23.25 (0.17)	24.83 (0.10)
	Specific*		32.53 (0.14)[a]	34.73 (0.04)[a]
5% DOT	Int A	10.24	19.22 (0.06)	20.54 (0.04)
	Int B		25.79 (0.07)	28.02 (0.04)
	Overall Avg.		23.26 (0.15)	24.90 (0.16)
	Specific*		33.34 (0.10)[a]	35.61 (0.09)[a]
8% DOT	Int A	10.23	22.36 (0.14)	23.33 (0.13)
	Int B		24.76 (0.03)	27.33 (0.02)
	Overall Avg.		23.96 (0.09)	26.00 (0.10)
	Specific*		32.99 (0.04)[a]	35.76 (0.05)[a]

* - MOE (GPa)/ρ (g/cm^3). Specific averages with the same letter (a-d) are statically equivalent. Three replicates were tested for Int A and five for Int B, with a total of eight replicates per treatment condition. MC=Moisture content.

Source: (GAUSS; KADIVAR; SAVASTANO JR, 2019)

3.1.3.2.2. Three-point bending

According to the previous discussion, there is a correlation between the dynamic MOE and apparent density. Similar behaviour could be observed with the modulus of rupture obtained by static bending, corroborating with the observations of other authors (DIXON et al., 2015). Therefore, specific values of MOR and MOE were also calculated for all the samples.

The stress-strain curves of several samples from all the conditions (Reference, Water, 5% and 8% DOT) are shown in Figure 3.5 and the results of MOR and MOE are shown in Table 3.5. It is possible to observe that all the curves, independently of the applied treatment, showed similar behaviour upon straining. The obtained average values of MOR, between 150.4 - 167.2 MPa, are similar to those observed by other authors in the same bamboo species, in which values between 140-258 MPa were reported using a comparable testing procedure (KRAUSE et al., 2016; OUNJAIJOM; MANEE-INTA; PUNYACUM, 2017).

Figure 3.5 - Stress vs specific strain curves obtained by static bending of samples treated with DOT, water and untreated.

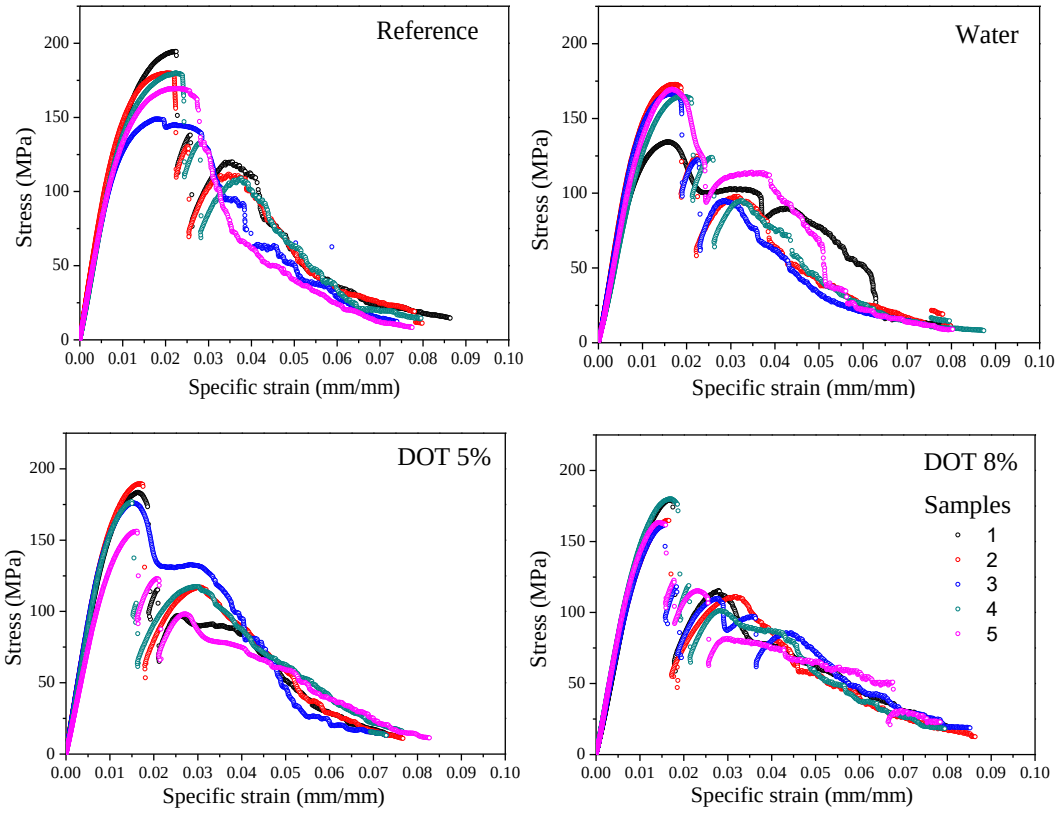

Source: (GAUSS; KADIVAR; SAVASTANO JR, 2019)

Table 3.5 - Summary of obtained results from three-point bending test.

Treatment conditions		MC (%)	MOR (MPa)	MOE (GPa)
Reference	Int A	10.92	125.8 (0.07)	16.16 (0.01)
	Int B		174.5 (0.10)	16.20 (0.06)
	Overall Avg.		156.2 (0.18)	16.18 (0.05)
	Specific*		209.4 (0.12)[a]	21.97 (0.10)[a]
Water	Int A	10.00	132.1 (0.10)	16.80 (0.07)
	Int B		161.4 (0.10)	15.13 (0.10)
	Overall Avg.		150.4 (0.14)	15.76 (0.10)
	Specific*		209.9 (0.07)[a]	23.24 (0.14)[a]
5% DOT	Int A	10.55	134.8 (0.09)	15.69 (0.06)
	Int B		176.4 (0.07)	17.12 (0.09)
	Overall Avg.		160.8 (0.15)	16.58 (0.09)
	Specific*		228.2 (0.09)[a]	23.70 (0.09)[a]
8% DOT	Int A	10.84	163.1 (0.22)	16.47 (0.07)
	Int B		169.7 (0.05)	15.57 (0.06)
	Overall Avg.		167.2 (0.13)	15.91 (0.07)
	Specific*		230.6 (0.10)[a]	22.03 (0.09)[a]

* - MOE (GPa)/ρ (g/cm^3) and MOR (MPa)/ρ (g/cm^3). Specific averages with the same letter (a-d) are statically equivalent. Three replicates were tested for Int A and five for Int B, with a total of eight replicates per treatment condition. MC=Moisture content.

Source: (GAUSS; KADIVAR; SAVASTANO JR, 2019)

According to the results shown in Table 3.5, although a slight increase in the average specific MOR of the samples treated with DOT was observed (8.5% and 10.1% for the 5% and 8% treatments, respectively), this difference is not statistically relevant using the ANOVA analysis ($p > 0.05$). The same behaviour was noticed for the results of MOE, in which case there was no considerable effect of the treatments with DOT. Comparing the results of MOE obtained

by static bending and by excitation pulse test, it was observed that the dynamic data were approximately 55% higher than the static MOE. In fact, this difference is normally found in NDT tests for the determination of dynamic MOE, with a difference between 40-50% (ARRUDA et al., 2011; CHUNG; WANG, 2018).

It is worth mentioning that since the same specimens were used for NDT and static bending tests, a correlation between the obtained data through both techniques can be made. In Figure 3.6 it is shown the relationship between the longitudinal dynamic MOE and static MOR. Interestingly, although they describe different mechanical properties, there is an almost linear correlation between them (R^2=0.8629). This observation can be very useful for quality control of bamboo products since a non-destructive test could be used to estimate other properties normally obtained only by destructive and time-consuming tests.

Figure 3.6 - Correlation between dynamic longitudinal MOE and the MOR obtained by static bending.

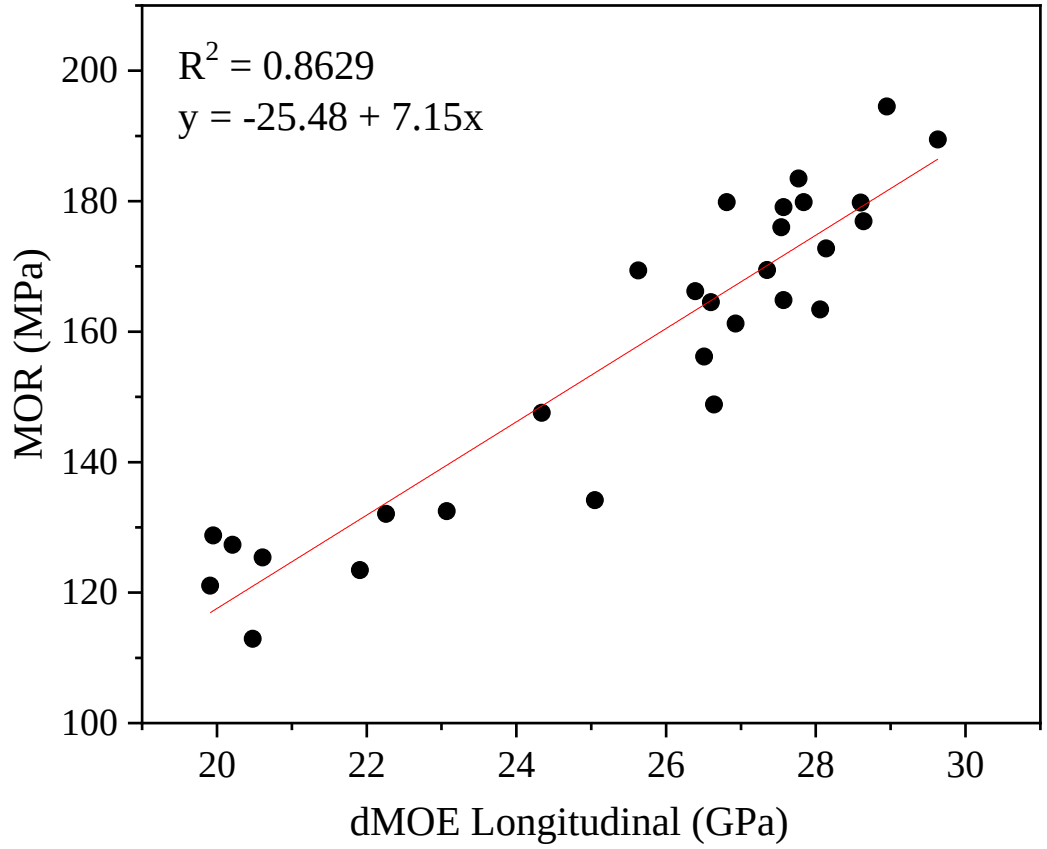

Source: (GAUSS; KADIVAR; SAVASTANO JR, 2019)

3.1.3.2.3. Compression parallel to the fibres

The compressive modulus of elasticity (E_c) was determined by following the stress-time pattern shown in Figure 3.1. Very good linearization (R^2 = 0.9998) of the stress-strain plot was obtained using the second loading step, assuring good quality of the extracted E_c.

A summary of the compressive strength (f_c) and E_c results obtained for the DOT treated, water treated and reference samples is presented in Table 3.6. From the results, the influence of preservative treatment also did not have any significant effect on the compressive modulus of elasticity, corroborating with the elastic properties obtained by static bending and excitation pulse tests. However, on compressive strength, a positive and statistically different effect ($p < 0.05$) of the treatment can be observed. The samples treated with 5% and 8% DOT solutions presented a specific f_c increase of 35.3% and 30.6%, respectively, in comparison with the Reference samples. The water treated samples also had a slight increase in the compression strength (17.1%). Similar behaviour was observed in the MOR obtained by static bending, although statistical analysis showed no valid difference.

According to the results of the mechanical tests, the solutions used for treatment did not cause any detrimental effect on the structure of bamboo even with high retention levels. Furthermore, it is possible to infer that the increase on the compressive strength can be correlated with the formed DOT salt crystals within the bamboo microstructure, in which could help to accommodate the applied forces during loading. Since the pH of 5 % and 8 % solutions have a close to neutral pH (between 7.9 and 7.7), which is one of the advantages over the use of only boric acid and borax as a source of boron, it is not expected chemical reactions during treatment. In fact, preservatives with pH above 4.1 are not expected to cause considerable detrimental effects on wood properties (LAHTELA; HÄMÄLÄINEN; KÄRKI, 2013). Therefore, the increase in the mechanical properties found in this study is hypothesized to be attributed partially by the accommodations of forces by DOT crystals inside the bamboo porous structure or other mechanisms not yet known.

Table 3.6 - Summary obtained results from compression tests parallel to fibre.

Treatment conditions		MC (%)	f_c (MPa)	E_c (GPa)
Reference	Int A	9.77	50.3 (0.06)	18.61 (0.03)
	Int B		65.4 (0.05)	32.00 (0.11)
	Overall Avr		60.8 (0.13)	27.54 (0.27)
	Specific*		82.5 (0.07)[a]	37.16 (0.20)[a]
Water	Int A	9.14	59.8 (0.06)	18.04 (0.13)
	Int B		74.3 (0.07)	25.49 (0.14)
	Overall Avr		67.1 (0.13)	22.30 (0.22)
	Specific*		95.80 (0.08)[b]	32.10 (0.17)[a]
5% DOT	Int A	9.56	68.0 (0.06)	17.07 (0.18)
	Int B		82.5 (0.04)	29.65 (0.10)
	Overall Avr		75.8 (0.11)	24.26 (0.30)
	Specific*		110.7 (0.06)[c]	34.49 (0.19)[a]
8% DOT	Int A	9.07	73.4 (0.11)	20.35 (0.13)
	Int B		78.0 (0.04)	30.57 (0.14)
	Overall Avr		75.7 (0.09)	26.19 (0.25)
	Specific*		106.8 (0.06)[c]	36.84 (0.18)[a]

E_c: Compressive modulus of elasticity; f_c: Compressive strength * - E_c (GPa)/ρ (g/cm^3) and f_c (MPa)/ρ (g/cm^3). Specific averages with the same letter (a-d) are statically equivalent. Six replicates were tested for Int A and eight for Int B, with a total of fourteen replicates per treatment condition. MC= Moisture content.

Source: (GAUSS; KADIVAR; SAVASTANO JR, 2019)

3.1.4. Conclusions

The effectiveness of an available commercial preservative - DOT - treatment on the mechanical properties of *D. asper* bamboo was investigated. In general, it was possible to conclude that there is no negative effect of DOT treatment on the investigated mechanical tests, even considering high DOT retention levels. The main conclusions are:

- *D. asper* bamboo strips can be successfully vacuum/pressure treated using boron compounds, achieving acceptable retention and penetration of DOT using 5% and 8% (wt/wt%) solutions.

- For the dynamic MOE determined from the excitation pulse tests, there was no statistically significant change ($p > 0.05$) among the investigated conditions.

- Although DOT treatment using both 5% and 8% concentration solutions positively affected specific MOR, the difference is not statistically valid ($p > 0.05$).

- There is a linear correlation between dynamic MOE (NDT) and MOR obtained by static bending.

- Bamboo treated with 5% and 8 % DOT solutions increased the compressive strength by 35.3% and 30.6%, respectively, but no significant difference ($p > 0.05$) was observed in the modulus of elasticity in compression.

Additional degradation tests with decay fungi (white-rot and brown-rot) are currently being performed for the achievement of information regarding the effectiveness of DOT on the protection of bamboo against fungi before and after severe leaching cycles.

3.2. Quality assessment and mechanical characterization of preservative-treated Moso bamboo (*P. edulis*)

3.2.1. Introduction

Bamboo as an engineered natural material is increasingly being explored for structural uses in construction (e.g., ANUAR AND KRAUSE, 2016; CHOW et al. 2019). Traditionally used for centuries for (so-called) informal or vernacular building construction, furniture, and daily necessaries (ZHANG et al., 2018), bamboo today has expanded into modern construction techniques. Extensive research on the generally good mechanical properties of bamboo is presented in the literature (DIXON; GIBSON, 2014a; JAKOVLJEVIĆ et al., 2017; AKINBADE et al., 2019). Fast-growing and maturing bamboo species such as *Phyllostachys edulis* (Moso) produce material with promising structural properties.

Without suitable treatment, however, bamboo is prone to biological degradation in a short period of time, reducing its utility as a structural material (JANSSEN, 2000). The "bamboo borer" or "powderpost" beetle (*Dinoderus minutus*) is a primary destructive agent of bamboo (WATANABE; YANASE; FUJII, 2015) and is present across the world's tropical zones (CABI 2019). Other xylophagous organisms, such as decay fungi and termites, can also affect the structural integrity of bamboo and consequently compromise the service life of structures (JAYANETTI; FOLLETT, 2008; TIBURTINO et al., 2015a). Today, conventional wood treatment solutions used in Brazil have good performance but are typically based on heavy metals and other toxic elements, such as CCA (Chromated Copper Arsenate), pentachlorophenol and others (MOHAJERANI; VAJNA; ELLCOCK, 2018). Whenever technically and economically feasible, the replacement of hazardous chemicals with less hazardous substances is an essential objective in the wood and bamboo industry. As a result, novel preservative formulations are being developed and used for interior and exterior applications.

Less hazardous substances that have been investigated and commercialized for the treatment of bamboo and wood for interior application include low-cost soluble salts, such as boron-based salts, specifically disodium octaborate tetrahydrate (DOT), boric acid and borax (CALDEIRA, 2010; KIM; TANG; LIESE, 2011; LIESE; TANG, 2015b; TIBURTINO et al.,

2015a). Boron compounds are some of the most effective and versatile preservative solutions used today since they combine broad-spectrum efficacy, low mammalian toxicity, and are odourless and colourless (TONDI et al., 2012a; DONMEZ CAVDAR; MENGELOĞLU; KARAKUS, 2015; JIT KAUR, 2018; ZHOU et al., 2018). Preservation with boron compounds can even improve the quality of bamboo, improving some mechanical properties in comparison with bamboo without preservatives in samples with high retention levels (PRININDYA; ARDIANSYAH, 2014; SULAEMAN et al., 2017; GAUSS; KADIVAR; SAVASTANO JR, 2019). Nevertheless, the use of boron compounds presents restrictions for the treated material because of the leaching of boron in the presence of water, making it unsuitable for use in exterior applications (HIDALDO-LÓPES, 2003; FREEMAN; MCINTYRE; JACKSON, 2009; CALDEIRA, 2010). For the exterior use, CCB (Chromated Copper Borate) was developed as an alternative to CCA, substituting arsenic with a boron source, reducing the toxicity to humans and the environment (VIDAL et al., 2015; BERALDO, 2016). Nonetheless, heavy metals are still used in its composition and the disposal of CCB treated wood/bamboo continues to be a problem (CALDEIRA, 2010).

From a structural engineering perspective, the challenge is to prescribe a treatment having sufficient retention and penetration in the culm to increase the bamboo service life without sacrificing physical or mechanical properties. Although chemical treatment is commonly used in the construction industry, its impact on material properties is often unclear. Recent investigations have demonstrated that the treatment method selected affects the mechanical properties of laminated bamboo material (SHAH; SHARMA; RAMAGE, 2018). The effects of preservative treatments such as steam, oil or dry heat treatment have been found to have adverse effects on both wettability and strength of the bamboo product (WAHAB et al., 2005, 2015; SULAIMAN et al., 2006; LI et al., 2015a; BUI; GRILLET; TRAN, 2017). Therefore, not only is a quality control assessment of the final structural material necessary but also the effects of chemical treatments on the mechanical properties of treated materials requires closer inspection.

Most structural projects utilising bamboo in Latin America and Asia use boron compounds (boric acid, borax or DOT) for bamboo used in a protected environment (typically referred to as interior exposure) and CCB or CCA for exterior exposure. Despite this dichotomy, there is no known design practice that differentiates the structural design of different-treated

bamboo. Indeed, there are no known studies of the treatability, mechanical performance and durability of different-treated bamboos. The present study aims to investigate the effects of DOT and CCB treatments – as the two most well-known commercially used preservatives – on treatability and mechanical properties of *P. edulis* bamboo (the most widely commercialized bamboo species). The applied methods of treatment for each material follow the same practical methods applied in the industry. Bamboo for exterior exposure is treated using CCB in a vacuum pressure process while bamboo for interior exposure is treated using DOT in an immersion method.

3.2.2. Materials and Methods

3.2.2.1. Material

Approximately 140 *Phyllostachys edulis* (Moso) bamboo culms were obtained from a supplier near Sao Paulo, Brazil. Culms between 3 and 5 years of age were harvested from which 4 to 4.5 m long poles (visually free of defects) were extracted. The diameters ranged from 70 to 90 mm, wall thickness from 6.5 to 10 mm and the oven-dry density prior to treatment was 760 kg/m^3.

The culms were divided into two batches (Figure 3.7). Batch A comprised of 130 poles treated with DOT by immersion (see below). From this large batch, twelve 1 m long samples were extracted from randomly selected poles for the evaluation of mechanical properties and boron penetration analysis. An additional two samples were extracted to assess boron retention following 7- and 10-days' immersion. This series of samples was intended as a means of quality assessment of the entire batch of bamboo and are indicated in this paper as "A-DOT".

A second smaller Batch B was used for direct comparison of CCB and DOT treatment. Adjacent 0.8 m long samples were extracted from untreated poles. The adjacent samples were then treated using CCB or DOT. Using adjacent samples in this way was intended to minimize the variation of mechanical properties from different poles and along the length of the same pole, permitting a direct comparison of the effects of treatment method. The samples intended for comparison are indicated B-DOT and B-CCB in this paper.

Figure 3.7 - Sampling and treatment methods.

<table>
<tr><td>140 P. edulis culms</td><td colspan="3"> 
</td></tr>
<tr><td>Batches</td><td>A-DOT</td><td>B-DOT</td><td>B-CCB</td></tr>
<tr><td>Treatment samples</td><td>130 - 4 to 4.5 m poles</td><td colspan="2">20 - 0.8 m samples cut from untreated culms
 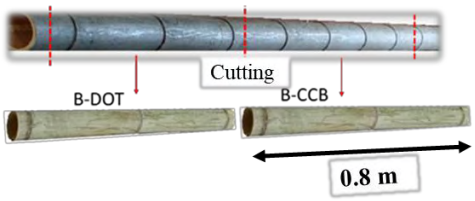
</td></tr>
<tr><td>Treatment</td><td colspan="2"> 
8% DOT in 4.7 m immersion tank</td><td> 
3.5% CCB in pressure/vacuum tank</td></tr>
<tr><td>Sampling for Tests</td><td> 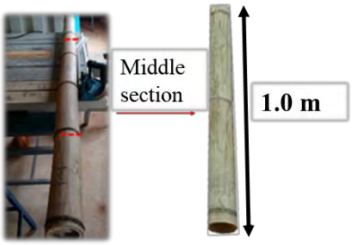

n = 12</td><td> 

n = 10</td><td> 

n = 10</td></tr>
</table>

Source: (GAUSS et al., 2020)

3.2.2.2. DOT Treatment[1]

Agricultural grade disodium octaborate tetrahydrate (DOT; $Na_2B_8O_{13}.4.H_2O$, molar weight of 412.5 g/mol) supplied by Sulboro (Brazil) was used. A-DOT and B-DOT samples were treated by immersion in an 8% (weight/volume) DOT aqueous solution. The 4.7 m long immersion tank is shown in Figure 3.7. A small amount of tannin extract supplied by Tanac (Brazil), was also added to the solution (0.5 kg per 1000 L) in order to facilitate the cleaning (and thereby reuse) of the solution and as an additional fungicide agent. The solution was conditioned, and the concentration adjusted after each treatment batch using a conductivity meter (according to a standard concentration curve). The A-DOT samples were kept in immersion between 7 and 10 days (depending on the batch) and the B-DOT samples immersed for 7 days.

3.2.2.3. CCB Treatment

B-CCB samples were treated using commercially available chromated copper borate (CCB), MOQ OX 50, supplied by Montana Química Ltda (Brazil). The product is an oxide-based CCB having approximately the following constituency of active ingredients: 32% CrO_3; 13% CuO; and 5% B (as trivalent boron); and 50% inert ingredients. The molar weight of the three active constituents is 100, 79 and 10.8 g/mol, respectively. A 3.5% (active ingredient weight/volume) aqueous solution was used in a pressure vessel using a full-cell process: -600mmHg (0.8 bar) vacuum for 30min, followed by 10 kgf/cm^2 (10 bar) pressure for 60 min, followed by -600mmHg vacuum for 15 min. Treatment was conducted in a pressure/vacuum tank shown in Figure 3.7.

[1] More information about this treatment is presented in section 3.4.2.

3.2.2.4. Treatment characterization

3.2.2.4.1. Retention and penetration analysis

Following treatment, samples subjected to boron (in case of DOT) and chromium, copper and boron (in case of CCB) retention analyses conducted according to Brazilian Standard ABNT NBR 6232:2013 (Penetration and retention of preservatives in pressure treated wood) and Indian Standard BIS 1902 (2006) (Preservation of bamboo and cane for non-structural purposes). For the chemical analyses, samples extracted from the middle part of each pole were subjected to (sulphuric) acid digestion, diluted and analysed by atomic absorption spectroscopy. The samples treated with DOT were analysed at IPT (Technological Research Institute, São Paulo) and the samples treated with CCB at Montana Química (São Paulo).

Penetration analysis was also performed in accordance with ABNT NBR 6232:2013 to observe the presence of boron (for DOT treated samples) and copper (for CCB treated samples). The cross-sectional area of samples extracted from the central region of the treated poles was reacted with the etching solutions:

For boron penetration analysis a solution composed of curcumin (earth turmeric) and ethyl alcohol (10% wt/vol alcohol) was applied to the treated bamboo section and permitted to dry. Then a saturated salicylic acid alcoholic solution (13 g per 100 mL solution) and 20 mL of concentrated hydrochloric acid was applied. The observation of red colour indicates the presence of boron. For copper penetration analysis, a solution with 0.5 g of chrome azurol S and 5.0 g of sodium acetate in 300 mL of water is applied; a dark blue colour indicates the presence of copper.

3.2.2.4.2. Optical and scanning electron microscopy

The transverse section of the treated bamboo samples was analysed in a ZEISS Smartzoom 5 optical microscope in order to evaluate the observable effects of the different treatment conditions. For the analysis, small samples were cut with a diamond disc and subjected to fine grinding and polishing with (sequentially) 15, 3 and 1 µm diamond polishing paste. After polishing the samples were cleaned with isopropyl alcohol and dried at room temperature.

Clean cuts of the longitudinal section of the bamboo samples (parallel to the fibres), obtained using a sharp chisel and subjected to no further surface preparation, were used for microstructural and chemical characterization in a FEI Apreo scanning electron microscope (SEM) equipped with a field-emission gun. This procedure was performed in order to preserve the chemicals within the bamboo structure for chemical analysis. Before analysis, the samples were coated with palladium in a Cressington Sputter Coater. Elemental mapping was performed using energy-dispersive X-ray spectroscopy (EDS) operated at 20 kV.

3.2.2.5. Mechanical characterization

Mechanical characterization of the samples treated with DOT and CCB was performed according to procedures described below. Full culm specimens were used for compression, shear and flat ring flexure tests while machined coupon specimens were used for tension and bending tests. All required specimen dimensions were obtained using a digital calliper having a precision of 0.01 mm. Digital Image Correlation (DIC) techniques were used in all tests to determine strain fields and thereby modulus. DIC is a well-established contact-free means of obtaining full-field surface deformations (and therefore strains). Specimens are painted with a speckle pattern prior to testing (photocopier toner broadcast onto wet white spray paint, the result is seen in Figure 3.8). During the test, consecutive high-resolution images (2448 x 2049 pixels) are taken every 0.5 sec. and deformation patterns (based on sampling of the speckle pattern) are recorded. Post-processing allows relative displacements and specified strain fields to be obtained in three dimensions. The system used in this study is a VIC-3D dual-camera system resulting in a resolution better than 1 microstrain on the surface of the specimens. All the obtained data was processed and analysed using the VIC-3D 2012 Digital Image Correlation software (Correlated Solutions). The sample was weighed prior to testing and afterwards dried at 100 °C ± 2 for at least 48 h to establish moisture content (MC) in accordance with ISO 22157:2019. Additional description and commentary on the mechanical test protocols are reported in (GAUSS; SAVASTANO; HARRIES, 2019).

Figure 3.8 - Mechanical test methods.

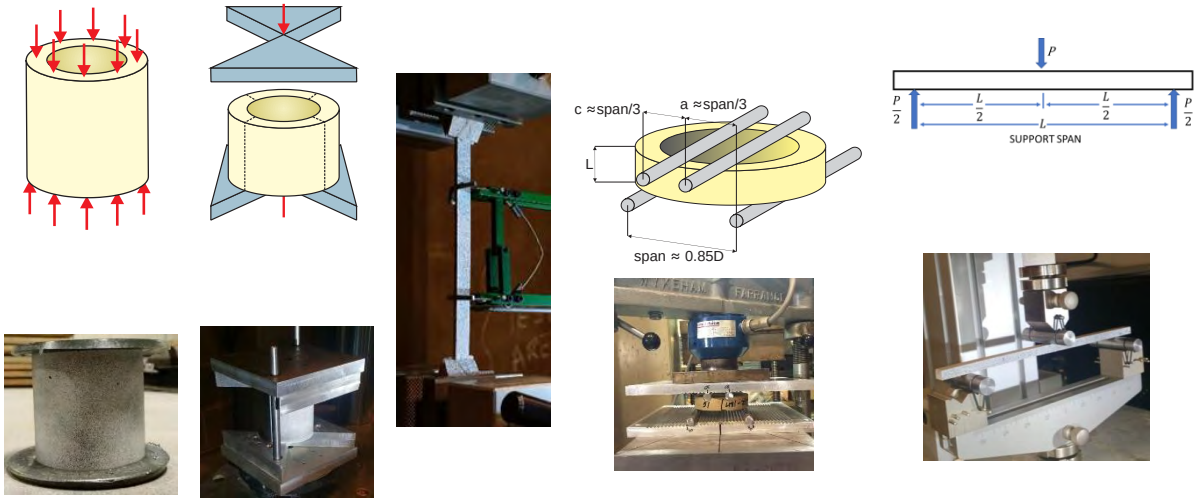

a) ISO 22157 compression test

b) ISO 22157 shear test

c) ISO 22157 tension test

d) flat ring flexure test (Virgo et al. 2017)

e) small coupon three-point bending test (ASTM D7264)

Source: (GAUSS et al., 2020)

3.2.2.5.1. Compression parallel to fibres

Full-culm compression tests (Figure 3.8a) were conducted according to ISO 22157:2019. Specimens had a height equal to their nominal diameter (i.e., L = D). A sulphur capping compound was used in order to ensure a flat loading surface and reduce the friction between the sample and the compression platen. Tests were performed in a 600 kN capacity universal testing machine; the load was applied at a crosshead displacement rate of 1.0 mm/min. Compression modulus, E_c, is determined from DIC analysis.

3.2.2.5.2. Shear parallel to fibres

Full-culm shear tests (so-called “bowtie” tests) were conducted according to ISO 22157:2019; also with specimens having a height equal to their nominal diameter (i.e., L = D). In this test (Figure 3.8b), the full culm specimen is supported at its lower end over two opposing quadrants and loaded at its upper end over the other two opposing quadrants. In this manner, loading the specimen results in four shear areas. The test is controlled by the first shear plane to

fail and therefore the shear strength, f_v, is interpreted as the lower bound shear strength. Tests were performed in a 600 kN capacity universal testing machine; the load was applied at a crosshead displacement rate of 1.0 mm/min. Shear modulus, *G*, is determined from DIC analysis.

3.2.2.5.3. Tension parallel to fibres

Tension tests were performed in accordance with ISO 22157:2019, with some modifications of the specimen design. Radially oriented bamboo strips, 200 mm in length, were extracted from sample poles. The samples were sanded to obtain uniform dimensions with a breadth (b) less than half of the culm wall thickness (t). Softwood tabs were glued on the specimen ends in order to facilitate gripping by the testing machine. Flat samples often exhibited failures associated with grip inconsistencies and/or stress raising effects; for an accurate comparison of treatment methods, these failures must be mitigated (in practice, grip failures are neglected – this is not possible in this study due to the limited number of samples available). A modified "dog bone" specimen was produced with a region of reduced breadth in the middle of the specimen. The tensile modulus of elasticity of the dog bone samples was validated comparing modulus values obtained from flat samples using both a mechanical extensometer and DIC (Figure 3.8c). Only specimens without nodes are considered in this paper. Tests were conducted in a 600 kN capacity universal test machine at a displacement rate of 1.0 mm/min.

3.2.2.5.4. Three-point small coupon bending test

The bending test perpendicular to the fibres for bamboo described by ISO 22157:2019 requires specimens having a length L > 30D. This test is intended as a component capacity test, not a materials evaluation test. Since the main objective of this work is to evaluate the influence of the preservative treatments on the mechanical properties of bamboo, reduced size specimens in prismatic form with 200 mm long x 10 mm wide x culm wall thickness deep were used (Figure 3.8e). Only specimens without nodes are considered in this paper. A span of 160 mm was used for all the tests, which resulted in an average shear span to depth ratio exceeding 10 in every test. The tests were conducted three-point bending following Procedure A of ASTM D7264

using a 10 kN capacity electromechanical testing machine. A displacement rate of 2.5 mm/min was used for all the tests. Tests reported in this study were conducted with the sample orientated such that the outer culm wall was in compression (OC) (see Gauss et al. 2019b for additional discussion of specimen orientation). Modulus of rupture (MOR) and modulus of elasticity (MOE) were calculated according to ASTM D7264.

3.2.2.5.5. Flat ring flexure test

In order to evaluate the mode I fracture behaviour of treated bamboo samples and better understand the splitting behaviour, a flat ring flexure test was performed (VIRGO et al., 2018; AKINBADE et al., 2019).

Samples with $0.18D \leq L \leq 0.22D$ (were cut from the 0.8 m bamboo poles and the dimensions were measured using a digital calliper at four quadrants of the specimen. The flat-ring flexure test was conducted in a four-point bending setup (Figure 3.8d) using a displacement rate of 0.76 mm/min (0.03 in/min) in a 45 kN mechanically driven testing machine equipped with a load cell having a precision of ± 0.4N. In the symmetric specimen, only circumferential stresses are present and the modulus of rupture is calculated only for samples that fail in the constant moment region (dimension "c" in Figure 3.8d) (VIRGO et al., 2018).

3.2.2.6. Statistical analyses

The averages of each test are presented with the corresponding coefficient of variation (COV) and number of samples. The differences between the treatment conditions on the mechanical properties were checked by a Tukey's test and analysis of variance (ANOVA) for significant ($p < 0.05$) differences. All analyses were performed using MINITAB® Release 18 Statistical Software.

3.2.3. Results and Discussion

3.2.3.1. Treatment characterization

Active ingredient penetration and retention analysis results are summarized in Table 3.7 and discussed in the following sections. Samples for treatment characterization were extracted from the middle part of the treated bamboo poles (away from the cut ends), which represents the region most susceptible to lower retentions.

3.2.3.1.1. Active Ingredient Penetration

Penetration analysis provides a qualitative measure of the efficacy of the treatment process and enables visualization of where the chemicals used in the treatment are located within the culm wall thickness. Depending on the degree of active ingredient penetration across the wall thickness (i.e., area reacting with the etching solutions) a grade between 0 to 4 can be assigned to each sample: 0 = no penetration); 1 = 0-25% penetration; 2 = 25-50%; 3 = 50-75%; and, 4 = greater than 75% penetration (KIM; TANG; LIESE, 2011). Examples of penetration grades for boron are shown in Figure 3.9.

Table 3.7 presents a summary of treatment parameters and penetration grade of each condition. For the A-DOT samples used for quality assessment, samples from 10 different poles were analysed resulting in penetration grades ranging from 2 to 4 (average = 3). For the B-DOT and B-CCB treatments, a single sample per condition was used resulting in penetration grades of 3 and 4, respectively.

Table 3.7 - Summary of treatment methods and assessment.

	A-DOT	**B-DOT**	**B-CCB**
Sample size, n	12	10	10
Treatment method	7- or 10-day immersion	7-day immersion	vacuum/pressure
Active ingredient and nominal concentration	8% DOT solution	8% DOT solution	3.5% CCB solution
Moisture content before treatment (%)	30.0	14.1	17.0
Weight gain following treatment (%) - (COV in parentheses)	-	17.0 (0.31)	30.2 (0.10)
Retention of active ingredient (kg/m^3)	2.2	2.2	7.2
Penetration grade	range from 2 to 4 (10 samples)	3 (single sample)	4 (single sample)

Source: (GAUSS et al., 2020)

Figure 3.9 - Boron penetration analysis of samples treated with DOT (untreated reference sample at left). Grade 4 (> 75% penetration); Grade 3 (50-75% penetration); Grade 2 (25-50% penetration).

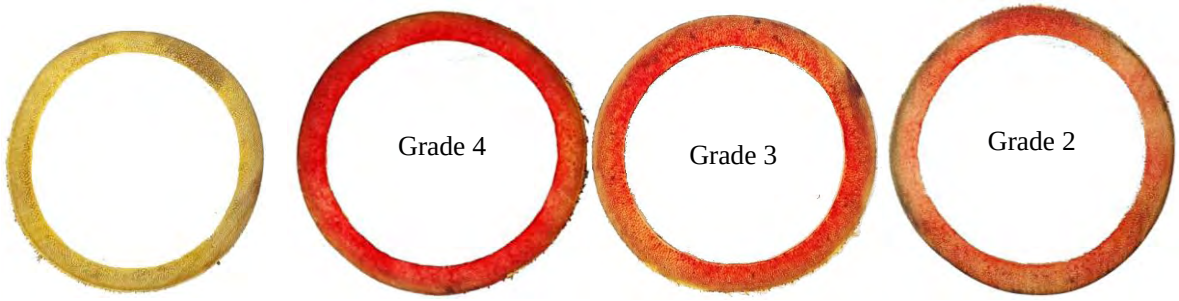

Source: (GAUSS et al., 2020)

3.2.3.1.2. Active Ingredient Retention

Active ingredient retention is assessed as mass retention of the chemical components of the treatment as given by Equations 3.4 and 3.5.

For DOT Total retention (kg/m^3) = $Na_2B_8O_{13}.4.H_2O$ (kg/m^3) Eq 3.4

For CCB Total retention (kg/m^3) = CrO_3 (kg/m^3) + CuO (kg/m^3) + B (kg/m^3) Eq 3.5

The samples treated with DOT exhibited lower retention levels (2.2 kg/m^3) mainly because this treatment is by "passive" immersion, rather than by "active" vacuum or pressure. Using pressure treatment for boron-based (BB: Boric acid + Borax) solutions, Kim et al. (2011) also observed lower retention levels in comparison with CCB for *B. stenostachya*, *T. siamensis* and *D. asper* bamboos. Values between 2.5 and 15.5 kg/m^3 were observed for BB proportional to the applied pressure (2.5-8.5 bar) and greater when the bamboo epidermal layer had been removed (an advantage for solution absorption). As reference values, the Indian Standard IS 9096:2006 recommends 6 kg/m^3 of active ingredient (borax + boric acid treatment, with the same proportion used for the formation of DOT) for indoor applications. A retention of 2.7 kg/m^3 of B_2O_3, equivalent to 4.0 kg/m^3 of DOT, is recommended by the American Wood Preservers's Association (AWPA) for boron-based treatments (CALDEIRA, 2010). Although boron-based treatments are widely used for structural use of bamboo, information regarding retentions values are scarce and are affected by treatment methods and bamboo species (KIM; TANG; LIESE, 2011; TIBURTINO et al., 2015b).

The A-DOT and B-DOT samples presented similar DOT retention values. Although the A-DOT samples have been extracted from 4.5 m poles (about 2 m to a cut end), and B-DOT samples were extracted from 0.8 m poles (no more than 0.4 m to a cut end), the length of the bamboo poles did not affect the retention of DOT. Furthermore, no difference was noticed for A-DOT samples from poles treated for 7 and 10 days in terms of retention or penetration.

The CCB treated samples exhibited retention of 7.2 kg/m^3, higher than that observed by Tiburtino et al. (2015b) in *D. asper* and *B. vulgaris* bamboo samples treated by immersion and by modified Boucherie methods (TIBURTINO et al., 2015b). For CCB treatments, Indian Standard IS401:2001 recommends retentions values of 10-16 kg/m^3 for applications exposed to weather and in contact with the ground, 6-10 kg/m^3 for applications exposed to weather but

without ground contact, and 6 kg/m^3 for applications undercover. Kim et al. (2011) reported values between 11.3 and 16.3 kg/m^3 retention of CCB in samples treated with similar pressure (8.5 bar) to the that used in this work. However, in their work, they used a 6% CCB solution and no information regarding the density of the material is reported (which can also greatly influence the treatability of bamboo). Baysal et al. (2016) reported that bamboo (*P. bambusoides*) presented lower retention values of several preservatives (CCB, boron, and other copper-based products) than those observed in wood (Scots pine), which was attributed to the anatomical characteristics of bamboo. The same behaviour was observed on the work of Lee et. al. (2001), using the same bamboo species used in this work, but treated with CCA instead of CCB.

3.2.3.2. Microstructural characterization and chemical analysis

Optical and scanning electron microscopy (SEM) were used to analyse the microstructure of the treated bamboo samples and investigate any difference between CCB and DOT treatments.

A typical microstructure obtained by optical microscopy of the bamboo used in this study is shown in Figure 3.10, in which its structure composed of parenchyma (P), fibre bundles (F), phloem (Ph) and vessels (V) is shown in detail. Using ImageJ analysis software (RASBAND, 2018) the fibre volume ratio of the *P. edulis* samples was determined. Sixteen images extracted from four randomly chosen culms resulted in determining a fibre volume content, V_f = 28.8 % (COV = 0.07). This value is similar to that reported in a number of other studies (AKINBADE et al., 2019).

Optical microscope images of CCB- and DOT-treated samples shown in Figure 3.11 show that there is no visual difference in terms of microstructure between treatments, especially around the vessels, where an effect might be expected.

Figure 3.10 - Microstructure of *P. edulis* bamboo used in this study. V=Vessels; F=Fibre bundles; Ph=Phloem; P=Parenchyma

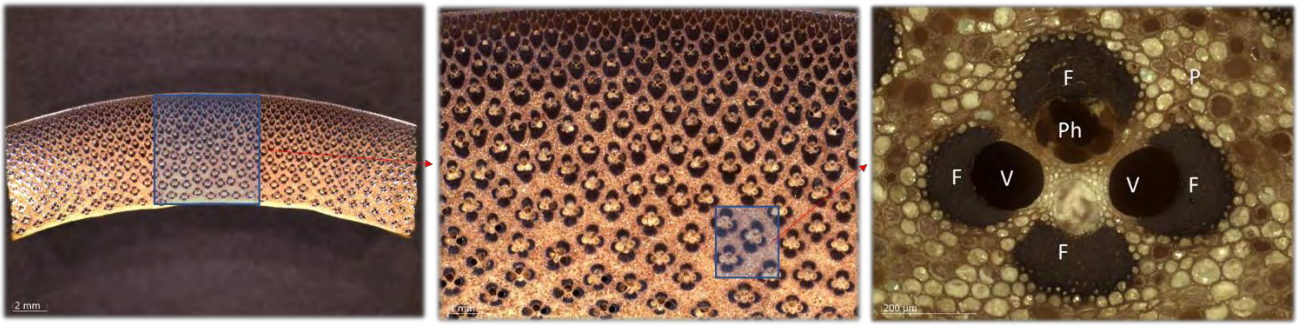

Source: (GAUSS et al., 2020)

Figure 3.11 - Optical microscopy images of the B-DOT and B-CCB samples

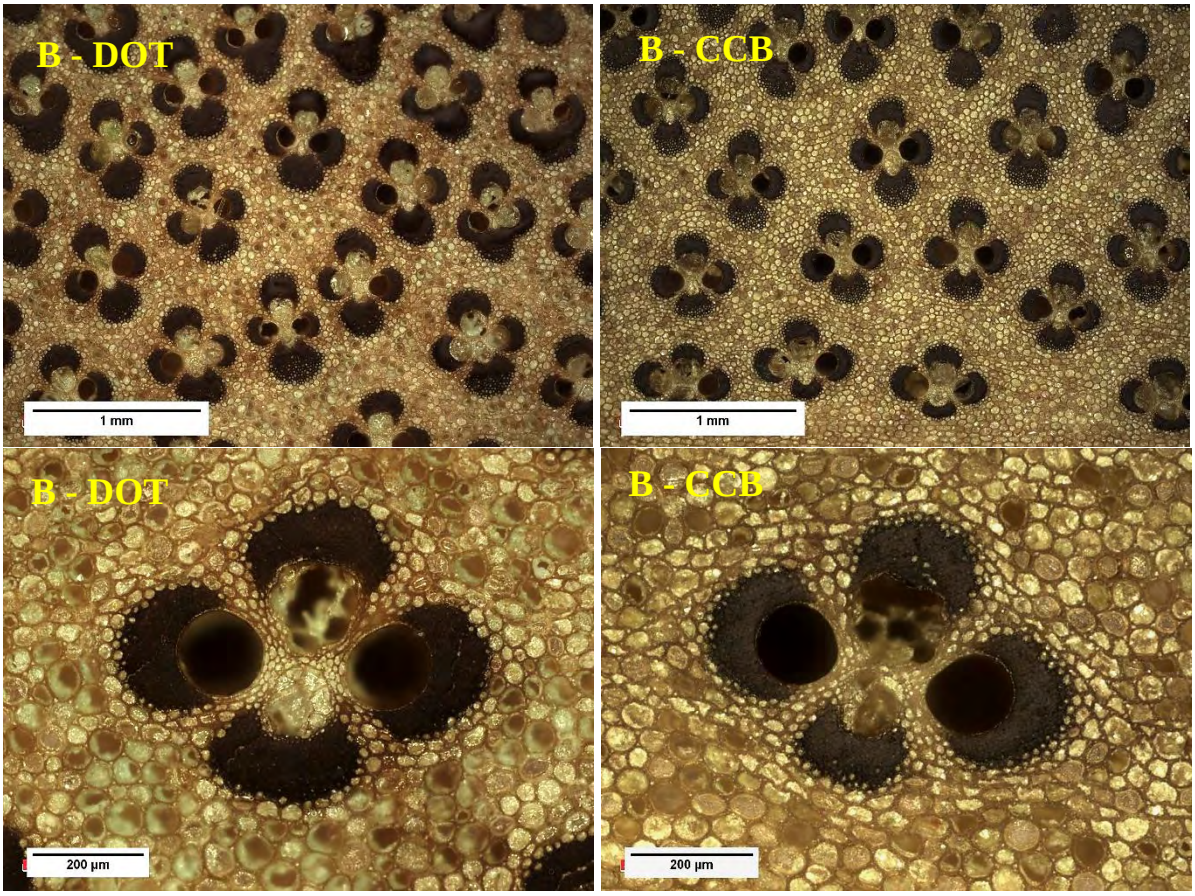

Source: (GAUSS et al., 2020)

Using SEM for the evaluation of a section parallel to the fibres, it is also possible to identify the main bamboo microstructural elements, i.e. parenchyma, vessels and fibre bundles, as shown in Figure 6. In this image, the structure of the vessel, including the pit openings on the inner surface of the vessel, can be clearly observed. The SEM images of CCB and DOT treated samples also do not show any visual difference in the parenchyma cells close to the vessel (Figure 3.12).

Elemental analysis using Energy Dispersive Spectroscopy (EDS) was performed to evaluate the distribution of the active ingredients through bamboo's microstructure. This technique has some limitations and is unable to detect light elements such as boron and sodium. Therefore, only the samples treated with CCB could be characterized. Figure 3.13 shows an elemental map and the corresponding tables of the semi-quantitative analysis of regions composed of parenchyma, vessels and fibres. It can be seen that most of the chromium and copper, in the form of CrO_3 and CuO, is concentrated in the large vessels (point 1 in the upper image). The entire analysed area of this image showed atomic weights of chromium and copper of 1.56% and 1.89%, respectively, whereas for the large vessel much higher values (Cr=12.47% and Cu=17.86%) were observed. Only traces of the elements were found in the fibres and parenchyma (points 2 and 3). The same effect can be observed in the lower image of Figure 3.13. Although the atomic weights of chromium and copper in the entire area are 3.49% and 4.05%, respectively, the two large vessels (points 1 and 2) presented significantly higher values of these elements. In this image, the phloem (point 3) presented similar values of chromium and copper in comparison with the entire area, but significantly lower than the large vessels. The phloem consists of large thin-walled sieve tubes with small cells, and it is used for the conduction of carbohydrates (instead of water that is conducted in the large vessels) (LIESE, 1987). It is assumed that the presence of carbohydrates can affect the penetration of the active ingredients in the phloem.

Although satisfactory retention levels were obtained in the CCB treated samples, there is a heterogeneous distribution of the active ingredients that cannot be detected by the penetration or retention tests. This poor distribution is explained by the low mobility of large and heavy elements such as chromium and copper in the bamboo microstructure. Additionally, there are no pathways for radial penetration in bamboo, like the rays in wood. The metaxylem

vessels of the vascular bundles are the main path for penetration and access to the parenchyma is difficult (LIESE, 2004; LIESE; TANG, 2015b).

The bamboo borer beetle (*Dinoderus minutus*), one of the main insects responsible for bamboo deterioration, lays its eggs on metaxylem vessels (GARCIA; MORRELL, 2009; WATANABE; YANASE; FUJII, 2015). Because the active ingredients are concentrated in the vessels, larval growth of the beetle is expected to be affected by the copper and chromium elements found in these regions and hence, prevent further insect infestation or new attacks. However, this assumption still needs to be validated in a controlled experiment to determine whether the concentration of active ingredients in the vessels prevents larval growth.

Figure 3.12 - SEM image of the longitudinal section parallel to the fibres of P. edulis bamboo showing its main constituents (upper image) and the parenchyma region of DOT and CCB-treated samples (lower images)

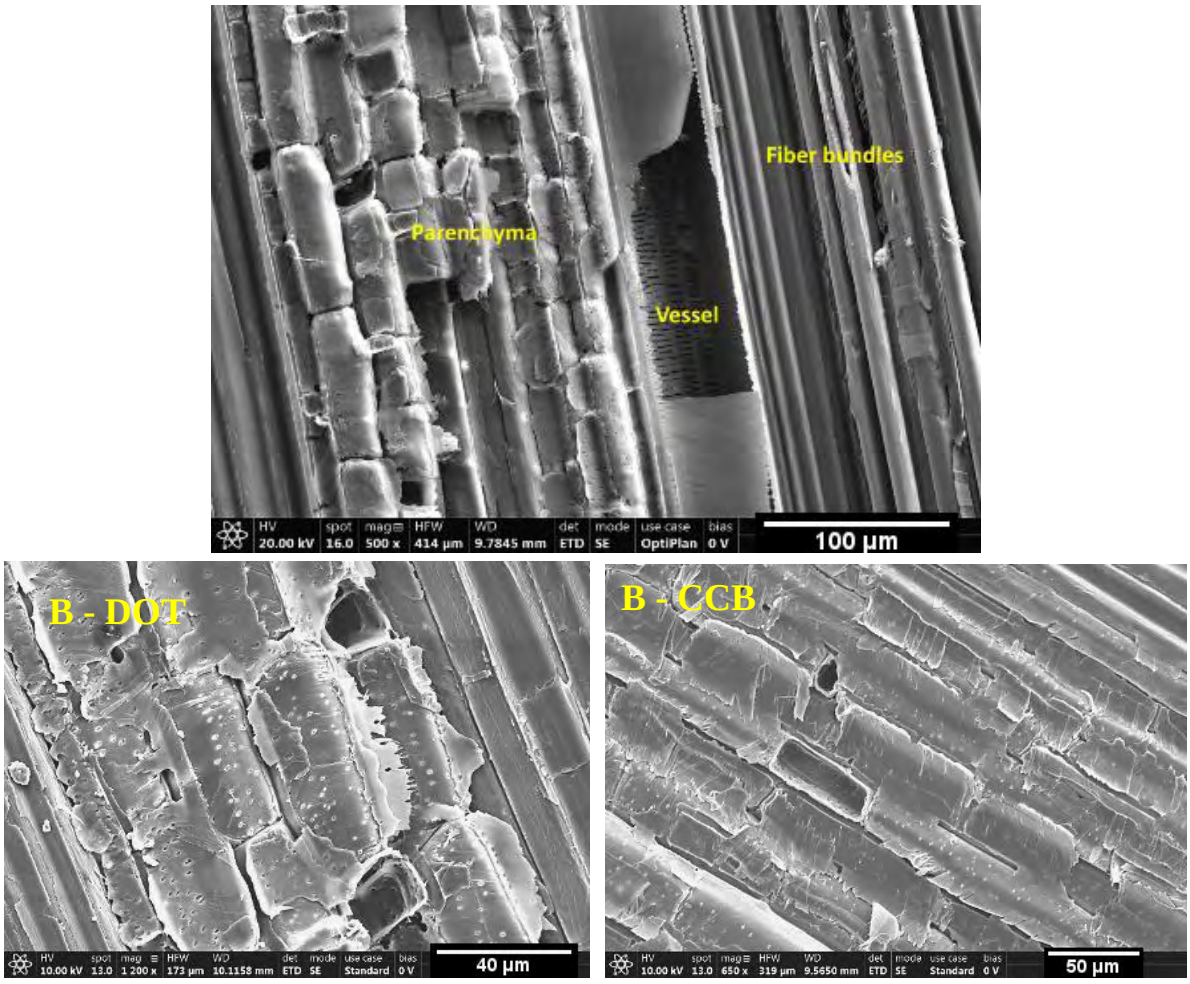

Source: (GAUSS et al., 2020)

Figure 3.13 - EDS mapping of a sample treated with CCB showing the higher concentration of chromium-Cr (yellow dots in right image) and copper-Cu (red dots) in the large vessels (LV) and phloem (PH) of the bamboo structure.

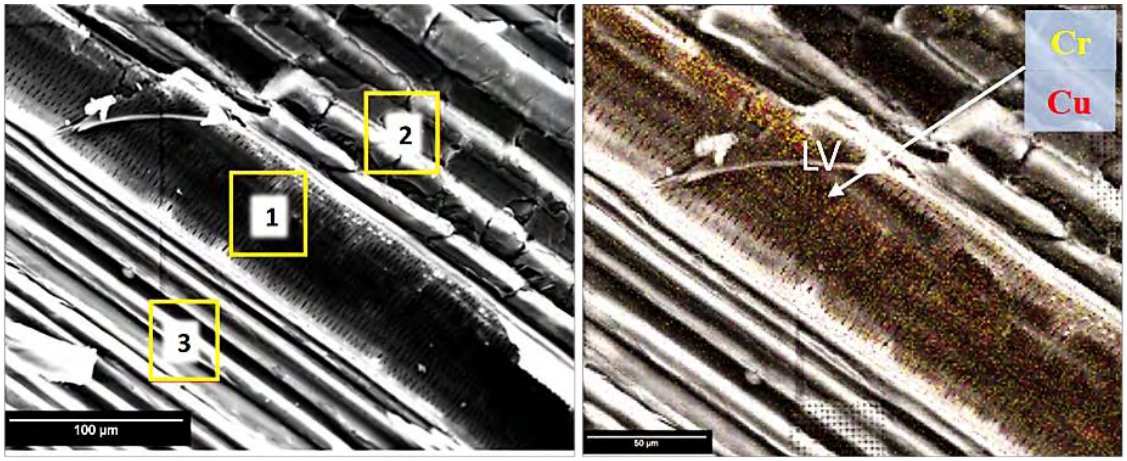

Element	Entire area		1 large vessel (LV)		2 parenchyma		3 fibre bundle	
	Weight (%)	Atomic (%)	Weight (%)	Atomic (%)	Weight (%)	Atomic (%)	Weight (%)	Atomic (%)
C	55.25	63.53	45.26	64.8	60.79	67.85	60.97	67.65
O	41.29	35.64	24.41	26.24	38.00	31.84	38.76	32.28
Cr	1.56	0.41	12.47	4.13	1.22	0.31	0.15	0.04
Cu	1.89	0.41	17.86	4.83	-	-	0.12	0.03

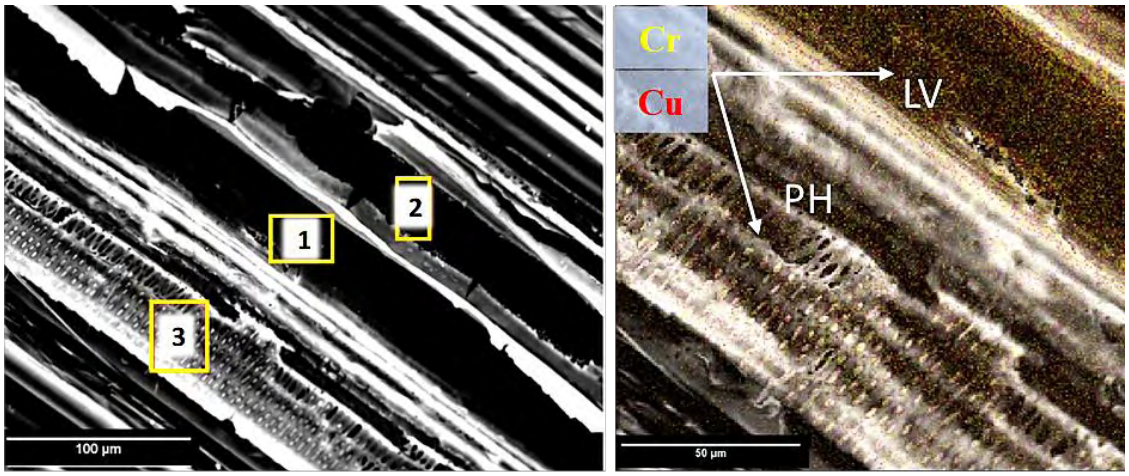

Element	Entire area		1 large vessel (LV)		2 large vessel		3 phloem (PH)	
	Weight (%)	Atomic (%)	Weight (%)	Atomic (%)	Weight (%)	Atomic (%)	Weight (%)	Atomic (%)
C	52.85	62.80	34.93	57.03	21.77	49.59	57.24	66.66
O	39.61	35.34	23.52	28.82	10.90	18.63	36.35	31.78
Cr	3.49	0.96	19.33	7.29	29.21	15.37	2.99	0.80
Cu	4.05	0.91	22.22	6.86	38.13	16.42	3.42	0.75

Source: (GAUSS et al., 2020)

3.2.3.3. Mechanical characterization

Results of the mechanical characterization tests are presented in Table 3.8 and summarized in Figure 3.14. In addition to strength (*f*) and modulus (E and G), the limit of proportionality (LOP) is reported. This value describes the stress at which the material ceases to behave in a linear manner having the modulus shown.

As seen in Table 3.8, there is little difference between A-DOT and B-DOT beyond the normal variation expected in bamboo material properties. An ANOVA analysis of the results of B-DOT and B-CCB indicates no significant (defined at 95% confidence) difference between the DOT and CCB treated samples for most mechanical properties. Only in compression (f_c and LOP) and shear (f_v) was observed a p-value < 0.05. These differences, however, are more a reflection of the relatively small coefficients of variation seen in this study than a real difference in material strength; this is seen in Figure 3.14. In fact, analysing the LOP in compression, shear and bending, the values obtained for B-DOT and B-CCB are practically the same.

Saikia et al (2015) investigated the tension and bending strength of three different bamboo species (*B. tulda*, *D. giganteus* and *B. balcoa*) treated with CCB and a new bio-chemical treatment. Although no information regarding retention and penetration of the active ingredients is reported, It was found that CCB treated and untreated samples had similar values of ultimate tensile and flexural strength, in samples exposed in environmental conditions for 6 months (SAIKIA et al., 2015). The treatment with DOT also does not negatively affect the mechanical properties of bamboo. In fact, a small increase of flexural and compression strength was observed in *D. asper* bamboo samples with high retentions of DOT (GAUSS; KADIVAR; SAVASTANO JR, 2019).

To the best of our knowledge, no paper was found addressing all the mechanical characterization used in this work. Nevertheless, some mechanical properties of *P. edulis* bamboo available in the open literature are consistent with the results shown in Table 2 (considering the average of all the samples). For compression and shear strength parallel to the fibres, values of f_c between 46.0 – 48.1 MPa and f_v between 11.2 – 15.9 MPa are reported (in this work the average f_c and f_v are 57.9 and 18.0 MPa, respectively) (XU et al., 2014; HUANG; HSE; SHUPE, 2015; DENG et al., 2016; AKINBADE et al., 2019). Dixon et al., using *P. edulis*

samples of density similar to this work, reported modulus of rupture and modulus of elasticity in bending of f_b=215 MPa and E_b=16,680 MPa, respectively (DIXON et al., 2015).

3.2.3.3.1. Characteristic Properties

Since no difference is found in properties of DOT- and CCB-treated bamboo, taking all data together (A-DOT + B-DOT + B-CCB), a sufficiently large sample (taken from 17 randomly selected culms of the original batch of 140 culms) is available to assess characteristic material properties suitable for design.

For strength, the characteristic value is defined as the 5th percentile value determined with 75% confidence (ISO 22156:2004) and for modulus, the mean value established with 75% confidence is used (ISO CD 22156:2019). The calculated characteristic values are shown in Table 2 and graphically compared with the mechanical properties of B-DOT and B-CCB samples in Figure 8.

Figure 3.14 - Comparison between DOT and CCB treated samples. The characteristic values are presented as red bars (denser pattern).

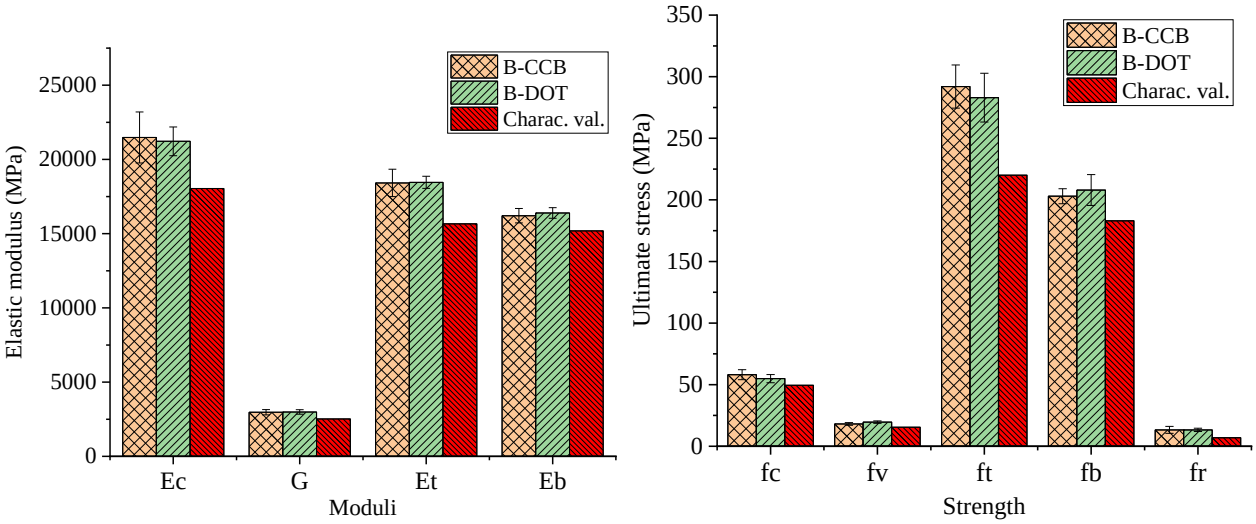

Ec=modulus of elasticity in compression; G=shear modulus; Et=modulus of elasticity in tension; Eb=modulus of elasticity in bending; fc=compression strength; fv=shear strength; ft=tensile strength; fb=modulus of rupture in bending; fr=transversal tensile strength. (Error bars represent ± 1 standard deviation)

Source: (GAUSS et al., 2020)

Table 3.8 - Summary of experimentally determined material properties (COV in parentheses). MC = Moisture content

Standard / Properties		A-DOT	B-DOT	B-CCB	B-DOT B-CCB *p*-value	A-DOT + B-DOT + B-CCB	Characteristic value
density (g/cm^3)		0.81	0.80	0.83	-	0.81	-
Compression // fiber (ISO 22157:2019)	n	24	15	16	-	55	-
	MC (%)	9.9 (0.04)	10.2 (0.02)	10.4 (0.03)	-	-	-
	f_c (MPa)	59.8 (0.10)	54.9 (0.06)	58.1 (0.07)	0.030	57.9 (0.08)	49.5
	E_c (GPa)	19.07 (0.11)	21.22 (0.09)	21.48 (0.08)	0.690	20.38 (0.10)	18.04
	LOP (MPa)	50.9 (0.12)	49.1 (0.06)	52.9 (0.08)	0.039	50.7 (0.10)	41.5
Shear // fiber (ISO 22157:2019)	n	25	9	15	-	49	-
	MC (%)	10.6 (0.03)	9.7 (0.01)	10.0 (0.02)	-	-	-
	f_v (MPa)	17.5 (0.08)	19.6 (0.05)	18.1 (0.06)	0.003	18.1 (0.08)	15.4
	G (GPa)	2.71 (0.10)	2.99 (0.10)	2.97 (0.06)	0.550	2.84 (0.10)	2.52
	LOP (MPa)	12.2 (0.09)	12.1 (0.08)	12.3 (0.11)	0.703	12.2 (0.09)	10.0
Tensile // fibers (ISO 22517:2019)	n	20	19	18	-	57	-
	MC (%)	6.8	6.9	6.8	-	-	-
	f_t (MPa)	247 (0.08)	283 (0.07)	292 (0.06)	0.466	275 (0.11)	220
	E_t (GPa)	15.83 (0.08)	18.31 (0.04)	18.42 (0.05)	0.894	17.47 (0.09)	15.66
Three-point bending (ASTM D7264)	n	18	18	18	-	54	-
	MC (%)	7.6 (0.07)	6.8 (0.07)	7.6 (0.08)	-	-	-
	MOR (MPa)	202 (0.07)	208 (0.06)	203 (0.03)	0.165	205 (0.06)	183
	MOE (GPa)	16.21 (0.07)	16.55 (0.05)	16.21 (0.03)	0.584	16.32 (0.06)	15.19
	LOP (MPa)	123 (0.07)	125 (0.06)	125 (0.06)	0.750	124 (0.06)	110
Flat-ring flexure (Virgo et al. 2018)	n	13	7	8	-	28	-
	MC%	9.5 (0.05)	9.7 (0.04)	9.7 (0.08)	-	-	-
	f_r (MPa)	10.7 (0.27)	13.3 (0.10)	13.3 (0.21)	0.989	12.1 (0.23)	6.9

Source: Author's authorship.

3.2.4. Conclusions

The treatment and mechanical properties of *P. edulis* bamboo treated with DOT and CCB were assessed. Penetration and retention assessment and microstructural analyses were conducted to investigate the efficacy of the treatment processes. Mechanical testing of treated samples was used to compare the resulting bamboo material properties after treatment. The following conclusions were drawn:

- The bamboo treated with CCB by a full-cell process exhibited higher retentions values than the bamboo treated with DOT by immersion: 7.2 kg/m^3 and 2.2 kg/m^3, respectively. Good penetration (between 50-100%) was observed in both cases.

- Microstructural analysis using optical and scanning electron microscopy showed no visual differences on the vessels and parenchyma cells between treatment conditions. Elemental analysis using EDS revealed a higher concentration of copper and chromium elements in the conducting vessels of the bamboo treated with CCB. Only traces of these elements were found in the parenchyma cells and fibre bundles.

- Compression, tension (parallel and transverse to fibres), bending, and shear properties were not affected by the treatment procedures. The quality assessment of samples treated with DOT demonstrated low variation in all the investigated mechanical tests, suggesting a uniform mechanical properties distribution within the batch of *P. edulis* bamboo used in this study.

- Combining all the investigated conditions, characteristic values of compression, tension, shear and bending were calculated according to ISO 22156-04: f_c=49.5 MPa; E_c=18,040 MPa; f_v=15.4 MPa; G=2520 MPa; f_t=220 MPa; E_t=15,660 MPa; f_b=183 MPa; E_b=15,190 MPa.

Today, bamboo remains primarily an “informal” structural material. Although standards are available for structural design, in comparison with other conventional materials, there is little or no guidance available regarding quality control of commercially treated bamboo poles. It is recommended that bamboo poles used for structural applications should be subject to a quality control protocol based on treatment evaluation (retention and penetration) and mechanical properties in order to reduce risks and improve the efficient use of bamboo as a load-bearing structural material.

3.3. Use of ISO 22157 mechanical test methods and the characterisation of Brazilian *P. edulis* bamboo

3.3.1. Introduction

In 2004, the International Organisation for Standardisation (ISO) promulgated ISO 22157:2004 *Bamboo – Determination of physical and Mechanical Properties.* The development of this test methods Standard (ISO 22157-1:2004) and accompanying *Laboratory Manual* (ISO 22157-2:2004) had as its aim "to bring bamboo towards the level of an internationally recognised and accepted building material and engineering material… in favour of the well-being of lower-income groups in developing countries, and in favour of a better environment in bamboo-growing countries." The development of ISO 22157:2004 initiated as early as 1988 and the initial draft, established in 1998 (INBAR, 1999), was the work of a handful of dedicated individuals – who are dutifully acknowledged in the 2004 ISO Standard. The accompanying Laboratory Manual has as its aim "to give a practical 'how to do' explanation on how to perform tests according in the ISO 22157-1.". Since 2004, ISO 22157:2004 has been used internationally, formally adopted by at least eight[2] countries and anecdotally known to be used more broadly. While an imperfect measure of industry penetration and use, as of July 2019, Google Scholar identifies 291 citations on searches of "ISO 22157" and "ISO Standard 22157". In 2019, a significantly revised ISO 22157:2019 was published and the *Laboratory Manual* withdrawn.

ISO 22157:2004 includes four mechanical property tests: a) full-culm longitudinal compressive strength; b) longitudinal tensile strength using a "dogbone" specimen taken from the culm wall; c) flexural capacity based on a three-point bend test of a long length of culm; and d) longitudinal shear using the "bowtie test" (JANSSEN, 1981). The Standard also provides guidelines for determining moisture content by drying, mass by volume, and shrinkage of bamboo.

The recently revised version, ISO 22157:2019, leveraged the considerable recent experience with bamboo materials which partially stemmed from the 2004 publication of ISO

[2] Colombia (NTC 5525), Ecuador (NTE INEN-ISO(DIS) 22157, Jamaica (JS ISO 22157), Vietnam (TCVN 8168), the Philippines (PNS ISO 22157), Netherlands (NEN-ISO 22157), Peru (Norma ISO/TC165/N315), India (IS 6874)

22157. The 2019 revision added two mechanical property tests: e) tension perpendicular to fibres (MITCH; HARRIES; SHARMA, 2010); and f) bending perpendicular to fibres (so-called circumferential compression) (SHARMA; HARRIES; GHAVAMI, 2013). In addition, moisture content by calibrated moisture meter and mass by culm length were added and existing mechanical tests (a) through d), above) were extensively revised. The 2004 method for determining shrinkage was withdrawn as a method that could not be practically performed.

Other mechanical test methods often used for bamboo materials but not [yet] included in ISO 22157 include g) interlaminar shear by tension (MOREIRA, 1991; INBAR, 1999); h) perpendicular shear (CRUZ, 2002); i) pin shear (JANSSEN, 1981; SHARMA, 2010); j) flat-ring flexure (VIRGO et al., 2018); and, k) small sample flexure (based on ASTM D7264 test method). A summary review of mechanical test methods a) through i) is provided in (HARRIES; SHARMA; RICHARD, 2012).

3.3.1.1. Selection of bamboo materials test methods

Those conducting material tests of bamboo may have limited access to complex test apparatuses. Nonetheless, "standard" testing needs to be just that: standard. Repeatability and minimising inter-laboratory variation to the greatest extent possible is critical so that a description of bamboo materials is as uniform as possible: creating a *lingua franca* among practitioners, as it were (HARRIES; BEN ALON; SHARMA, 2019). Simple test methods are those that a) require minimal specimen preparation; b) do not require a complex test apparatus; and, c) are based on applying compression forces (HARRIES; SHARMA; RICHARD, 2012).

Due to the dimensional variability and curved shape of bamboo, extracted test specimens are often not symmetric or require some of the material to be lost during specimen fabrication; in a functionally graded material such as bamboo, this may result in test specimens that do not represent the material as it is used *in situ*. Thus, full-culm section specimens should be preferred for obtaining material properties reflective of *in situ* properties. A simple test apparatus will mitigate operator bias and accommodate the variable geometry of bamboo specimens. Finally, compression-based tests are simple to conduct and can often be carried out with quite fundamental instrumentation (GLUCKSMAN; HARRIES, 2015). Tension-based tests, on the

other hand, require fixtures to interface with the highly anisotropic bamboo that can bias test results.

3.3.1.2. Objectives of study

The objective of this paper is to describe the use of bamboo material characterisation tests and identify some factors affecting the performance of these. Using digital image correlation (DIC), the behaviour of the tests specimens, their interaction with boundary conditions, and the progression of damage during testing is illustrated. Understanding specimen behaviour will lead to more robust mechanical testing practice. In addressing these objectives, an example of the mechanical characterisation of a batch of Brazilian *P. edulis* is described.

3.3.2. Bamboo materials

Phyllostachys edulis (Moso) bamboo was obtained from a supplier near Sao Paulo, Brazil. Approximately 140 culms between 3 and 5 years of age were harvested and subsequently treated (as described in section 3.2) from which 4 m long poles were extracted. The diameters ranged from 80 to 100 mm, wall thickness from 6 to 9 mm and the average oven-dry density prior to treatment was 760 kg/m^3. Image analysis determined an average fibre bundle content of 29%.

The bamboo reported in this study was also subject of a study of treatment processes, as reported in the previous section. The specimens were treated in one of the following manners:

- culms were treated with chromated copper borate (CCB) in a pressure vessel using a vacuum (-600 mmHg for 30 min.) – pressure (10 kgf/cm^2 for 60 min.) – vacuum (-600 mmHg for 30 min.) process.
- culms were treated by seven- to ten-day immersion in an 8% concentration of agricultural grade disodium octaborate tetrahydrate (DOT).

Description of each treatment study was presented in the previous section. Analysis of variation (ANOVA) of all data indicated that the effect of the treatment conditions had no significant effect on the mechanical properties of bamboo. All mechanical properties reported in this study were found to fall within the 95% confidence interval band and have a normal

distribution irrespective of treatment. Therefore, in support of the objectives of this paper, data from the treatment processes have been combined. The density of the treated *P. edulis* specimens was found to be 810 kg/m^3 (COV = 0.05), also using the method of ISO 22157:2019. For all tests, moisture content at the time of testing was determined using the oven-method of ISO 22157:2019 and ranged from 7% to 10%.

3.3.3. Test methods

Test specimen sampling was random within the batch described (resulting in 17 poles from the batch of 140). Full culm section specimens were used for compression and shear tests while machined coupons were used for tension and small coupon bending.

3.3.3.1. Full culm compression parallel to fibres

Full culm compression tests based on that prescribed by ISO 22157:2019 were conducted. Apart from some minor revisions (none affecting the samples tested in this study), the conduct of this test is the same as ISO 22157:2004. ISO 22157 specifies "The length of the specimen shall be taken as the lesser of the outer diameter, *D*, or 10 times the wall thickness, 10t. For the *P. edulis* specimens reported these values were essentially the same: the average values of *D* and *t* of the compression specimens were 78.3 mm (COV = 0.04) and 7.23 mm (COV = 0.09), respectively. For this study, specimen length (77.9 mm; COV = 0.04) was taken as the culm diameter, in all cases. ISO 22157:2019 requires an "intermediate layer" be placed at both ends of the specimen in order to minimise friction, causing radial restraint of the specimen ends. Compliant with ISO 22157:2019, sulphur 'capping compound' was used as shown in Figure 3.15a. The applied load was determined from the test machine load cell and all other strain data was determined using digital image correlation (DIC) techniques described below. A total of 55 specimens, 41 internode and 14 with a node at their mid height, were tested. Compression strength parallel to the fibres is calculated from test results as:

$$f_c = F/A_{culm} \qquad \text{Eq. 3.6}$$

In which F is the applied axial load and $A_{culm} = \pi/4 \times [D^2 - (D - 2t)^2]$ is the cross sectional area of the culm. Compression modulus, E_c, is determined from DIC analysis.

3.3.3.2. Full culm shear parallel to fibres

The so-called 'bowtie' shear test was developed by Janssen (1981) and is standardised in ISO 22157:2019. Apart from a minor revision (again, not affecting the samples tested in this study) this test is identical to the ISO 22157:2004. In this test (Figure 3.15b), the full culm specimen (having the same dimensional requirements as the compression test) is supported at its lower end over two opposing quadrants, and loaded at its upper end over the other two opposing quadrants. In this manner, loading the specimen results in four shear areas (a typical failure is seen in Figure 3.15b). Specimens were generally sampled immediately adjacent compression specimens, therefore dimensions are essentially identical: average specimen length was 77.3 mm (COV = 0.03) and diameter and culm thickness were 78.1 mm (COV = 0.03) and 7.28 mm (COV = 0.08), respectively. Applied load was determined from the test machine load cell and all other strain data was determined using DIC. A total of 49 specimens, 36 internode and 13 with a node at their mid height, were tested.
Shear strength parallel to the fibres is calculated from test results as:

$$f_v = F/4Lt \qquad \text{Eq. 3.7}$$

in which F is the applied load and $L \times t$ is the area of each shear plane (L is specimen length and t is culm wall thickness). The test is controlled by the first shear plane to fail and therefore f_v is interpreted as the lower bound shear strength. Shear modulus, G, is determined from DIC analysis.

3.3.3.3. Tension parallel to fibres test

Significant revisions were made to the ISO 22157 tension test between 2004 and 2019. In ISO 22157:2019 the specimen orientation as it is cut from the culm and subsequently tabbed is specified (as seen in Figure 3.15c). Additionally, rotationally-restrained boundary conditions

of the test machine were as specified in ISO 22157:2019. Both specimen orientation and boundary conditions were shown by Richard and Harries (2015) to significantly impact tension test results due to the graded nature of the culm wall (RICHARD; HARRIES, 2015). ISO 22157:2019 standardises these parameters; the present tests are compliant with ISO 22157:2019.

Specimens were extracted from culm walls as shown in Figure 3.15c. The average wall thickness, t = 7.07 mm (COV = 0.10) and the average specimen breadth, b = 2.68 mm (COV = 0.16). All specimens were 200 mm long and had a gauge length of 100 mm as shown in Figure 3.15c. Applied load was determined from the test machine load cell. In addition to DIC, an external 50 mm gauge length extensometer (seen in Figure 3.15c) was used to determine tensile modulus and validate DIC data. A total of 84 specimens, 57 internode and 27 with a node in the middle of the gauge length, were tested.

Tension strength parallel to the fibres is calculated from test results as:

$$f_t = F/A \quad \text{Eq. 3.8}$$

in which F is the applied axial load and $A = bt$ is the cross-sectional area of the gauge length of the specimen. Tension modulus, E_t, is determined from DIC analysis or using an external extensometer as:

$$E_t = \Delta f_t/\Delta\varepsilon \quad \text{Eq. 3.9}$$

Where the change in stress (f_t) and measured strain (ε) is taken only between two points in the elastic region of behaviour (i.e., below any observed limit of proportionality).

3.3.3.4. Small coupon bending

ISO 22157 promulgates a full-culm bending test but not a small coupon bending test. The full-culm test can be difficult to conduct – requiring a long specimen (a minimum span length of 30D is prescribed) which corresponds to large deflections requiring a versatile test arrangement and a series of ‘saddles’ to conduct the test. Additionally, ISO 22157 is silent on how taper (D and/or t) over the long specimen length should be limited and how this will affect results. Richard et al. (2017) argue that even at a length of 30D, the ISO 22157 full-culm flexure test does not determine modulus of rupture, but rather the member flexural capacity of the culm being tested (RICHARD et al., 2017). This capacity is rarely governed by compression or

tension behaviour but is most always governed by longitudinal shear of the culm in flexure which itself is a mixed mode of failure due to the stress state of the culm. Trujillo et al. (2017) proposed that the full-culm flexure test is appropriate for grading schema (ISO 19624:2018) based on member capacity (TRUJILLO; JANGRA; GIBSON, 2017). Nonetheless, the test does not provide a meaningful stress that may be used in a stress-based design.

For these reasons, like some other researchers, a small coupon flexural test is adopted (GOTTRON; HARRIES; XU, 2014; RICHARD et al., 2017). In the longitudinal direction, bamboo is often described as a unidirectional fibre-reinforced material. For this reason, *ASTM* D7264 – 15 Standard Test Method for Flexural Properties of Polymer Matrix Composite *Materials* was adopted. A three-point bending test (Figure 3.15d; ASTM D7264 Procedure A) was selected in order to maximise the test shear span and therefore minimise the effects of shear.

Bending specimens were extracted from culm walls as shown in Figure 3.15c. However, for flexure, b is greater than t and bending is about an axis perpendicular to the dimension t. Due to the curvature of the culm wall, the coupons are sanded flat in their through-thickness direction. The average resulting specimen dimensions were, t = 6.57 mm (COV = 0.08) and b = 9.95 mm (COV = 0.06). Coupons were 200 mm long and tested in three-point bending over a span length of 160 mm. The average shear span to depth ratio exceeded 10 in every test (average was 12.3 (COV = 0.09)); this exceeds the minimum recommended ratio of 8 (ASTM D7264).

Two test orientations are possible (Figure 3.15d) resulting the outer culm wall being in compression (OC) or in tension (OT); 54 tests of the former and 10 of the latter were conducted. In addition, 24 specimens having a node at midspan were tested; these were conducted in the OC orientation in every case.

The modulus of rupture based on an assumption of a homogeneous material is determined as:

$$MOR = 3FL/2wt^2 \qquad \text{Eq. 3.10}$$

where F is the maximum applied load at midspan, L is the simple test span and w and t are specimen width and depth, respectively.

The apparent axial modulus of the homogeneous specimen derived from bending, MOE, is determined from the midspan displacement, Δ. For three-point bending:

$$MOE = FL^3/4\Delta wt^3 \qquad \text{Eq. 3.11}$$

More complex analysis of the test is possible using data from DIC; this will be described in the discussion of results, below.

3.3.3.5. Digital image correlation

Digital image correlation (DIC) is a well-established contact-free means of obtaining full-field surface deformations (and therefore strains). Specimens are painted with a speckle pattern prior to testing (photocopier toner broadcast onto wet white spray paint, the result is seen in Figure 3.15a. During the test, consecutive high-resolution images (2448 x 2049 pixels) are taken every 0.5 sec. and deformation patterns (based on sampling of the speckle pattern) are recorded. Post-processing allows relative displacements and specified strain fields to be obtained in three dimensions. The system used in this study is a VIC-3D dual camera system and DIC processing software (Correlated Solutions). The advantage of a dual camera system when viewing full-culm bamboo is that the strain field can be accurately obtained on the curved surface of the bamboo. The resolution of DIC data is a function of the field of view and camera resolution. For the small material samples tested in this study, theoretical strain resolution better than 1 microstrain is obtained; nonetheless strains are reported with a precision of 10 microstrain. Subsequent figures show a variety of DIC-obtained images that will be discussed below.

Figure 3.15 - Bamboo test methods.

a) compression specimen showing sulphur capping and DIC speckle pattern. Specimen height is approximately 90 mm.

b) "bowtie" test set-up and typical specimen failure. Specimen height is approximately 90 mm.

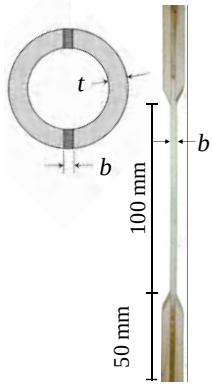

c) test specimen geometry and test set-up showing DIC speckling and extensometer

Outer culm wall in compression (OC)

Outer culm wall in tension (OT)

d) three-point bending test of coupon and specimen orientation. Flexural span is 160 mm and specimen depth is approximately 7 mm

Source: (GAUSS; SAVASTANO; HARRIES, 2019)

3.3.4. Test results

ANOVA analysis of all data indicated that mechanical properties reported in this study were found to fall within the 95% confidence interval band for having a normal distribution.

3.3.4.1. Full culm compression parallel to fibres

A summary of full culm compression test results is given in Table 3.9. Representative compressive stress versus strain data is shown Figure 3.16a. The strain shown in Figure 3.16 is obtained by DIC as the axial (longitudinal) strain 'averaged' over a vertical section (shown by dotted lines in Figures 3.16b and 3.16c). As is typical with a correctly executed test, the stress-strain behaviour shown in Figure 3.16a is essentially linear to failure. The strain fields at lower load levels are uniform over the specimen. As the stress approaches ultimate, restraint from the loading platens results in larger axial strains near the middle of the specimen (Figure 3.16b); typically, the specimen will bulge-out at this location and eventually split. Once split, the linear behaviour of the compression stress-strain curve will typically become negligible (Figure 3.16a, post-peak behaviour). The effect of the initiation of splitting is seen in Figure 3.16b: near the bottom of the specimen to the right of the dotted line, a small region of low axial strain is forming. Nonlinear behaviour may also result from uneven loading of the culm end; this was generally not seen in this study since sulphur capping compound was used. Using a sulphur capping compound (as is used for testing reinforced concrete cylinders) largely addresses uneven loading as the capping results in uniform distribution of force to the culm and, if done correctly, results in parallel specimen end surfaces. The capping compound provides a low friction interface and relatively little lateral restraint from the thin layer of material. To minimise restraint, once capped, the material in the culm annulus (internal diameter, no contact with the culm wall) can be broken leaving only the culm walls capped.

The limit of proportionality (LOP) is defined as the limit of observed elastic behaviour (see Figure 3.16a for example). A relatively high LOP indicates a good test procedure likely to yield a representative value of bamboo compression strength. As described above, behaviour beyond the LOP, is indicative of other mechanisms of failure.

As shown in Table 3.9, neither compression capacity, modulus of elasticity or LOP are affected by the presence of a node. Indeed, considering the natural variation present, tests with and without nodes cannot be statistically distinguished (see unpaired t-test *p*-values shown in Table 3.9). Locally, however, the node is seen to be stiffer than the surrounding internode region. As seen in Figure 3.16c, the local compressive strain at the node is to about one half the average

strain over the height of the specimen. The behaviour affected by the presence of the node is discussed further below.

Table 3.9 - Full culm compression parallel to fibre test results.

	Internode specimen			Specimen with node			*p*-value	All specimens		
	n	average	COV	n	average	COV		n	average	COV
f_c, MPa	41	57.5	0.09	14	59.5	0.06	0.19	55	57.9	0.08
E_c, GPa		20.30	0.10		20.64	0.12	0.61		20.38	0.10
LOP, MPa		50.9 0.89f_c	0.10		50.1 0.84f_c	0.10	0.90		50.7 0.88f_c	0.10
NOTES:	Moisture content = 10.2% (COV = 0.04) Specimens sampled from 17 different culms *p*-value from unpaired t-test comparing internode specimens to specimens with nodes									

Source: (GAUSS; SAVASTANO; HARRIES, 2019)

Figure 3.16 - Representative results of longitudinal full-culm compression test (compressive strain shown as positive in this figure).

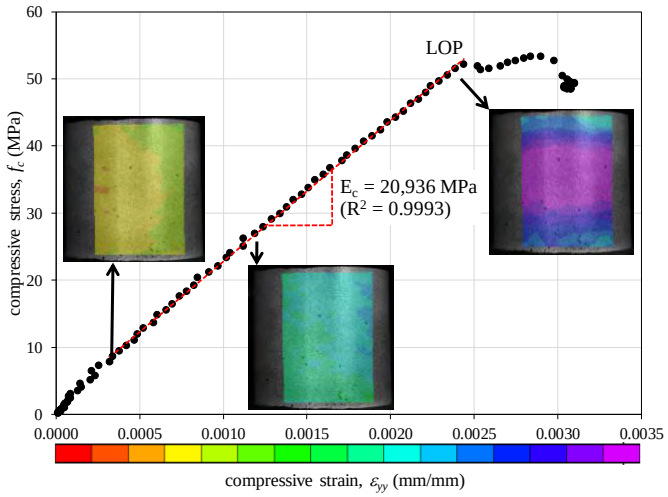

a) longitudinal stress-strain progression of internode compression test

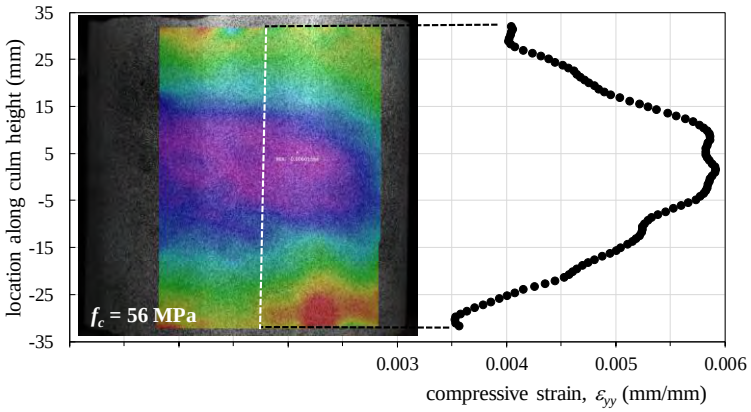

b) longitudinal strain distribution in internode specimen at stress = 56 MPa

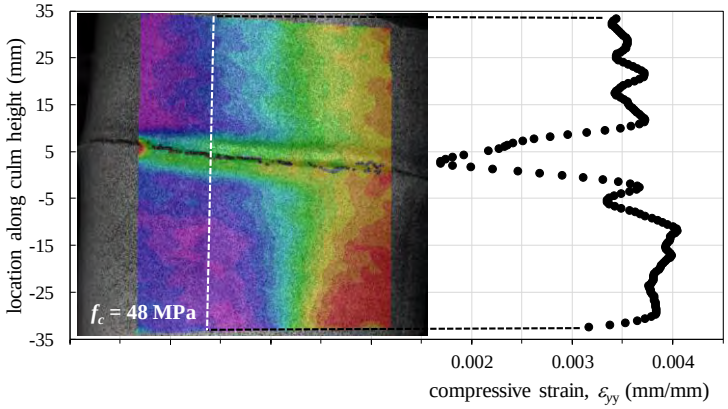

c) longitudinal strain distribution in specimen with node at stress = 48 MPa

Source: (GAUSS; SAVASTANO; HARRIES, 2019)

3.3.4.2. Full culm shear parallel to fibres

A summary of shear test results is given in Table 3.10. Representative shear stress versus strain data is shown Figure 3.17a. The strain shown in Figure 3.17 is obtained by DIC along one of the four shear planes. At lower stress levels, the shear strain is relatively uniformly distributed along the height of the specimen. Similar to compression tests, as the LOP is exceeded, the shear strains tend to increase near the loading platens where the shear cracks and eventual failures initiate. This behaviour results from the stress concentrations at the edges of the loading platens and is clearly seen in Figure 3.17b where the strain at the top and bottom of the specimen is about 40% greater than at mid-height. Due to this stress concentration, the LOP is lower in the shear tests than in compression. Also similar to the compression tests, the presence of the node has no significant effect on the measured capacity (*p*-values, Table 3.10) and a stiffening effect on the local shear response (Figure 3.17c).

Table 3.10 - Full culm shear parallel to fibre test results.

	Internode specimen			Specimen with node			*p*-value	All specimens		
	n	average	COV	n	average	COV		n	average	COV
f_v, MPa	36	18.0	0.08	13	18.1	0.07	0.83	49	18.1	0.08
G, GPa		2.86	0.10		2.79	0.10	0.52		2.84	0.10
LOP, MPa		12.2 $0.68f_v$	0.09		12.2 $0.67f_v$	0.10	1.00		12.2 $0.67f_v$	0.10
NOTES:	Moisture content = 10.3% (COV = 0.04) Specimens sampled from 16 different culms *p*-value from unpaired t-test comparing internode specimens to specimens with nodes									

Source: (GAUSS; SAVASTANO; HARRIES, 2019)

Figure 3.17 - Representative results of longitudinal “bowtie” shear test.

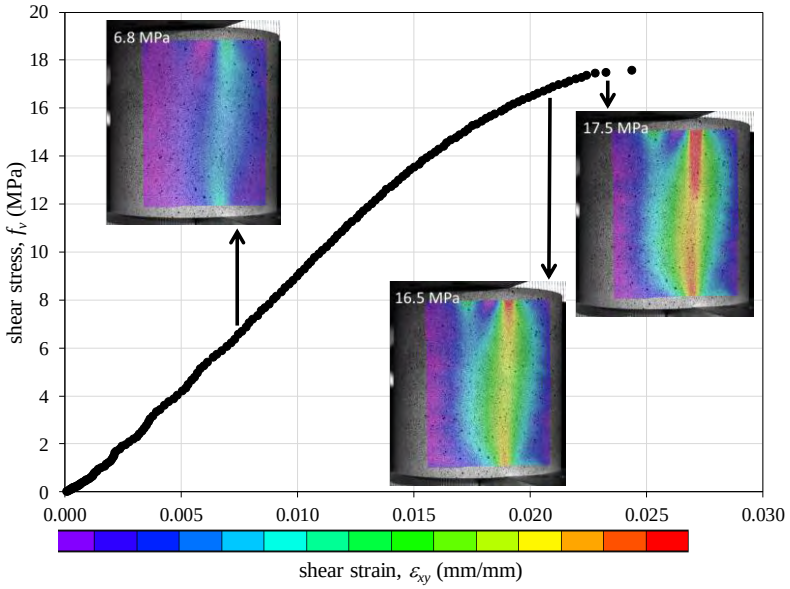

a) shear stress-strain progression of internode shear test

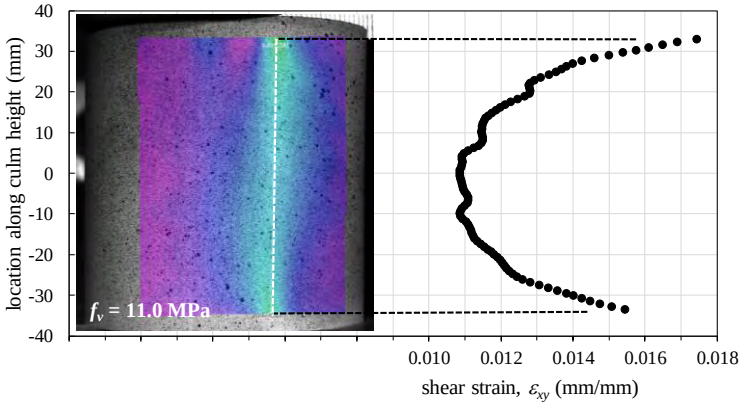

b) shear strain distribution in internode specimen at shear stress = 11.0 MPa

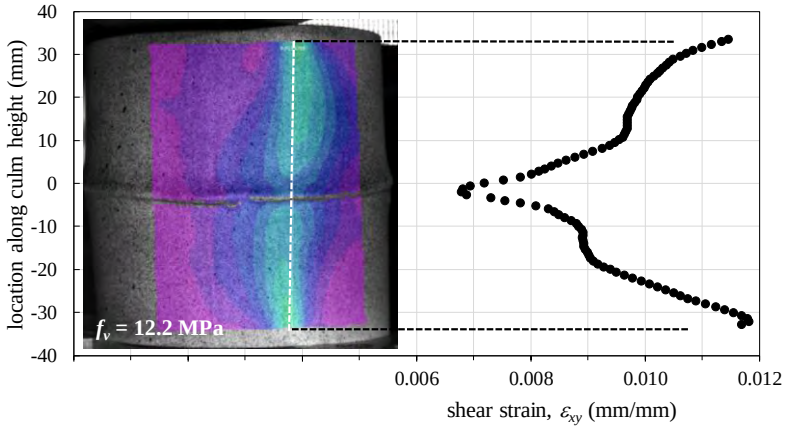

c) shear strain distribution in specimen with node at shear stress = 12.2 MPa

Source: (GAUSS; SAVASTANO; HARRIES, 2019)

3.3.4.3. Tension parallel to fibres test

A summary of tension test results is given in Table 3.11. Representative tension stress versus strain data is shown Figure 3.18a. The preference for the through-culm wall orientation tested using rotationally-restrained boundary conditions (RICHARD; HARRIES, 2015) is evident in Figure 3.18a. There is no apparent strain gradient across or along the 100 mm gauge length. The solid data points in Figure 3.18b, showing the axial strain along the middle 40 mm gauge length indicate some variation but no gradient along the gauge length. The efficacy of the DIC data is validated by the data from the external extensometer from which the average strain over a 50 mm gauge length is determined. The behaviour is essentially linear to a brittle failure; there is no marked difference between LOP and failure. This lack of nonlinearity – even near failure – indicates a failure dominated by fibre rupture.

The effect that the presence of a node has on the tension behaviour is dramatic. In this study, the tensile capacity with a node is approximately 36% of the internode counterpart. While stiffness over the gauge length (including the node) is reduced, the local stiffness of the node itself is significantly lower. As seen in Figure 3.18b, the strain at the node increases about four times over the strain in the adjacent internodes. The behaviour affected by the presence of the node is discussed further below.

Table 3.11 - Tension parallel to fibre test results.

	Internode specimen			Specimen with node			*p*-value
	n	average	COV	n	average	COV	
f_t, MPa	57	275	0.11	27	100	0.20	0.0001
E_t, GPa		17.47	0.09		11.19	0.18	0.0001
NOTES:	Moisture content = 6.8% Specimens sampled from 11 different culms *p*-value from unpaired t-test comparing internode specimens to specimens with nodes						

Source: (GAUSS; SAVASTANO; HARRIES, 2019)

Figure 3.18 - Representative results of tension test.

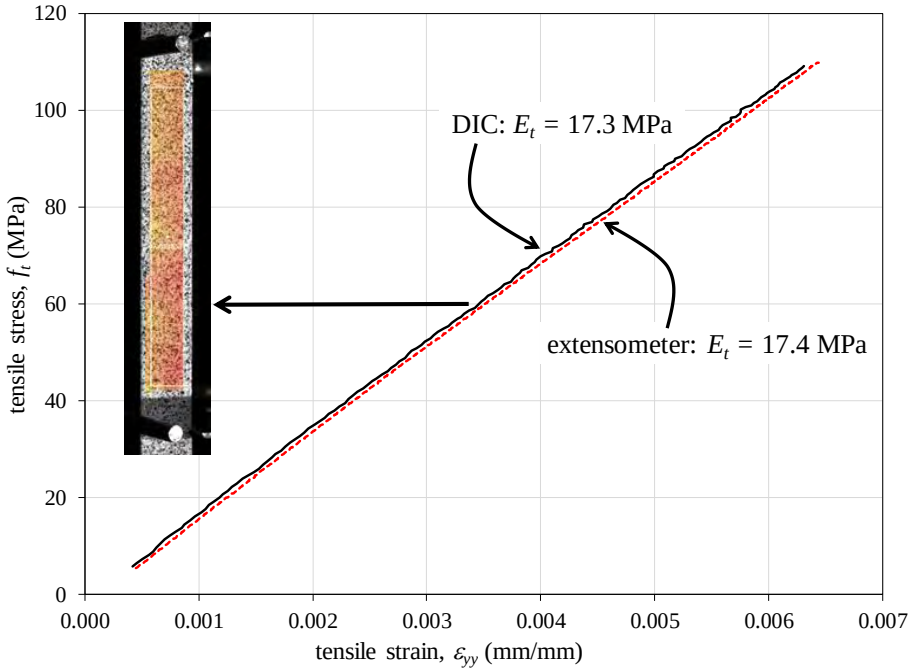

a) comparison between DIC and extensometer derived longitudinal stress-strain curve for internode specimen

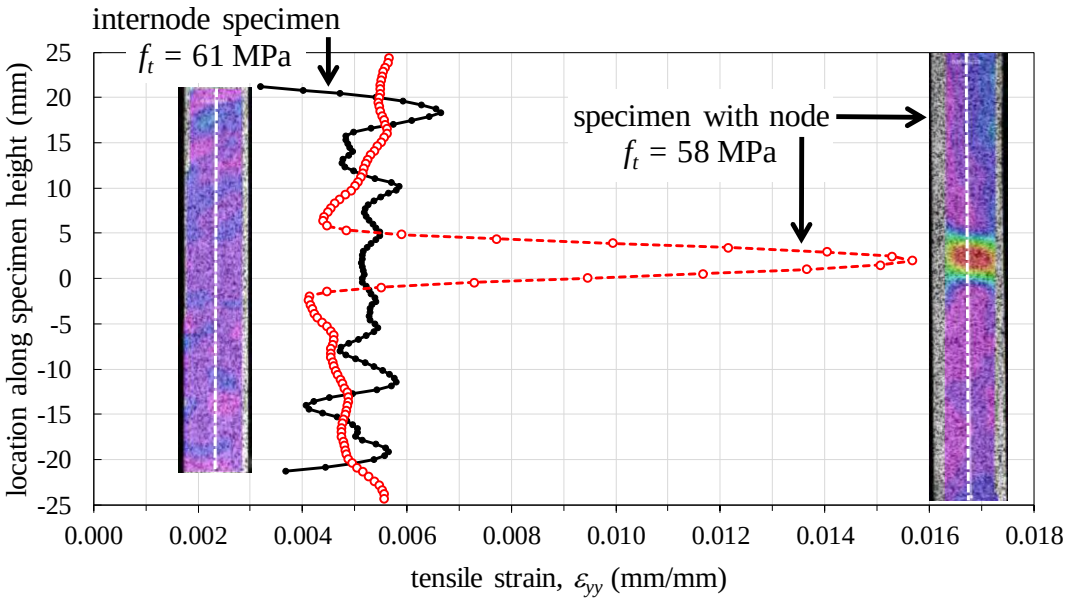

b) longitudinal strain distribution in specimens with and without nodes

Source: (GAUSS; SAVASTANO; HARRIES, 2019)

3.3.4.4. Small coupon bending

A summary of coupon bending test results is given in Table 3.12; these results assume gross sections properties and homogenous material properties and should be interpreted as being 'average' properties for a cross section. Representative flexural stress versus extreme fibre strain data is shown in Figure 3.19a. Bending behaviour is clearly different for OC and OT orientation (*p*-values in Table 3.12) and the behaviour is more nonlinear (especially for OT); having a lower LOP than previous tests types. As an additional measure of this behaviour, the cumulative energy (or specific energy), *SE*, taken as the area under the stress-extreme fibre strain curve is also given in Table 3.12.

From extreme fibre strains, shown in Figure 3.19b, the behaviour of the specimens becomes evident. For both OC and OT specimens, flexure is described by a softer nonlinear response of the compression zone and a stiffer tension behaviour having a higher LOP. The greater nonlinearity observed in the compression strains indicates more local damage in the matrix-dominated compression zone. Compression behaviour drives the failure of OT specimens which are generally unable to develop large tensile strains despite the culm wall being oriented such that the greater fibre density is in tension. Based on observation, it appears that OC specimen failure is driven by excessive tensile strains resulting in failure of the relative lightly 'fibre reinforced' tension zone. Bending tests having a node a midspan are very clearly dominated by the poor tensile behaviour of the node as is discussed below.

Table 3.12 - Coupon flexure test results.

	Internode specimen outer culm wall in compression (OC)			Internode specimen outer culm wall in tension (OT)			*p*-value	Specimen with node at midspan		
	n	average	COV	n	average	COV		n	average	COV
MOR, MPa	54	205	0.06	10	183	0.08	0.0001	24	127	0.11
MOE, GPa		16.32	0.06		15.57	0.06	0.03		15.05	0.07
SE, kJ/m^2		39.5	0.13		78.5	0.23	0.0001		13.6	0.23
LOP, MPa		124 0.61*MOR*	0.06		67 0.37*MOR*	0.15	0.0001		87 0.68*MOR*	0.11
NOTES:	Moisture content = 7.3% (COV = 0.09) Specimens sampled from 11 different culms *p*-value from unpaired t-test comparing OC specimens to OT specimens									

Source: (GAUSS; SAVASTANO; HARRIES, 2019)

Figure 3.19 - Representative results of three-point coupon bending test.

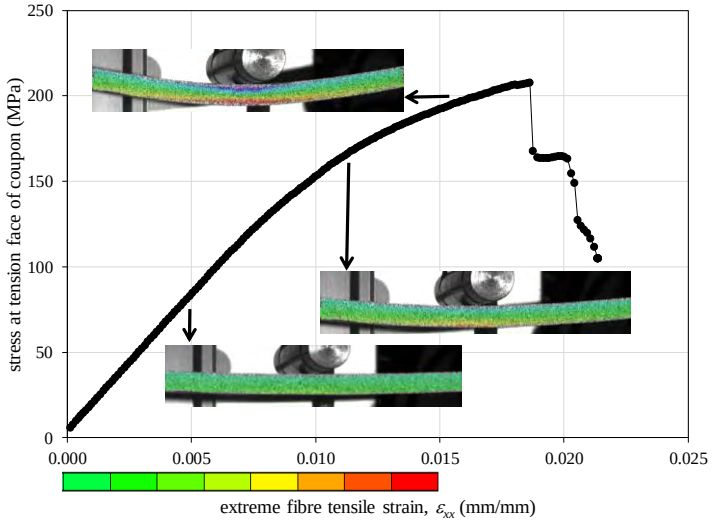

a) longitudunal shear stress-strain progression of OC internode coupon test

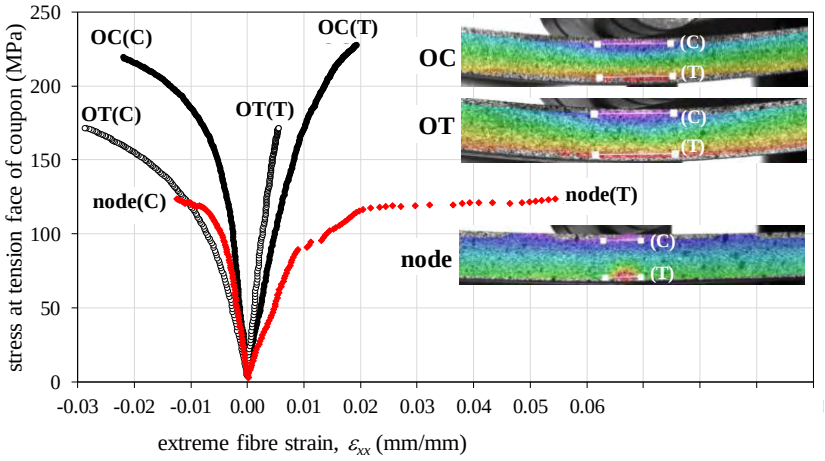

b) longitudinal strain of the compression (C) and tension (T) sides in the OC, OT and node specimens bending tests

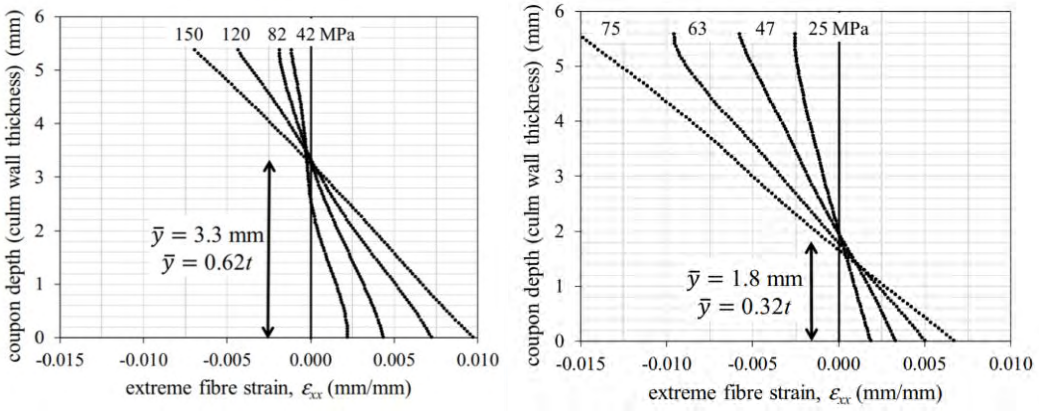

c) strain distributions through depth of coupon (culm wall thickness) (horizontal axis for OT shifted 0.02 to right for clarity)

Source: (GAUSS; SAVASTANO; HARRIES, 2019)

3.3.4.5. Assessing “real” bending behaviour

The difference in tensile and compression behaviour in flexure results in a shift in the neutral axis of the specimen toward the stiffer outer culm wall; this is illustrated in Figure 3.19c for representative OC and OT specimens. This shift reflects mainly the differences of moduli along the wall thickness, with higher fibre density (and hence higher moduli) towards the outer layer (AKINBADE et al., 2019). If the strain distribution through the culm wall can be determined as is the case using DIC, the actual behaviour of the culm wall in flexure can be determined. Assuming a linear strain distribution (Figure 3.19c), the moment applied to the coupon, M, is resisted by a tension-compression couple having a lever arm equal to $(2/3)t$. From equilibrium, and the recorded extreme fibre strains, ε_T and ε_C, the tensile and compression moduli can be determined:

$$E_{TF} = 3M/t\bar{y}\varepsilon_T \quad \text{Eq. 3.12}$$

$$E_{CF} = 3M/t(t - \bar{y})\varepsilon_c \quad \text{Eq. 3.13}$$

Where $\bar{y} = t\varepsilon_T/(\varepsilon_T - \varepsilon_C)$ is the location of the neutral axis (relative to the tensile face of the coupon).

The approach using Equations 3.12 and 3.13, however, is affected by a number of test parameters and is only practical when sufficiently robust strain data is available. In three-point flexure, the recorded strain at the compression face is significantly impacted by local deformation caused by the application of the load and local strains in this region are unreliable. Using four-point flexure, having a constant moment region, addresses this issue but such tests are limited by available internode length and the need to have a shear span to depth ratio greater than 8. The utility of E_{TF} and E_{CF} in practice is also limited. For this reason, the use of stress at tension face (Eq. 3.10) is believed sufficient to represent the flexural behaviour of small coupon bending samples.

3.3.4.6. Effect of node

In compression and shear, the presence of a node in the test specimen has a local stiffening effect. This is attributed to the reduction in unidirectional fibre alignment and the thickening of the culm wall in the nodal region (Figure 3.20). In the node, the bamboo fibres are shorter than in the internode. Additionally, as many fibre bundles simply pass through the node, others rearrange themselves into the sheath (outwards) and diaphragm (inwards) (LIESE, 1998). Liese (1998) illustrates the rearrangement of the vessels (vascular anastomoses) in the nodal region (Figure 3.20); the 'vascular skeleton' supporting the primary vessels also becomes less anisotropic. The total fibre volume in *P. edulis* is typically less than 30% and, in general, fibre volume in other species rarely exceeds 40% (AKINBADE et al., 2019). As a result, both compression and shear in the longitudinal direction are matrix-dominated behaviours. As the fibres become less unidirectionally aligned in the node, there is a natural stiffening effect as fibres now reinforce the weaker parenchyma matrix in directions other than longitudinal. The additional section thickness at the node further reinforces the behaviour resulting in a stiffer response. The local stiffening effect has no statistically significant effect on the global, or specimen stiffness as illustrated in Tables 3.9 and 3.10.

The same bamboo node morphology results in a softening of the fibre-dominated tension behaviour; this is evident in Table 3 and Figure 4, reporting direct tension results. However, the same mechanism also drives the small coupon bending tests in which a node is included. The presence of the node dominates the tension behaviour of the flexural specimen leading to brittle failure. Unlike in compression, in tension, the node becomes a 'weak link'. The strains shown in Figure 3.19b illustrate this dramatically, where then tension strain increases essentially unbounded while the compression strain has considerable reserve capacity (In Figure 3.19b, the compression strain has barely achieved half that observed in the OC or OT specimens without a node).

Figure 3.20 - Fibre morphology at node.

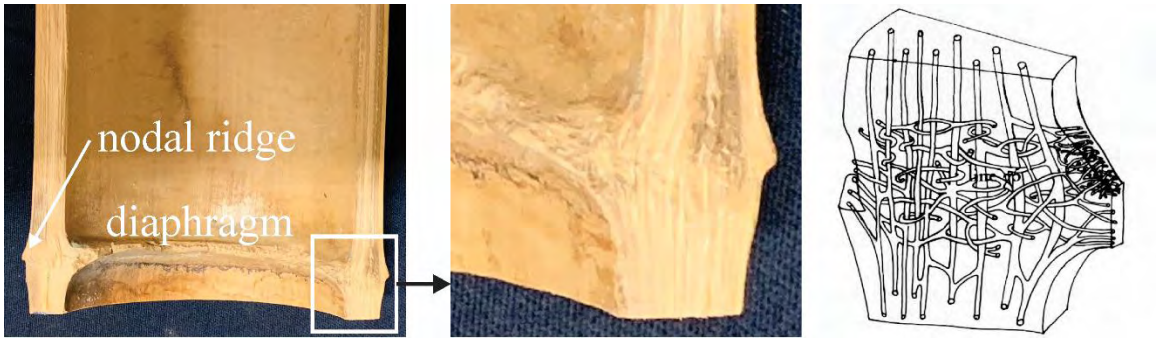

a) nodal region of *P. edulis* showing fibre orientation and local thickening of culm wall

b) skeleton of vascular bundle at node (LIESE, 1998)

Source: (GAUSS; SAVASTANO; HARRIES, 2019)

3.3.4.7. Characteristic properties of *P.edulis*

The average mechanical properties determined for the Brazilian *P. edulis* tested are summarised in Table 3.13 and Figure 3.21. In Table 3.13 these are compared to other such data reported in the literature and seem to be in general agreement. The characteristic design strengths that resulted from this study are also summarised in Table 3.13. These values are defined as the 5th percentile value determined with 75% confidence (ISO 22156:2004; ISO CD 22156:2019) and are calculated for data having a normal distribution as:

$$f_{ik} = f_{i\,average} - K \times \text{standard deviation of } f_i \qquad \text{Eq. 3.14}$$

where K is the confidence level factor associated with the confidence interval (75%), data percentile (5%) and the number of samples tested (n). Values of K are tabulated in multiple sources; the tables included in ASTM D2915-17 were used in the present study. For a test series having $n = 50$, $K = 1.811$.

Stiffness values used in design are conventionally the mean value established with 75% confidence (ISO CD 22156:2019) calculated for data having a normal distribution as:

$$E_{ik} = E_{i\ average} - 1.15\ x\ standard\ deviation\ of\ E_i \quad \text{Eq. 3.15}$$

The characteristic values apply only to the batch of *P. edulis* tested. The relatively high characteristic values reflect the low variation observed in the tests. Coefficient of variation (COV) for both strength and modulus of elasticity remained below 0.11 in all performed tests. The process of testing illustrated in this paper reflects what is required to establish characteristic design values which may be then used to grade the batch of bamboo (ISO 19624:2018).

3.3.4.7.1. Minimising material damage in bamboo design

While the characteristic values of strength are conventionally used in design (ISO 22156:2004; ISO CD 22156:2019), the application of the limit of proportionality (LOP) may be more appropriate since exceeding this limit is associated with damage and material degradation. Additionally, stipulating the LOP as the design value of interest is consistent with the use of the modulus of elasticity which is calculated at strains below the LOP. The average LOP values and associated characteristic values (Eq. 3.14) are summarised in Table 3.13. The authors argue, that these are the appropriate values of stress for use in design.

Table 3.13 - Comparison with *P.edulis* data available in literature.

Source	ρ	MC	f_c	E_c	f_v	G	f_t	E_t	*MOR*	*MOE*
	kg/m^3	%	MPa	GPa	MPa	GPa	MPa	GPa	MPa	GPa
This study strength	810	7-10	57.9	20.38	18.1	2.84	275 (no node) 100 (node)	17.47 11.19	205 (OC) 183 (OT)	16.32 15.57
This study LOP			50.7		12.2				124 (OC) 67 (OT)	
This study characteristic strength			49.5	18.04	15.4	2.52	220 (no node) 63 (node)	15.66 8.87	183 (OC) 152 (OT)	15.19 14.49
This study characteristic LOP			41.5		10.0				110 (OC) 49 (OT)	
(AKINBADE et al., 2019)	896	14	48.1	-	15.1	-	-	-	-	-
(DENG et al., 2016)	655	8-12	-	-	11.8	-	48 (node)	-	-	-
	799		-	-	15.9	-	62 (node)	-	-	-
(DIXON et al., 2015)	400	4	-	-	-	-	-	-	52	4.35
	850		-	-	-	-	-	-	215	16.68
(HABIBI et al., 2015)	-	-	-	-	-	-	-	-	146 (OC) 125 (OT)	11.40 9.90
(HUANG; HSE; SHUPE, 2015)	-	12	61.3	-	12.9	-	197 (no node)	-	149	-
(XU et al., 2014)	-	10	46.0	11.20	11.2	-	-	-	-	-
(YU et al., 2008)	703	10	-	-	-	-	168 (no node)	16.4	-	-

Source: (GAUSS; SAVASTANO; HARRIES, 2019)

Figure 3.21 - Mechanical characterisation of *P edulis*: strength and modulus. (Error bars represent ± 1 standard deviation).

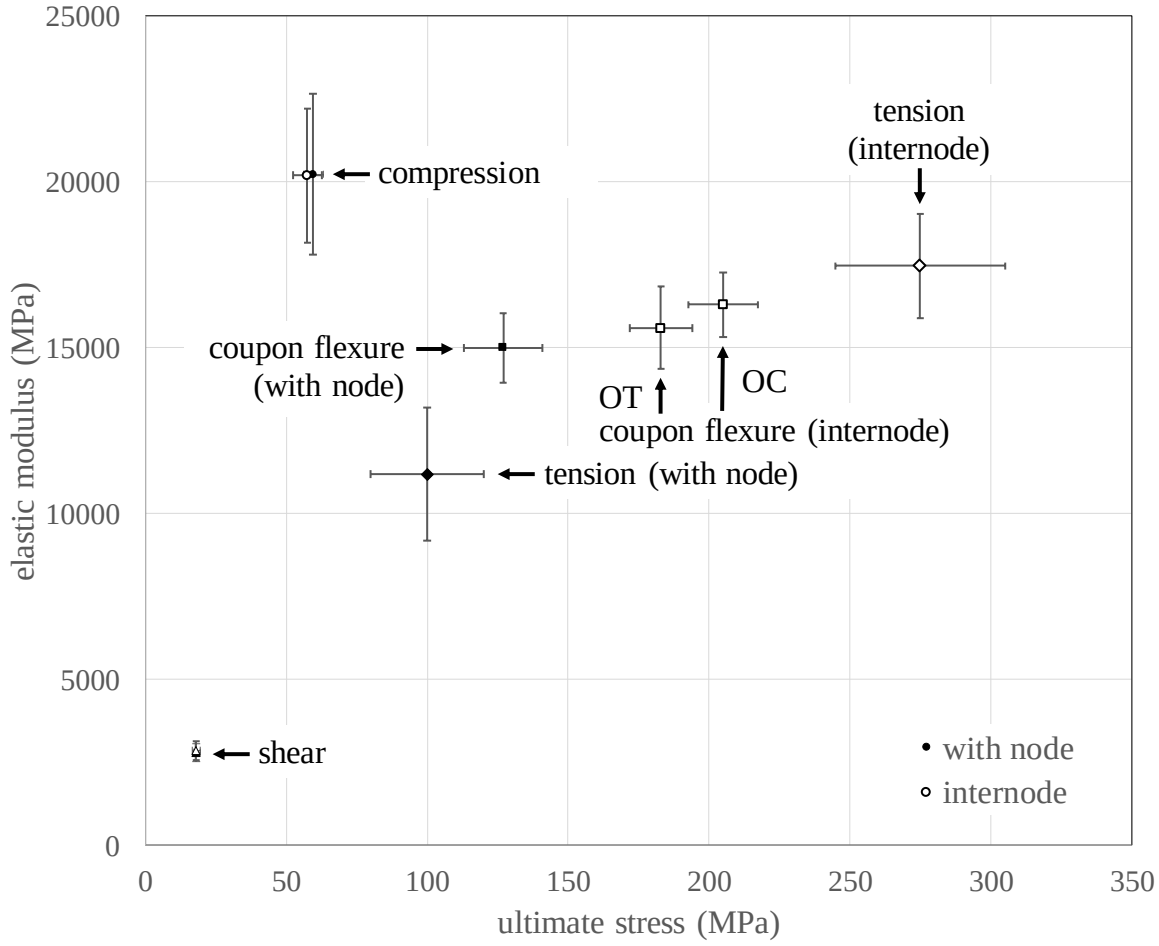

Source: (GAUSS; SAVASTANO; HARRIES, 2019)

3.3.5. Conclusions and recommendations

The characterisation of Brazilian *P. edulis* bamboo is presented as an example of the adoption of ISO 22157 test methods. The efficacy of the parameters affecting the test specimen behaviour were investigated using digital image correlation (DIC) techniques. The DIC helped to identify and quantify specimen behaviour, particularly in the presence of a node. In particular, nodes are shown to have a significant local effect on behaviour. In compression and shear, the presence of a node has little impact. In tension, however, the node is a 'weak link' significantly

reducing the available capacity of the culm. This behaviour is an artefact of the morphology of the bamboo fibres in the nodal regions. Specimen damage development was also described by DIC and the adoption of the limit of proportionality (LOP) was proposed as a measure of useful material capacity.

3.3.5.1. Recommendations for testing mechanical properties of bamboo

While this study has demonstrated the efficacy of using DIC, such instrumentation is available to only a handful of bamboo researchers and is not presently suitable for field implementation. Nonetheless, the observations made using DIC can inform bamboo materials testing practice. The following recommendations are made.

- In addition to ultimate capacity, the limit of proportionality (LOP) should be reported for all tests. This requires a measure of either specimen displacement or strain. Absent such a method, machine crosshead travel can be used as a surrogate for displacement sufficient to identify the LOP. Machine crosshead travel should never be used to calculate a real displacement, strain or modulus however.

- Full-culm compression and 'bowtie' shear tests parallel to the fibres are relatively insensitive to the presence of a node. ISO 22157:2019 prescribes that both tests use 50% samples including a node to establish characteristic values. While reasonable, a small degree of conservativeness will result if values are determined for a sample containing no nodes.

- The ISO 22157:2019 tension test has not been validated considering the new restrictions placed on specimen orientation and boundary conditions. In the present study – enforcing these restrictions – relatively low variability (COV = 0.11) was observed. Some issues with the tabs affecting test performance were observed; further investigation of alternative tension tab arrangements and materials is required to improve the utility of this test method.

- The ISO 22157:2019 tension test also specifies that specimens contain one node in the gauge length. This will result in conservative values of tension strength (Table 3.11).

However, the relatively local effect of the node (Figure 3.18b) will make strains and modulus of elasticity obtained from this test unreliable and a function of the gauge length used. While bamboo tensile strength is conservatively represented in the presence of a node, modulus of elasticity may be unrealistically low. In this perspective, the utility of the ISO 22157 tension test requires further investigation.

- Although beyond the scope of the present study, researchers and practitioners are reminded that it is critical to report bamboo density and moisture content since both of these parameters are well known to affect material properties.

Small coupon bending of bamboo specimens has been demonstrated applying a method used for reinforced plastics, ASTM D7264 (Procedure A: three-point bending). It is proposed that a similar method be adopted into ISO 22157. The small coupon geometry is appropriate for determining the material properties for bamboo intended to be used in engineered products such as glue-laminated bamboo or cross-laminated bamboo timbers. In such applications, bamboo strip orientation should be randomised, therefore standardising the bending test in the OT orientation will result in uniformly conservative design values. It is not believed that the inclusion of a node is necessary in bending tests.

If strain data is to be determined or data beyond that derived from Equations 3.10 and 3.11 is necessary, four-point bending (ASTM D7264 Procedure B) is required in order to establish a constant moment region unaffected by the application of load. However, maintaining the geometry of the four-point bend specimen while also ensuring that the shear span remain greater than 8t requires a test specimen that is at least 32t long. This may be impractical for many species considering the internode length available. Further development of a small coupon flexural test for bamboo is recommended.

3.4. Complementary information

3.4.1. DIC analysis procedure

In this section, the procedure used for the DIC analysis (related to the results presented in the last two sections) is further detailed. The procedure herein presented was also used for the tested samples from Chapter 4 (*D. asper* bamboo specimens). This is a powerful method for strain analysis and relatively underused for bamboo characterization. Therefore, a detailed description of the application of this method can be useful for future researchers.

The samples used in all the tests (compression, tension, bending, and shear) were painted with a speckle pattern prior to testing. The stereo cameras (VIC-3D dual-camera system) were adjusted at a specific distance (focal distance) and calibrated using a calibration pattern composed of equidistant dots (a distance of 5 mm), as shown in Figure 3.22a. Then, the samples were positioned in the testing machine (in Figure 3.22b a compression sample is presented as an example), illuminated by LED lights, and submitted to testing and image recording. High-resolution images (2448 x 2049 pixels) were recorded every 0.5 sec. and processed in a DIC processing software (Correlated Solutions).

Figure 3.22 - Setup used for a) calibration and b) test of the DIC analysis.

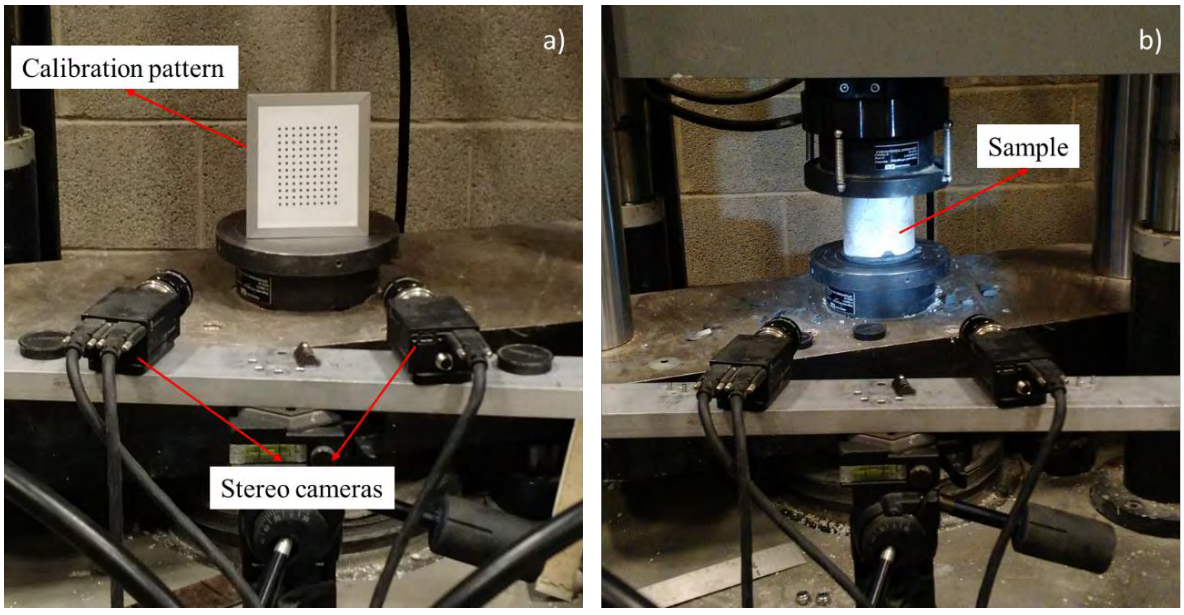

Source: Author's authorship.

In order to analyse the strain distribution and displacement maps during the tests, an area of interest (AOI) was selected for each sample and the subset size (the minimum area used for the correlation between images) defined to have a mean pixel uncertainty below 0.01 (Figure 3.23). Figure 3.23d shows a representation of the resulting strain map during the calculation process.

Figure 3.23 - a) Selection of the area of interest (AOI), b, c) the definition of the subset size, and d) resulting strain mapping in a 3D view.

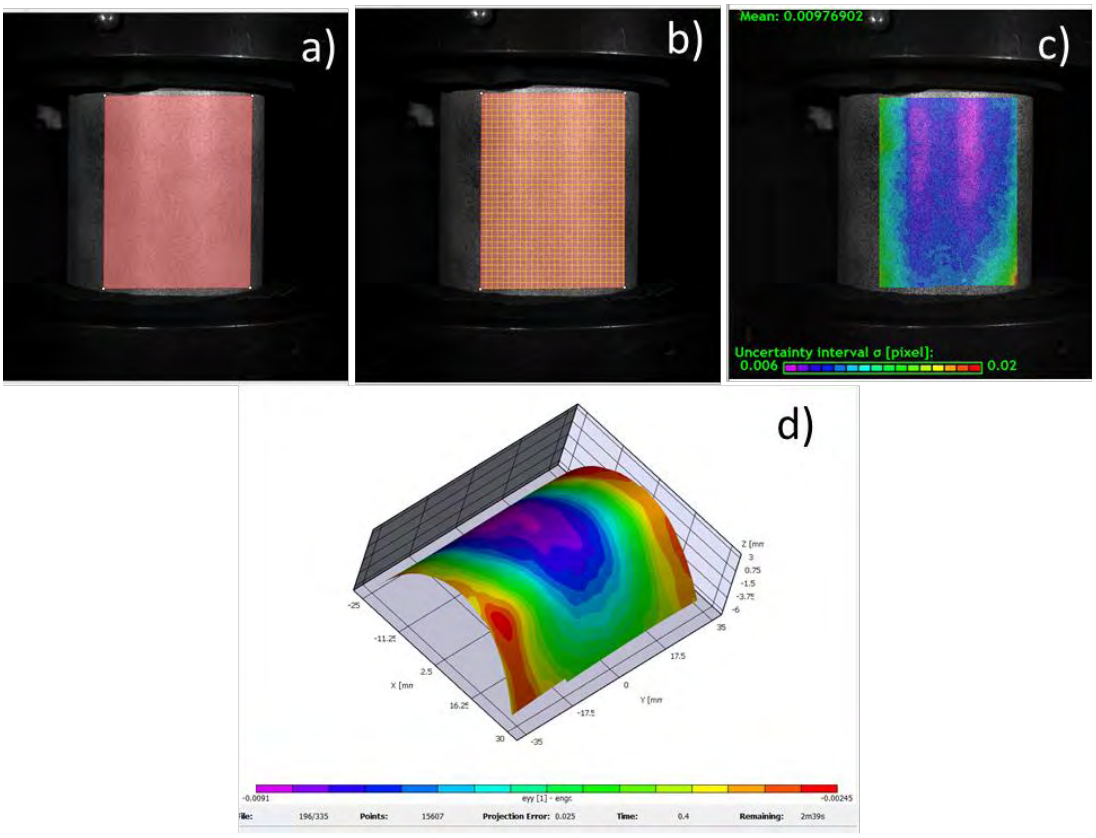

Source: Author's authorship.

The DIC system is independent of the testing machine. The synchronization between the acquired data from the cameras (two images per second) and the mechanical testing machine was made by using a time correction, obtained through a time/displacement plot for each sample, as shown in Figure 3.24. The recording of the images started before the starting of the mechanical test and, therefore, the time shown in the x-axis of Figure 3.24 is related to the DIC

system. After the time synchronization, the corresponding stress of each image could be obtained.

Figure 3.24 - Time versus displacement plot used for the determination of time correction for DIC/Testing machine synchronization.

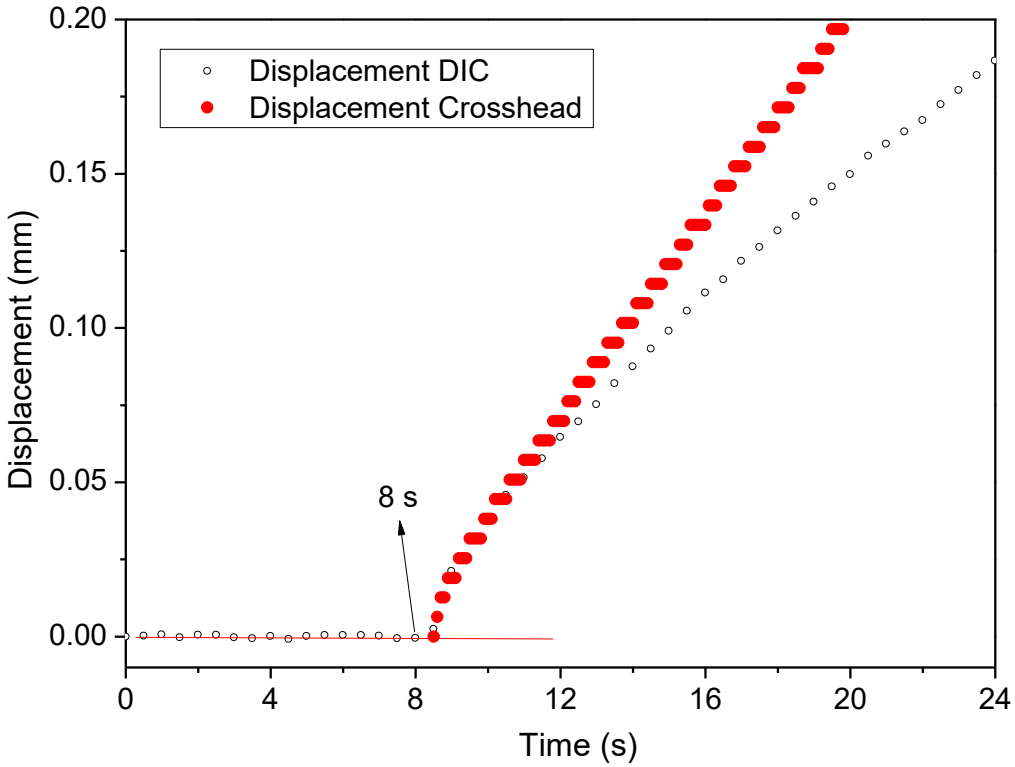

Source: Author's authorship.

3.4.1.1. Compression tests

The calculation of the modulus of elasticity in compression was performed after previous analysis of the method. It was tested the difference between the strain calculation by using the mean ε_{yy} strain of a selected area or by using virtual extensometers. Both methods are represented in Figure 3.25. For the strain calculated using virtual extensometers (Figure 3.25a), E_c of 16.5 GPa (Left), 17.6 GPa (Right), and 16.83 GPa (Average) were observed. Using the area (Figure 3.25b), a E_c of 17.05 GPa was obtained. Since the E_c values are similar and considering that by using the area measurement, a more representative value can be acquired, it

was decided to use this procedure for the other samples. As previously discussed, during the elastic region, the strain distribution is uniform and, therefore, should not affect the E_c - calculation if the entire AOI is considered.

The importance of using extensometry/strain analyses methods can be observed in Figure 3.26, as advised in section 3.3. The difference between the stress/strain curve obtained by the DIC measurements and the cross-head displacement of the testing machine shows a considerable influence on the E_c calculation. This effect is caused by the deformation/accommodation of all the moving parts of the testing machine, in which not all the incremental displacement is transferred to the specimen.

Figure 3.25 - Different procedures used for the determination of strain within the AOI. a) virtual extensometer (calculates the strain using the selected initial length, b) Mean strain (ε_{yy}) of a selected area.

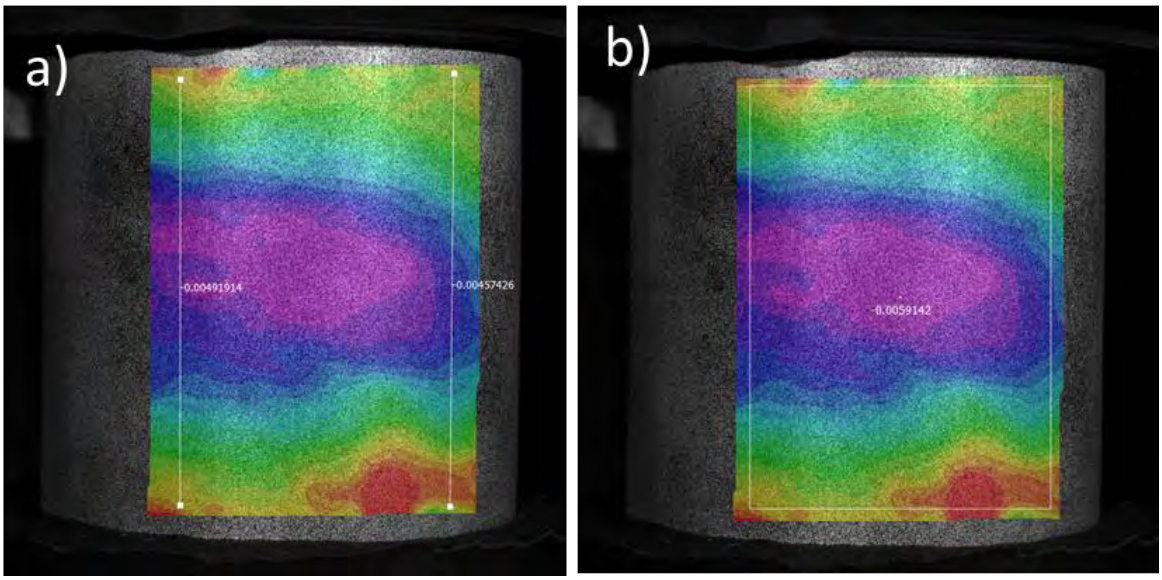

Source: Author's authorship.

Figure 3.26 - Stress x strain curves obtained using DIC (red) and the cross-head displacement (black). The E_c was calculated using the DIC curve through linearization of the elastic region.

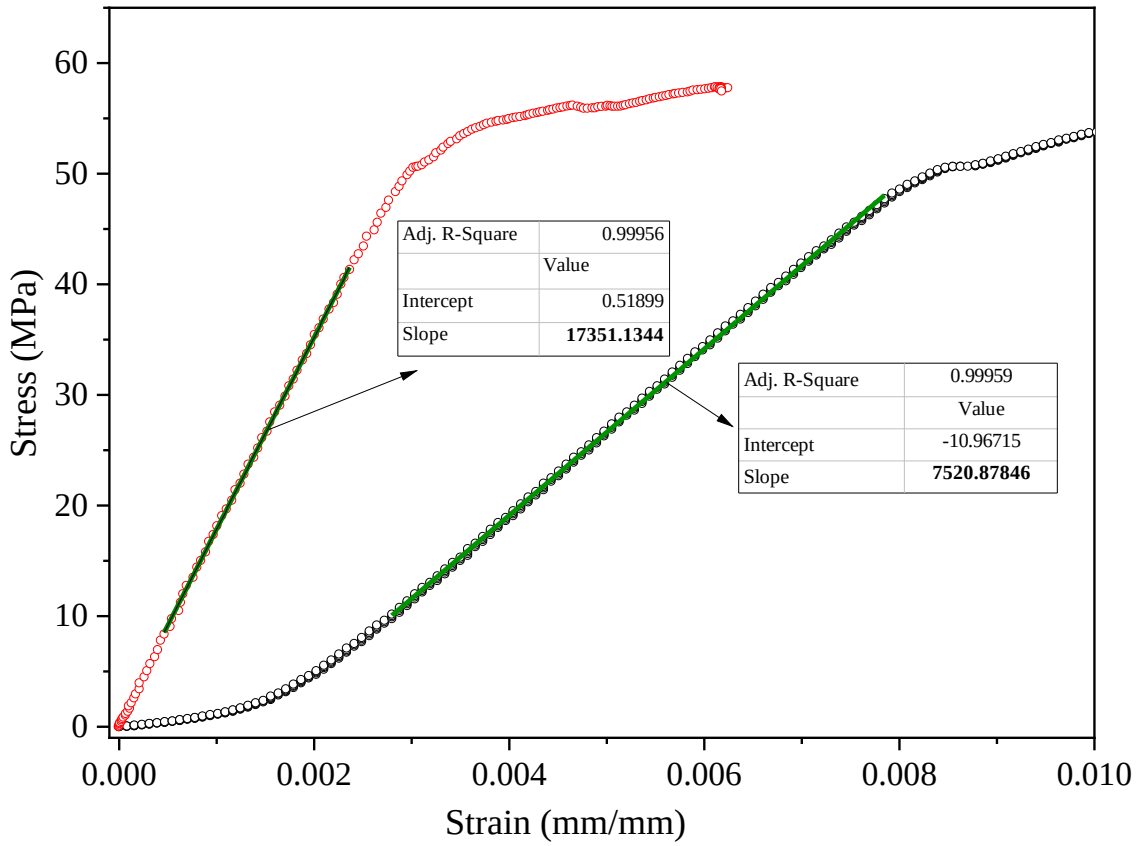

Source: Author's authorship.

Besides the strain mapping and E_c calculation, through the results obtained with DIC, it was also possible to analyse the strain behaviour in the xx and yy directions, as shown in the plot of Figure 3.27. Although not published elsewhere, additional information such as the apparent dilation in the xx direction in compression could be also evaluated. Table 3.14 gives the average apparent dilation of 18 samples (*P. edulis*) in the longitudinal (ε_{yy}) / tangential (ε_{xx}) directions using the method described in Figure 3.27. Interestingly, the obtained average of 0.45 is within the Poisson's ratio reported for different wood species used for construction [between

0.28 and 0.64 for hardwoods and softwoods in longitudinal (loading axis) / tangential (deformation axis) direction] (KRETSCHMANN, 2010).

Figure 3.27 - Strain in the xx and yy directions in the elastic region of a bamboo sample submitted to axial compression loads.

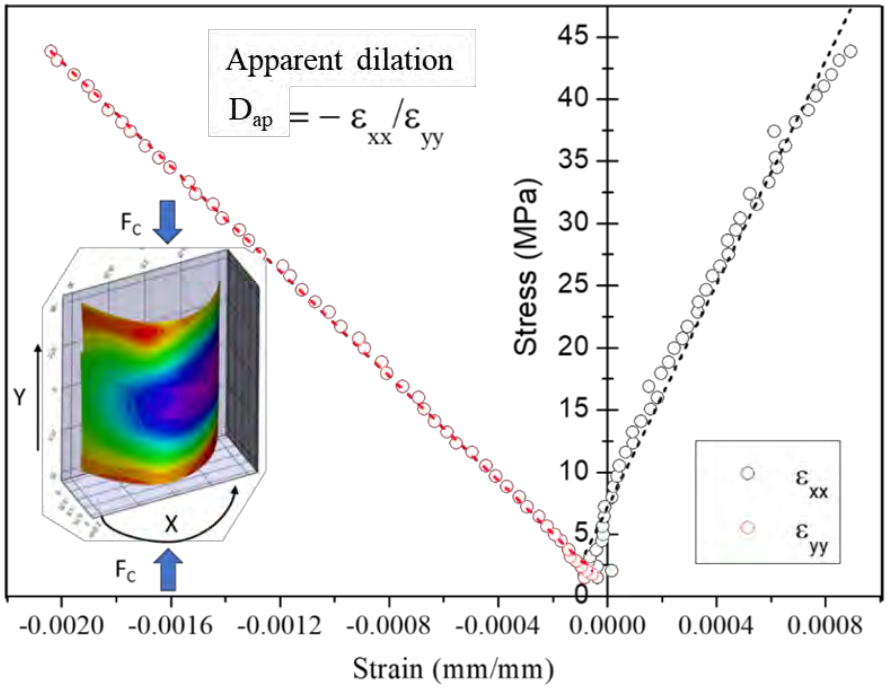

Source: Author's authorship.

Table 3.14 – Apparent dilation calculated through DIC analysis.

N	ρ (g/cm^3)		Moisture content (%)		Apparent dilation	
	average	COV	average	COV	average	COV
18	0.811	0.051	10.17	0.047	0.45	0.104

Source: Author's authorship.

3.4.1.2. Shear tests

In order to standardize the calculation of the modulus of elasticity in shear (G), the displacement in the Y axis (loading direction) has been tracked in the loading side of the shear plates. Figure 3.28b shows a representation of the Y displacement map in relation to the reference (first image). Using the displacement values during loading (tracking area) divided by the initial sample length we can obtain the shear strain. Then, G is calculated by the linearization of the stress/shear strain plot in the elastic region, as can be seen in Figure 3.29.

Figure 3.28 - a) AOI showing the shear plates and b) mapping of the displacement in the Y direction and the tracking area used for the calculation of G.

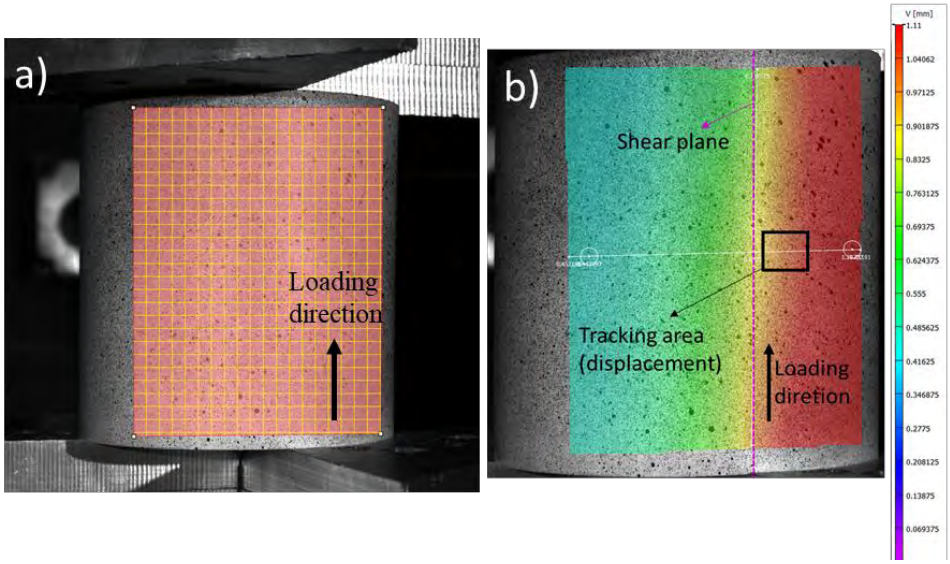

Source: Author's authorship.

Figure 3.29 - Linearization of the stress/shear strain plot used for the G calculation.

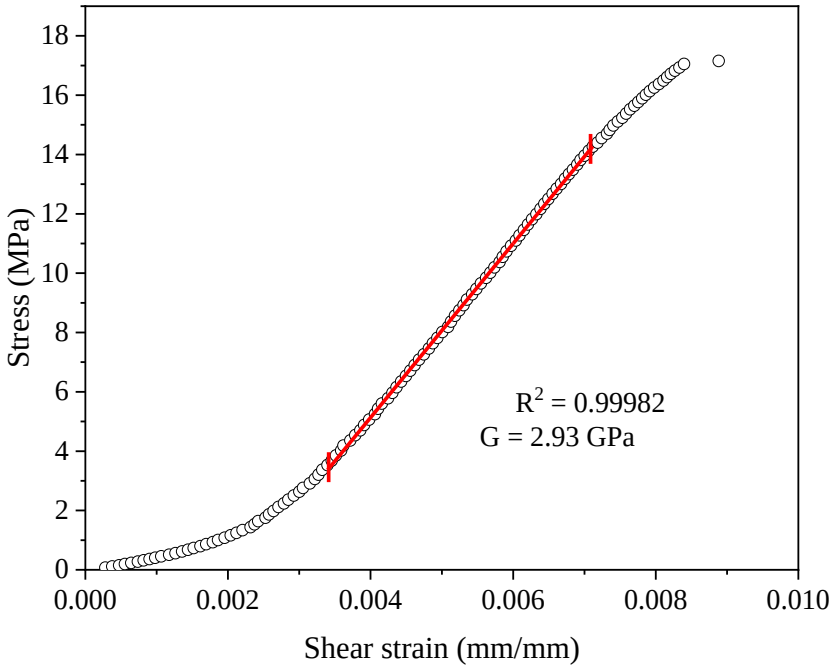

Source: Author's authorship.

3.4.1.3. Bending tests

The advantage of using DIC analysis on bending tests is that it brings the possibility to observe the real neutral zone of the specimens; due to the heterogeneous nature of bamboo, the neutral zone is not in the middle of the thickness, as described and proved in section 3.3. Instead of the common practice of using a deflectometer, the displacement of the sample in the Y axis of the central region was tracked according to the procedure presented in Figure 3.30. The same sample (and image) are presented in Figure 3.30a and Figure 3.30b. However, different mapping methods are shown: a) displacement in Y direction and b) ε_{xx} strain. It is possible to observe that the tracking point of Figure 3.30a is positioned in the neutral zone shown in Figure 3.30b (light blue colour region).

The obtained values of the tracked point shown in Figure 3.30 were then used for the calculation of the corresponding specific strain, as described by ASTM D7264-15. Figure 3.31 shows graphically the resulting stress/strain plot and the corresponding measurements that were performed for each sample: MOE, MOR, LOP, and SE (see section 3.3 for the definitions).

Figure 3.30 - a) Mapping of the displacement in the Y axis (upper image) and b) the strain in the X direction (ε_{xx}). A point positioned approximately in the neutral zone was used to track the real displacement throughout the test.

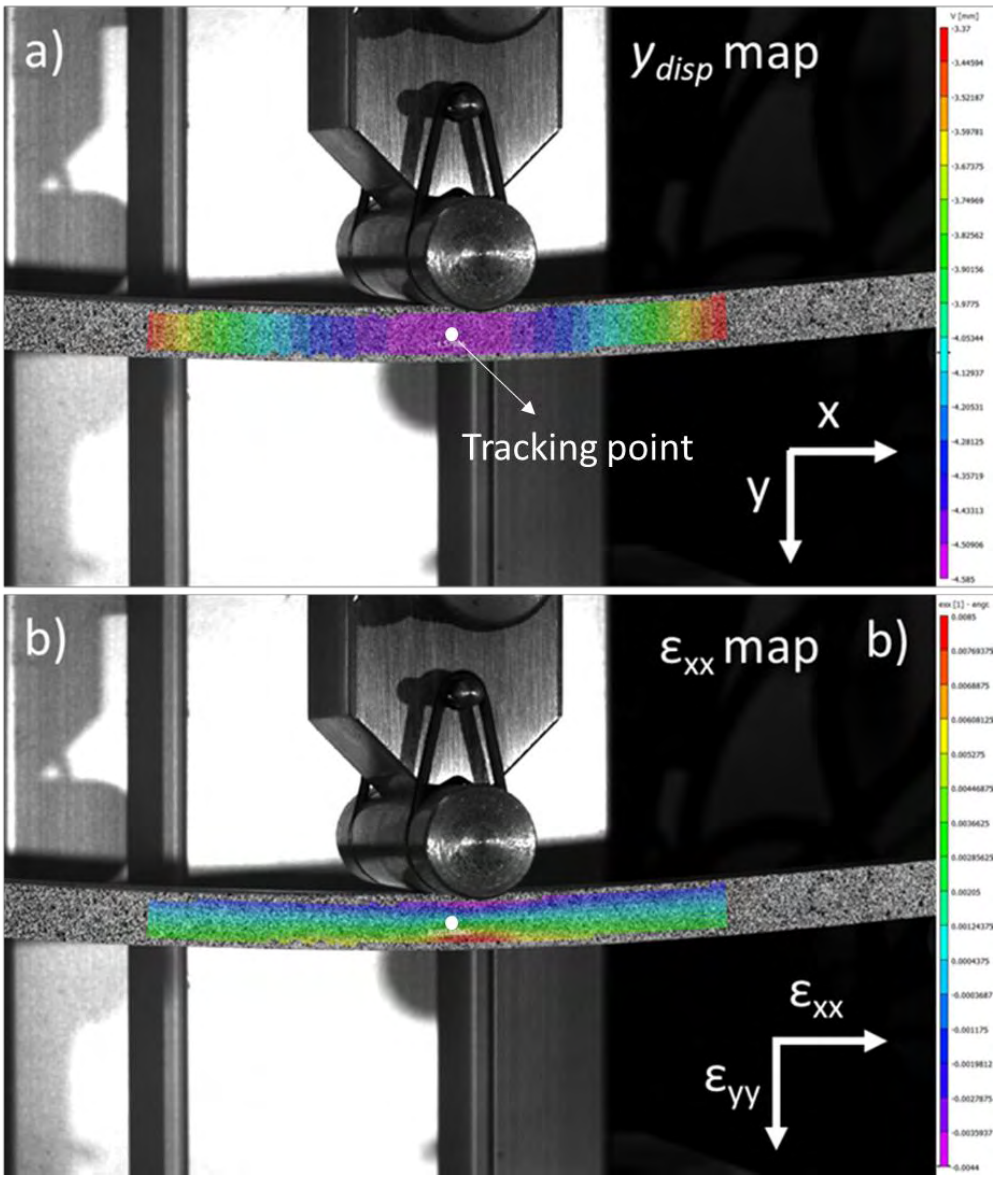

Source: Author's authorship.

Figure 3.31 - Representation of all the extracted information of each sample submitted to the bending test.

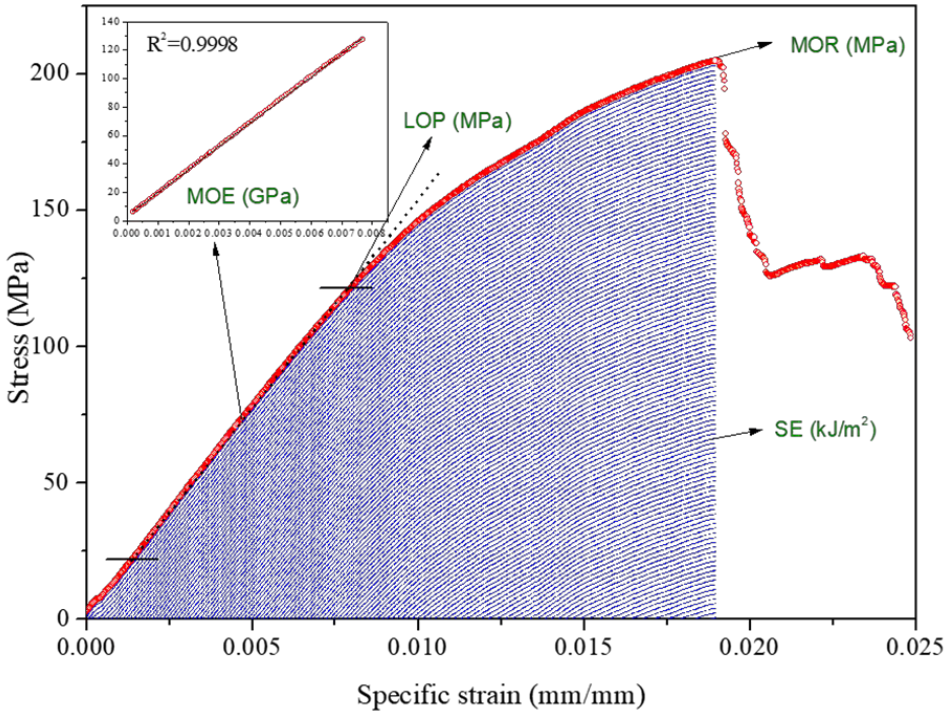

Source: Author's authorship.

3.4.1.4. Tension tests

The tension specimen suggested by the ISO 22157:2019 standard has the inconvenient of causing types of failure of bamboo that sometimes are not directly related to the properties of the material (related to gripping failure or shear). Therefore, modified specimens with a reduced region in the centre of the sample were utilised for calculation of the tensile strength (f_t). The modification proposed in this study was necessary to reduce external influences on the effect of the treatments on the tensile behaviour. The reduced region ("dog bone") was easily made by using a circular grinding machine. In addition, the DIC enables the strain mapping of the entire area of interest, which gives the possibility of calculating the E_t in different regions.

A representation of flat and modified samples is presented in Figure 3.32. Before the complete characterization of the bamboo samples, different tests were conducted to verify the reliability of this modification on the calculation of the modulus of elasticity in tension (E_t) using the DIC system.

Figure 3.32 - Specimens designs for the tension parallel to the fibre tests.

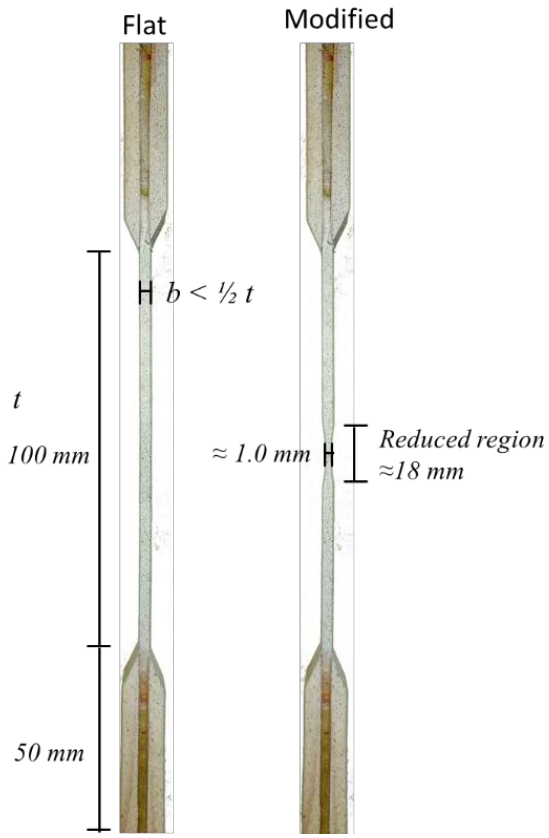

Source: Author's authorship.

First, the calculation of E_t using the strain from the DIC analysis was compared with a conventional clip-on extensometer (both measured simultaneously), as shown in Figure 3.33. The E_t obtained by both methods for the same sample, which was tested only in the elastic region, is presented in Figure 3.34. Almost identical values were observed. In order to confirm this observation, 15 samples were submitted to the same procedure. The obtained values were then used to verify the E_t calculated using the modified specimens.

An example of the obtained ε_{yy} strain map of a modified specimen is presented in Figure 3.35. The E_t was calculated by using the average strain determined in two regions. In method 1, the strain in the middle of the sample, corresponding to the reduced thickness region (see the 3D representation of Figure 3.35), was considered for the calculation. In method 2, the average strain of the upper and lower parts of the specimen (relative to the reduced region), which have the same thickness and width of the original sample (without the modification), was used for

the E_t calculation. This experiment was conducted in 15 different samples, which were twin samples (same internodes) of the previous tests using the clip-on extensometer. The obtained results of all the methods are given in Table 3.15. The method 2 proved to be more reliable, presenting E_t values considerably similar to the ones determined by DIC and extensometer of the flat specimens. Therefore, method 2 was used for the remnant samples used in this study.

The samples with node were tested without the reduced region since all the failures occurred in the middle of the sample, where the node was positioned, as discussed in section 3.3.

Figure 3.33 - Flat sample used for the simultaneous determination of the E_t using DIC and a clip-on extensometer.

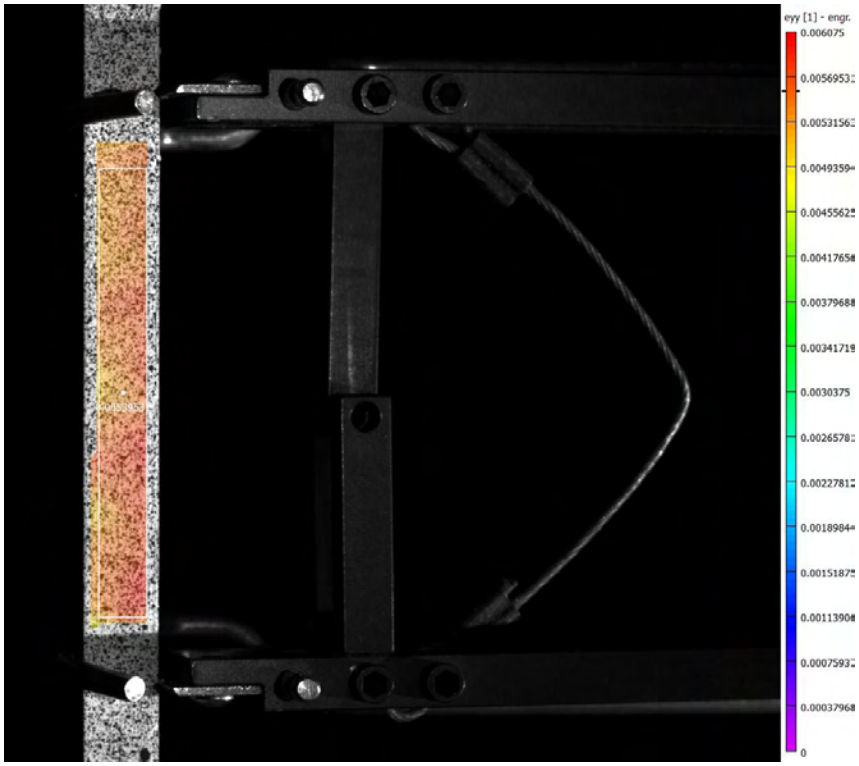

Source: Author’s authorship.

Figure 3.34 - Linearization and determination of E_t using DIC and extensometer. Same results.

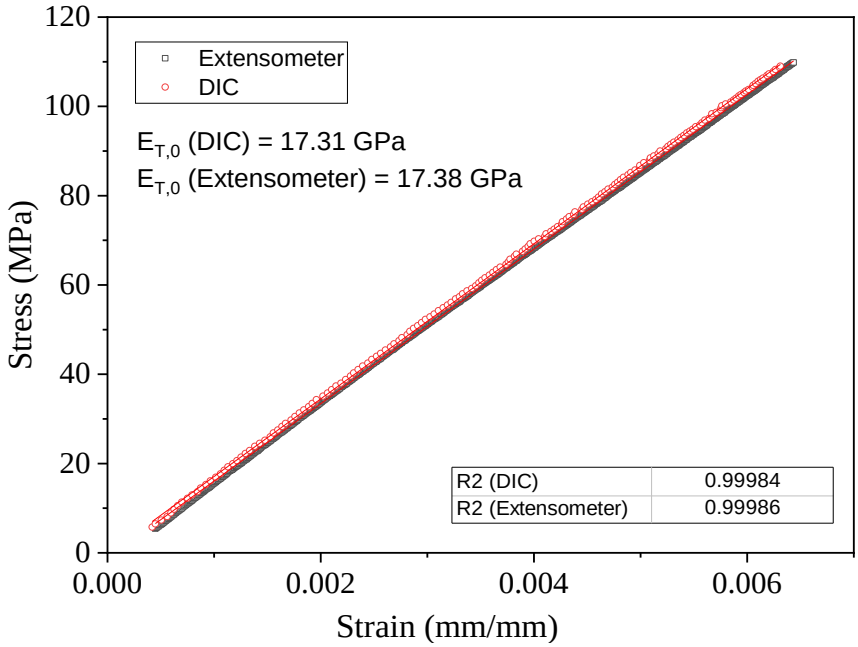

Source: Author's authorship.

Figure 3.35 - DIC mapping of a modified sample and the areas used for the determination of E_t. Method 1 – Top and Bottom part (original width and thickness) and Method 2 – Middle part (width and thickness of the reduced region). On the left: a 3D representation of the analysed area.

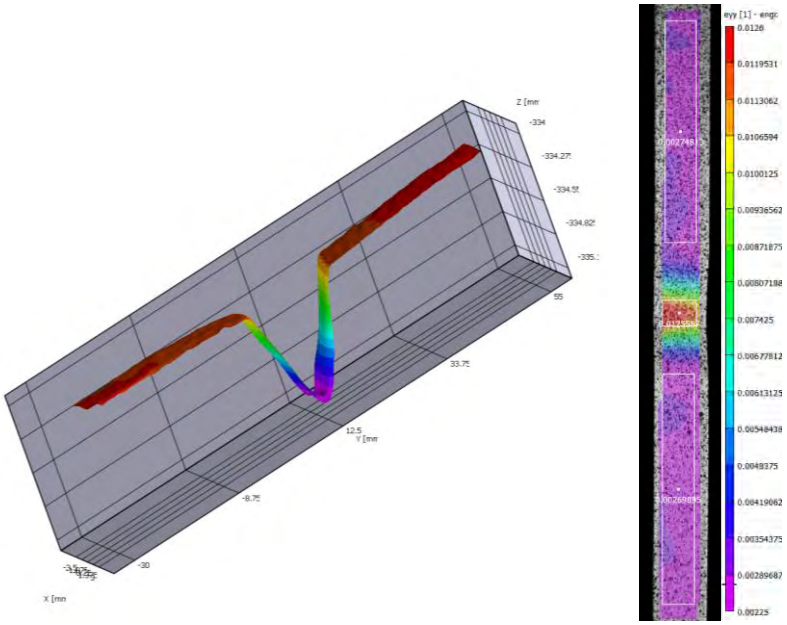

Source: Author's authorship.

Table 3.15 - Comparison between the E_t calculation methods.

Flat sample (DIC x Extensometer)					Modified sample (DIC)				
n	E_t (GPa) DIC		E_t (GPa) Extensometer		n	E_t (GPa) Method 1 (Middle/reduced region)		E_t (GPa) Method 2 (Upper and lower regions)	
	average	COV	average	COV		average	COV	average	COV
15	17.60	0.064	17.39	0.105	15	15.99	0.106	17.72	0.079

Source: Author's authorship.

3.4.2. Guidelines for bamboo treatment by the immersion method

In this section, guidelines for bamboo treatment by immersion method are presented. This procedure has been used for part of the development of this doctorate work and had been used to advise workers/companies commercializing or using treated bamboo. The procedures described below are for treatment using DOT only.

The immersion method, also called as soaking and diffusion process, according to Indian Standard IS 1902:2006 and IS 9096:2006, can be used for the treatment of full-culm bamboo as well as for bamboo strips, slivers, and other bamboo units. This is a scalable and straightforward method based on the immersion of bamboo materials in a water-borne treatment solution for a specific time.

Although green bamboo culms should be used for this treatment method (IS 9096:2016), culms dried in the shadow have been used to describe this procedure because of logistic reasons. This condition is considered as a "worst-case" scenario and, additionally, the purpose of this work is to describe the methods advised for maintenance of the treatment solution and for quality control of treated bamboo poles. During the development of this doctorate work more than 300 bamboos poles of *D. asper* and *P. edulis* have been treated using this method (Figure 3.36) and after 3 years of storage, there were no signs of *D. minutus* attack. On the other hand, reference samples (without treatment) stored in the same building were severely attacked.

Figure 3.36 - Bamboo poles of *D. asper* and *P. edulis* bamboo treated during the doctorate project.

Source: Author's authorship.

3.4.2.1. Treatment procedure

A steel tank of 4.8 x 0.5 x 0.5 m^3 has been used for the immersion treatment. The tank was previously coated with an anti-corrosion paint layer and coated with a PU-based resin. In order to have a closed system and reduce the direct contact with the treatment solution, the treatment operation can be performed in a setup composed of the treatment tank, storage, and filter, with a drainage/reflux system. This system can be easily built using off the shelf and used materials, as shown in Figure 3.37. In this case, the following materials have been utilised:

- Metallic tank of (4.8 x 0.5 x 0.5) m^3;
- Hydraulic centrifugal pump - 220 V of 1 CV (inlet 1" / outlet ¾");
- Flexible 1" hose;
- PVC pipes, filling fabric and connections (Filter);
- Flanges, clamps, fittings and registers;
- Polyethylene drums of 200 L;

The built treatment system and details about hydraulic connections and the filtering system are given in Figure 3.37. In this case, most parts of the components were in used condition and were refurbished. A total of R$ 320.00 Brazilian reais was necessary to build the entire system, with most of the costs related to new hoses, pipes and connections. The use of a hydraulic pump enables the filling and drainage of the tank and filtering/cleaning operations of the preservative solution. The installation of a filter is optional, but it helps on the maintenance of the preservative solution, avoiding the accumulation of organic particles. The model presented in Figure 3.37 can be substituted by commercial filters used in pools and irrigation systems.

Figure 3.37 - Layout of the treatment tank with a solution storage/circulation system.

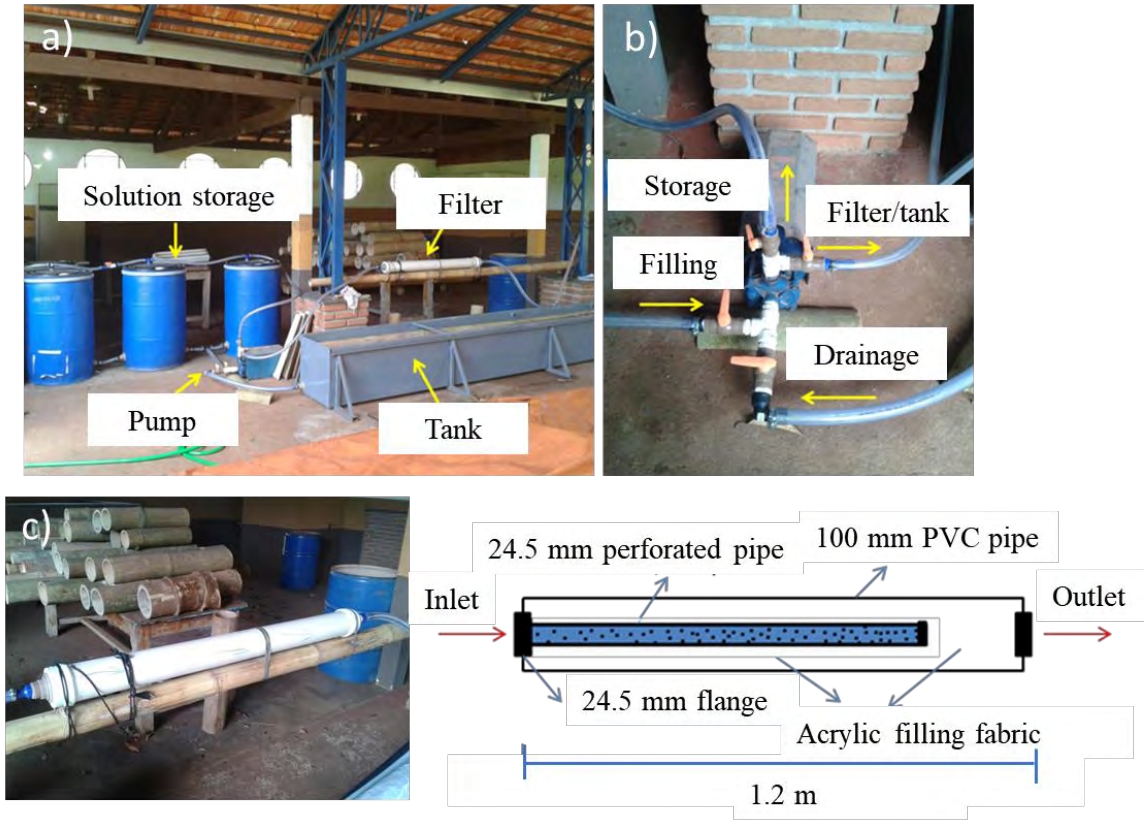

Source: Author's authorship.

Bamboo poles of the species *D. asper* and *P. edulis* with moisture contents between 12-30% and with 3-4.5 m in length were submitted to a treatment process using a DOT solution with a nominal concentration of 8% wt/vol.

Prior treatment, the bamboo poles must be clean; manually with water, brush, and sand or using a high-pressure water pump. The dirt on the bamboo surface can contaminate the treatment solution and result in more filtering/cleaning operations. After washing, all the nodes of each pole must be perforated. This process can be performed by using a steel rod (3/8" with 3 m in length) coupled in an electric drill. The holes are necessary for the correct penetration of the solution within each internode of the pole.

The treatment process consists of first positioning the cleaned bamboo poles into the treatment tank without the solution. Since bamboo has a lower density than water, locks must be used to maintain the poles completely immersed in the solution, as can be seen in Figure 3.38a. After this procedure, the preservative solution is pumped to the immersion tank, passing

through the filter (Figure 3.37) until the complete immersion of the poles (Figure 3.38b). The poles should be maintained immersed for at least 7 days. If possible, a longer period of immersion is advised (up to two weeks), depending on productivity demands. Each batch is composed of all the bamboo poles treated in the same cycle. After the immersion time, the preservative solution is pumped back to the storage drums and the poles are withdrawn from the tank. Since bamboo is hollow, the poles must be left in a standing position to drain the solution from its interior before storage.

The procedures used to guarantee the correct concentration of the preservative solution are described below.

Figure 3.38 - a) Organization of bamboo poles inside the empty immersion tank and b) tank filled with the preservative solution.

Source: Author's authorship.

3.4.2.2. DOT solution concentration control

Disodium octaborate tetrahydrate (DOT) is formed from the combination of boric acid and disodium tetraborate decahydrate (borax), according to the following stoichiometric reaction:

$Na_2B_4O_7.10\ H_2O + 4H_3BO_3 \rightarrow Na_2B_8O_{13}.4\ H_2O + 12H_2O$

Disodium octaborate tetrahydrate ($Na_2B_8O_{13}.4\ H_2O$) – 412.46 g/mol
Disodium tetraborate decahydrate ($Na_2B_4O_7.10\ H_2O$) – 381.87 g/mol
Boric acid ($H_3BO_{3)}$ – 61.83 g/mol

DOT is a white, odourless solid, with a melting temperature of 813/803 °C and a water solubility at 223.65 g/L at room temperature (CIRCABC, 2009). According to this reaction, for each mole of borax, 4 moles of boric acid are necessary to form DOT. This balance corresponds to 1.544 parts of borax for 1 part of boric acid in weight. Taking this into consideration, bamboo or wood treatment can be performed using directly commercial DOT or by the combination of borax and boric acid in the correct proportion. The main advantage of using DOT is its higher water solubility than boric acid (63 g/L) and borax (47 g/L) and a higher proportion of boron per mas unity.

A conductivity test can indirectly determine the concentration of a specific solution. Since the electrical conductivity (measured by Siemens/length unit, e.g. mS/cm) of a solution is proportional to the concentration of dissociated ions of the same salt, though a calibration curve, it is possible to estimate the concentration of an unknown solution (in case of a solution with the same salt used for the calibration curve). Figure 3.39 shows a calibration curve of solutions prepared with commercial agricultural grade DOT with concentrations between 1-10% wt/vol. With the corresponding conductivity, the data can be fitted as a polynomial function and the concentration of an unknown solution determined by the equation given in Figure 3.39. Although these standard solutions were prepared using distilled water, the influence of tap water on the conductivity is minimal (µS/cm) and, in this case, neglected. However, whenever necessary, the conductivity of the water used for the solution preparation should be checked.

Table 3.16 gives an example of the procedure applied to correct a used DOT solution. After measuring the solution conductivity, the corresponding concentration is calculated. Then, the mass of equivalent DOT present in the solution can be determined and the necessary DOT addition calculated (considering a target solution concentration of 8%).

Figure 3.39 - Calibration curve of the concentration of DOT in relation to the solution conductivity.

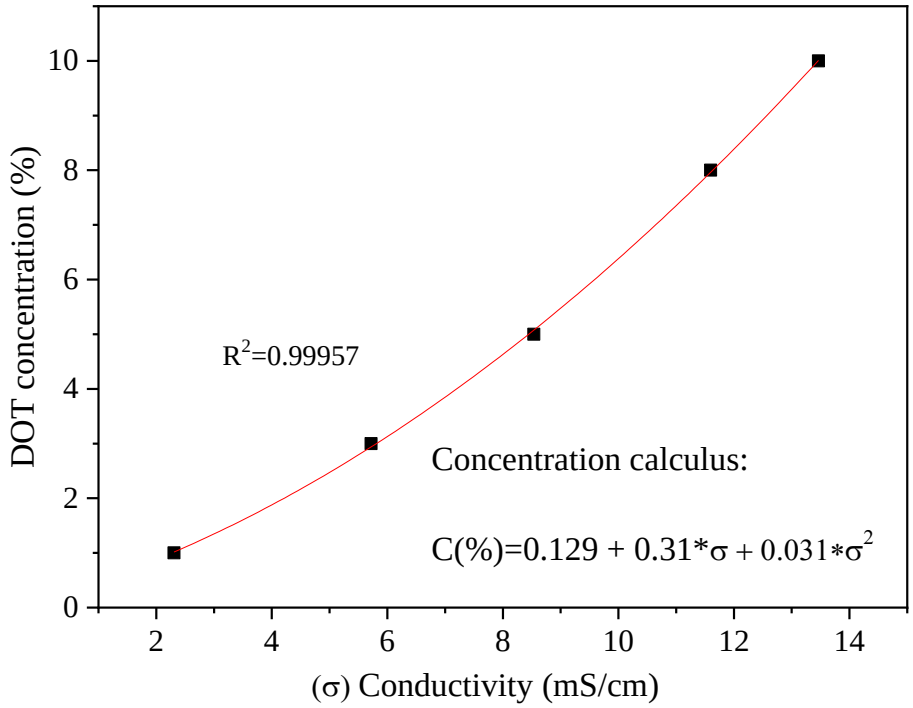

Source: Author's authorship.

Table 3.16 - Example of the correction of DOT solution using a calibration curve.

Tank Volume (L)	Current conductivity - σ (mS/cm)	Current concentration – C (% wt/vol)	Mass of DOT in the solution (kg)	Mass of DOT necessary for an 8% solution (kg)	Necessary DOT addition (kg)
750	4.91	2.40	18.00	60.00	42.00
750	9.95	6.28	47.10	60.00	12.90

$C(\%)=0.129 + 0.31\sigma + 0.031\sigma^2$

Source: Author's authorship.

As part of the quality control of a specific product, traceability is a crucial issue. In the case of bamboo poles that will be used for structural applications, the records of each batch and corresponding poles can be easily organized with basic information, such as date of treatment, solution concentration, moisture content (MC) before treatment, species, and batch size. Table 3.17 gives an example of a tracking records table for treated bamboo production. Instead of recording information of each pole, the information regarding each batch is considered. However, each bamboo pole should be marked with the ID of the corresponding batch. Simple identification systems can be used; a sequential number followed by the year of treatment in the last two digits, for example (118, where 1 is the sequential number, and 18 is the year).

The main idea of this simple methodology is to bring more confidence in the seller/buyer relationship, proved by tracking records report. It would be useful, especially in large scale projects that demand high amounts of bamboo. In addition, an accredited procedure has the possibility to increase the added value of products. Comments about the qualification of the treatment procedure are presented below.

Table 3.17 - Suggestion of an organization table for quality control and tracking records of treated bamboo poles.

Batch ID	Species	Pole length (m)	n	Solution conductivity (mS/cm)	Solution concentration (%)	Average MC (%)	In	Out
317	*P.edulis*	4-4.5	33	12.200	8.53	29.8%	11/18/2017	11/25/2017
118	*P.edulis*	4-4.5	30	11.530	7.82	25.4%	5/15/2018	5/22/2018
218	*P.edulis*	4-4.5	35	11.692	7.99	22.3%	6/5/2018	6/12/2018
318	*D. asper*	4-4.5	10	12.038	8.35	10.7%	6/12/2018	6/19/2018
				.				
				.				
				.				
				.				
				.				
				.				

Source: Author’s authorship.

3.4.2.3. Boron penetration

The penetration analysis is an important tool to easily determine how the active ingredient of the treatment is distributed in bamboo. According to the Standard ABNT NBR 6232:2013, for boron penetration, a solution composed of curcumin (earth turmeric) and ethyl alcohol (10% wt/vol alcohol) is applied in the material to be analysed and permitted to dry. Then a solution composed by a saturated salicylic acid alcoholic solution (13 g per 100 mL solution) and 20 mL of concentrated hydrochloric acid is applied. The observation of red colour indicates the presence of boron. This effect can be observed in Figure 3.40, where an untreated sample is compared with a treated sampled with DOT. If no boron is present, a yellow colour is maintained.

Figure 3.40 - Resulting colour change after the penetration analysis of untreated and treated samples.

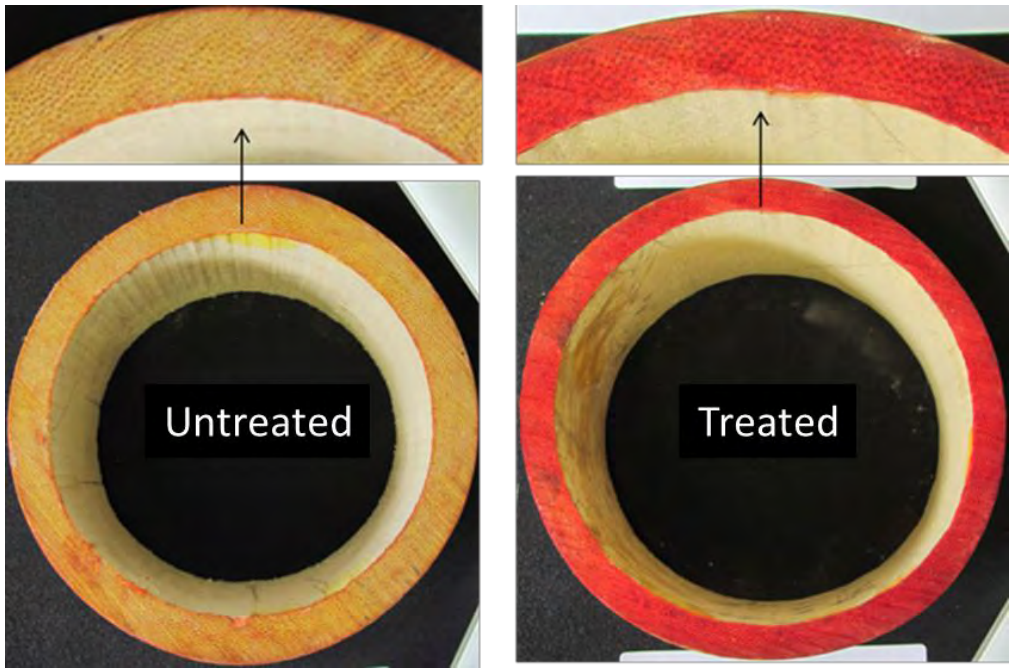

Source: Author's authorship.

Depending on the degree of active ingredient penetration across the wall thickness (i.e., area reacting with the etching solutions) a grade between 0 to 4 can be assigned to each sample: 0 = no penetration); 1 = 0-25% penetration; 2 = 25-50%; 3 = 50-75%; and, 4 = greater than

75% penetration (KIM; TANG; LIESE, 2011). In addition, the grade of penetration can be represented as types of penetration, as shown in Figure 3.41 (SALES-CAMPOS; VIANEZ; MENDONÇA, 2003).

This test can also be used to detect problems in the treatment process. In case of partial penetration is observed along the thickness, but uniformly distributed throughout the circumference, the problem can be related to the immersion time or solution concentration. On the other hand, if there is a homogeneous penetration along the thickness but concentrated in some regions of the circumference, the problem can be related to the lack of solution in the interior of the bamboo poles. Examples of results obtained by this method are presented below.

Figure 3.41 - Resulting colour change after the penetration analysis of untreated and treated samples.

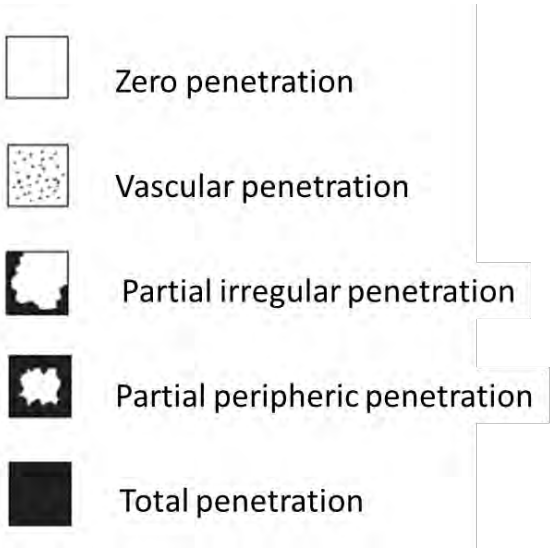

Source: (SALES-CAMPOS; VIANEZ; MENDONÇA, 2003).

Penetration analyses of *D.asper* poles showed relatively uniform boron penetration across the wall thickness (grade 4). Figure 3.42 presents the resulting penetration analysis of 6 different culms randomly selected from the bamboo storage. All these samples were extracted 40 cm from the poles ends.

The boron penetration along the pole length was also evaluated. In Figure 3.43, the resulting penetration analyses of the top (T1), middle (M), and bottom (T2) parts of a 4.5 m long *D. asper* pole are presented. In this example, a uniform distribution of boron can be observed in

all the analysed sections. These results show that diffusion of boron occurred through the bamboo wall thickness (although dry poles were used for treatment).

Figure 3.42 - Boron penetration analyses of different treated bamboo poles (*D. asper*).

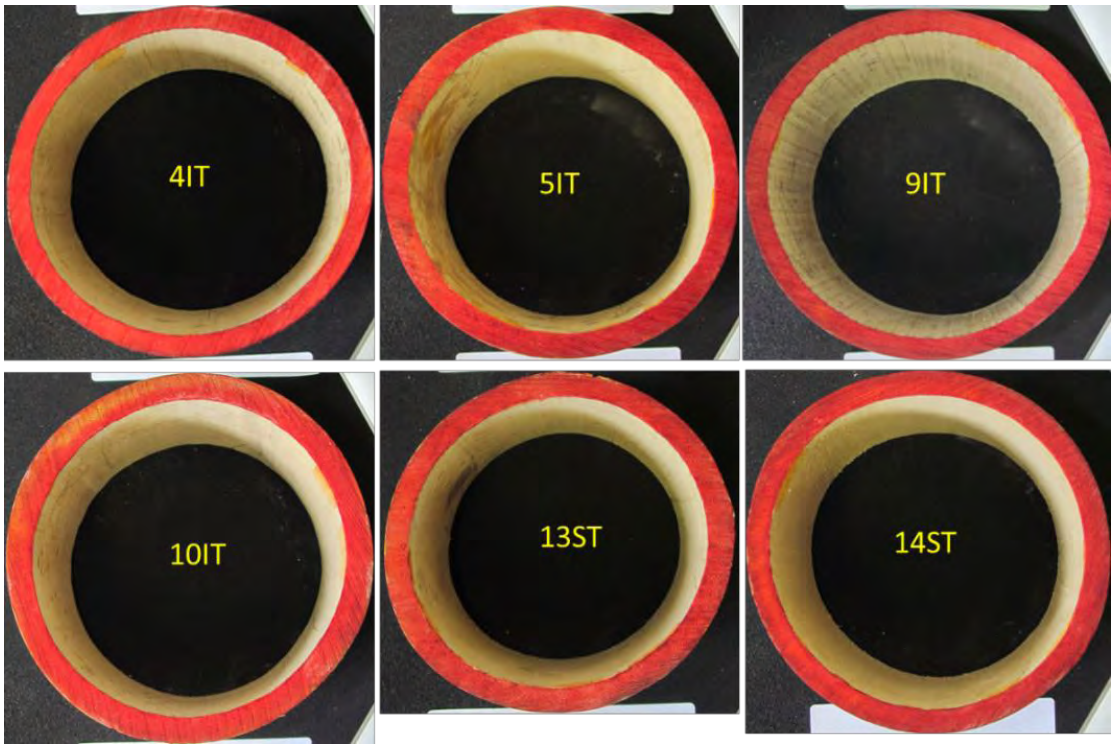

Source: Author's authorship.

Figure 3.43 - Boron penetration analyses of samples extracted from different positions along the culm length (T1=Top; M=Middle; T2=Bottom).

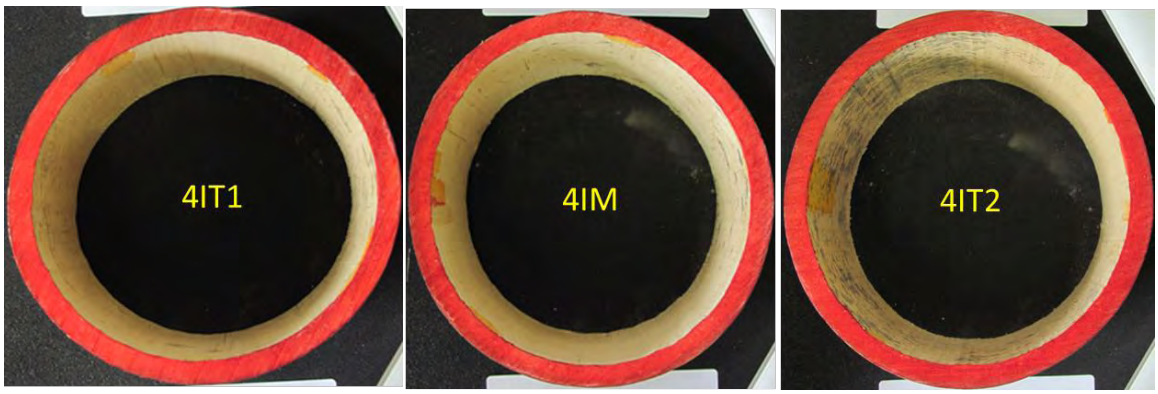

Source: Author's authorship.

3.4.2.4. Boron retention

The chemical analysis is used to determine the actual amount of active ingredient present in the treated material (retention analysis), which is very important for quality assurance (LEBOW, 2010). The main purpose of this section is to briefly describe this methodology and how it can be used in combination with the penetration analysis.

For boron detection, chemical procedures based on the digestion of the material can be performed according to the Brazilian standard NBR 6232:2013. In this method, the ground material is subjected to sulphuric acid digestion, filtered, diluted, and analysed by atomic absorption spectroscopy. By using a calibration curve, the amount of boron per mass of material can be determined (g/kg, or ppm).

Other procedure based on simpler methods can also be utilised. The AWPA A65-15 standard (*Standard method to determine the amount of boron in treated wood using azomethine-H or carminic acid*) is based on a colourimetric analysis, in which the target material is analysed through a UV-light spectrophotometer. In this method, boron is extracted by boiling a specific mass of ground material in water for 30 min. After filtering, the obtained solution is diluted in 250 mL volumetric flask and an aliquot (1 mL) is reacted with an Azomethine-H solution (a buffer solution is also added for pH control). The analysis is then conducted in a spectrophotometer with the absorbance measured at 420 nm. The amount of boron of an unknown solution is determined by using standard boron solutions (1 – 10 ppm) with known absorbances.

Although used for treated wood, both methods can be successfully applied for treated bamboo. However, the first method (based on NBR 6232:2013) depends on more expensive equipment and normally the analyses are expensive to be performed in third-party laboratories. The second method, although not common in the wood industry, is similar to the procedure used for boron determination in soil, which is almost ten times cheaper than the former one.

For comparison purposes, bamboo samples with different retention levels were evaluated through both methods. For each method, samples originated from the same original specimens were used. The NBR 6232:2013 method was conducted in an accredited laboratory for wood analysis at the Institute for Technological Research (IPT), São Paulo Brazil. The AWPA A65-15 method was performed in the Laboratory of Soil Analysis, at the USP in

Pirassununga, Brazil. Table 3.18 gives the results obtained by both methods in g/kg. Although there is a difference in the results of both methods, that can be related to the preparation/dilution process, the AWPA method is recommended for quality control purposes taking into account the accessibility and costs of the analyses (around R$ 10.00 for AWPA and R$ 70.00 for NBR).

Table 3.18 - Comparison between two methods for boron retention analysis.

Sample	Boron retention (g/kg)	
	NBR 6232:2013	AWPA A65-15
1	2.30	2.92
2	2.00	2.29
3	0.60	0.75
average	1.63	1.98

Source: Author's authorship.

Knowing the density of the original sample used for the analysis, the retention of the active ingredient can be obtained in kg/m^3 (kg of active ingredient per m^3 of bamboo/wood). Boron retention in wood/bamboo can be represented as BAE (boric acid equivalent), equivalent B_2O_3 or DOT. For total retention of DOT, the amount of boron determined by one of the previously described methods (in kg/m^3) is multiplied by a factor of 4.77 (1 g of B is related to 4.77 g of $Na_2B_8O_{13}.4H_2O$, in other words, DOT has 20.97% of boron in mass).

Table 3.19 presents the retention values of DOT in *P.edulis* and *D.asper* bamboo samples that were extracted from the middle part of 3-4.5 m long poles treated by the immersion method (immersion of 7-8 days). Average retention of 2.475 kg/m^3 of DOT was observed, with no considerable difference between species. As reference values, the Indian Standard IS9096:2006 recommends 6 kg/m^3 of active ingredient (borax + boric acid treatment, with the same proportion used for the formation of DOT) for indoor applications. Retention of 2.7 kg/m^3 of B_2O_3, equivalent to 4.0 kg/m^3 of DOT, is recommended by the American Wood Preservers's Association (AWPA) for boron-based treatments.

Although retention values presented in Table 3.18 are lower than those recommended by Standards, as discussed in section 3.2, the treatment procedure provided sufficient/uniform

boron penetration and showed no sign of fungi or insect attack in a stored stock of more than 300 poles during 3 years of storage. Additionally, increasing the immersion time or solution concentration, the retention values can be improved. A *D. asper* bamboo pole immersed for 19 days, for example, presented DOT retention of 4.152 kg/m^3. Each treatment method has its limitations and advantages, especially considering the passive ones, such as the immersion method. However, methods to assess the quality and real conditions of treated bamboo is strongly recommended as an important step for bamboo standardization.

Table 3.19 - Average retention values of DOT for *D. asper* and *P. edulis* bamboo treated by immersion method.

Species	n	Dry apparent density (g/cm^3)	Retention of DOT (kg/m^3)	
			Average	COV
D. asper	4	0.70	2.586	0.15
P. edulis	6	0.75	2.401	0.14
All	10	0.72	2.475	0.14

Source: Author's authorship.

4. CHAPTER 4 – Development of alternative treatments for bamboo

In this chapter, results related to the development and application of new preservatives for bamboo treatment by a vacuum/pressure process are presented. This chapter is organized into three main parts composed of results submitted to publication and complementary information.

First, the use of tannin extract in combination with disodium octaborate tetrahydrate for bamboo treatment is assessed. In this part, the polymerization of tannin in the presence of boron compounds and hexamine is evaluated. Solutions based on tannin were then used for the treatment of bamboo samples that were subjected to physical-mechanical and thermal characterizations, and accelerated fungi decay tests. Second, the use of citric acid for the chemical modification of bamboo is explored. In this part, a complete characterization of the physical, mechanical, and chemical properties, and thermal degradation of bamboo are reported using treatment solutions determined after preliminary studies, shown in Gauss, Dominguez and Savastano (2018). Lastly, the results of accelerated fungi decay tests of samples chemically modified with citric acid (still not published) and additional information regarding the vacuum/pressure process are presented as complementary information.

The following published/submitted publications are related to this Chapter:

GAUSS, C.; KADIVAR, M.; PEREIRA, R.; SAVASTANO JR, H. Assessment of *Dendrocalamus asper* bamboo treated with tannin-boron preservatives. Manuscript submitted to Construction and Building Materials, 2020.

GAUSS, C.; KADIVAR, M.; HARRIES, K.; SAVASTANO JR, H. Chemical modification of *Dendrocalamus asper* bamboo with citric acid: effects on the physical-chemical, mechanical and thermal properties. Manuscript submitted to Journal of Cleaner Production (under revision), 2020.

GAUSS, C.; DOMINGUEZ, A. L. S.; SAVASTANO JUNIOR, H. Dimensional stability and water absorption of *Dendrocalamus asper* bamboo treated with citric acid and boron salts (In Portuguese). In: 3º Congresso Luso-Brasileiro Materiais de Construção Sustentáveis, 2018, Coimbra, Portugal

4.1. Assessment of *Dendrocalamus asper* bamboo treated with tannin-boron preservatives

4.1.1. Introduction

Although the use of bamboo as a sustainable material has received more attention in the last ten years (based on the numbers of related publications in this field), it has been questioned due to several drawbacks. Owing to its chemical composition; high amount of starch (2-6%), sugar (2%) and protein (1.5-6%) and low content of resin, wax and tannin (LIESE, W., KUMAR, S., 2003; F.L. SUN, Y.Y. ZHOU, B.F. BAO, A.L. CHEN, 2011; LI et al., 2014; JIT KAUR, 2018), bamboo is very vulnerable to deterioration. Biological degradation such as decay fungi, termites and borers (*D. minutus*) attack are the major restrictions on bamboo use, especially in the construction industry (KAUR et al., 2016; SINGHA; BORAH, 2017; GAUSS; KADIVAR; SAVASTANO JR, 2019). Therefore, it needs preservative treatments.

Investigations on the bamboo degradation when exposed to biological attacks or outdoor conditions, lead the industry and academia to suggest and use different preservative methods and solutions to protect bamboo (LUGT; VOGTLÄNDER; BREZET, 2009; KAUR et al., 2016; TANG et al., 2019a). The chemical treatment methods serve as one of the most appropriate means of bamboo preservation and are recommended for large-scale construction projects (JANSSEN, 2000; CORREAL, 2016). However, careful considerations should be given to the selection of the materials for avoiding human health hazards because of illnesses that might be traced to hazardous chemicals (SCHULTZ, T. P., NICHOLAS, D. D., AND PRESTON, 2007; XU, G., WANG, L., LIU, J., AND HU, 2013). Sustainability, as well as its effect on the physical and mechanical properties of bamboo, must be considered. Accordingly, nowadays, less hazardous preservatives such as boron salts and tannins are becoming increasingly critical to diminish environmental impact (LUGT; VOGTLÄNDER; BREZET, 2009; KAUR et al., 2016; LI et al., 2019).

Boron salts are very common for wood and bamboo treatment and are recommended worldwide for structural use, in situations where the bamboo is protected from external adversities, such as water and sun exposure, and without contact with the ground/soil (JAYANETTI; FOLLETT, 2008; MOHAREB et al., 2011; TANG, 2013). Tannins, which are

naturally derived substances (GUJRATHI; BABU, 2007; DE HOYOS-MARTÍNEZ et al., 2019), have been used as preservatives in wood products offering protection against light and weathering factors, and against deterioration by insects, fungi and bacteria (H. YAMAGUCHI, 1998; YAMAGUCHI, H., YOSHINO, K., AND KIDO, 2002; HU et al., 2017; TOMAK et al., 2018; LI et al., 2019). Tannin extracts can be obtained from different sources, especially from tree barks, such as *Acacia mearnsii* (SILVEIRA et al., 2017; DE HOYOS-MARTÍNEZ et al., 2019). Normally they are used for leather production, animal feed, wood resins and other chemicals (DE HOYOS-MARTÍNEZ et al., 2019). At the best of our knowledge, there is no publication which reports tannin extract used for bamboo protection yet, and its effectiveness as a sustainable treatment that can protect bamboo from degradation is one of the hypotheses of this paper.

Although each of these two materials are efficient against termites, borers and some fungi, they are extremely leachable when are used alone (GARCI, A. A.; TADEO, J. L., 2006; SEN; TASCIOGLU; TIRAK, 2009; HU et al., 2017), which limits the application of bamboo in more exposed conditions. Several formulations as alternative treatment have been developed to overcome this negative aspect in the wood industry. The use of tannin extracts in combination of boron has been highlighted to reduce the leaching of boron and tannin compounds because of in-situ polymerization within wood structure (PIZZI; BAECKER, 1996; THEVENON MF, PIZZI A, 1998; THEVENON; TONDI; PIZZI, 2009; TONDI et al., 2012b; TONDI; HU; THEVENON, 2015; HU et al., 2017; LI et al., 2019). This combined preservative solution with a cross-linking agent (formalin, hexamine) at elevated temperature turns out to be a whole new material with improved characteristics and properties compared to the characteristics of the individual components, possessing positive results in terms of leachability, fungi decay tests and stability (TONDI et al., 2012b; TONDI; HU; THEVENON, 2015).

The role of tannin in this mixed new treatment product is the formation of an insoluble polymerized network, while boron compounds such as boric acid can facilitate this reaction and be partially incorporated in the polymerized tannin (TONDI et al., 2012a; HU et al., 2017). With a hard polymerized material partially occupying the wood's cavities, acceptable results have been published in terms of mechanical properties of tannin-boron treated wood. However, there is a lack of information focused on this treatment for bamboo. Although bamboo is also a porous material and its main chemical composition is similar to wood (LI et al., 2015c), it has been

proved that the deterioration behaviour of bamboo is quite different from that of wood (LI et al., 2014). Microstructural and chemical modifications might be induced as the results of chemical treatment, and consequently, the bamboo macro characteristics, physical, and mechanical properties can change.

The necessity of having information regarding the use of tannin-boron treatment for bamboo as a new treatment method prompted the authors starting research in this area to take a step towards high added-value bamboo-based materials. In this work, the mechanical and physical properties, as well as fungi decay performance and thermal stability of *D. asper* bamboo treated with tannin and tannin-boron solutions were evaluated.

4.1.2. Materials and methods

4.1.2.1. Materials and samples preparation

Mature culms (more than three years old) of *D. asper* bamboo were collected and conditioned in a protected environment. The culms were harvested at an experimental field in the USP campus, Pirassununga, Brazil. Pirassununga is located at an altitude of 630 m above the sea level, with an annual average rainfall of 1363 mm and a tropical climate with well-defined seasons (rainy summer and dry winter).

The treatment process was conducted using six different internodes from the middle part (more uniform) of three different culms. Tangentially oriented strips, approximately 200 mm long and 30 mm wide, were cut from the internode sections.

The apparent densities at approximately 7% MC and in the dry condition, the real density, fibre volume fraction, and chemical composition are shown in Table 4.1. The apparent densities were measured by the water immersion method at 27 °C (water density = 0.9965 g/cm^3), as described in ASTM D2395−17 Standard. The fibre volume fractions were determined using images obtained by an optical stereoscope and analysed through ImageJ analysis software (RASBAND, 2018). The real density was determined using a helium pycnometer, in which bamboo particles (dried at 60 °C for 48 h) representative of all the internodes (A-F) were used for the analysis. The same particles were used for the chemical analysis that was carried out following the methodology proposed by Van Soest (1994) described in Morais, Rosa and

Marconcini (2010) (EMBRAPA Technical Document - Procedures for Lignocellulosic Analysis) (MORAIS; ROSA; MARCONCINI, 2010). This method basically consists of separating cellular (lipids, fats, starch, water-soluble compounds) and cell-wall contents (holocellulose, lignin, insoluble protein) by using neutral and acid detergent solutions. The balance between the solubilised and filtered fractions using both detergent solutions is used to calculate alpha-cellulose, hemicellulose, lignin, and extractives. The percentage of ashes was obtained by burning the sample at 500 °C for 4 h (MORAIS; ROSA; MARCONCINI, 2010).

Table 4.1 - Physical properties and chemical composition of *D. asper* bamboo used in this work.

Internode	Apparent density (g/cm^3)	MC (%)	Oven-dry apparent density (g/cm^3)	Real* density (g/cm^3)	Fibre** volume fraction (%)	Chemical composition*				
						α-C	L	H	E	A
A	0.978	7.5	0.949	-	-	-	-	-	-	-
B	0.979	7.6	0.942							
C	0.853	7.4	0.827							
D	0.882	7.5	0.845							
E	0.887	7.4	0.867							
F	0.894	7.8	0.864							
Avg	0.912	7.5	0.882	1.303	44.82	54.8	20.2	13.7	9.6	1.7
COV	0.06	0.02	0.06	0.03	0.08	-	-	-	-	-

α-C: alpha-cellulose; L: lignin; H: hemicellulose; E: extractives; A: ashes

* Real density and chemical composition were determined using ground material obtained from all internodes. ** Determined by the analysis of eight samples randomly chosen.

Source: Author’s authorship.

4.1.2.2. Tannin, boron compounds and hexamine reaction

Before bamboo treatment, the polymerization of tannin with hexamethylenetetramine (hexamine) and the boron compounds boric acid, borax and DOT (1.54:1 ratio borax/borax acid) was explored. Several formulations were prepared with different concentrations of hexamine, boric acid and DOT in relation to tannin. Table 4.3 gives the investigated solutions and corresponding compositions. The concentration of hexamine is based on the dry weight of tannin, and the concentrations of boric acid and DOT are based on the total solution weight. All the solutions were adjusted to a pH = 9 using a 50% wt/vol NaOH solution. After preparation, the solutions were oven-dried at 103 ± 2 °C and then maintained in this temperature for 48 h for complete polymerization reaction.

After drying/curing process, the obtained samples were crushed into particles (28 mesh) and submitted to a leaching process. For each condition, 4 g of solid material and 80 mL of distilled water were added into glass beakers. The samples were stirred every 24 h and maintained immersed for 72 h. Then the samples were filtered and dried at 103 °C up to a constant weight. The obtained materials were submitted to a second leaching cycle (using the same previous procedure) and again filtered and dried at 103 °C.

The obtained samples were classified into unleached and leached samples and were submitted to a boron analysis using a colourimetric method (CAPELLE, 1961), the same one used for the determination of boron in plants (CARMO et al., 2000). The samples were calcined in a furnace at 550 °C for 4 h and the ashes were then digested with 25 mL of HNO_3 solution (0.1 M). Then, 1 mL of the obtained solution was diluted to 100 mL of HCl (0.1 M) and a buffer solution was added to control the pH. Azomethine-H was added to the diluted solution to react with boron. The obtained solution was analysed in a UV-Visible spectrophotometer with a wavelength of 430 nm. The obtained absorbance was used to calculate the boron concentration according to a calibration curve, previously prepared.

Boric acid, disodium borate decahydrate, hexamine and sodium hydroxide of analytical grade supplied by Labsynth®, Brazil, were used. *Acacia mearnsii* tannin powder (Phenotan AG) was gently provided by Tanac®, Brazil.

Table 4.2 - Tannin-based solutions used for the leaching test.

Sample	ID	Solution composition
1	T10H0.6	Tannin 10% + Hexamine 6%
2	T10H1.0	Tannin 10% + Hexamine 10%
3	T10H0.6BA1	Tannin 10% + Hexamine 6% + Boric acid 1%
4	T10H1.0BA1	Tannin 10% + Hexamine 6% + Boric acid 5%
5	T10H0.6BA5	Tannin 10% + Hexamine 10% + Boric acid 1%
6	T10H1.0BA5	Tannin 10% + Hexamine 10% + Boric acid 5%
7	T10H0.6DOT1	Tannin 10% + Hexamine 6% + DOT 1%
8	T10H1.0DOT1	Tannin 10% + Hexamine 10% + DOT 1%
9	T10H0.6DOT5	Tannin 10% + Hexamine 6% + DOT 5%
10	T10H1.0DOT5	Tannin 10% + Hexamine 10% + DOT 5%

Obs.: % of hexamine in relation to the dry mass of tannin and % of DOT and BA in relation to the total solution weight

Source: Author's authorship.

4.1.2.3. Treatment process

Five samples per internode (total of 30 samples) were used for each treatment condition, according to Table 4.2. Before the treatment procedure, the samples were air-dried at 103 ± 2 °C until constant weight and after that conditioned in a climatic chamber at 25 °C and 70% RH for 240 h. This procedure was used to track weight changes after treatment and at the same time treat the samples in a more realistic condition (with moisture). The samples were treated in a pressure vessel following a vacuum/pressure schedule (Figure 4.1): initial vacuum (-650 mmHg) without any solution for 15 min, vacuum phase with the solution for 60 min, pressure phase (14.1 kgf/cm^2) for 180 min and final vacuum phase for 15 min. Then, the obtained samples of each treatment condition were dried at room temperature for 48 h, oven-dried at 60 ±2 °C for 24 h, and finally cured at 103 ± 2 °C for 48 h for the reaction of tannin polymerization to occur.

The treatment solutions were prepared by dissolving first the tannin extract in 8 L of distilled water (10% wt/wt solution) and adding the cross-linking agent hexamethylenetetramine (hexamine) to the solution. For the tannin solution (T10H), 6% (by tannin dry weight) of hexamine was used. For the samples treated with the presence of boron (B5 and T10HB5) in the formulation, a combination of boric acid and disodium borate decahydrate (borax) was used in the ratio of 1: 1.54 by mass for the formation of DOT ($Na_2B_8O_{13}.4H_2O$). The tannin-boron solution (T10HB5) was prepared by first dissolving the boric acid and borax (5% wt/wt) and

then adding the tannin extract (10% wt/wt) and hexamine (10% on tannin dry weight). The pH of all the tannin-based solutions was maintained at pH=9 using a NaOH 50% wt/vol solution.

Table 4.3 - Treatment conditions with tannin-based formulations.

ID	Treatment solution (wt/wt)	Number of samples	Temperature treatment after impregnation (°C)
Reference	none	30	103
B5	DOT 5%	30	103
T10H	Tannin 10% + Hexamine 6%*	30	103
T10HB5	Tannin 10% + Hexamine 10%* DOT 5%	30	103

* Based on dry tannin weight

Source: Author's authorship.

Figure 4.1 - Layout of the samples and pressure vessel used for the impregnation process.

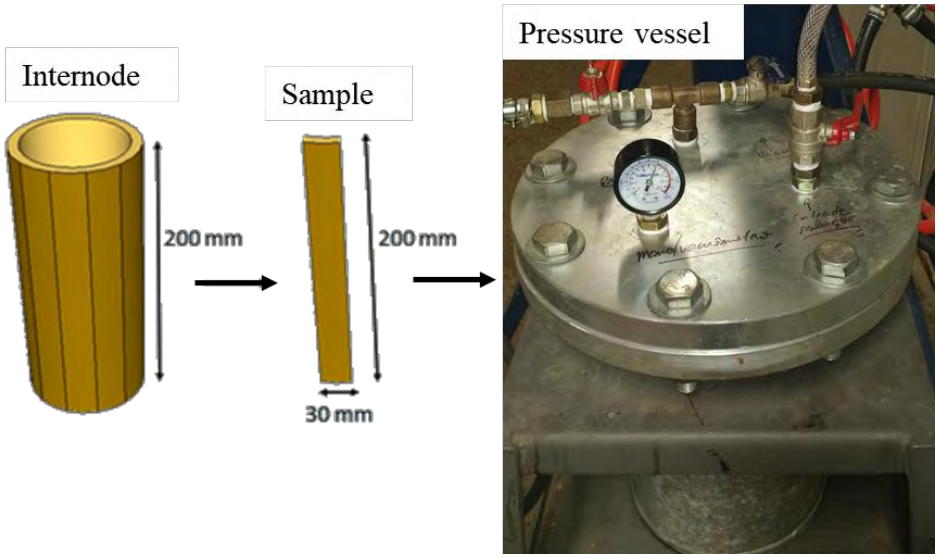

Source: Author's authorship.

4.1.2.4. Water absorption, swelling and leaching test

The water absorption and swelling behaviours of treated bamboo were determined during a leaching test procedure. Sixteen 20 mm x 20 mm x thickness (t) samples per condition (see Figure 4.2) were extracted from the middle part of four different specimens after treatment.

These samples were subjected to a leaching process for 12 days according to recommendations of AWPA E10:16. The treated samples were first dried at 60 °C until a constant weight was achieved. The samples were then immersed in distilled water for the determination of water absorption (WA) and thickness and width swelling (TS and WS respectively) after 12 h and 24 h of immersion. The dimensions of the samples were obtained with an accuracy of 0.01 mm and the weight determined with a precision of 0.001 g. WA, TS and WS were calculated in relation to the initial weight and dimensions of the samples after drying at 60 °C. After the measurements, the water was changed, and the samples were conditioned in a steel vessel where a vacuum (-650 mmHg) was applied for 60 min. to guarantee total penetration of water. Following this, the water was replaced after 12 h and then every 24 h for 12 days. After the completion of the leaching process, the final weight and dimensions of the samples were obtained, and they were again dried at 60 °C until a constant weight was achieved.

Figure 4.2 - Bamboo samples used for the water absorption, swelling and leaching tests. Where t = bamboo wall thickness; OL = outer layer; IL = inner layer.

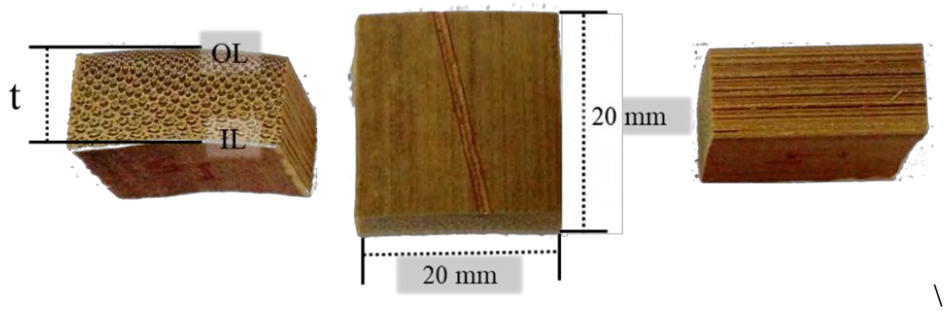

Source: Author's authorship.

4.1.2.5. Boron retention analysis

The samples treated with formulations based on DOT were subjected to boron retention analyses conducted according to Brazilian Standard ABNT NBR 6232:2013. For the chemical analyses, samples extracted from the middle part of four different specimens of the samples treated with boron (leached and unleached) were ground into a powder and passed through a 28-mesh sieve. The obtained material was subjected to sulphuric acid digestion, diluted and

analysed by atomic absorption spectroscopy. The chemical analyses were performed in the Trees, Wood, and Furniture Laboratory at the Institute for Technological Research (IPT), São Paulo, Brazil, following the same procedures used for treated wood. The amount of equivalent B_2O_3 was calculated according to:

$$Retention\ (B_2O_3) = \left(\frac{B \times \rho}{100}\right) \times 3.22 \qquad \text{Eq. 4.1}$$

Where B is the weight percentage of boron in the analysed sample (in%), ρ is the oven-dry apparent density of the sample (in kg/m^3), and 3.22 is a stochiometric factor for obtaining the amount of B_2O_3 based on the amount of boron.

4.1.2.6. Accelerated fungi decay test

A modified fungi decay test was performed in the Institute for Technological Research (IPT), São Paulo, Brazil, based on the work conducted by (MONTEIRO, 1997) and adapted from AWPA E10-16 Standard. Small samples of 20 x 3 x thickness (t) mm³ were extracted from the middle section of four different specimens and tested in Petri dishes, as shown in Figure 4.3. Samples extracted from the specimens submitted to the leaching cycles described in 4.2.2.3 were also tested. 16 samples per condition were tested against the fungi strains *Pycnoporus sanguineus* (white-rot) and *Gloeophyllum trabeum* (brown-rot), obtained from IPT. First, the fungi were cultivated in potato dextrose agar (PDA) for two weeks in Petri dishes. Before the exposure of the samples, they were conditioned at 26 °C and 70% RH for two weeks until a constant weight (initial weight). Then the samples were sterilized at 120 °C for 15 min and allocated aseptically in the Petri dishes (four Petri dishes with four samples per condition per fungus) to be exposed to the fungi (see Figure 4.3). After eight weeks of test, the samples were removed from the climatic chamber, cleaned, dried at 60 °C for 2 hours, and then conditioned at 26 °C and 70% RH until a constant weight (final weight). The initial and final weights were used to calculate the weight loss.

Figure 4.3 - Layout of the samples and pressure vessel used for the impregnation process.

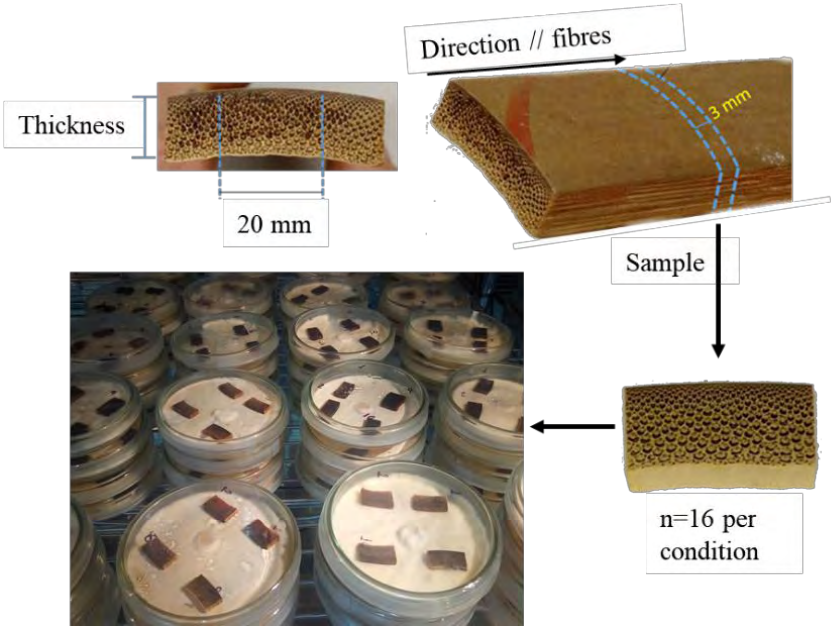

Source: Author's authorship.

4.1.2.7. Mechanical characterisation

The effects of the proposed treatments on the mechanical properties of bamboo were evaluated. Machined coupon specimens, representing the full wall thickness, were used for compression, bending, and shear tests. For all the tests, the samples were extracted from six to eight different specimens, representing all the internodes. All required specimen dimensions were obtained using a digital calliper having a precision of 0.01 mm. The moisture contents at the time of test were determined by weighing the samples before testing and afterwards drying at (100 ± 2) °C for at least 48 h.

The compression tests parallel to the bamboo longitudinal axis (parallel to fibres) were performed with samples with transverse sections having the same size as the culm wall (t x t) and length four times the thickness (L= 4t). The tests were conducted in a 600 kN capacity Instron universal testing machine (model 600DX) at a cross-head displacement rate of 0.5 mm/min. The tests and results calculation followed the recommendations of ASTM D143-14. The longitudinal compression strength (f_c) is reported as the maximum load divided by the cross-section area of the sample.

Three-point bending tests were conducted using samples in a prismatic form with 200 x 10 x thickness (t) mm^3. A span of 190 mm was used for all the tests, which resulted in an average shear span to depth ratio exceeding 10 in every test. The samples were orientated such that the outer culm wall was in compression (OC). The tests were conducted following Procedure A of ASTM D7264-15 as modified by others (DIXON; GIBSON, 2014b; GIBSON et al., 2016; GAUSS; SAVASTANO; HARRIES, 2019) using a 10 kN capacity Testresources electromechanical universal testing machine at a displacement rate of 2.5 mm/min. The modulus of rupture (MOR), modulus of elasticity (MOE) and specific strain were calculated according to ASTM D7264-15. The displacement of midheight (t/2) of the sample at midspan was tracked using a Digital Image Correlation (DIC) setup (GAUSS; SAVASTANO; HARRIES, 2019).

The shear behaviour of the treated bamboo samples was evaluated through an interlaminar shear test by tension (MOREIRA, 1991; INBAR, 1999). Coupon specimens are scored halfway through their depth perpendicular to the loading direction at two locations resulting in a shear plane having an area $A = L_s \times t$. Since the shear plane is at the middle of the specimen, when loaded in tension, the plane is subject to pure shear. The shear strength is then calculated using the maximum load at failure divided by the shear area A. All the interlaminar shear tests were conducted using a 10 kN capacity Testresources electromechanical universal testing machine using a displacement speed of 1.0 mm/min.

4.1.2.8. Thermal characterisation

The thermal characterisation was performed in order to understand the thermal degradation of bamboo treated with DOT and tannin-based solutions. For the analyses, samples extracted from the middle part of four different specimens of each condition were ground into a powder, passed through a 60-mesh sieve and dried at 60 °C for 48 h. The tests were conducted in a Netzsch TGA/DSC model STA 449 F3 Jupiter using synthetic airflow (flow rate of 100 mL/min.) from room temperature up to 800 ^oC at 10 ^oC/min. The synthetic airflow was used to better understand the behaviour of the material in a real environment, in the presence of oxygen. This procedure has been demonstrated to be correlated with limiting oxygen index (LOI) flammability tests (LIODAKIS; ANTONOPOULOS; KAKARDAKIS, 2010; LIODAKIS et al., 2013; JIANG; LI; GAO, 2015; PARK et al., 2015; WANG; LIU; LV, 2017).

4.1.2.9. Statistical analyses

The averages of each test for each test condition are presented with the corresponding coefficient of variation (COV) and the number of samples. The differences among the treatment conditions on the evaluated properties were checked by a Tukey test and analysis of variance (ANOVA) for significant ($p < 0.05$) differences. All analyses were performed using MINITAB Release 18 Statistical Software.

4.1.3. Results and discussion

4.1.3.1. The polymerization reaction of tannin, boron compounds and hexamine

Several works report the use of tannin solutions based on mimosa tannin extract (10-35% solution), hexamine (6% by mass on dry tannin), and boric acid (5% on total solution) as a source of boron (THEVENON; TONDI; PIZZI, 2009; TONDI et al., 2012c, 2012a, 2013). The pH of the solution can also influence the polymerization process. Usually, a pH correction of the tannin-based solutions to a pH = 9 is performed with a NaOH solution before the curing heat treatment (TONDI et al., 2012c, 2013). In fact, pH can influence the solubility of the formed compounds and the viscosity of the solution before polymerization (GARCIA; PIZZI, 1998; PEÑA et al., 2009; TONDI et al., 2013). Another important aspect is that normally only boric acid is utilised in the formulations reported in the literature and to the best of our knowledge, there is no comprehensive study on the effect of hexamine on boron leaching and solubilization of the formed polymer.

Figure 4.3 shows the samples before, during, and after the leaching test. It was possible to observe that some unreacted tannin was solubilized in water. The results obtained after the leaching process are presented in Table 4.4. Firstly, it can be seen that the increase of the hexamine concentration in the formulation had no considerable influence on the solubility of the formed compounds, especially when observing samples 1 and 2. The samples with higher concentrations of boric acid and DOT showed the highest losses after leaching, which may be related to boric acid or DOT in excess or unreacted with the tannin polymer network. Regarding

the loss of boron, it is observed that all formulations had a considerable loss of boron, but still maintaining more than 50% even after the leaching process. It should be noted that both boric acid and DOT are very soluble, and if not in combination with tannin, the loss of boron would be total. Additionally, it can be observed that in samples 4, 6 and 10, the increase in hexamine concentration reduced boron leaching, especially in sample 4. However, among the formulations with higher concentrations of boric acid and DOT, sample 10 presented the lowest boron and weight losses after leaching.

Figure 4.4 - Procedure used for the leaching test. a) Particles of solid polymerized tannin, b) solids with different compositions (samples 1-10) at the beginning of the leaching test and c) at the end of the test, and d) obtained solid material after filtering.

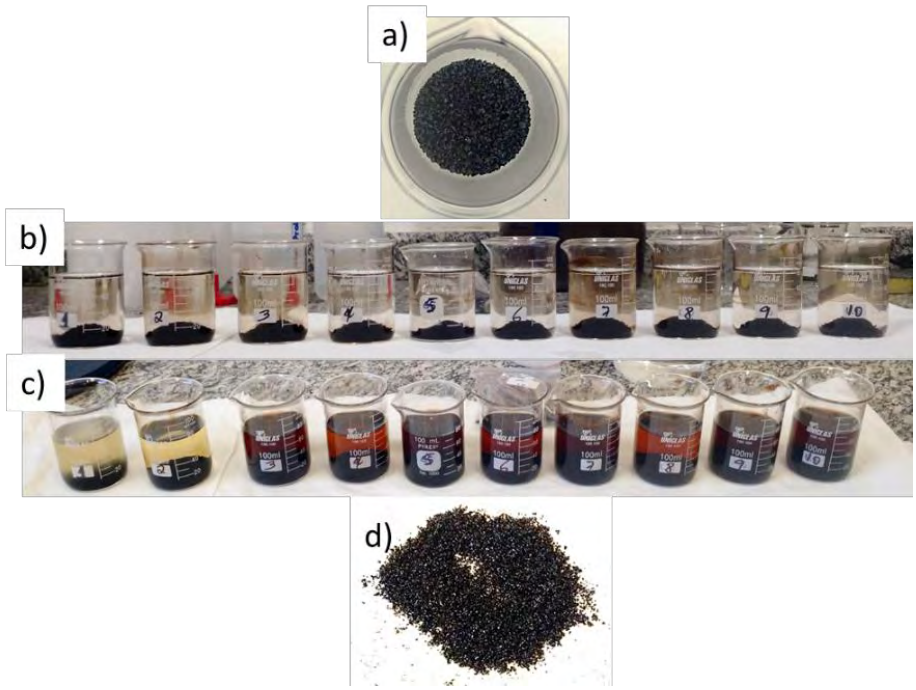

Source: Author's authorship.

Figure 4.5 depicts the FT-IR spectra of tannin-based compounds (pure tannin; T10H1.0; T10H1.0B5; T10H1.0DOT5). The addition of hexamine alters the tannin structure, due to the differences of the obtained spectrum and consequently of the chemical bonds. It is mainly noted a difference regarding the groups C = C of aromatics (1600 cm^{-1}) and the absence of peaks between 1450 cm^{-1} and 1500 cm^{-1} in tannin samples with DOT and BA + Hexamine, which is related to the tannin polymerization process (PEÑA et al., 2009; YUBOCHAI et al., 2017). A

difference in the 1600 cm^{-1} peak (aromatics) is observed in the samples with and without boron. The more pronounced hump between 1350-1500 cm^{-1} of the TH1.0DOT5 and TH1.0BA5 samples may be attributed to B–N stretching (1465–1330 cm-1) and B–O stretching (1380–1310 cm-1) (STUART, 2004). However, there is no noticeable difference between the samples with BA and DOT.

Concerning the results presented in Table 4.4, solutions based on the formulations of the samples 1 (T10H0.6) and 10 (T10H1.0DOT5) were used for bamboo treatment by vacuum/pressure process. For the tannin + hexamine samples, the amount of hexamine did not change the weight loss after leaching, therefore a higher amount of hexamine is unnecessary. In the case of the tannin + hexamine + boron samples, sample 10 had the lowest weight loss (among the high boron content samples) and the increase of hexamine helped to reduced boron loss.

Table 4.4 - Results of weight loss and boron analysis of all the conditions submitted to the leaching cycles.

Sample	ID	Weight loss after leaching (%)	Boron analysis (mg/kg - ppm)		
			Unleached	Leached	Boron loss (%)
1	T10H0.6	1.99	-	-	-
2	T10H1.0	1.94	-	-	-
3	T10H0.6BA1	3.04	11,478	8,744	23.81%
4	T10H1.0BA1	2.74	12,973	11,542	11.03%
5	T10H0.6BA5	24.84	33,055	16,768	49.27%
6	T10H1.0BA5	23.96	34,535	18,536	46.32%
7	T10H0.6DOT1	0.29	12,137	7,136	41.20%
8	T10H1.0DOT1	0.68	11,044	6,477	41.35%
9	T10H0.6DOT5	19.19	33,570	17,668	47.37%
10	T10H1.0DOT5	18.48	31,030	18,552	40.21%

Source: Author’s authorship.

Figure 4.21 – FT-IR spectra of polymerized tannin formulations.

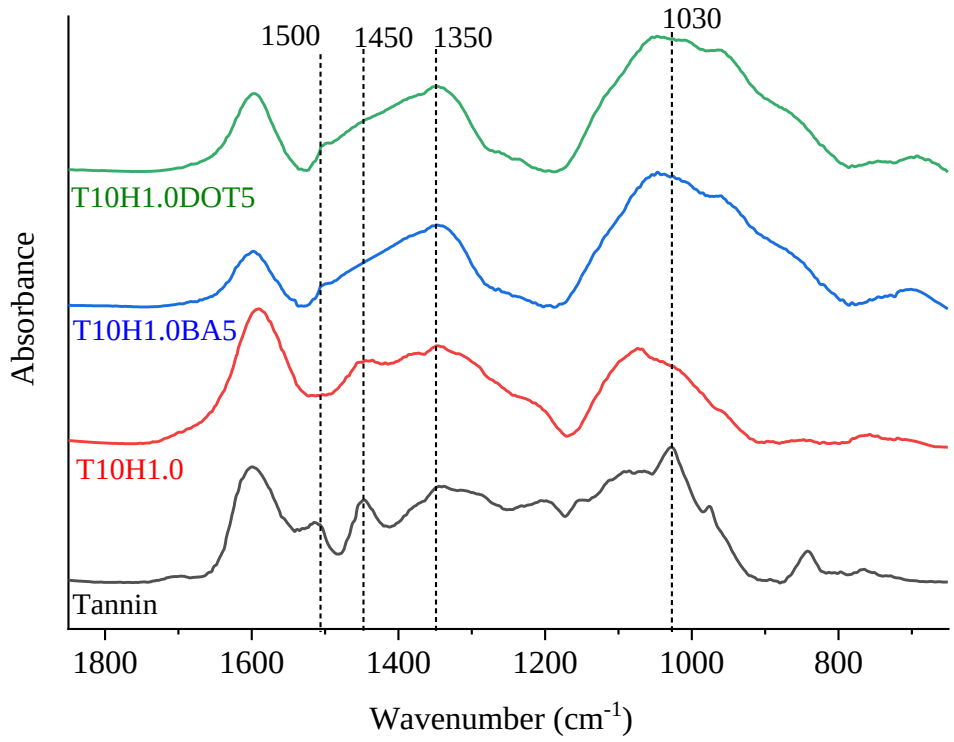

Source: Author's authorship.

4.1.3.2. Bamboo treatment

Table 4.5 gives the solution absorption (weight of preservative solution absorbed in relation the weight of the samples before treatment) and weight percentage gain (WPG) (the relation between the dry weight of the samples after and before treatments).

Although the bamboo samples presented reasonable solution absorption, a low WPG was observed. Bamboo has a considerable high amount of extractives, which can leach during treatment and explain the low WPG. For the tannin based solutions, the WPG are equivalent to retention values (R) of 24.17 kg/m^3 and 24.7 kg/m^3 for TH10 and TH10B5, respectively, calculated by the formula: $R\left(\frac{kg}{m^3}\right) = \frac{W_{A.I}\,(g)}{\rho_{a\,(\frac{g}{cm^3})}}.10$, where $W_{A.I}$ is the weight of retained active ingredient and ρ_a the dry apparent density of bamboo. Tondi et al. (2013) reported absorptions (or also called impregnation rate) of up to 180% and 120% for scots pine and beech woods, respectively, using 10% tannin extract solutions and vacuum impregnation. These wood species have a porosity of 65.7% (scots pine) and 48.4% (beech) (TONDI et al., 2012b). In comparison, the porosity of the bamboo used in this study, using the dry apparent density and real density

(Table 4.1), was found to be 32.3%, which explains the lower absorption values observed in bamboo. Additionally, since bamboo does not have pathways for radial penetration, like in wood, the penetration within bamboo's microstructure mainly occur in the metaxylem vessels and the access to parenchyma is limited (LIESE, 2004; LIESE; TANG, 2015b). Therefore, even using vacuum/pressure impregnation for treatment, the accessibility of the solutions into the bamboo structure is limited by anatomical features.

Table 4.5 - Sample conditions after the treatment processes.

Conditions	MC Before Treat. (%)		Solution absorption wt (%)		WPG After drying (%)	
	avg.	COV	avg.	COV	avg.	COV
Reference	7.1	0.05	-	-	-	-
B5	7.1	0.04	49.5	0.09	0.04	-
TH10	7.2	0.05	42.6	0.10	2.74	0.12
TH10B5	7.2	0.04	38.9	0.11	2.80	0.10

Source: Author's authorship.

4.1.3.3. Water absorption, swelling and leaching

Table 4.6 gives the results of water absorption (WA), thickness (TS) and width swelling (WS) after 12, 24 and 288 h (end of the leaching process). The statistical analysis presented in the Tables refers only to the comparison among the treatment conditions (Reference, B5, T10HB5, and T10H) for each analysed property. The change in dimensions was tracked measuring the thickness and width in the middle of the samples. Because of the bamboo samples natural curvature, the volumetric changes were not considered. The changes in length were negligible.

The three treatments had a small positive effect on WA, TS, and WS reduction. In the properties measured at 12 h, all the results are similar. However, at the end of the experiment (t = 288 h) the treatments caused a small decrease in WA, TS, and WS, especially the T10HB5 condition. The change in WA and dimensions were more pronounced in the first 24 h of immersion.

Tondi et al. (2012c) studied the dimensional stability of wood in different values of relative humidity treated with 10% and 20% tannin solutions. They concluded that there is no

considerable difference in comparison to the reference, with only a small increase in radial swelling of the treated wood (TONDI et al., 2012c). To the best of our knowledge, there is no available data in the literature about physical properties of bamboo treated with tannin and boron preservatives. From the obtained results, we can conclude that the treatments investigated in this work had little effect on the hydrophilicity behaviour of bamboo.

Table 4.6 - Summary of water absorption and swelling results. Same letters in the same row (a, b, or c) mean there is no statistical difference among treatment conditions.

Treatment conditions							
n = 16				Reference	B5	T10HB5	T10H
Water absorption (%)		12h	Avg.	28.96 [a,b]	27.67 [b]	29.37 [a]	30.23 [a,b]
			COV	0.06	0.13	0.08	0.05
		24h	Avg.	39.72 [a]	36.09 [b]	37.61 [a,b]	38.56 [a,b]
			COV	0.05	0.10	0.07	0.04
		288h	Avg.	67.43 [a]	59.18 [b]	59.62 [b]	61.96 [b]
			COV	0.05	0.07	0.06	0.03
Swelling (%)	Thickness	12h	Avg.	6.81 [a]	6.09 [a,b]	5.86 [b]	5.96 [a,b]
			COV	0.11	0.18	0.13	0.10
		24h	Avg.	10.13 [a]	8.49 [b]	8.11 [b]	7.94 [b]
			COV	0.10	0.14	0.14	0.11
		288h	Avg.	13.12 [a]	11.19 [b]	10.35 [b,c]	9.70 [c]
			COV	0.08	0.16	0.15	0.13
	Width	12h	Avg.	3.93 [a]	3.92 [a]	3.67 [a]	3.85 [a]
			COV	0.16	0.14	0.09	0.14
		24h	Avg.	5.43 [a]	5.12 [a,b]	4.54 [b,c]	4.76 [c]
			COV	0.14	0.09	0.10	0.13
		288h	Avg.	6.95 [a]	6.75 [a]	5.67 [b]	5.81 [b]
			COV	0.11	0.08	0.08	0.13

Source: Author's authorship.

Water causes severe degradation of wood preservatives, especially for boron-based formulations. Therefore, leaching tests are essential to evaluate the performance of treated wood/bamboo. Table 4.7 shows the results of the leaching tests with the corresponding boron loss. This was a severe leaching test, with the main idea of testing the treated materials in harsh conditions. After the test, the samples treated with T10HB5 had the lowest weight loss among all the analysed conditions. However, the boron loss was the same as the B5 samples, treated only with DOT. Although the main purpose was to reduce boron leaching by using a polymerized tannin network, the severe leaching cycles used in this study seemed to be capable of solubilizing most part of boron. Interestingly, the same formulation when tested independently (results of section 4.2.3.1), preserved 60% of boron. In the work of Tondi et al. (2012c), they reported that between approximately 20% of tannin was leached using 20% tannin solution and 35% was leached using a 10% tannin solution. Although using hexamine as a cross-linking agent, the tannin loss was attributed to unreacted tannin within wood's structure. After leaching cycles according to the standard EN 1250-2 (1995), Tondi et al. 2012a reported a boron loss of approximately 30% for scots pine and approximately 22% for beech wood after 80 h of test with the water changed 6 times. In the same work, it is possible to observe that most part of unreacted boron leaches out in the first leaching cycles. Although the tannin-based solutions reduced significantly boron leaching in the investigated conditions, the effect of longer-term and harsher leaching tests were not performed, which could lead to further boron loss.

The polymerization of tannin network within bamboo's structure could have had its reaction affected by the presence of bamboo constituents and therefore, affected the boron fixation. Nevertheless, we can observe that a small amount of boron is still present in the leached samples.

Table 4.7 - Mass loss after leaching cycle and B_2O_3 equivalent retention before and after leaching.

Conditions		Weight loss after leaching cycle (%)	B_2O_3 eq. retention (kg/m^3)		Boron loss (%)
			Before leaching	After leaching	
Reference	Avg.	6.65	-	-	-
	COV	0.07			
B5	Avg.	6.63	4.66	0.82	82.4
	COV	0.10	-	-	-
T10H	Avg.	6.77	-	-	-
	COV	0.10			
T10HB5	Avg.	5.66	3.01	0.55	81.7
	COV	0.08	-	-	-

Source: Author's authorship.

4.1.3.4. Fungi decay tests

Bamboo samples were tested in pure fungi cultures of *P. sanguineus* and *G. trabeum* to evaluate the efficiency of the proposed treatments against fungi decay.

Figure 4.5 shows the reference and T10HB5 samples at the end of the test after exposure to the *P. sanguineus* fungi. The treated samples did not show mycelium growth on the surface, while the reference samples were completely covered. Table 4.8 shows the results of the weight losses (WL), with the corresponding ANOVA analysis, of all the conditions (leached and unleached) for both *P. sanguineus* and *G. trabeum* fungi. The first thing to notice is that *P. sanguineus* caused higher WL than *G. trabeum* in all treatment conditions. The effect of the leaching process is also clearly noticeable. Interestingly, even with the high boron loss of the T10HB5 samples (see Table 4.7), this condition presented the lowest WL among the leached samples in both fungi tests. On the other hand, although the B5 samples had the best performance in the unleached condition (4.50% and 3.37% for the *P. sanguineus* and *G. trabeum* respectively), the leached samples had WLs similar to the reference.

Figure 4.5 - Examples of reference and T10HB5 samples after the test against *P. sanguineus* fungi.

Source: Author's authorship.

Table 4.8 - Results of fungi decay tests presented in weight loss percentage. Same letters (a, b, or c) mean there is no statistical difference among treatment conditions.

Weight loss – WL (%)								
Condition	*P. sanguineus* n=16				*G. trabeum* n=16			
	Unleached		Leached		Unleached		Leached	
	Avg.	COV	Avg.	COV	Avg.	COV	Avg.	COV
Reference	9.26 [a]	0.23	15.03 [a]	0.22	6.02 [a]	0.11	10.52 [a]	0.66
B5	4.50 [c]	0.28	10.51 [a,b]	0.51	3.37 [c]	0.39	13.37 [a]	0.53
T10H	6.98 [b]	0.25	9.79 [b]	0.65	3.81 [b,c]	0.27	3.48 [b]	0.63
T10HB5	5.28 [c]	0.27	7.58 [b]	0.88	4.47 [b]	0.21	1.35 [b]	0.90

Source: Author's authorship.

White-rot fungi (such as *P. sanguineus*) degrade lignin and hemicellulose while brown-rot fungi (such as *G. trabeum*) are selective for cellulose (WEI; SCHMIDT; LIESE, 2013). Results of bamboo fungi decay are scarce, especially about treated bamboo. In the work of Suprapti (2010) different bamboo species were subjected to decay by white-rot, brown-rot and soft-rot fungi. For *D. asper* bamboo the highest values of weight loss were caused by the white-rot fungi *P. sanquineus,* being classified as non-durable. On the other hand, Wei, Schmidt and Liese (2013) found a weight loss below 5% of *D. asper* bamboo tested against the brown-rot fungi *G. trabeum*.

Tiburtino et al. (2015) tested *B. vulgaris* and *D. giganteus* (normally confused with *D. asper* in Brazil) samples treated with CCB against *Postia placenta* (brown-rot) and *Polyporus fumosus* (white-rot). For the reference (control) samples, they reported a weight loss in *D. giganteus* of 10.83% and 8.35% for *P. placenta* and *P. fumosus* respectively. *B. vulgaris* presented similar values; 8.33% and 11.24% for *P. placenta* and *P. fumosus* respectively. They also tested the effect of different treatment methods using 1% and 3% CCB (oxide based) solutions. The 3% CCB treated samples had the best results for both species (lowest weight loss in both fungi).

Tannin treatments also presented promising results in wood. In the work of Silveira et al. (2017), acacia wood samples treated with A*cacia mearnsii* tannin extract showed good results in terms of fungi decay by *P. sanguineus*. The treatment using a tannin solution of 10% decreased the WL from 28.07% (reference without treatment) to 5.96%. In comparison, CCB (2.5% solution) treated samples presented a WL of 2.67%. By using tannin-hexamine-boron formulations, Tondi et al. (2012b) studied fungi degradation of treated European beech and pine woods. Pine wood treated with solutions with different compositions (between 10-20% of tannin and 0.1-4.1% of boric acid), decayed by *C. puteana* fungi (brown-rot) after leaching, presented WL between 0.1-3.2%. The reference (without treatment) had an average WL of 42.6%. Tannin-only solution was not tested. Similar values are reported for European beech decayed by *C. versicolor* (white-rot).

The data from Table 4.8 can be better visualized in the boxplot of Figure 4.6. There is a considerable deviation of the weight loss data, especially on the leached samples, which may be attributed inhomogeneous leaching of the preservatives. Nonetheless, we can see the positive effects of the tannin-based treatments even after the leaching cycles, especially on the samples decayed by *G. trabeum* fungi. It is also possible to notice graphically that the leached reference and B5 samples have the same behaviour.

The samples treated with tannin-based formulations can be classified (as per EN 350-1:1996) as durability Class 2 (durable – 5% < WL ≤ 10%) against *P. sanguineus* and Class 1 (highly durable - WL < 5%) against *G. trabeum* for both leached and unleached samples. Concerning the B5 samples, although Class 1 is achieved against both fungi for the unleached samples, the leached ones had the same classification of the reference, Class 3 (moderately durable - 0% < WL ≤ 15%). A high boron loss was observed in the T10HB5 samples after

leaching but both tannin-based formulations presented satisfactory results after fungi decay test. It suggests that part of the polymerized tannin was stable even after the leaching cycles and sufficient to reduce the fungi decay on bamboo.

Figure 4.6 - Boxplot of the results obtained with the fungi decay tests.

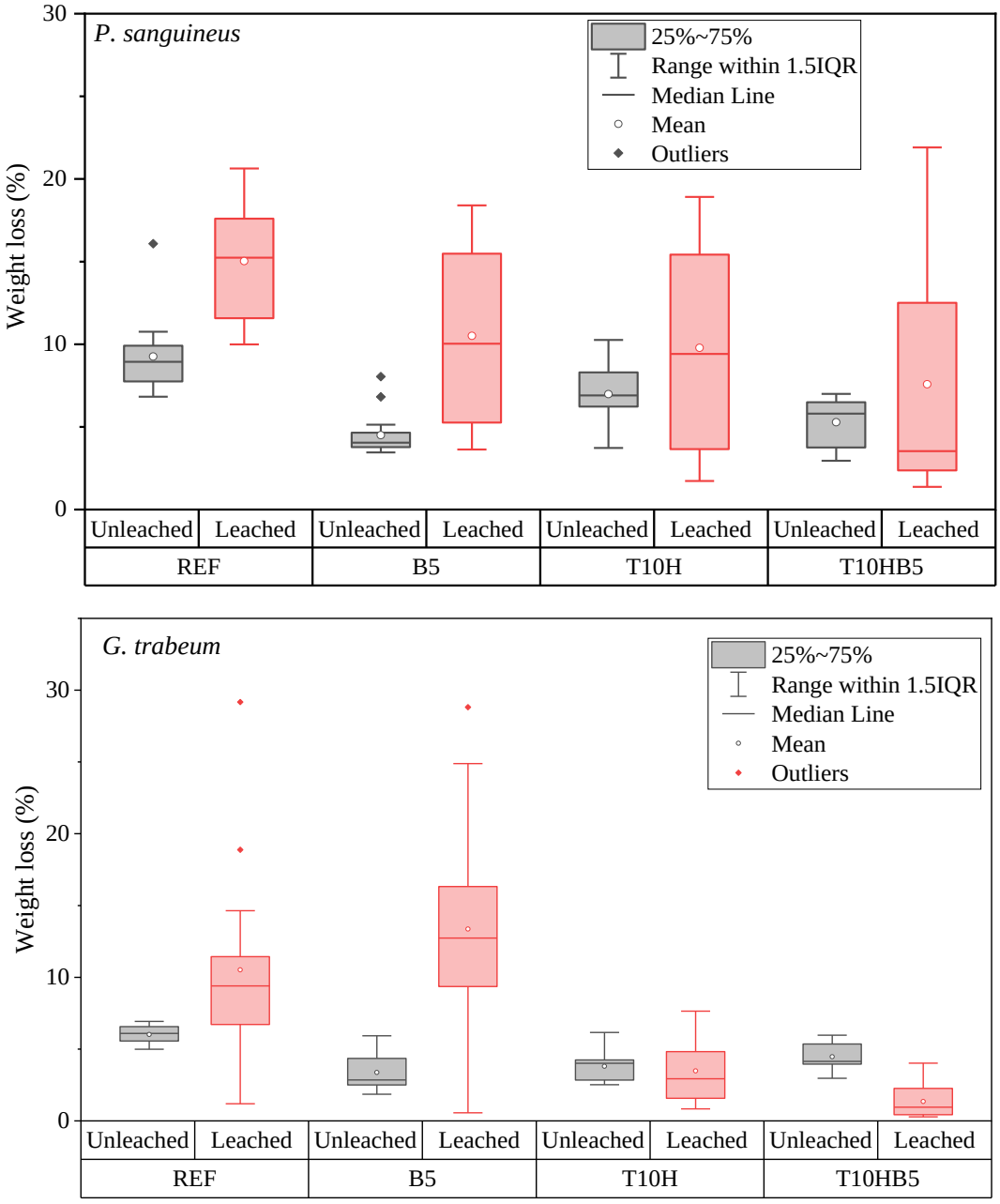

Source: Author's authorship.

4.1.3.5. Mechanical properties

Table 4.9 presents a summary of the mechanical properties obtained by compression, inter-laminar shear and three-point bending of all the investigated conditions. The first thing to notice is the small increase in the density of the treated samples, which may be attributed to the solid particles of boron and tannin occupying part of the voids. In bamboo and wood, the increase in density is normally accompanied by an improvement of the mechanical properties. Figure 4.7a presents an optical microscopy image of a typical microstructure of the bamboo used in this study, mainly composed of parenchyma, fibre bundles and vessels. The tannin-based solutions were found to be concentrated in the vessels of bamboo, as indicated in Figure 4.7b on the left. However, some of the vessel walls collapsed on the samples treated with tannin-based solution, which is assumed to be caused by the high pressure used for impregnation.

An increase in the compression strength (f_c) of all the treated samples was observed; 24.12%, 10.45%, and 18.90% for the B5, T10H, and T10HB5, respectively. In the bending tests, there appeared to be clearly positive results for all three treated samples groups. The T10HB5 treatment presented the highest values for MOR and MOE, with an increase of 13.38% and 8.9% respectively, in comparison with untreated samples. The observed increase on the f_c, MOR and MOE of the samples treated with boron corroborates with the results reported by Gauss, Kadivar and Savastano Jr. (2019) confirming that DOT improves the overall mechanical properties of bamboo.

According to the results of inter-laminar shear, although it was observed a slight increase of 1.19% in the case of DOT treated samples and a slight decrease of 5.95% and 7.14% in the case of T10H and T10HB5 samples, respectively, this difference is not statistically significant ($p > 0.05$). The small reduction in f_v may be caused by the collapse of part of the conductive vessels (Figure 4.7b).

The improvement of the mechanical performance by using tannin-based treatments is in line with the outcome of research performed by Tondi et al., where especially hardness is improved because of the reticulation of the tannin-hexamine resins in the wood cells (TONDI et al., 2012b). The polymerization reaction of tannin-hexamine within bamboo's structure is also thought to contribute on strength improvement.

Table 4.9 - Summary of mechanical properties results. Same letters (a, b, c, or d) mean there is no statistical difference among treatment conditions.

Condition	Average		Compression // fibres n=12		Interlaminar shear n=10		Three-point bending n=16			
	ρ (g/cm^3)	MC (%)	f_c (MPa)		f_v (MPa)		MOR (MPa)		MOE (GPa)	
			Avg.	COV	Avg.	COV	Avg.	COV	Avg.	COV
Reference	0.88	7.2	105.3^{a}	0.05	8.4^{a}	0.11	215.3^{a}	0.09	21.45^{a}	0.04
B5	0.92	7.1	130.7^{d}	0.04	8.5^{a}	0.13	242.6^{b}	0.09	23.34^{b}	0.05
T10H	0.90	7.0	116.3^{b}	0.03	7.9^{a}	0.13	222.5^{a,b}	0.13	22.01^{a,b}	0.05
T10HB5	0.91	7.3	125.2^{c}	0.03	7.8^{a}	0.11	244.1^{b}	0.10	23.36^{b}	0.04

Source: Author's authorship.

Figure 4.7 - Optical microscopy of *D. asper* bamboo and a) its main constituents (F – Fibre bundles; Ph – Phloem; V – Vessels; P – Parenchyma) and b) samples treated with a tannin-based solution.

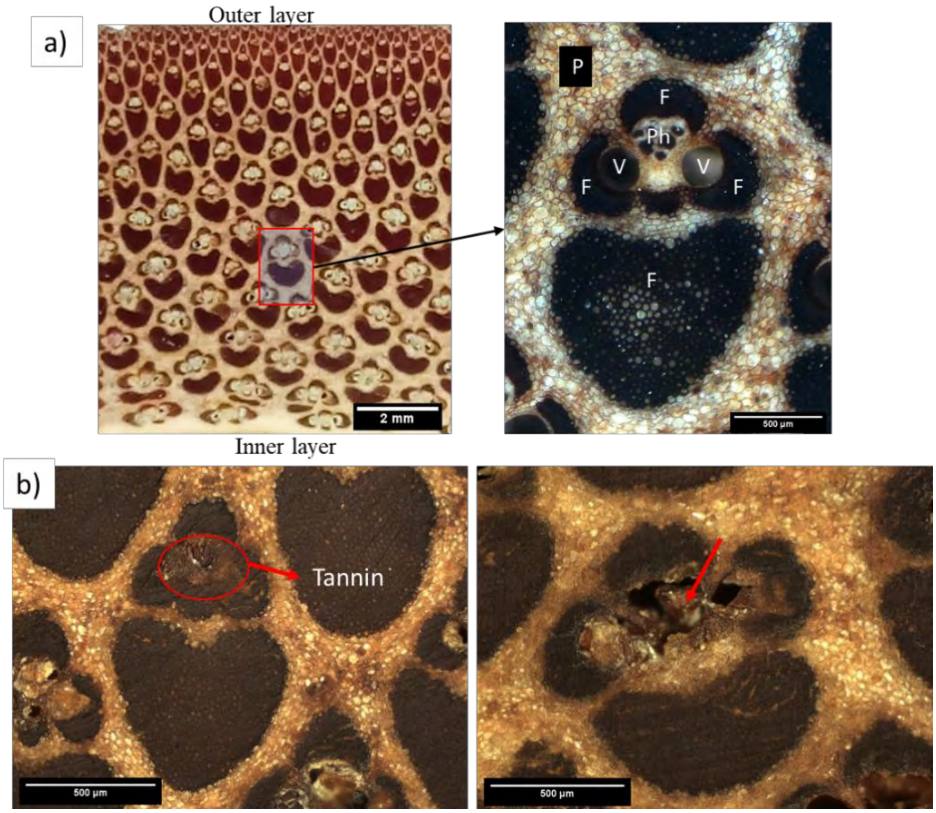

Source: Author's authorship.

4.1.3.6. Thermal degradation[3]

Thermogravimetric analysis (TGA) can be a powerful tool to understand the thermal stability of bamboo. Characteristics from the TG curve can be correlated with flammability tests by using synthetic air during the test. In the work of Jian et al. (2015), they studied the effect of flame retardants on Chinese fir wood and reported that there is an increase of char formed at 400 °C in the TG test under synthetic air as the limiting oxygen index (LOI) increases. Higher temperatures of pyrolysis and slower weight loss at a specific temperature range imply better thermal stability of wood. Flame retardants are used to achieve these properties (WANG; LIU; LV, 2017). By using urea-formaldehyde oligomer and phosphorus acid flame retardants Jiang et al. (2015) observed the suppression of combustibility in wood, leading to the formation of more char over flammable products of pyrolysis.

Figure 4.8 shows the TG curves and its derivative with respect to time (DTG) for the reference and treated samples. Considerable differences in weight loss behaviour among the treated conditions in relation to the reference can be observed, especially the samples with boron (B5 and T10HB5). Table 4.10 gives the residual char at 400 °C, and the T_{max} (temperature of maximum weight loss rate) obtained using the TG and DTG curves. The boron retention values are also presented. The B5 and TH10B5 samples showed the highest char yield, with an increase of 25.9% and 14.7%, respectively, in relation to the reference. T_{max} also increases in both conditions, proportionally with boron retention values. These results can be attributed to the suppression of part volatile gases by the boron compounds. The effect of boron compounds as fire retardant is well known (SHARMA et al., 2015b; WANG; LIU; LV, 2017). The flame-retardant mechanism of boric acid is primarily physical. During heating, it forms a glassy coating (boron trioxide) on the solid surface trapping volatile pyrolysis products which decreases oxygen diffusion and, consequently, prevents the propagation of exothermic combustion reactions (SHARMA et al., 2015b). It is worth mentioning that DOT had demonstrated better fire retardant effect than pure boric acid or borax (UNER et al., 2016).

Notably, although no boron is present in the T10H condition, there is an increase of 14.7% in the percentage of residual char but no change in the T_{max}. In fact, Tondi et al. (2012a)

[3] The procedure used for the thermo degradation analysis is further elucidated in section 4.2.3.8.

reported the positive effects of polymerized tannin-hexamine treatment on the reduction of ignition, flame and ember times of Scots pine and European beech woods (tannin only and tannin with boric acid/phosphoric acid).

The TG and DTG curves in Figure 4.8 can be divided into different stages. The samples without boron presented 3 stages while the B5 and T10HB5 conditions presented 4 stages (delimited in Figure 4.8a). Table 4.11 summarizes the characteristics of each stage, showing the weight loss, initial temperature (T_i), and final temperature (T_f). Between room temperature and around 160 °C (T_1) the weight loss is mainly caused by the evaporation of water. The second stage (from 160 to 370 °C) is characterized by the decomposition of hemicellulose and cellulose into char, CO_2, CO, CH_4, CH_3OH, CH_3COOH, and other components (WANG; LIU; LV, 2017). In this phase, the positive effects of the presence of boron are evident. The decrease in weight loss and T_f are proportional to boron retention. The T10H condition also had a decrease in weight loss, which corroborates with the result of residual char. Lignin and cellulose degrade in temperatures between 370 and 550 °C (T_3) (WANG; LIU; LV, 2017). Although the TH10 condition had an increase in the temperature of maximum degradation ($T4_f$), the weight loss in this stage was similar to the reference. In this temperature range, the samples B5 and T10HB5 presented a fourth stage (T_4), which extended the temperature of maximum degradation to 590 °C and 578 °C for the B5 and T10HB5 conditions respectively. This effect can be related to the suppression of combustible gases and dehydration of DOT in this temperature range, increasing the temperature of maximum weight loss.

Table 4.10 - Residual char and T_{max} of bamboo samples subjected to TG analysis.

Condition	B_2O_3 eq. retention (kg/m^3)	Residual Char (%) at 400°C	T_{max} (°C)
Reference	-	35.77	288
B5	4.66	45.05	320
T10H	-	41.04	286
T10HB5	3.01	42.88	307

Source: Author's authorship.

Figure 4.8 - TG (a) and DTG (b) curves of the bamboo samples with different treatment conditions.

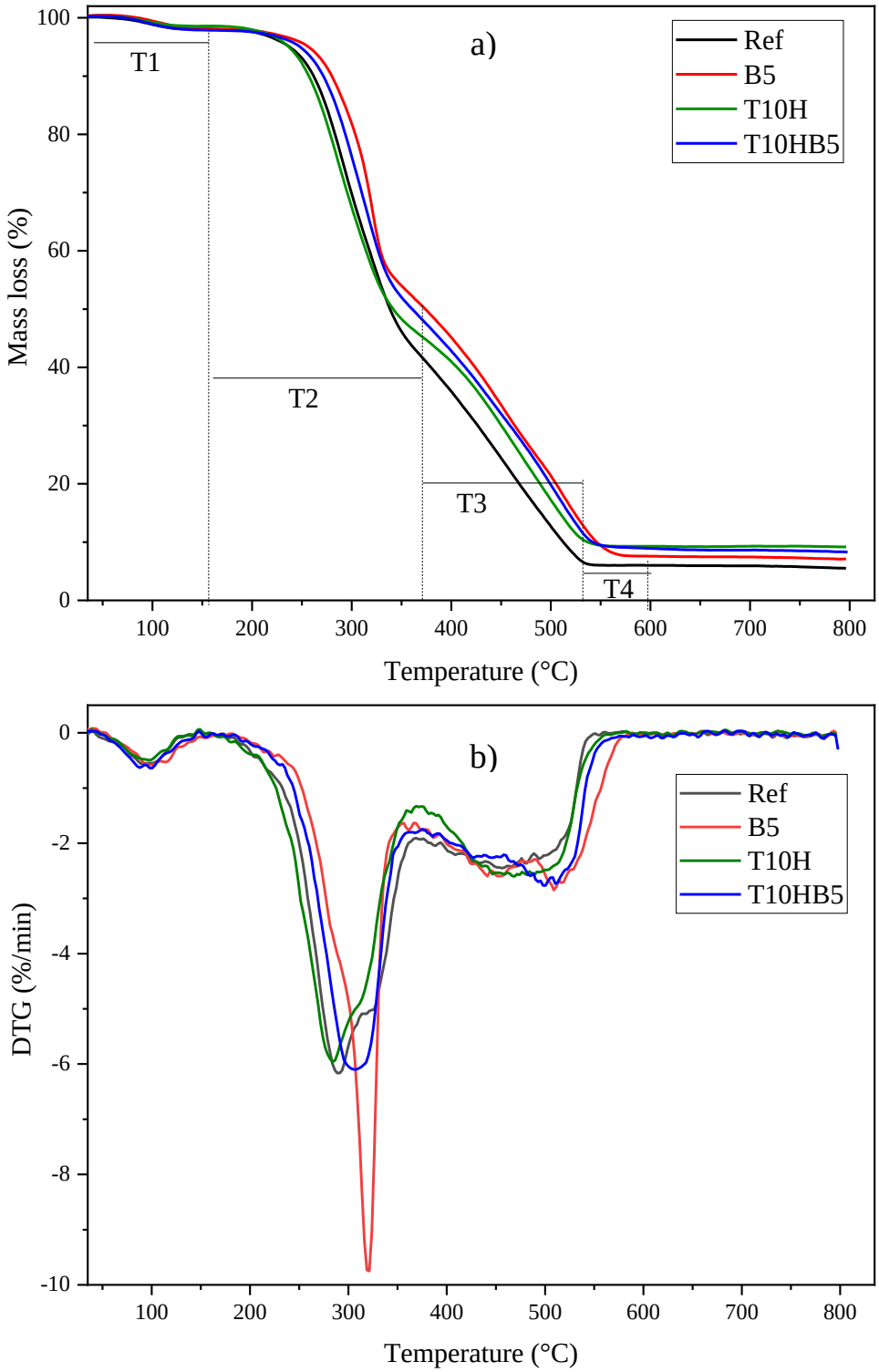

Source: Author's authorship.

Table 4.11 - Characteristics of thermal decomposition stages. The ranges were determined according to the DTG curve.

Condition	$T1_i$ (°C)	$T1_f$ (°C)	WL_1 (%)	$T2_i$ (°C)	$T2_f$ (°C)	WL_2 (%)	$T3_i$ (°C)	$T3_f$ (°C)	WL_3 (%)	$T4_i$ (°C)	$T4_f$ (°C)	WL_4 (%)
Reference	40	134	2.02	184	371	56.29	376	549	34.65	-	-	-
B5	43	166	2.40	191	353	44.42	371	484	25.35	489	590	16.39
TH0.6	40	135	1.66	172	369	53.04	376	563	35.25	-	-	-
TH1.0B5	44	154	2.38	184	359	47.45	372	460	18.19	460	578	20.72

Where WL = Weight loss at a specific stage; T_i = Initial temperature; T_f = Final temperature.

Source: Author's authorship.

4.1.4. Conclusions

In trees, tannin is one of the substances developed by nature for protection against external adversities. In this work, we presented an alternative treatment method for bamboo based on the combination of polymerized tannin and boron. Through extensive characterization methods, the main conclusions are as follow:

- In comparison to wood, the treatability of bamboo is more difficult. The low solution uptake of bamboo is thought to be related to its anatomical structure and lower porosity. The treatments did not cause meaningful differences in water absorption (WA) and dimensional stability. However, the tannin/hexamine/boron samples had the lowest values of WA, thickness and width swelling.

- Although the formulation of pure T10HB5 (10% tannin, 10% hexamine (based on dry tannin) and 5% boric acid+ borax) presented low weight losses after leaching, when applied to bamboo it was not capable of fixing boron after severe leaching cycles.

- White and brown-rot fungi decay tests showed that the samples treated with tannin-based solutions (leached and unleached) could be classified as durable and highly durable, showing better performance than untreated and boron treated samples. The

effect of remnant polymerized tannin was enough to decrease the weight loss against the tested fungi.

- The mechanical tests results revealed positive effects of all the investigated treatments, improving the compression strength, modulus of rupture (MOR) and modulus of elasticity (MOE) in bending. The samples submitted to the tannin-hexamine-boron treatment presented the highest values of MOR and MOE, 244.1 MPa and 23.36 GPa, respectively.

- Thermogravimetric analyses using synthetic airflow revealed that the use of boron in the treatment solutions improve the thermal stability of bamboo in the evaluated conditions. Tannin/hexamine treatment also caused a mild increase in the char yield at 400 °C and, consequently, had a positive effect on thermal degradation.

Along with its wide range of applications, tannin-based solutions can be an interesting option for bamboo treatment, especially when leaching can be a problem. Nevertheless, more research is necessary to improve the reaction for a tannin-boron network and the treatability of bamboo materials.

4.2. Chemical modification of Dendrocalamus asper bamboo with citric acid: effects on the physical-chemical, mechanical and thermal properties

4.2.1. Introduction

To be used in construction, bamboo must be treated to enhance its resistance to fungal and insect attack. Significant developments in the area of bamboo treatment have been achieved during the last decades. These developments are attributed to increased environmental concerns, worldwide demand for 'clean' chemicals and high-quality bamboo products; interest in bamboo is driven by the rising prices of durable tropical timber and its limited availability (MANTANIS, 2017). Various bamboo treatment techniques such as chemical, heat, and oleo-thermal treatments have been demonstrated, in both academic and industrial levels. Treatment using chemicals, as an effective way to improve durability and stability, is the most frequently investigated treatment for wood and bamboo materials (HILL, 2006; ZHANG et al., 2014; ESSOUA et al., 2016; SCHORR; BLANCHET; ESSOUA ESSOUA, 2018; GAUSS; KADIVAR; SAVASTANO JR, 2019). Chemical preservatives can permanently alter material cell wall polymers and deposit chemicals in cell voids (HILL, 2006; FENG et al., 2014).

However, most traditional bamboo and wood preservatives, such as copper, arsenic, chromium, and other chemical reagents have a high toxicity. While some chemical reagents are not toxic by themselves, they can be transformed into poisonous substances and released into the environment (WANG et al., 2018) posing a risk to ecological quality and environmental health. Chemical preservatives can be leached out and released from the material into soil, ground and surface water, and eventually into oceans, causing water and sediment pollution (SHUKLA; ZHANG; KAMDEM, 2019). Appropriate disposal of such treated material at the end of bamboo or wood service life is also a significant concern (DUBEY, 2010). Novel preservative formulations are being investigated. The key target is the replacement of conventional hazardous preservatives with more environmentally safe chemicals for improving the moisture sensibility, dimensional stability, and resistance to fungal decay of bamboo. Additionally, treatment must not sacrifice the mechanical properties of the bamboo.

Chemical modification has been investigated and applied at an industrial scale to improve the durability and stability of wood products. The acetylation process with acetic

anhydride, for example, is used to stabilise wood, increase hydrophobicity, improve dimensional stability and provide resistance to biological degradation, making this modified wood appropriate for exposed applications (HILL, 2006; ROWELL, 2012). As in the acetylation process, an esterification process using citric acid as the primary solution can chemically modify wood or other lignocellulosic materials. This approach has been used as a binder for particleboards, wood veneers, and for the esterification of hydroxyl groups from wood following thermal treatment between 100 ºC and 140ºC (DESPOT; HASAN; JUG, 2008; ŠEFC et al., 2009a; ROMAINOR et al., 2014; WIDYORINI et al., 2014; ESSOUA et al., 2016; DEL MENEZZI et al., 2018).

Using renewable chemical products, such as citric acid, is a significant development for treatments for the wood industry. Citric acid is widely available in nature at relatively low cost, and it satisfies requirements related to health and safety concerns (RAMIREZ et al., 2017; SÁNCHEZ-RIVERA et al., 2017; YE et al., 2019). Citric acid has the potential to be a cross-linking agent for cellulose (Figure 4.9) and to react with cell wall polymers (FENG et al., 2014; WIDSTEN et al., 2014). In the wood industry, citric acid not only improves the product but also contributes to reducing the final environmental footprint of buildings (ESSOUA et al., 2017). Esterifying wood with citric acid can improve dimensional stability and biological durability. However, while compression strength parallel to the grain remains unaffected, there is a decrease in tensile strength and modulus of rupture in citric acid treated wood (DESPOT; HASAN; JUG, 2008; ŠEFC et al., 2009b, 2009a, 2012; GUO et al., 2019). According to studies of the reaction of citric acid with cellulosic materials conducted using FTIR spectroscopy analysis, it appears that the two adjacent carboxylic acid groups dehydrate and form a five-membered cyclic anhydride intermediate, which may further react with a hydroxyl group of cellulose via esterification (FENG et al., 2014).

Several catalysts, such as sodium hypophosphite, have been proposed to enhance the formation rate of anhydride intermediates in citric acid-modified wood in order to minimise cellulose degradation during the curing stages. However, it is not necessary to use the catalyst for the reaction between wood and citric acid to occur (FENG et al., 2014). Larnøy et al. (2018), impregnated pine wood with an aqueous solution containing citric acid and sorbitol and cured this at 140°C. They concluded that this combination enhances dimensional stability, durability against decay fungi and exhibits reduced susceptibility to blue-stain fungi. Essoua et al. (2016),

L'Hostis et al. (2018), and Berube et al. (2017) treated different wood samples with citric acid and glycerol curing the samples at temperatures higher than 100 °C. Wood treated with the combination of citric acid and glycerol exhibited improved resistance to fungal decay and higher mechanical strengths.

There are many similarities between wood and bamboo. For this reason, the agents that have shown good results in wood preservation are believed to be appropriate for the chemical modification of bamboo as well. Using citric acid as a renewable-based chemical for bamboo treatment can be an innovative alternative to the petrochemical treatment materials commonly used. Nonetheless, some components of bamboo (hemicellulose, lignin, and some other extractives) may degrade under treatment, which can negatively affect the mechanical properties of the final bamboo products; this requires investigation. Moreover, the effect of disodium octaborate tetrahydrate (DOT) and other boron compounds, which are the most common chemicals used in conventional bamboo treatment, in combination with citric acid is a matter of interest, since these chemicals combine broad-spectrum efficacy and fire-retardant properties (TONDI et al., 2012a; DONMEZ CAVDAR; MENGELOĞLU; KARAKUS, 2015; YU et al., 2017; ZHOU et al., 2018).

The main goal of the present study is to investigate the effects of citric acid treatment and compare these with DOT-treated and untreated *Dendrocalamus asper* bamboo samples. The effects were evaluated through the investigation of the physical (water absorption, swelling, and leaching) and mechanical properties (compression, tension, bending, and shear), thermal degradation under synthetic airflow, and the chemical changes, tracked by FTIR and XRD.

Figure 4.9 - Mechanism for the citric acid crosslinking of cellulose.

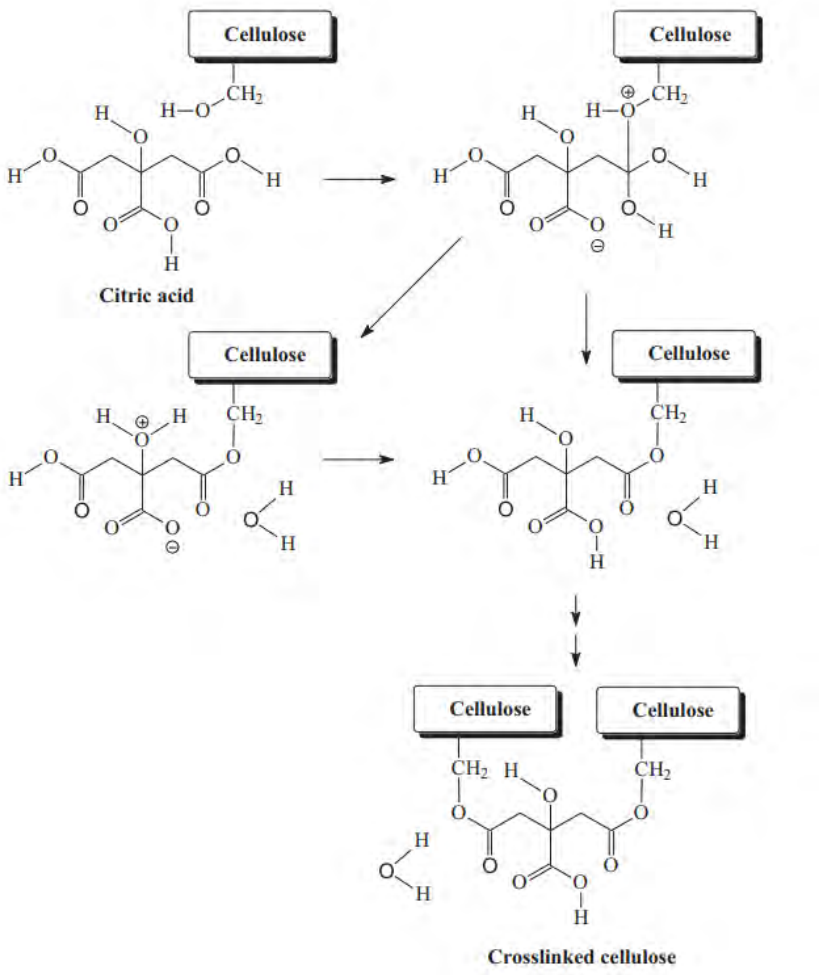

Source: (WIDSTEN et al., 2014).

4.2.2. Materials and methods

4.2.2.1. Materials and samples preparation

The *D. asper* bamboo species has been used for this study due to its availability in several regions in Brazil. Bamboo culms were harvested at an experimental field on the USP campus in Pirassununga, state of São Paulo, southeast region of Brazil (21°59′S 47°26′W). Pirassununga is located at an altitude of 630 m above sea level, has an annual average rainfall of 1363 mm and has a tropical climate with well-defined wet and dry seasons.

Mature culms (more than three years old) were collected and conditioned in a protected environment for drying until reaching an equilibrium moisture content. The treatment process

was performed using six different internodes from the middle (more uniform) part of three different culms. Tangentially oriented strips, approximately 200 mm long and 30 mm wide, were cut from the internode sections, as shown in Figure 4.10.

Fibre volume fractions and the apparent densities at approximately 10% moisture content (before the conditioning steps described in section 4.1.2.2) and in the oven-dry condition are shown in Table 4.12. The apparent densities were measured by the water immersion method at 27 °C, as described in ASTM D2395−17. The fibre volume fractions were determined using images obtained using an optical stereoscope and analysed using ImageJ software (RASBAND, 2018), in which the same threshold procedure described by Akinbade et al. (2019) was used. A typical microstructure of *D. asper* bamboo composed of fibre bundles, parenchyma, vessels, and phloem, as well as the threshold procedure used for fibre fraction determination, is shown in Figure 4.11.

Figure 4.10 - Samples layout used for the treatment process and the number of samples obtained from each internode.

Sample layout	Internode – n
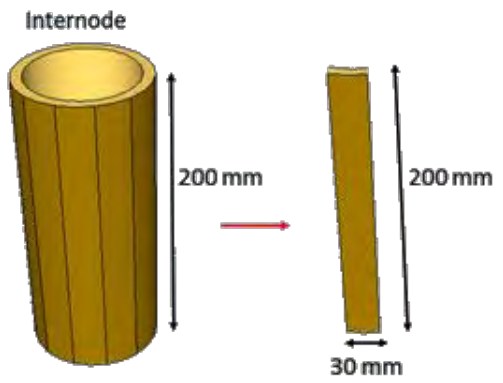	A – 20
	B – 20
	C – 20
	D – 20
	E – 20
	F - 20

Source: Author’s authorship.

Table 4.12 - Apparent density and fibre volume fraction of *D. asper* bamboo samples used in this study.

Internode	Apparent density (g/cm^3)	Moisture content (%)	Oven-dry apparent density (g/cm^3)	Fibre volume fraction (%)
A	0.742	9.9	0.716	42.4
B	0.750	9.8	0.726	39.0
C	0.778	10.2	0.747	43.0
D	0.794	10.0	0.763	34.6
E	0.782	10.2	0.761	37.8
F	0.797	10.5	0.750	39.5
Average	0.774	10.1	0.744	39.4
COV	0.04	0.03	0.04	0.08

Source: Author's authorship.

Figure 4.11 - Typical microstructure of *D. asper* bamboo samples used in this study and threshold procedure used for fibre volume fraction determination. V=Vessels; F=Fibre bundles; Ph=Phloem; P=Parenchyma.

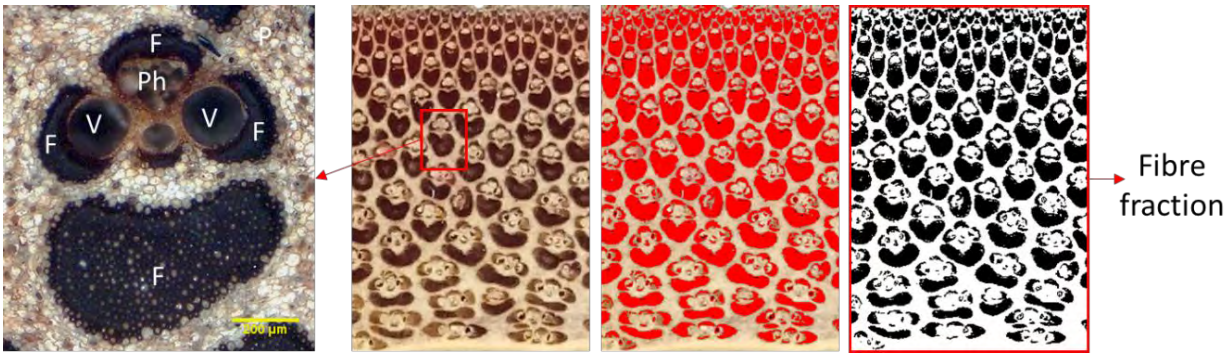

Source: Author's authorship.

4.2.2.2. Treatment process

The samples were submitted to different treatment processes. Five samples per internode (total of 30 samples) were used for each treatment condition, using the solutions presented in Table 4.13. Before treatment, the samples were air-dried at 103 ± 2 °C until a constant weight was achieved; following this they were conditioned in a climatic chamber at 25 °C and 70% RH for 240 h. This procedure that was used permit weight changes after treatment to be accurately assessed and at the same time treat the samples in a more realistic moisture condition. Following

conditioning, the moisture content of the samples was approximately 8% (reported later in Table 4.14). The samples were treated in a pressure vessel following a vacuum/pressure schedule: initial vacuum (-650 mmHg) without any solution for 15 min., vacuum phase with the solution for 60 min., pressure phase (14.1 kgf/cm^2) for 180 min. and a final vacuum phase for 15 min. Following treatment, samples were dried at room temperature for 48 h, oven-dried at 60 ± 2 °C for 24 h, and finally cured at 120 ± 2 °C for 48 h in order that the reaction between citric acid and bamboo can occur. The heating initiates citric acid dehydration to form an anhydride and its carboxyl (COOH) groups, which reacts with bamboo hydroxyls forming ester bonds (FENG et al., 2014; SÁNCHEZ-RIVERA et al., 2017).

For the samples treated with the presence of boron in the formulation, a combination of boric acid and disodium borate decahydrate (borax) was used in the ratio of 1: 1.54 by mass for the formation of DOT ($Na_2B_8O_{13}.4H_2O$) (GAUSS; KADIVAR; SAVASTANO JR, 2019). In the case of CA10B5 solution, first the boric acid and borax were dissolved in the correct proportion, and then the citric acid was added.

Boric acid, disodium borate decahydrate and citric acid of analytical grade supplied by Labsynth, Brazil, were used. Reference samples were subject to the same conditioning (103ºC followed by 25ºC at 70% RH for 240 h) and curing (120ºC for 48 h) protocols but were not subject to the vacuum/pressure treatment cycles.

Table 4.13 - Impregnation schedule and treatment solutions.

Condition	Treatment solution (wt/wt)	Number of samples	Heat treatment temperature (after impregnation)
Reference	none	30	120 °C
B5	DOT 5%	30	120 °C
CA10	citric acid 10%	30	120 °C
CA10B5	citric acid 10% + DOT 5%	30	120 °C

Source: Author's authorship.

4.2.2.3. Moisture uptake

The treated and untreated samples were conditioned at 25 °C and 70% RH in order to observe the moisture uptake in relation to time. The samples were weighed after 48, 168, 336 and 504 hours and the moisture content calculated using the dry weight of the samples, obtained after the heat treatment process (at 120 ^{o}C).

4.2.2.4. Water absorption, swelling, and leaching

Samples with 20 mm x 20 mm x thickness were extracted from the middle part of four different specimens after treatment. These samples were subjected to a leaching process for 12 days according to recommendations of AWPA E10:16. Before this process, the treated samples were first dried at 60 °C until a constant weight was achieved. Samples were then immersed in distilled water for the determination of water absorption (WA) and thickness and width swelling (TS and WS, respectively) after 12 h and 24 h immersion. The weight of the samples was determined with a precision of 0.001 g and the dimensions with an accuracy of 0.01 mm. WA, TS and WS were calculated in relation to the initial weight and dimensions of the samples after drying at 60 °C. After these measurements, the water was replaced, and the samples were conditioned in a steel vessel where a vacuum (-650 mmHg) was applied for 60 min. in order to guarantee total penetration of water. Following this, the water was replaced after 12 h and then every 24 h for 12 days. After the completion of the leaching process, the final weight and dimensions of the samples were obtained, and they were again dried at 60 °C until a constant weight was achieved.

4.2.2.5. Boron retention analysis

Following treatment, samples were subjected to boron retention analyses conducted according to Brazilian Standard ABNT NBR 6232:2013. For the chemical analyses, samples extracted from the middle part of four different specimens of the samples treated with boron (leached and unleached) were ground into a powder and passed through a 60-mesh sieve. The obtained material was subjected to sulphuric acid digestion, diluted and analysed by atomic

absorption spectroscopy. The chemical analyses were performed in the laboratory of trees, wood, and furniture at the Institute of Technological Research (IPT), São Paulo, Brazil, following the same guidelines used for treated wood. The amount of equivalent B_2O_3 was calculated according to:

$$Retention\ (B_2O_3) = \left(\frac{B \times \rho}{100}\right) \times 3.22 \qquad \text{Eq. 4.2}$$

Where B is the weight percentage of boron in the analysed sample (in%), ρ is the oven-dry apparent density of the sample (in kg/m^3), and 3.22 is a stochiometric factor for obtaining the amount of B_2O_3 based on the amount of boron.

4.2.2.6. Fourier Transformed Infrared (FTIR) spectroscopy

The chemical modifications involved after treatment were investigated through Fourier transform infrared (FTIR) spectroscopy. Samples extracted from the middle part of four different specimens of each condition were ground into a powder and passed through a 100-mesh sieve. The analyses were conducted using a PerkinElmer Spectrum One FTIR with the ATR (Attenuated Total Reflectance) universal sample accessory. For each analysis, 32 scans were used in the spectral region of 4000-600 cm^{-1} with a resolution of 4 cm^{-1}. Before the measurements, all the samples were dried at 60 °C until a constant weight was achieved.

4.2.2.7. Microstructural characterisation

The transverse section of the treated bamboo samples was analysed in a HITACHI model TM-3000 (with an acceleration voltage of 15 kV) scanning electron microscope (SEM) to observe possible effects of the different treatment conditions. For the analysis, small samples were cut with a diamond disc and subjected to fine grinding and polishing with (sequentially) 6, 3 and 1 μm diamond polishing suspension. After polishing, the samples were cleaned with isopropyl alcohol and dried at room temperature. The fractured surfaces of samples submitted to interlaminar shear tests (see below) with no further preparation were also submitted to microscopy analysis.

4.2.2.8. X-ray diffraction

An X-ray diffractometer (Horiba LA-960, with CuKα radiation generated at a voltage of 40 kV and a current of 30 mA) was used to scan the samples between 5–65° 2θ at 10°/min. The samples were prepared by the same procedure described for FTIR analysis. The crystallinity of cellulose, *CrI*, was calculated using the Segal peak height method (NAM et al., 2016), according to the following equation:

$$CrI = \frac{I_{002} - I_{am}}{I_{002}} \, x \, 100 \qquad \text{Eq. 4.3}$$

Where I_{002} represents the maximum intensity of the (002) plane reflection of the cellulose I structure at approximately 2θ = 22.7° and I_{am} is the intensity of the amorphous reflection at 2θ = 18°.

4.2.2.9. Thermal characterisation

The thermal characterisation was performed in order to understand the thermal degradation of bamboo treated with citric acid and boron compounds. The tests were conducted in a Netzsch TGA/DSC model STA 449 F3 Jupiter using synthetic airflow (flow rate of 100 ml/min.) from room temperature up to 800 ºC at 10 ºC/min. Differential scanning calorimeter (DSC) measurements were also performed with the thermogravimetric analysis (TGA). The samples were prepared by the same procedure used for FTIR analysis. The synthetic airflow was used to better understand the behaviour of the material in a real environment, in the presence of oxygen. This procedure has been demonstrated to be correlated with limiting oxygen index (LOI) flammability tests (LIODAKIS; ANTONOPOULOS; KAKARDAKIS, 2010; LIODAKIS et al., 2013; JIANG; LI; GAO, 2015; PARK et al., 2015; WANG; LIU; LV, 2017).

4.2.2.10.Mechanical characterisation

Machined coupon specimens were used for compression, tension, bending, and shear tests, as presented in Figure 4.12. All required specimen dimensions were obtained using a digital calliper having a precision of 0.01 mm. Samples were weighed before testing and afterwards dried at (100 ± 2) °C for at least 48 h to establish moisture content at the time of test.

Figure 4.12 - Mechanical test methods.

<table>
<tr>
<td> 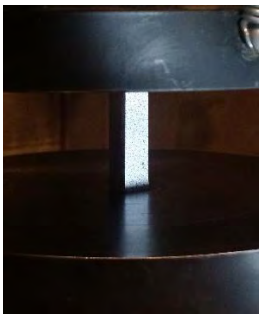 </td>
<td>  </td>
<td> 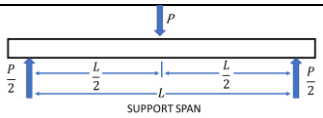

 </td>
<td> 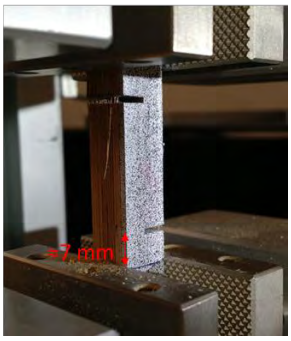
</td>
</tr>
<tr>
<td>a) compression test</td>
<td>b) tension test</td>
<td>c) small coupon three-point bending test</td>
<td>d) interlaminar shear</td>
</tr>
</table>

Source: Author’s authorship.

4.2.2.10.1. Compression parallel to fibres

Sub-sized specimens with square transverse sections were used to investigate the effect the alternative treatments on compression behaviour parallel to the bamboo longitudinal axis (i.e. parallel to fibres). Samples with transverse sections having the same size as the culm wall (t x t) and length four times the thickness (L= 4t) were tested in a 600 kN capacity Instron universal testing machine (model 600DX) at a cross-head displacement rate of 0.5 mm/min. (Figure 4.4a). The samples were extracted from six different specimens (Figure 4.2) of each treatment condition. The tests and results calculation were conducted according to recommendations of ASTM D143-14. The longitudinal compression strength (f_c) is reported as the maximum load divided by the cross-section area of the sample. The modulus of elasticity

(E_c) in compression was determined using strain mapping obtained through a Digital Image Correlation (DIC) setup, as is described elsewhere (GAUSS; SAVASTANO; HARRIES, 2019).

4.2.2.10.2. Tension parallel to fibres

The tension parallel to fibres tests were performed based on ISO 22157-19. Radially oriented bamboo strips 200 mm in length were extracted from six different specimens (Figure 4.2) of each treatment condition. The strips were sanded to obtain uniform dimensions with a breadth (b) less than half of the culm thickness (t). Softwood tabs were glued on the gripped ends to facilitate gripping by the testing machine. Although ISO 22157-19 provides for prismatic specimens, because DIC was used to determine strains, the specimens were provided with a reduced section at the middle of the gauge length in order to concentrate the tension failure region (this region can be seen in Figure 4.4b). Tests were conducted in 10 kN capacity Testresources electromechanical universal testing machine (model 100). A displacement rate of 1.0 mm/min was used for all the tests. The longitudinal tensile strength (f_t) was calculated using the maximum load divided by the reduced area cross-section area at the thinnest part of the specimen. The modulus of elasticity (E_t) in tension was determined using the strain mapping obtained through a Digital Image Correlation (DIC) setup (GAUSS; SAVASTANO; HARRIES, 2019).

4.2.2.10.3. Three-point small coupon bending test

Samples in a prismatic form with 200 x 10 x thickness (t) mm^3 were used. They were extracted from eight different specimens (Figure 4.2) of each treatment condition. A span of 190 mm was used for all the tests, which resulted in an average shear span to depth ratio exceeding 10 in every test. The tests were conducted following Procedure A of ASTM D7264-15 as modified by others (DIXON; GIBSON, 2014b; GIBSON et al., 2016; GAUSS; SAVASTANO; HARRIES, 2019) using a 10 kN capacity Testresources electromechanical universal testing machine at a displacement rate of 2.5 mm/min. The modulus of rupture (MOR), modulus of elasticity (MOE) and specific strain were calculated according to ASTM D7264-15. Tests reported in this study were conducted with the sample orientated such that the outer culm wall

was in compression (OC). The displacement of midheight (t/2) of the sample at midspan was tracked using a Digital Image Correlation (DIC) setup (GAUSS; SAVASTANO; HARRIES, 2019).

4.2.2.10.4. Interlaminar shear

The behaviour of the treated bamboo samples in shear was evaluated through an interlaminar shear test. Coupon specimens are scored halfway through their depth perpendicular to the loading direction at two locations resulting in a shear plane having an area $A = L_s \times t$, as can be seen in Figure 4.13. Since the shear plane is at the middle of the specimen, when loaded in tension, the plane is subject to pure shear. The shear strength is then calculated using the maximum load at failure divided by the shear area A. All the interlaminar shear tests were conducted using a 10 kN capacity Testresources electromechanical universal testing machine using a displacement speed of 1.0 mm/min.

Figure 4.13 - Specimen layout used for interlaminar shear tests.

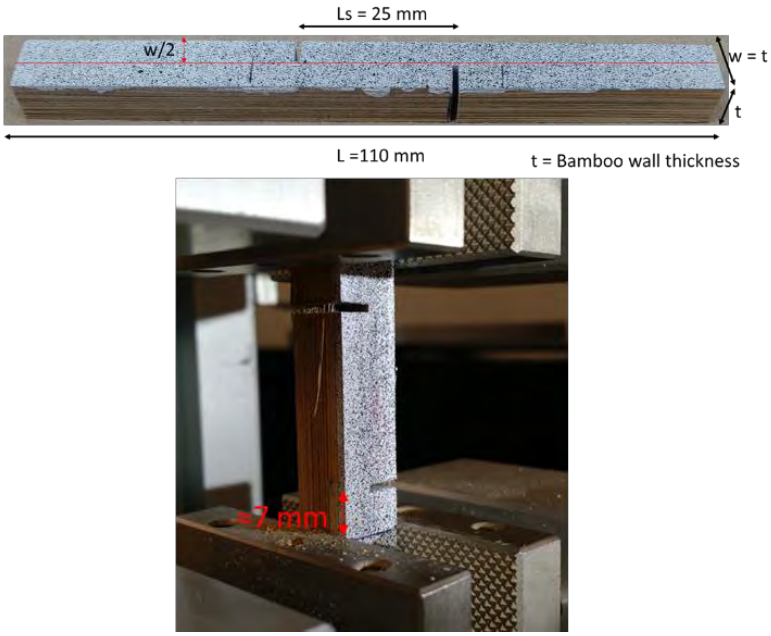

Source: Author's authorship.

4.2.2.11. Statistical analyses

The averages of each test for each condition are presented with the corresponding coefficient of variation (COV) and the number of samples. The differences among the treatment conditions on the evaluated properties were checked by a Tukey test and analysis of variance (ANOVA) for significant ($p < 0.05$) differences. All analyses were performed using MINITAB Release 18 Statistical Software.

4.2.3. Results and Discussion

4.2.3.1. Treatment process

Table 4.14 presents a summary of the solution absorption, moisture content (MC) before treatment and weight percentage gain (WPG) for all analysed conditions. The averages and corresponding COV were calculated based on 30 samples for each treatment.

Differences were observed on the average absorption of the same solution (B5, CA10, CA10B5) in different internodes sets. Even using high pressure for the treatments, this difference is explained by the different densities of the samples. In fact, by using the real density of bamboo (obtained using a helium pycnometer) and the oven-dry apparent density, it is possible to estimate the volume attributed to pores. Similar values of average real density (1.303 g/cm^3 was obtained for all internodes. By dividing the apparent density by the real density, a "void" volume of 43% for the bamboo samples used in this study was found. Higher apparent densities are closer to the maximum real density of the material (without any pores) and therefore, have less available space for the solution absorption. This effect can be observed in Figure 4.14, where an almost linear relation between density and solution absorption is presented. Preservative absorption is also a function of the solution molecular weight and concentration (TONDI et al., 2013; GAUSS; KADIVAR; SAVASTANO JR, 2019). The most concentrated solution, CA10B5, had the lowest solution uptake compared with the samples treated only with DOT or CA. This effect can also be observed in Figure 4.14, where solution absorption is less for the CA10B5.

Low WPG values were obtained in all the analysed conditions as compared to those reported for wood (ŠEFC et al., 2009a; TONDI et al., 2012a; FENG et al., 2014). During

treatment, it is assumed that bamboo can also leach some extractives and starch into the treatment solution and therefore, influence the WPG calculation.

Table 4.14 - Sample conditions after the treatment processes.

Conditions (active ingredients)	Total solution concentration of active ingredient (%)	MC Bef. Treat. (%)		Solution absorption (%)		WPG After drying (%)	
		Avg.	COV	Avg.	COV	Avg.	COV
Reference	-	7.7	0.04	-	-	-	-
B5	5	8.2	0.08	59.1	0.08	0.48	0.35
CA10	10	7.9	0.05	58.7	0.09	3.55	0.11
CA10B5	15	8.4	0.07	46.4	0.11	3.45	0.12

Source: Author's authorship.

Figure 4.14 - Solution uptake in relation to the oven-dry apparent density of bamboo samples from different internodes. In this plot, the error bars are the standard deviations.

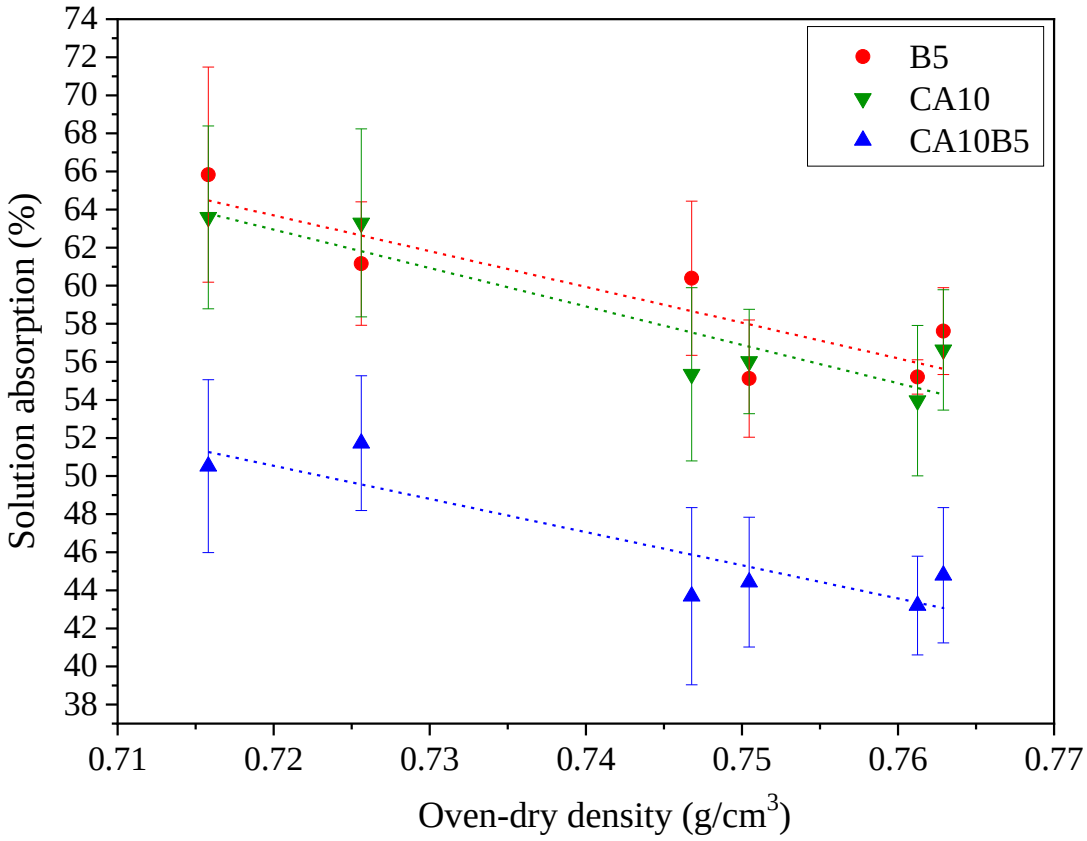

Source: Author's authorship.

4.2.3.2. Moisture uptake

Bamboo, like wood, is a hygroscopic material that absorbs and releases moisture to the surrounding environment. In fact, the data used for wood, correlating equilibrium moisture content (EMC) to temperature and relative humidity, can also be used for the bamboo moisture uptake in some situations (LIESE; TANG, 2015a). The chemical modification with citric acid is expected to decrease the equilibrium moisture content of lignocellulosic materials, as it decreases the number of available free hydroxyls through the reaction with acid carboxylic groups (COOH) from citric acid (ESSOUA et al., 2016). This effect can be observed in Figure 4.15, in which the sorption curves of all the samples (30 per condition) conditioned at 25 °C and 70% RH are presented. To the best of our knowledge, there is no publication regarding bamboo modification using citric acid. Therefore, comparisons with other bamboo species or even wood are difficult.

According to Figure 4.15, even after more than 500 hours of conditioning, the equilibrium moisture content was not achieved for all the analysed conditions. At 25 °C and 70% RH, conditions recommended by ISO 22157-19 and other wood Standards for material conditioning, it is expected that an EMC between 10 – 12% will be achieved (NGUYEN et al., 2012). Since the samples were dried after treatment (120 °C), including the reference samples, the collapse of cell micropores may have led to a reduction of the moisture absorption rate (HILL, 2006). The absorption curves of all conditions could be fitted to a power-law ($y = a.x^b$) with a relatively good coefficient of correlation (R^2). The obtained functions for each condition are also shown in Figure 4.15. Treatment with citric acid clearly affected the kinetics of moisture absorption of the bamboo samples. The CA10 treatment presented the lowest moisture content after 504 h, 4.7% (COV = 0.08), while the reference had a moisture content of 6.9% (COV = 0.09), a decrease of 32%. The changes in the kinetics can also be represented by the fitting coefficients, in which a continuous decrease of the scalar (a) is observed.

Figure 4.15 - Moisture content change in relation to time in a climatic chamber at 25 °C and 70% RH. In this plot, the error bars are the standard deviations.

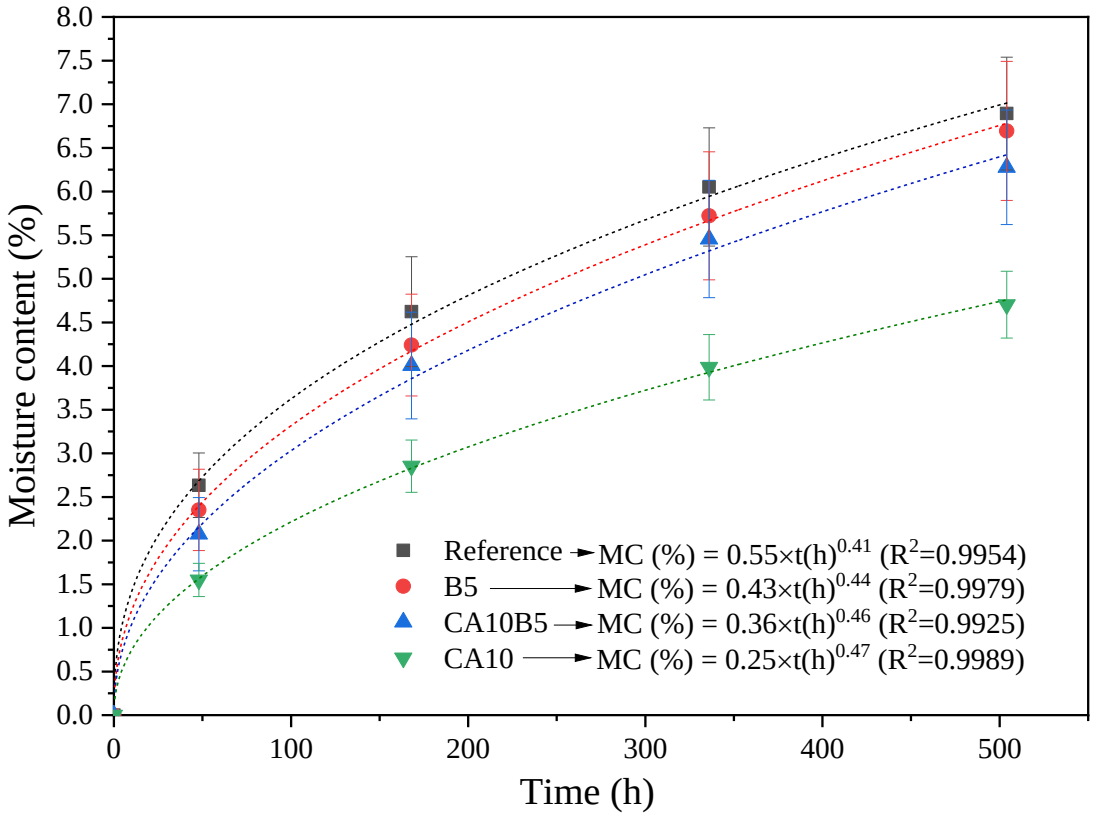

Source: Author's authorship.

4.2.3.3. Water absorption, swelling and leaching

Reduction in water absorption and swelling leads to increased dimensional stability, a primary goal of chemical modification of lignocellulosic materials. In Table 4.15 a summary of the WA, TS, and WS of all the investigated conditions is presented. The effect of citric acid on the modification of bamboo can be observed by the statistically relevant changes in WA, TS and WS.

For WA, the samples treated with CA10 show a WA reduction, in comparison with the reference, of 26% even after 288 h of immersion. After 288 h, the samples treated with DOT had no difference in comparison with the reference. The samples treated with CA and DOT (CA10B5) also had a considerable reduction of WA (16% after 288 h).

In this study, the change in dimensions was tracked measuring the thickness and width in the middle of the samples used for water absorption and swelling tests. Since bamboo is not completely flat (the samples have a natural curvature), the volumetric changes were not considered. The changes in length were almost negligible. Therefore, in Table 4.15, the changes in thickness and width only are reported. The samples treated with citric acid presented statistically significant changes in their dimensions. The CA10 and CA10B5 treatments had similar thickness swelling (TS) reduction after 288 h, 43% and 42%, respectively. Reductions in the width swelling (WS) were also observed: 33% and 26% for the CA10 and CA10B5 treatments, respectively. The treatment using only boron compounds showed no statistically significant difference in comparison with the reference.

Vukusic et al. (2010) modified fir and beech wood with different polycarboxylic acids. The treatments using citric acid resulted in WPG of up to 18% for Fir and 9% for Beech wood. For these conditions, anti-swelling efficiency (ASE) values of 54% and 38% and water absorption reductions of 21% and 19% for Fir and Beech wood, respectively, are reported. Šefc et al. (2009b) reported WPG between 6% and 18% also for fir and beech wood using a solution composed of citric acid and sodium hypophosphate (SHP) and curing at temperatures between 140 and 180 °C. They observed ASEs from 39% to 57% and reduction in water absorption from 15% to 22%. Pine wood treated with a solution of glycerol and citric acid presented a WPG between 30 – 35% resulting in an ASE between 50-60% (ESSOUA et al., 2016). Berube et al. (2017) investigated the use of citric acid and glycerol for esterification of different wood species achieving a maximum ASE of 69% for white pine, although no information about WPG is reported.

In the present study, promising values of TS and WS reductions were obtained considering the low WPG achieved (see Table 4.14). Furthermore, no catalyst was used while most of the papers addressing chemical modification with citric acid use SHP. Feng et al. (2014) demonstrated that the addition of SHP had little influence on the ASE of chemically-modified poplar wood: a WPG of about 4.6% resulted in an ASE close to 36%.

After the leaching process, the samples were dried at 60 °C until a constant weight was achieved and compared to the initial weight (before the test). This procedure was performed to evaluate the boron loss and mass change after leaching. The obtained results are presented in Table 4.16. For the samples that were treated with boron compounds, around 90% of boron was

leached. The combined treatment of boron compounds and citric acid did not have an effect on boron fixation. Additionally, the weight losses of the B5 and CA10B5 treatments, 6.98% and 9.27% respectively, were higher than the reference or the CA10 treatment, which presented the lowest weight loss (5.04%). The difference between the CA10B5 and CA10 conditions is attributed to the boron loss and leaching of unreacted citric acid.

Table 4.15 - Summary of water absorption and swelling results. Same letters (a, b, or c) mean there is no statistical difference among treatment conditions.

Treatment conditions							
n = 16				Reference	B5	CA10	CA10B5
Water absorption (%)		12h	Avg	28.93[a]	32.83[b]	22.64[c]	24.68[c]
			COV	0.07	0.17	0.14	0.09
		24h	Avg	41.17[a]	44.16[a]	29.26[b]	33.17[c]
			COV	0.06	0.13	0.09	0.07
		288h	Avg	79.87[a]	81.06[a]	59.10[b]	66.96[c]
			COV	0.05	0.13	0.07	0.1
		WA reduction – 288 h (%)*		-	**+ 1.5**	**- 26.0**	**- 16.2**
Swelling (%)	Thickness	12h	Avg	5.37[a]	5.18[a]	3.63[b]	3.84[b]
			COV	0.15	0.18	0.12	0.11
		24h	Avg	8.12[a]	7.48[a]	4.83[b]	5.38[b]
			COV	0.13	0.12	0.08	0.11
		288h	Avg	10.45[a]	9.76[a]	5.92[b]	6.03[b]
			COV	0.11	0.15	0.09	0.11
		TS reduction – 288 h (%)*		-	**- 6.6**	**- 43.3**	**- 42.3**
	Width	12h	Avg	3.37[a]	3.17[a]	2.61[b]	2.69[b]
			COV	0.15	0.15	0.12	0.16
		24h	Avg	4.42[a]	4.01[a]	2.94[b]	3.28[b]
			COV	0.19	0.1	0.17	0.15
		288h	Avg	5.10[a]	4.88[a]	3.41[b]	3.78[b]
			COV	0.18	0.12	0.11	0.15
		WS reduction – 288 h (%)*		-	**- 4.3**	**- 33.1**	**- 25.9**

Source: Author's authorship.

Table 4.16 - Mass loss after leaching cycle and B_2O_3 equivalent retention before and after leaching.

Conditions		Mass loss after leaching cycle (%)	B_2O_3 eq. retention (kg/m^3)		Boron loss (%)
			Before leaching	After leaching	
Reference	Avg	5.59	-	-	-
	COV	0.07			
B5	Avg	6.96	5.47	0.46	91.6
	COV	0.09	-	-	-
CA10	Avg	5.04	-	-	-
	COV	0.06			
CA10B5	Avg	9.30	4.76	0.48	89.9
	COV	0.07	-	-	-

Source: Author's authorship.

4.2.3.4. Mechanical properties

In order to evaluate the effect of the chemical treatments on the mechanical properties of *D. asper* bamboo, compression, tension, three-point bending, and shear tests were performed on each investigated condition. Table 4.17 shows a summary of the compression, tension and shear properties. In Table 4.18, the results of the three-point bending tests are presented. The influence of the different treatments on the mechanical properties was assessed by ANOVA where the results with different letters are statistically different at a confidence level of 95% ($p < 0.05$). Although some influence of the low moisture content of the samples can be present on the results of the mechanical tests, the primary purpose of the mechanical characterisation in this study is a relative analysis among the different treatment conditions. In this sense, despite the differences in the samples modified by citric acid (lower EMC), the evaluated conditions presented moisture contents in the same range and therefore, are not thought to affect the relative analysis.

Through Table 4.17, it is possible to observe the effect of citric acid and boron treatment on the mechanical properties of bamboo. Interestingly, there is an 18% improvement in the compressive strength and modulus of elasticity of samples treated with only citric acid. This

increase in the compressive properties is also reported to occur in wood modified with citric acid and SHP (ŠEFC et al., 2012; FENG et al., 2014). For wood, this effect is explained by the cross-linking of cell wall polymers and cell wall bulking, increasing the stiffness (FENG et al., 2014). However, the modification with citric acid had a deleterious effect on interlaminar shear strength (decrease of 19%) and especially in tensile strength (decrease of 29%). No change was observed on the tensile modulus of elasticity. Analysing the samples treated with only DOT, there was an increase in all the evaluated properties, including the modulus of elasticity in compression and tension. This effect of DOT on the mechanical properties of bamboo was evaluated in detail and reported elsewhere (GAUSS; KADIVAR; SAVASTANO JR, 2019)

The samples treated with a combination of citric acid and DOT presented similar behaviour as the CA10 treatment. In this case, the compression properties (strength and modulus) were preserved, and shear and tensile strength were affected, with a decrease of 24% and 26%, respectively. It is possible to infer that there was a selective change in some components of bamboo, like hemicellulose or cellulose. This aspect is discussed in more detail in the next sections.

Three-point bending tests were used to determine additional features, such as a) a limit of proportionality (LOP), corresponding to the limit of the elastic region of the stress-strain curve; b) specific energy (SE), calculated as the area under the stress-strain curve up to the MOR; and c) the failure modes of the specimens, classified based on ASTM D143-14. Table 4.18 summarises all the results, and the failure modes are illustrated in Figure 4.16. As observed in other studies and the results shown in Table 4.18, the treatment with DOT promoted an increase in the MOR (14%), MOE (10%), LOP (22%) and SE (16%). However, most of the samples failed in a combination of splintering tension failure (ST) and horizontal shear failure (HS). The reference samples, on the other hand, exhibited mainly ST failures.

The samples treated with citric acid (alone or in combination with DOT) presented the lowest SE values, which correlates with the decrease of interlaminar shear strength (Table 4.17). Additionally, most samples of the CA10 and CA10B5 treatments failed as HS or ST+HS. However, MOR, MOE and LOP were preserved for the CA10B5 treatment, and an increase of LOP (21%) was observed for the CA10 samples. Although the citric acid treatment caused a decrease in the tensile strength, it did not have a deleterious effect on the bending properties.

Based on the overall results, the chemical modification of bamboo had a marginal effect on the mechanical properties, although resulted in a more brittle material behaviour (decrease in shear strength, specific energy in bending, and tensile strength). Similar results are reported related to chemical modification of wood (XIE et al., 2007; FENG et al., 2014).

Table 4.17 - Summary of the mechanical properties of all the analysed treatment conditions. The COV is presented in parenthesis. Same letters (a, b, or c) mean there is no statistical difference.

Condition	Average ρ	Compression // fibres n=12			Interlaminar shear n=10		Tension // fibres n=12		
		MC	f_c	E_c	MC	f_v	MC	f_t	E_t
	g/cm^3	%	MPa	GPa	%	MPa	%	MPa	GPa
Reference	0.75	6.4	97.5 [a] (0.06)	21.40 [a] (0.08)	5.9	5.9 [a] (0.08)	5.6	269.4 [a] (0.10)	23.34 [a] (0.04)
B5	0.77	7.1	113.4 [b] (0.06)	26.00 [b] (0.14)	6.4	6.2 [a] (0.07)	5.4	295.6 [a] (0.09)	25.91 [b] (0.05)
CA10	0.77	4.5	115.0 [b] (0.07)	25.34 [b] (0.07)	4.8	4.8 [b] (0.16)	4.7	190.6 [b] (0.18)	23.19 [a] (0.06)
CA10B5	0.74	5.4	98.3 [a] (0.06)	21.50 [a] (0.10)	5.3	4.5 [b] (0.16)	5.5	200.6 [b] (0.21)	22.54 [a] (0.07)

Source: Author's authorship.

Figure 4.16 - Predominant types of failure observed in the tested bamboo samples and classified according to ASTM D143-94. Where, ST = Splintering tension failure; HS = Horizontal shear failure; ST+HS = Combined ST and HS failure.

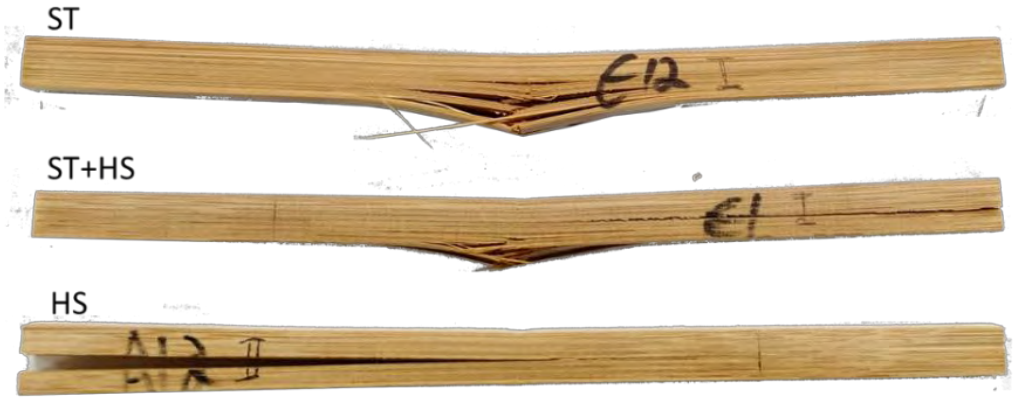

Source: Author's authorship.

Table 4.18 - Summary of bending properties of all the analysed treatment conditions. The COV is presented in parenthesis. Same letters (a, b, or c) mean there is no statistical difference.

Condition	Three-point bending								
	n	MC	*MOR*	*MOE*	*LOP*	*SE*	Failure mode		
		%	MPa	GPa	MPa	kJ/m^2	ST	HS	ST+HS
Reference	14	6.1	193.9 [a] (0.07)	20.6 [a] (0.09)	127.1[a] (0.11)	29.1[a] (0.11)	10	4	0
B5	16	6.3	220.5 [b] (0.08)	22.7 [b] (0.04)	155.7 [b] (0.07)	33.7 [b] (0.15)	2	3	11
CA10	16	4.7	196.2 [a] (0.13)	21.9 [b] (0.09)	154.1[b] (0.08)	24.5 [c] (0.20)	6	2	8
CA10B5	15	5.5	184.8 [a] (0.08)	21.1 [a,b] (0.05)	136.8 [a] (0.11)	24.3 [c] (0.11)	2	7	6

Where, ST = Splintering tension failure; HS = Horizontal shear failure; ST+HS = Combined ST and HS failure; LOP = Limit of proportionality; SE = Specific energy.

Source: Author's authorship.

4.2.3.5. Microstructural analysis

Following the mechanical characterisation, some of the samples were investigated through SEM analysis. One of the observable effects of citric acid treatment was the decrease in shear and tensile strength (Table 4.17). In Figure 4.17, SEM images of the interlaminar shear test fracture surfaces of B5 samples, having the highest interlaminar shear strength, and CA10B5 samples, having the lowest, are shown. Comparing these treatments, it is possible to observe an evident detachment between the parenchyma and fibre bundles on the CA10B5 sample (red arrows in Figure 4.17). On the other hand, on the B5 sample, fragments of the parenchyma were found attached to the fibre bundles. This observation suggests that the CA10B5 treatment affected the fibre-parenchyma interface in a deleterious manner. Analysing the cross-section of regions close to the fibre bundles from these two treatments (see Figure 4.18), small cracks (red arrow) along the interface between the fibre bundles and parenchyma were identified on the CA10B5 condition. The presence of inter-fibril cracks within the fibre bundle of the CA10B5 sample was also more significant than on the B5 sample. It is possible to infer that these defects played a role in the decrease of shear and tensile strength since in tension the bond of the matrix

(parenchyma) and fibre bundles (reinforcement phase) is vital for maintaining continuity and permitting load redistribution between fibre bundles. Although apparently effected by treatment type in this study, inter-fibril cracks are observed in many studies having different conditioning histories; these are thought to initiate cracking in the parenchyma (AKINBADE et al., 2019). Such inter-fibril cracking may increase in older (at harvest) culms (LIESE; WEINER, 1996) and has been attributed to shrinkage associated with culm drying (CHEN et al., 2018; AKINBADE et al., 2019) but also may be an artefact of SEM sample preparation (OSORIO et al., 2018).

Figure 4.17 - SEM images of the interlaminar shear fracture surfaces of samples from the B5 and CA10B5 conditions. F=Fibre bundles; P=Parenchyma. Red arrows indicate the P/F detachment.

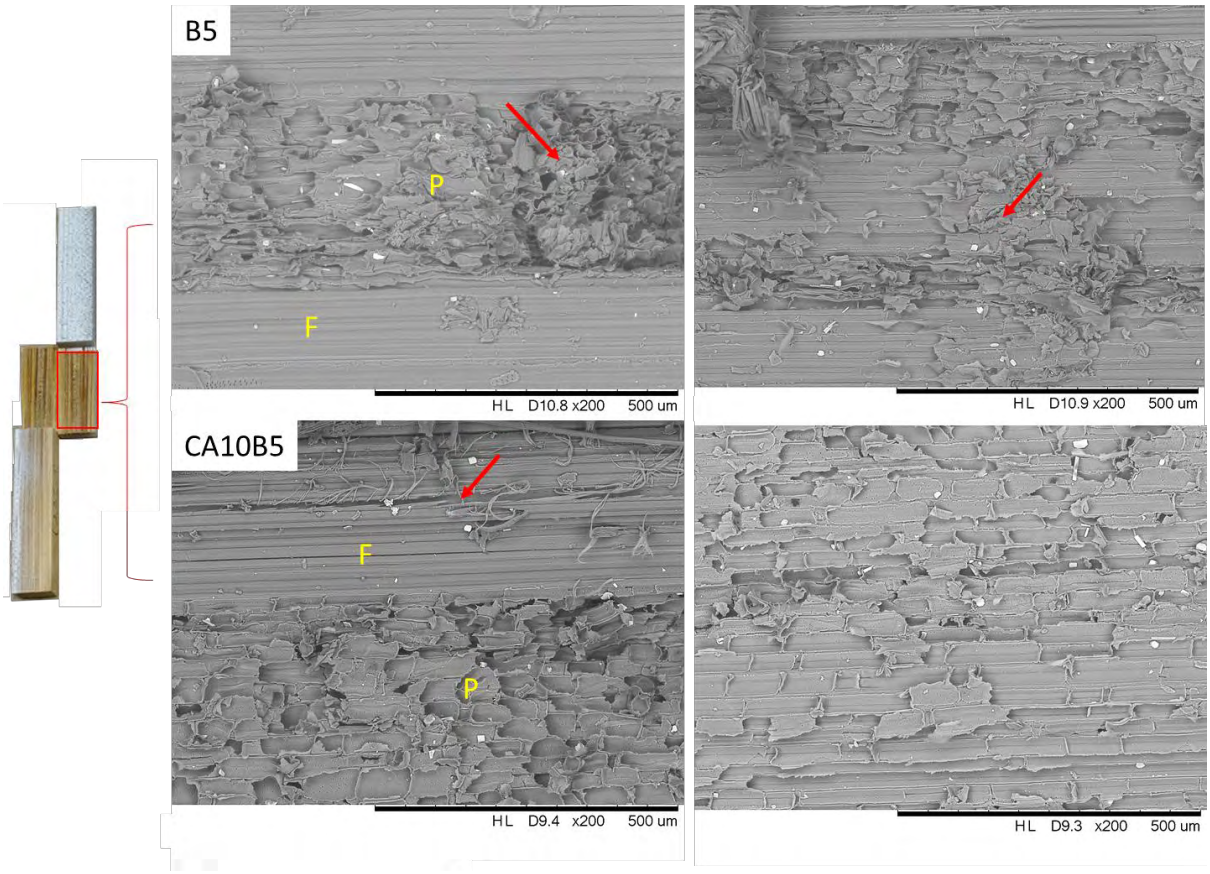

Source: Author's authorship.

Figure 4.18 - SEM images of the cross-section of B5 and CA10B5 samples. V=Vessels; F=Fibre bundles; P=Parenchyma. The Red arrow indicates the presence of cracks between F and P.

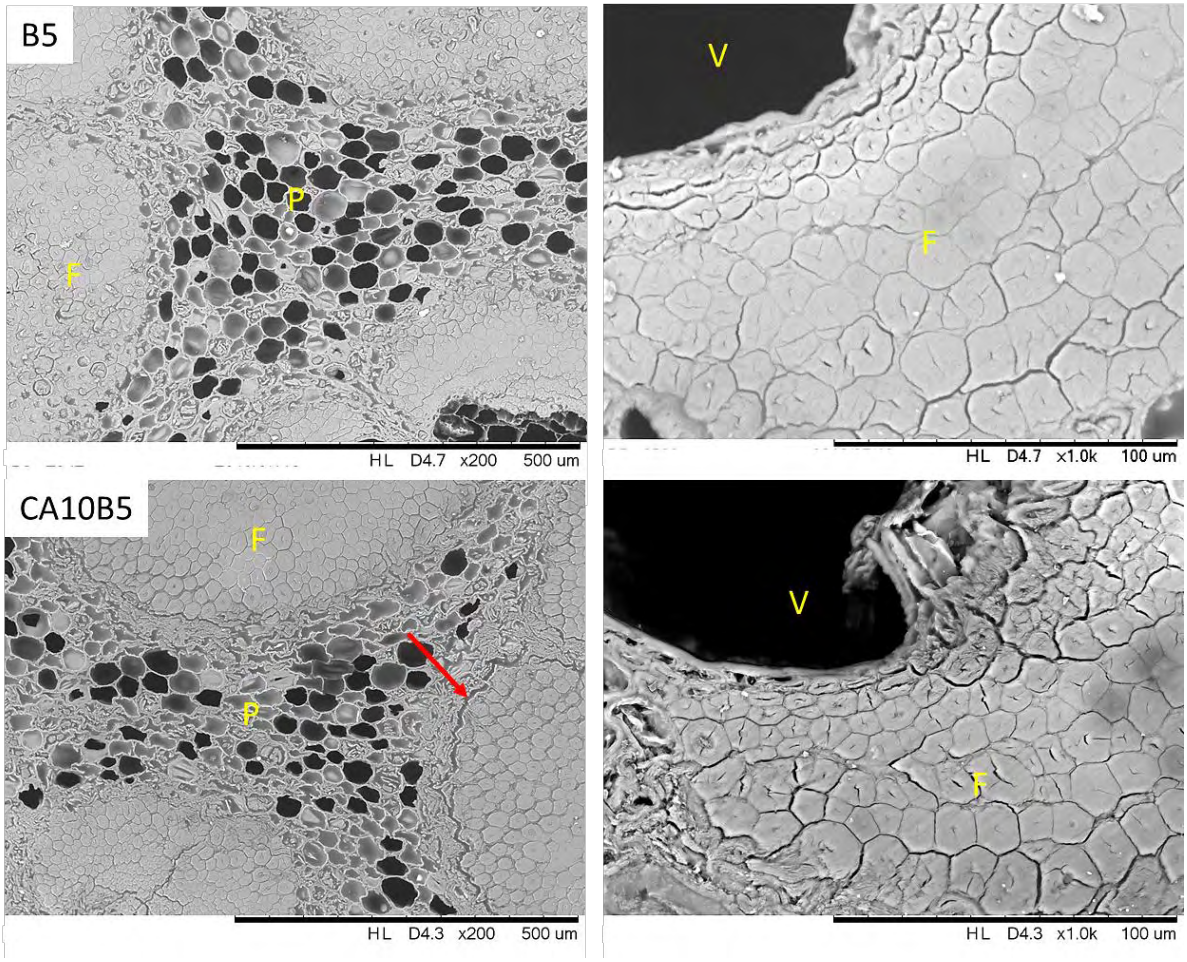

Source: Author's authorship.

4.2.3.6. Fourier Transformed Infrared (FTIR) Spectroscopy

FTIR spectroscopy was used to analyse bamboo chemical functional groups and changes after treatments. This technique is commonly used to evaluate the efficacy of chemical modifications on wood or other lignocellulosic materials. Figure 4.19 presents the FTIR spectra of the reference and treated conditions. All the spectra were normalised using the maximum absorbance.

A summary of the main functional groups between 3400 – 600 cm^{-1}, mainly assigned to stretching and vibrations of functional groups of wood and bamboo components, is presented in Table 4.19 (PANDEY; PITMAN, 2003; XU et al., 2013). The functional region between 3800 – 2700 cm^{-1} can be attributed to different CH stretching vibration groups and O-H hydrogen bonds (DIOUF et al., 2011).

Figure 4.19 - FTIR spectra of all the analysed conditions. The main functional groups' wavenumbers are identified.

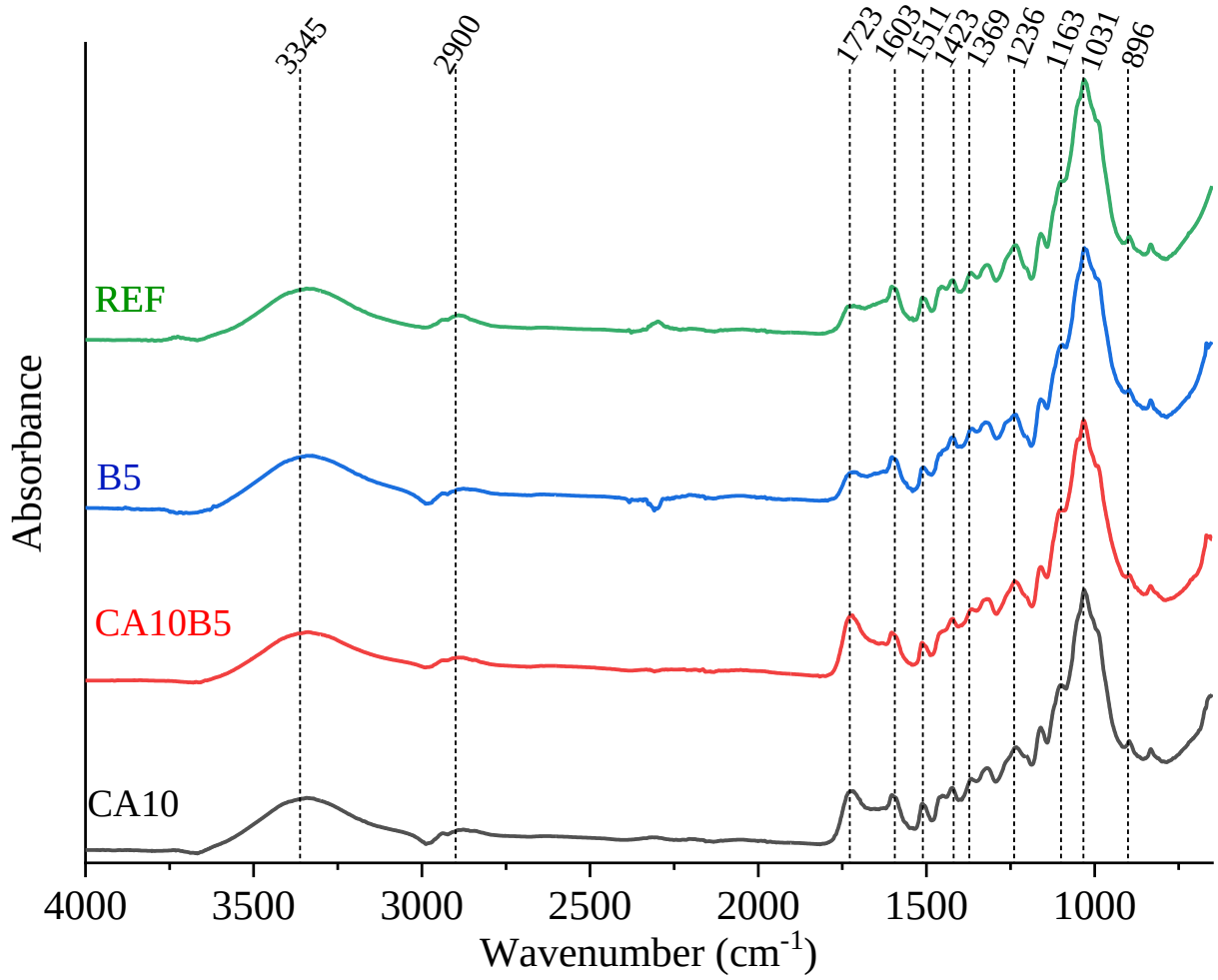

Source: Author's authorship.

Table 4.19 - Summary of the main functional groups found in wood and bamboo samples.

Wavelength (cm^{-1})	Functional group	Assignment
3345	-OH	Present in water and wood/bamboo components
2900	C=H, - CH_2 -	Stretching of the methyl and methylene groups, hydrocarbon chains
1723	− COOH (C = O)	free carbonyl groups, Stretching of acetyl or carboxylic acid (hemicelluloses)
1601	C = C	Aromatic ring (lignin)
1511	C =C	Aromatic ring (lignin), stronger guaiacyl element than syringyl
1460	C−H	Asymmetric bending in CH_3 (lignin)
1425	CH_2	Aromatic skeletal vibrations (lignin) and CH deformation in plane (cellulose)
1369	C-H	C-H deformation in cellulose and hemicellulose
1317	O−H	phenol group (cellulose)
1248	CO	Guaiacyl ring breathing with CO-stretching (lignin and hemicelluloses), esters
1163	C − O − C	Carbohydrate
1120	C−H	Guaiacyl and syringyl (lignin)
1039	C−O, C−H	Primary alcohol, guaiacyl(lignin)
896	C−H	C H deformation in cellulose

Source: (XU et al., 2013; MENG et al., 2016).

FTIR fingerprint region (1500-600 cm^{-1}) contains many well-defined peaks that provide abundant information on various functional groups present in wood/bamboo constituents. The main peaks analysed in the bamboo samples are identified in Figure 4.19. The main change among the investigated treatments is the increase in the peak at 1723 cm^{-1} which corresponds to the C=O stretching vibration. This effect can be better seen in Figure 4.20, which highlights only 1900-1300 cm^{-1}. The increase at 1723 cm^{-1} is related to the formation of esther bonds through reactions between the carboxylic groups of citric acid and bamboo hydroxyl (OH) groups (ESSOUA et al., 2016). In Table 4.20, the peak height (absorbance) ratios between the 1723 cm^{-1} peak and other relevant peaks are presented. The ratio analysis in FTIR results helps

to understand chemical changes during a specific process (MORRIS; CATALANO; ANDREWS, 1995; XU et al., 2013). Comparing the carbonyl group with the hydroxyl peak at 3345 cm^{-1} there is a clear increase in the ratio, which suggests an esterification process consuming part of the available hydroxyls. The same behaviour is observed in the ratio of the 2900 cm^{-1} (C=H, CH_2), and 1317 cm^{-1} (phenol group of cellulose) peaks, which can also be used to estimate the degree of esterification of cellulose (MORRIS; CATALANO; ANDREWS, 1995). If compared to the reference and boron treated samples, a higher degree of esterification was found for the samples modified with citric acid. These reactions explain the decrease in water absorption and swelling of the chemically modified bamboo samples.

Other interesting changes can be identified through the peak ratios presented in Table 4.20. The ratios of peaks related to cellulose and hemicellulose, I_{1369}/I_{1317} and I_{896}/I_{1317}, (where 1369 cm^{-1} corresponds to C-H deformation in cellulose and hemicellulose, 1317 cm^{-1} to O−H, phenol group in cellulose, and 896 cm^{-1} to C-H deformation in cellulose), had a small decrease in the samples treated with citric acid, which suggests structural changes in cellulose and hemicellulose may have occurred. The curing process with citric acid can also cause hydrolysis of glycosidic bonds in hemicelluloses (AZEREDO et al., 2015). These changes in cellulose and hemicellulose might explain the decrease in tensile strength of the CA10 and CA10B5 samples.

Table 4.20 - Ratio between absorbance intensities of different functional groups.

Condition	Peak intensity ratios of different functional groups*				
	I_{1723}/I_{3345}	I_{1723}/I_{2900}	I_{1723}/I_{1317}	I_{1369}/I_{1317}	I_{896}/I_{1317}
REF	0.65	1.34	0.44	0.90	1.38
B5	0.69	1.87	0.42	0.93	1.39
CA10	1.13	2.93	0.72	0.87	1.33
CA10B5	1.34	2.83	0.80	0.88	1.30

* - Each subscript number is the wavelength relative to a specific functional group (Table 4.19).

Source: Author's authorship.

Figure 4.20 - Detailed FTIR spectra of all the analysed conditions in the 1900-1300 cm^{-1} region. The main change among the samples is found at 1732 cm^{-1} (C=O group).

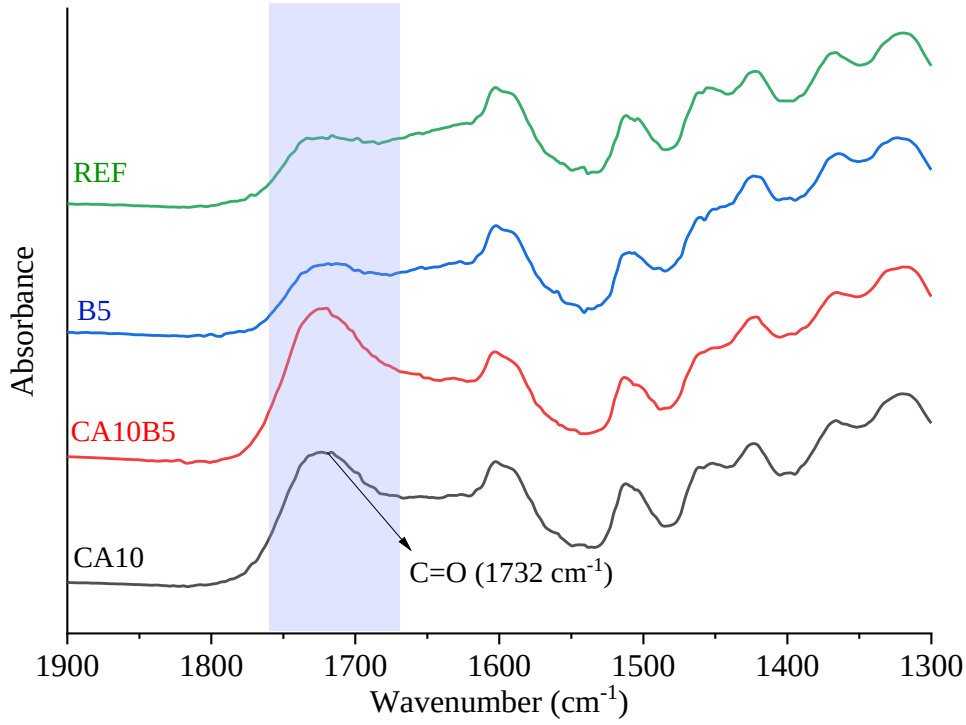

Source: Author's authorship.

4.2.3.7. XRD analysis

The strength of lignocellulosic materials is mainly related to cellulose. Additionally, the relationship between amorphous and crystalline cellulose may affect the mechanical properties of wood and bamboo (JIANG et al., 2018; TANG et al., 2019b). During chemical or thermal treatment, changes in the cellulose structure can occur. Therefore, crystallinity index (CrI) of cellulose for each treatment condition was determined using the Segal method.

Figure 4.21 shows the XRD patterns of all the investigated treatments. Typical peaks assigned to cellulose Iβ structure, 22.4° (002), 16.3° (101) and 35.0° (040), can be observed (NISHIYAMA et al., 2003; TANG et al., 2019b). All the conditions exhibited similar patterns, with minor changes in the peak height of the (002) plane, as shown in the magnified plot of the 10-30° region shown in Figure 4.21. The crystallinity indices of the samples are presented on the top of each diffraction pattern. Although there are no substantial changes in the CrI, the samples

treated with citric acid had the lowest values. Samples treated with only boron compounds, however, presented the highest CrI, which was similar to the reference.

Changes in the CrI of cellulose are generally reported in processes involving temperature, where an increase of CrI accompanies an increase in mechanical properties. However, this effect is typically observed for treatment temperatures above around 140 °C (FATRIASARI et al., 2016; KADIVAR et al., 2019; TANG et al., 2019b).

According to the FTIR results, it is possible to infer that minor changes in the cellulose structure occurred in the chemically modified bamboo. These changes could also be reflected in the proportion of amorphous and crystalline cellulose. Interestingly, the samples treated with boron compounds had the best overall mechanical properties and also presented the highest value of CrI, which is consistent with other studies related to cellulose structure (TANG et al., 2019b). On the other hand, the bamboo samples modified with citric acid showed the lowest tensile strengths (highly dependent on the cellulose) and accordingly, the lowest values of CrI.

Figure 4.21 - XRD patterns of all the investigated conditions. The inset shows the 2θ positions used for cellulose crystallinity index calculation. (101) and (002) planes refer to cellulose Iβ crystal structure.

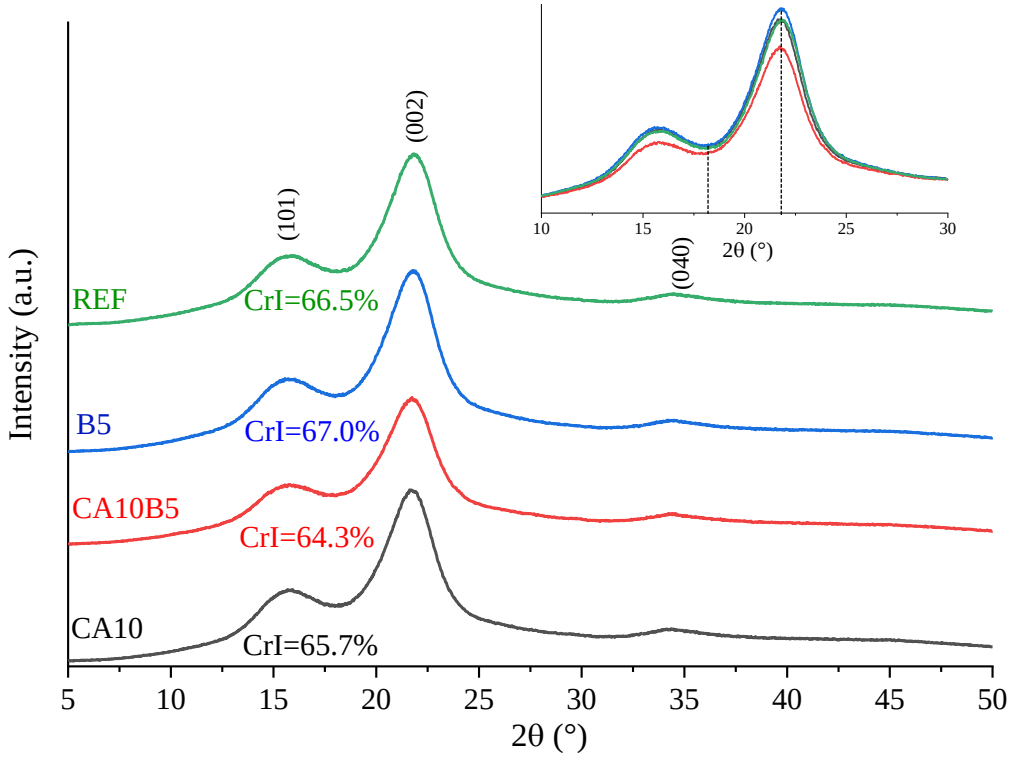

Source: Author's authorship.

4.2.3.8. Thermal degradation

Jiang et al. (2015) analysed the effect of urea-formaldehyde oligomer and phosphorus acid flame retardants on Chinese fir wood in terms of thermal degradation and flammability tests. Using TGA/DTA analysis, it was possible to observe the relationship among the formation of char at 400 °C (using static air), limiting oxygen index (LOI) and the temperature of the maximum of the first derivative of the TGA curve (T_{max}). There is an increase in the residual char with an increase of LOI values. This effect may be attributed to the suppression of combustibility by the addition of flame retardants, leading to the formation of more char instead of the flammable, volatile products of pyrolysis (JIANG; LI; GAO, 2015). Therefore, the use of TGA under synthetic air can be a reliable tool to understand thermal degradation behaviour in more realistic conditions.

In Figure 4.22, the TG curve and its derivative with respect to time (DTG) of bamboo samples without any treatment using synthetic air and nitrogen flow are presented. The effect of oxygen on the thermal decomposition of bamboo is clearly evident and similar to results reported in the literature (Azadeh, 2018; LeVan and Jerrold. E., 1990; Uner et al., 2016; Wang et al., 2017). From Figure 4.22, comparing the TG curves with synthetic air and nitrogen flow, it is possible to observe considerable differences above 300 °C. At the temperature range between 400 °C and 500 °C, the second DTG peak in the sample tested with synthetic air is related to the combustion of volatile gases produced by the decomposition of cellulose and lignin (WU et al., 2018). Additionally, higher temperatures of pyrolysis and/or slower weight loss at a particular temperature mean better thermal stability of wood samples (WANG; LIU; LV, 2017). These effects can be achieved by using flame retardants.

Figure 4.22 - Comparison between TG/DTG curve of the reference sample tested with synthetic air and nitrogen flow.

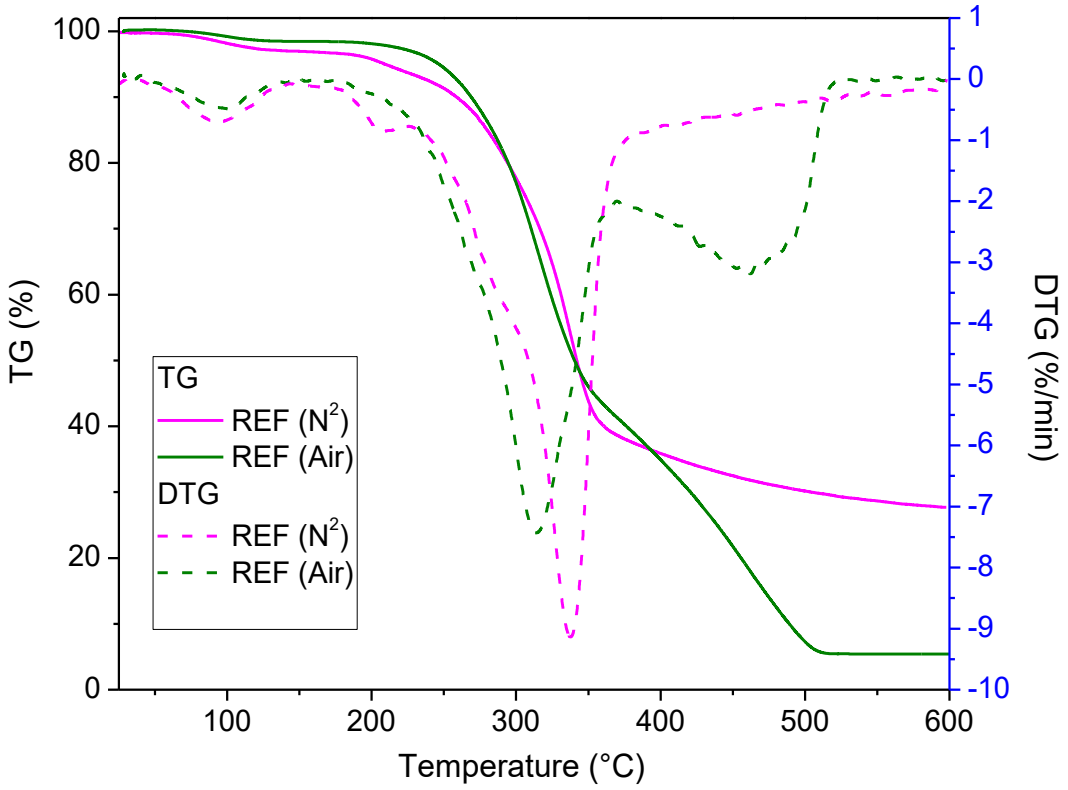

Source: Author's authorship.

Figure 4.23 presents the TG and DTG curves of all the investigated treatments. Firstly, it is possible to observe considerable differences among the different treatment conditions, mainly when boron compounds are used (B5 and AC10B5). In Table 4.21, the residual char obtained at 400 °C and T_{max} of the bamboo samples are shown. The B5 and CA10B5 samples had the highest amount of char (up to 25% increase), proportional to the boron retention, while T_{max} increased from 314 °C to 321 °C. These results show the suppression of part of the volatile gases during heating by boron compounds; this can be attributed to a flame retardancy effect. DOT, which is formed by the proportion of boric acid and borax used in this work, is a better fire retardant than pure boric acid, borax or the combination of both in other proportions (UNER et al., 2016). On the other hand, the citric acid treatment presented a lower amount of char than

the reference, but similar T_{max}. The addition of boron compounds in the citric acid solution (CA10B5), however, had a positive result in terms of char formation.

Figure 4.23 - TG (a) and DTG (b) curves of different treatment conditions of bamboo samples.

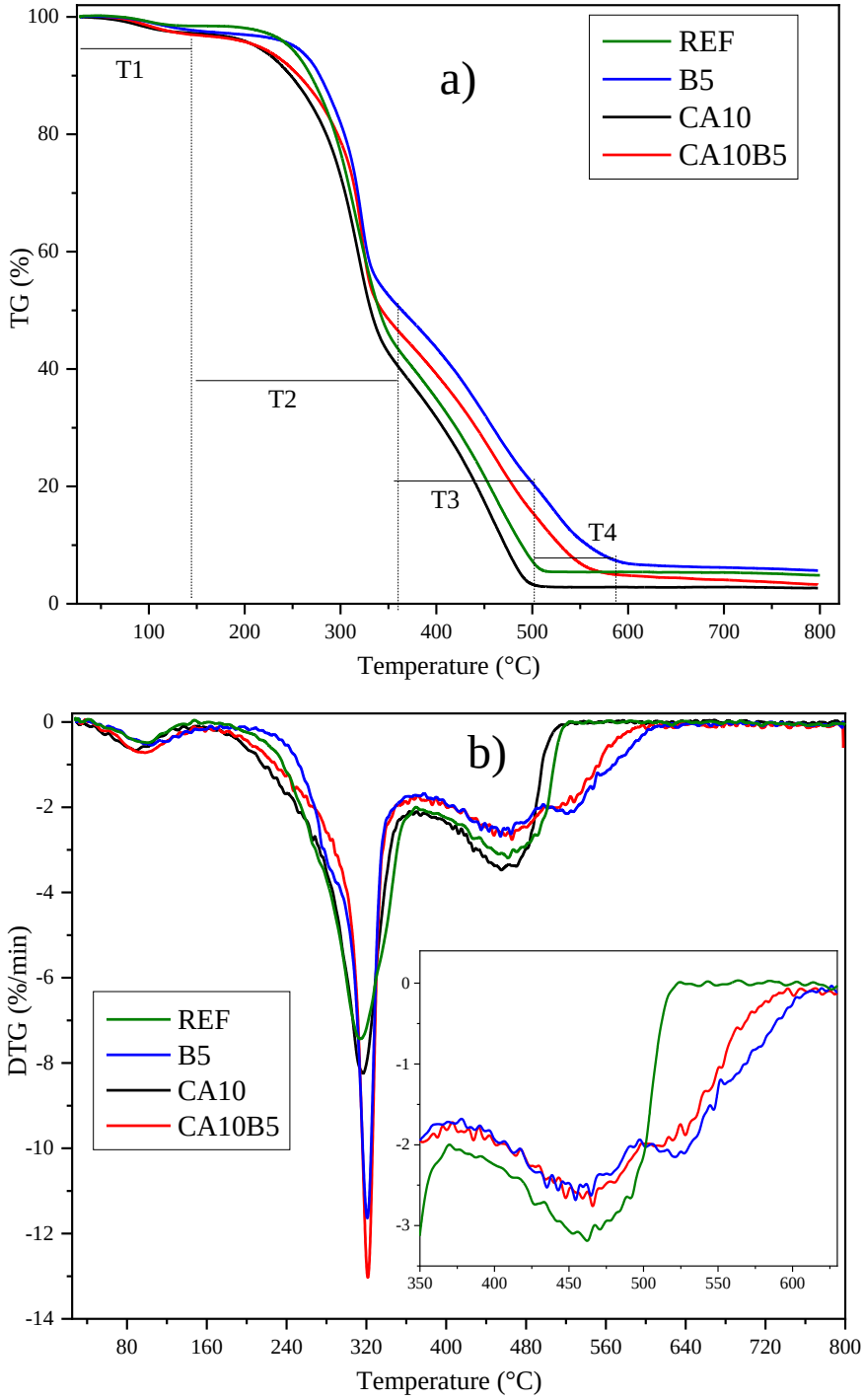

Source: Author's authorship.

Table 4.21 - Residual char and T_{max} of bamboo samples subjected to TG analysis.

Condition	B_2O_3 eq. retention (kg/m^3)	Residual Char (%) at 400°C	T_{max} (°C)
REF	-	34.91	314
B5	5.47	43.59	321
CA10	-	31.71	316
CA10B5	4.76	39.14	321

Source: Author's authorship.

Although in the work of Jiang et al. (2015) an inverse relationship between T_{max} and LOI is reported, in the present work, from Figure 4.22, it is possible to observe higher T_{max} for the sample tested with nitrogen flow, for which, in theory, the combustion of the sample is negligible. Materials that undergo thermal decomposition in the presence of oxygen are supposed to have higher thermal resistance if their thermal decomposition behaviour is closer to situations using an inert gas (JIANG; LI; GAO, 2015). Therefore, in this work, a higher T_{max} is seen as advantageous for the flammability behaviour of the tested samples

Analysing the DTG and TG curves shown in Figure 4.23, it is possible to divide the temperature range into four different stages. The reference and CA10 conditions presented three stages (T1, T2, and T3) while the samples that had boron in the treatment solution also revealed a fourth stage (T4). In Table 4.22, the characteristics of each stage are summarised, including the initial temperature (T_i), final temperature (T_f) and corresponding weight loss for each stage.

At stage T1, between room temperature up to about 160 °C, evaporation of water is the leading cause of weight loss. Interestingly, the samples modified with citric acid ended this stage at a lower temperature than the other samples, suggesting that the modification facilitated the removal of water in the bamboo samples. At the second stage, from 160 to 370 °C, the weight loss is driven mainly by decomposition of hemicellulose and cellulose into char, CO_2, CO, CH_4, CH_3OH, CH_3COOH, and other components (WANG; LIU; LV, 2017). In this case, the effect of boron compounds is evident, increasing the initial temperature and decreasing the weight loss considerably, to 47% for B5 from and 57% for the Reference conditions. At the third stage, from 370 °C and 550 °C, degradation of lignin and cellulose take place (WANG; LIU; LV, 2017). In this stage, lower weight losses were also observed for the B5 and CA10B5 samples, falling to

26% for B5 from 34% for the Reference condition. Additionally, the samples treated with boron had a secondary peak within this temperature range (identified as T4), extending the degradation temperature to around 600 °C. At this fourth stage, exhibited only by the B5 and CA10B5 conditions, the maximum weight loss temperature was found to be 614 °C and 605 °C for B5 and CA10B5, respectively. Therefore, the use of boron in the formulations increased the temperature of maximum degradation, which can be explained by the suppression of combustible gases and dehydration of the formed DOT at around 600 °C.

DSC measurements can be used to observe the exothermic reactions occurring during heating. According to the DSC curves shown in Figure 4.24, the heat flow is smaller in the samples that were treated with boron compounds, which represents a lower release of energy. Additionally, in the temperature range of 500-600 °C, the samples treated with boron presented a secondary peak; the same behaviour observed in the DTG curves of Figure 4.23.

Table 4.22 - Characteristics of thermal decomposition stages. The ranges were determined according to the DTG curve.

Condition	$T1_i$ (°C)	$T1_f$ (°C)	WL_1 (%)	$T2_i$ (°C)	$T2_f$ (°C)	WL_2 (%)	$T3_i$ (°C)	$T3_f$ (°C)	WL_3 (%)	$T4_i$ (°C)	$T4_f$ (°C)	WL_4 (%)
REF	45	162	1.76	172	370	57.13	377	524	34.43	-	-	-
B5	41	180	2.86	211	367	47.32	380	498	26.26	498	614	14.34
CA10	38	134	2.57	164	362	56.97	379	522	33.59	-	-	-
CA10B5	44	145	3.13	173	363	50.58	391	506	26.50	507	605	9.43

Where WL = Weight loss at a specific stage; T_i = Initial temperature; T_f = Final temperature.

Source: Author's authorship.

Figure 4.24 - DSC results of the different treatment conditions of bamboo samples.

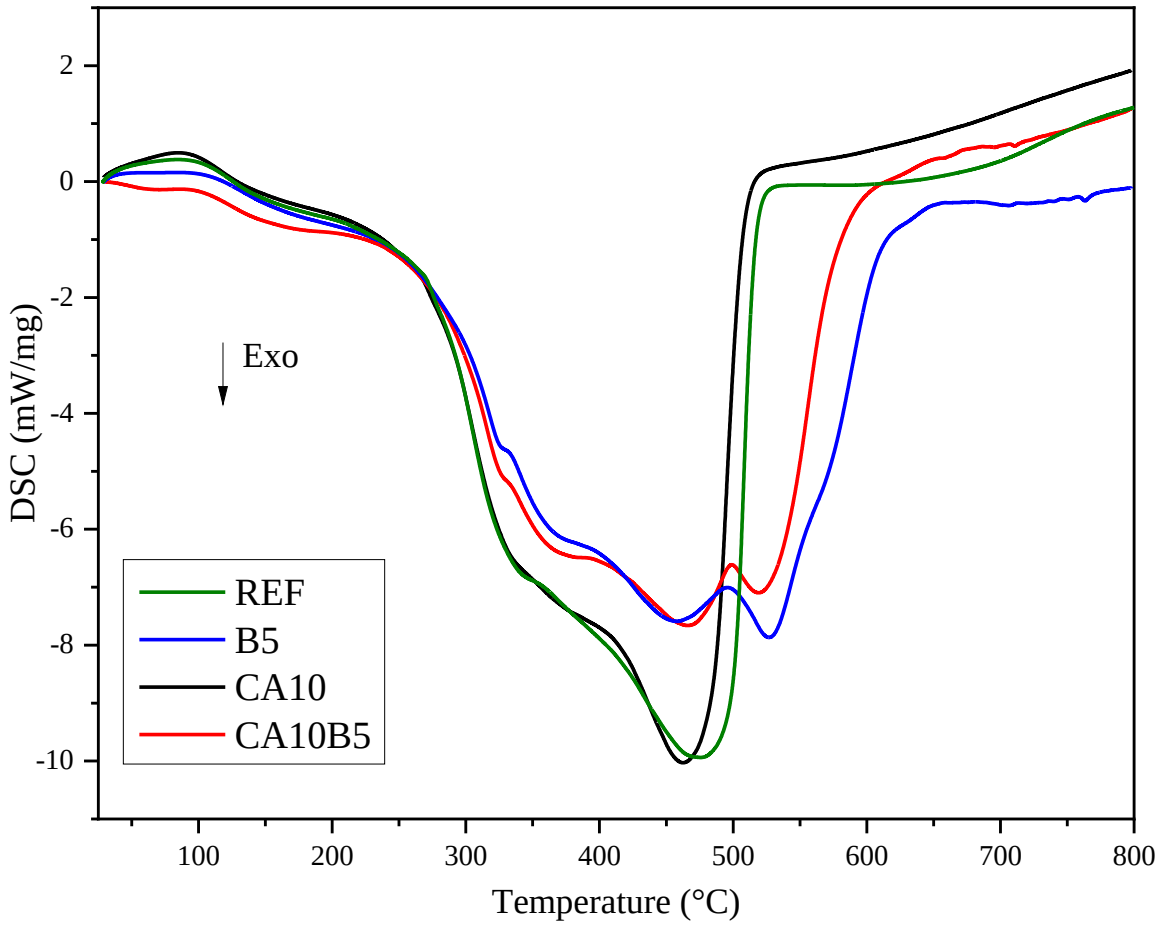

Source: Author's authorship.

4.2.4. Conclusions

The chemical modification with citric acid over the physical-mechanical properties and chemical composition of bamboo did not cause considerable chemical degradation, physical damage, or strength reduction. This treatment approach caused considerable improvement in water absorption, moisture uptake, and swelling properties in comparison with reference and DOT treated samples. Although higher three-point bending and compression strength were observed, caution should be adopted for the bamboo treated with citric if it is subjected to tensile and shear forces in a structural application. Furthermore, citric acid resulted in some changes in cellulose structure, with the reduction of crystallinity index, possible hydrolysis of the amorphous phase and glycosidic bonds in hemicelluloses, and detachment between the

parenchyma and fibre bundle regions. Samples treated only with citric acid had higher weight losses upon heating than those of the reference samples, while the treatment only with DOT resulted in the best thermal stability. The combination of both citric acid and DOT was found to be an alternative to overcome this problem.

This work provides insights into the use of non-hazardous materials as an alternative for chemicals in bamboo treatment, opening new opportunities for the development of more durable bamboo-based materials with improved stability.

4.3. Complementary information

4.3.1. Comments on vacuum/pressure impregnation

Before proceeding with the impregnation process using the solutions based on tannin and citric acid, a brief test was performed. The main goal was to verify the appropriate time and pressure conditions during the process, evaluating the advantages over the impregnation using only vacuum and atmospheric pressure. The impregnation was compared to the immersion process at room temperature and at 40 °C.

In this case, a solution composed of 10% tannin + 5% DOT solution was used due to higher viscosity (more critical situation). Five bamboo samples with 200 mm x 30 mm x thickness (see Figure 4.10) from the same internode were used for each test condition. The samples were oven-dried at 62 ° C and weighed before, during, and at the end of the process. The impregnation process was conducted in a pressure/vessel equipped with a pressure gauge, vacuometer and inlet/outlet valves for the solution (Figure 4.25). With this system, it was possible to achieve a relative vacuum of -630 mmHg (or in absolute terms 2.1 psi) and pressure of around 200 psi by using a compressed nitrogen cylinder. Different treatment times were tested, and the effect of the vacuum and pressure phases evaluated. The tested conditions are presented in Table 4.23. Before the vacuum phase, an initial vacuum of 15 min was applied without the solution. After each step (a-d) the weight of each sample was recorded. The time used for the vacuum phase also has been analysed (tests 1 and 2).

Figure 4.25 - Setup used for vacuum/pressure impregnation.

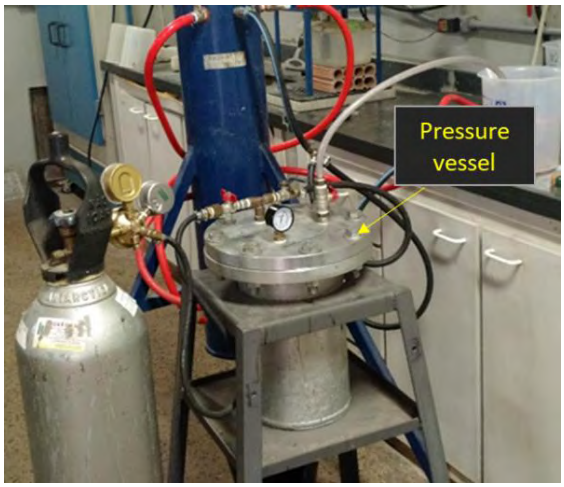

Source: Author's authorship.

Table 4.23 - List of tests used to evaluate the absorption of the preservative solution in relation to the process.

Test	Process
1 Vacuum/pressure	a. 1 h vacuum b. + 1 h high pressure c. + 2 h high pressure d. + 12 h atmospheric pressure
2 Vacuum/pressure	a. 3 h vacuum b. + 1 h high pressure
3 Immersion (room temperature)	a. 2 h immersion b. + 2 h immersion c. + 12 h immersion d. + 12 h immersion
4 Immersion (at 40 °C)	a. 2 h immersion b. + 2 h immersion c. + 12 h immersion d. + 12 h immersion

Source: Author's authorship.

From monitoring the weight throughout these processes, it was possible to observe which test provided the highest solution absorption (penetration) in relation to the treatment time. Figure 4.26 shows the relationship between the solution absorption and process time of tests 1, 3, and 4. With 2 hours of process in test 1 (1 h vacuum + 1 h pressure), the solution absorption is higher than those observed in the treatment by immersion at 40 °C and at room temperature after 28 hours. The extra 2 hours in the pressure stage (4 hours of process) increased the solution absorption in 15%, achieving 58.3%. On the other hand, the additional 12 h of atmospheric pressure did not cause a considerable increase in penetration.

Regarding the vacuum/pressure process, it was noted that the time in the vacuum phase does not effectively interfere with the absorption of the solution. After 3 h in the vacuum phase (test 2), the samples had an average solution absorption of 15.7% while in test 1, 17.5% of weight increase was observed after 1 h. Accordingly, the highest increment of solution penetration occurs during the pressure phase.

In comparison to wood, bamboo has more limitations for the penetration of fluids. By using the same treatment schedule in pine and balsa wood, an absorption between 100 – 200%

could be achieved. As explained in the former chapters, this difference is related to the difference in the apparent density and in conductive vessels available in bamboo and wood. Nonetheless, the obtained results helped to understand the importance of vacuum/pressure impregnation for high concentration solutions. Considering the solution uptake and time, 4 hours of process using test 1 was considered appropriate for bamboo impregnation. The selected process for the treatment used in Chapter 4 is summarized in Figure 4.27.

Figure 4.26 - Comparison of the treatment tests in relation to process time and solution absorption.

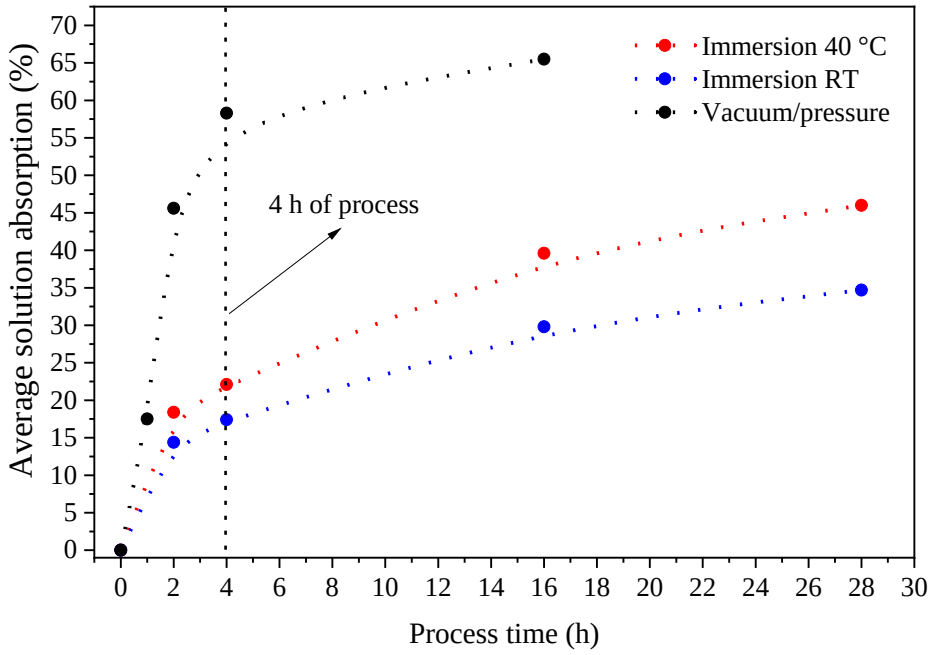

Source: Author's authorship.

Figure 4.27 - Treatment scheduled defined after the treatment tests.

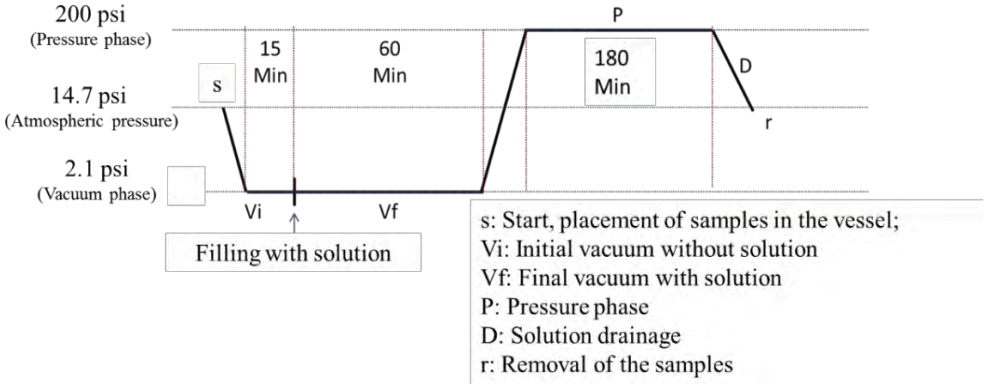

Source: Author's authorship

4.3.2. Fungi decay tests of *D. asper* bamboo treated with citric acid and DOT

Complementing the results presented in the paper of section 4.2, fungi decay tests of *D. asper* bamboo samples treated with citric acid were conducted using the same procedure used for the analysis of tannin-treated samples in section 4.1.

4.3.2.1. Testing method and samples conditions

The samples used in the fungi decay tests were obtained from the same set of samples treated in the study presented in section 4.2. As a reminder, those samples were treated using solutions composed of 10% of citric acid (CA10), 5% disodium octaborate (B5) and a combination of both (CA10B5) and cured at 120 °C. Two sets of samples were used as a reference; both submitted to the same drying scheduled. These two sets were extracted from different groups of internodes with similar densities. Leached and unleached samples were evaluated. The leached samples were obtained from the leaching process described in section 4.2.2.4 with the results presented in section 4.2.3.3. Table 2.24 gives a summary of the investigated conditions with the corresponding solution absorptions, WPGs, and boron retention before and after leaching.

The decay tests were performed using white-rot and brown-rot fungi, *Pycnoporus sanguineus* and *Gloeophyllum trabeum*, respectively. Sixteen samples per condition were tested according to the methodology described in 4.1.2.5. The samples of this study were concomitantly tested with the ones used in section 4.1.

Table 4.24 – Results of the leaching process of samples used for fungi decay test.

Conditions		Solution absorption (%)	WPG After drying (%)	Mass loss after leaching cycle (%)	B_2O_3 eq. retention (kg/m^3)		Boron loss (%)
					Before leaching	After leaching	
Reference 1	Avg.	-	-	5.59	-	-	-
	COV			0.07			
Reference 2	Avg.	-	-	5.75	-	-	-
	COV			0.06			
B5	Avg.	59.1	0.48	6.98	5.47	0.46	91.6
	COV	0.08	0.35	0.08	-	-	-
CA10	Avg.	58.7	3.55	5.04	-	-	-
	COV	0.09	0.12	0.06			
CA10B5	Avg.	46.4	3.45	9.27	4.76	0.48	89.9
	COV	0.11	0.11	0.07	-	-	-

Source: Author's authorship

4.3.2.2. Fungi decay results

White-rot fungi are selective for lignin and hemicellulose, while brown-rot fungi degrade mainly cellulose (YANG; CAO; MA, 2019). Although being susceptible to fungi decay, lab tests indicate that bamboo presents higher resistance then softwood. Weight losses around 5% for *G. trabeum* and up to 34% for *P. sanguineus* are reported for untreated *D. asper* bamboo (SUPRAPTI, 2010; WEI; SCHMIDT; LIESE, 2013). However, the fungi degradation can considerably vary depending on the fungi strains, testing method and origin of the bamboo samples.

The resulting weight losses (WL) after the fungi decay tests are given in Table 4.25 and the variation of the data presented in the boxplot of Figure 4.28. The difference among the treatment conditions was statistically evaluated through ANOVA (Tukey's test, $p < 0.05$). In the case of the unleached samples, *P. sanguineus* caused higher WL than *G. trabeum*. The samples treated only with DOT (B5) had the lowest WL among the treated conditions, with similar results from the ones presented in section 4.1.3.4. The two sets of reference samples had the highest WL, followed by the CA10 and CA10B5 conditions when decayed by *P. sanguineus*. The effect of leaching is evident, especially in the B5 samples. Interestingly, the WL of the citric acid-treated samples decreased after leaching, with the lowest value observed in the CA10B5

condition, despite having a high COV. However, the behaviour of the samples decayed by *G. trabeum* was utterly different. First, the reference samples had relatively low WL, especially Reference 1. As expected, the B5 condition also presented low WL, 3.61%, while the CA10 and CA10B5 conditions had equivalent WL of the Reference 2. After leaching, there was a great increase in the WL of all the conditions. The data from the B5 samples are not presented due to contamination problems in the Petri dishes and therefore, were not considered. Nevertheless, we can see that the chemical modification with citric acid did not protect bamboo properly against brown-rot, presenting the same performance of untreated samples, especially after leaching. Even the AC10B5 samples, with 4.76 kg/m^3 of equivalent B_2O_3, was not properly protected against *G. trabeum*. Although these results are somewhat counterintuitive, some assumptions about this behaviour are presented in the section of partial conclusions (4.2.2.3).

In Figure 4.28, the boxplot of all the analysed conditions clearly shows the high deviation of the results, specifically in the leached samples. We may assume that a selective modification of the bamboo components by citric acid, could have caused the evident difference between the two fungi. In addition, chemical treatment might have caused unintentional structural changes in cellulose that could have been further degraded upon leaching.

Table 4.25 – Weight loss of samples submitted to fungi decay tests. Same letters (a, b, or c) mean there is no statistical difference among treatment conditions.

Weight loss (%)								
Condition	*P. sanguineus* n=16				*G. trabeum* n=16			
	Unleached		Leached		Unleached		Leached	
	Avg.	COV	Avg.	COV	Avg.	COV	Avg.	COV
Reference 1	16.86^{a}	0.31	16.06^{ab}	0.30	2.94^{b}	0.15	24.51^{ab}	0.51
Reference 2	13.84^{b}	0.19	13.31^{bc}	0.30	8.01^{a}	0.19	16.54^{b}	0.39
B5	3.83^{d}	0.26	18.49^{a}	0.43	3.61^{b}	0.19	-	-
AC10	11.45^{bc}	0.16	8.45^{cd}	0.22	7.23^{a}	0.55	24.89^{ab}	0.29
AC10B5	8.67^{c}	0.21	3.83^{d}	0.77	8.06^{a}	0.60	30.70^{a}	0.33

Source: Author's authorship

Figure 4.28 - Boxplot of the results obtained with the fungi decay tests of the reference, B5, CA10, and CA10B5 samples (leached and unleached).

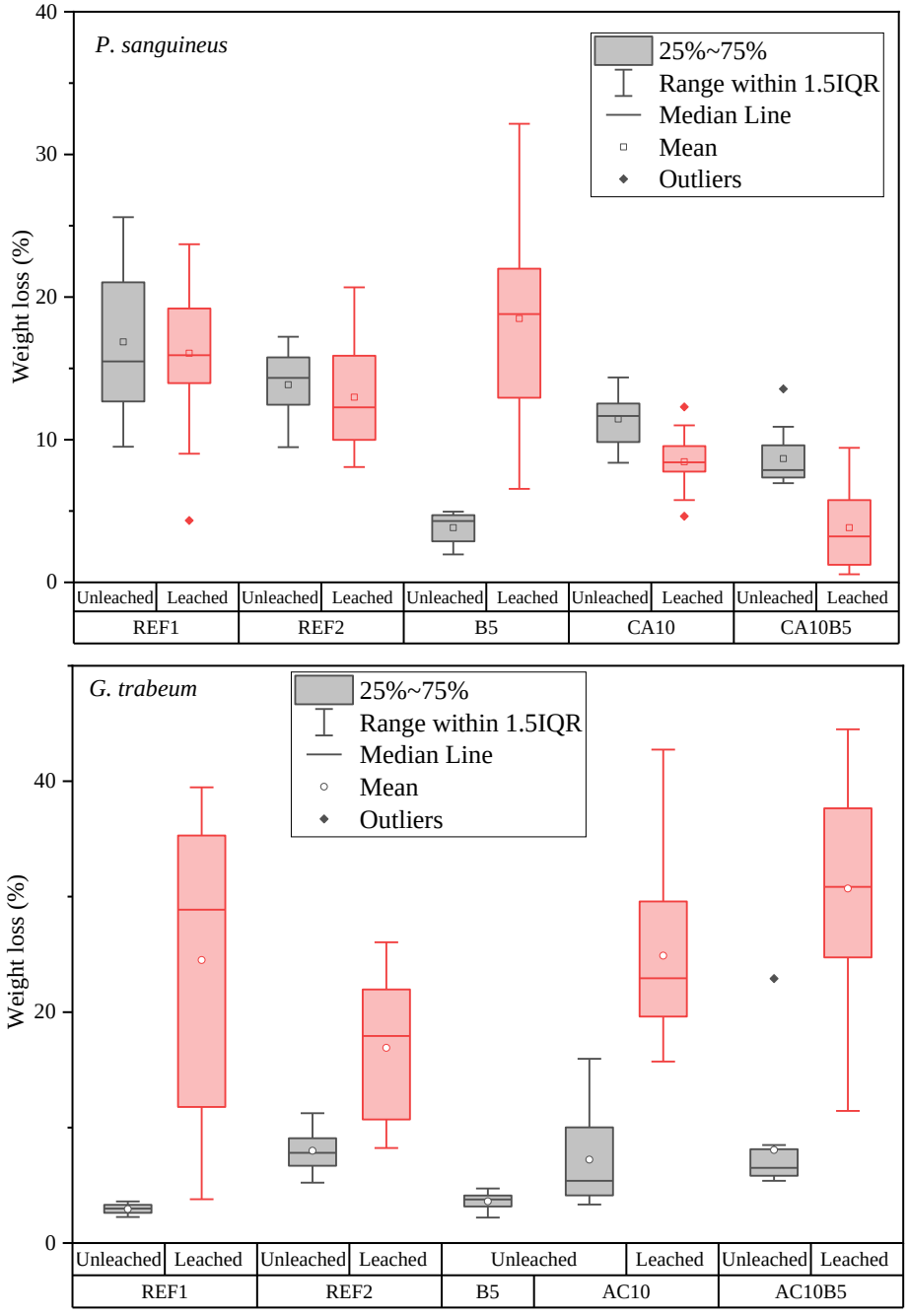

Source: Author's authorship

Although no publications were found addressing fungi degradation of bamboo treated with citric acid, chemical modification processes commonly improve the degradation resistance of wood materials (SANDBERG; KUTNAR; MANTANIS, 2017). In only one work, beech

wood modified by citric acid with a WPG of 6.1% had an eight-fold increase in the durability against *Poria placenta* fungus. However, no information regarding the effects of leaching is presented (DESPOT; HASAN; JUG, 2008).

4.3.2.3. Partial conclusions

According to the obtained fungi decay results, the samples treated with only DOT (B5), unleached, can be classified according to EN 350-1:1996 as Class 1 (highly durable) for both *P. sanguineus* and *G. trabeum* fungi. However, after leaching, the B5 condition is classified as Class 4 (slightly durable) against *P. sanguineus*. The treatments with citric acid, considering the leached and unbleached samples, ranged between Classes 1 and 3 (moderately durable) for P. sanguineus and between Classes 3 and 4 for *G trabeum*.

As the main conclusion based on the statistical analyses, the citric acid treatment used in this study did not protect bamboo against the brown-rot fungi *G. trabeum*. However, it showed some fungicide properties for the white-rot fungi *P. sanguineus*, especially after leaching. To explain the observed results, some assumptions have been raised.

Assumption 1 – *P. sanguineus* degrades mainly lignin and hemicellulose. In this case, the citric acid modification could have modified especially those components and hence, protected from decay. Since *G. trabeum* degrades cellulose, and the modified samples had the same behaviour of the references, it is possible to infer that the cellulose was not modified, as previously thought.

Assumption 2 – The chemical modification with citric acid degraded hemicellulose and lignin and some of those components leached out after the leaching cycles, reducing the amount of available material to be consumed by the fungi. This effect would then explain the decrease in WL of the samples decayed by *P. sanguineus*. On the other hand, unintentional chemical changes on the cellulose could also have facilitated its consumption by *G. trabeum*.

Assumption 3 – Fungi degradation may be more sensitive to the modification degree and perhaps, higher WPGs are necessary for satisfactory protection. Nonetheless, problems with the adapted fungi decay test could have happened, compromising the results of the samples tested against *G. trabeum*.

5. CHAPTER 5 – Conclusions and final remarks

In a general context, and according to all the information presented throughout this thesis, bamboo is indeed an interesting and promising material. However, many areas related to its production and use have space for improvement, especially related to basic quality protocols and preservation. The adoption of standardized methods for treatability evaluation is strongly advised, especially for more sensitive applications, such as for structural use.

A set of methods to evaluate the treatability of bamboo was deeply investigated and presented. Understanding the effect of treatments on mechanical properties was an important issue that was addressed in a meaningful way. Therefore, useful tools for mechanical, physical and chemical characterizations of bamboo will be available for the public. Additionally, new possibilities for bamboo treatment based on less hazardous chemicals were investigated. The proposed treatment systems, based on chemical modification and tannin-based polymers impregnation, presented interesting and promising results that can be further improved.

A summary of conclusions and recommendations related to chapters 3 and 4 are presented below.

5.1. Conclusions and recommendations

Chapter 3 – Assessment of conventionally treated bamboo

This chapter was divided into three independent, but correlated, studies: the effect of disodium octaborate (DOT) in the mechanical properties of *D. asper* bamboo; quality assessment and mechanical characterization of chromated copper borate (CCB) and DOT treated *P. edulis* bamboo; and the use of digital correlation for standardized ISO 22157 mechanical tests.

Several characterization methods for the evaluation of bamboo treated with (DOT) and (CCB) were explored. Both preservatives are advised for different applications; for exterior use, CCB and for interior use, DOT. In the first study, the effect of DOT on the mechanical properties of *D. asper* bamboo was directly investigated through small coupon compression and dynamic and static three-point bending tests. By using 5% and 8% DOT solutions in a vacuum/pressure treatment, complete penetration and high solution absorption were achieved.

The main outcome of this study is that there is no deleterious effect of DOT on the mechanical properties, but in fact, an increase in bending and compression strength. However, no evident change was observed in the modulus of elasticity in bending (static and dynamic) and compression.

In the second study, a small batch of full-culm *P.edulis* bamboo poles treated by the immersion method with DOT solution was assessed in terms of treatability (penetration and retention evaluation) and mechanical properties. Considering the mild effects of DOT on the mechanical properties, a direct comparison of the DOT treated samples with full-culm bamboo treated with CCB in a commercial vacuum/pressure (full-cell) process was conducted. In relation to the DOT treated samples, 12 different poles (randomly chosen from a 130 batch) were fully characterized. Although low DOT retention was observed (2.2 kg/m^3), the penetration throughout the wall thickness was satisfactory. The additional samples used for the comparison with CCB also presented the same retention level while the CCB-treated samples had a retention of 7.2 kg/m^3. The preferential path for the preservative penetration was observed by SEM-EDS analysis. Higher concentrations of chromium and copper (components of CCB) were identified in the conducting vessels of bamboo while only traces of these elements were present in the parenchyma or fibre bundles. Despite these differences in retention, interestingly, there were no statistical differences ($p > 0.05$) between the treatments in all the evaluated mechanical properties: compression, shear and tension parallel to the fibres, coupon three-point bending, and tension perpendicular to the fibres (flat ring flexure test). Therefore, the combination of the mechanical results of all the samples (originated from 17 different bamboo culms) was used for the calculation of the characteristic values of compression, tension, shear and bending according to ISO 22156 – 04: f_c=49.5 MPa; E_c=18,040 MPa; f_v=15.4 MPa; G=2520 MPa; f_t=220 MPa; E_t=15,660 MPa; f_b=183 MPa; E_b=15,190 MPa.

In the third study, the same set of results obtained by the characterization of the samples in the previous study was utilised. In this part, the use of ISO 22157 standard was assessed and deeply discussed using complementary analyses performed using strain mapping obtained by digital image correlation (DIC) technique. The DIC helped to identify and quantify specimen behaviour in compression, shear, tension and bending tests, particularly in the presence of a node, where its local effect could be analysed. In compression and shear, the node has an insignificant impact. However, in tension and bending, the node acts as a ‘weak link’, reducing

the loading capacity of the culm significantly. This effect was explained by the morphology of the fibres in the nodal region. Additionally, the real bending behaviour of small coupon tests was evaluated in different bending orientations (outer layer in the compression side and in the tension side). The displacement of the neutral line towards the outer layer (higher fibre content/density) could be experimentally demonstrated. Depending on the sample orientation, the bending behaviour is consistently different. With the outer layer in compression, higher modulus of elasticity, modulus of rupture and limit of proportionality are observed. On the other hand, the outer layer in tension almost doubles the specific energy, increasing toughness. Last but not least, the specimen damage development was also described by DIC and the adoption of the limit of proportionality (LOP) was proposed to measure the material capacity. Albeit the characteristic values of strength are conventionally used in design, the application of the limit of proportionality (LOP) may be more appropriate since exceeding this limit is associated with permanent material damage.

At the end of this chapter, guidelines for bamboo treatment by the immersion method using DOT preservative were presented. The maintenance of the preservative concentration is one important aspect that can be successfully adjusted by simply measuring the conductivity of the treatment solution. The treatability of the bamboo culms can be verified with penetration and retention analyses. The retention analysis is advised for the qualification of a specific treatment schedule since it is labour intensive and requires an appropriate chemical laboratory. Nonetheless, the penetration tests are straightforward and can give reliable results directly in the field or treatment plant and, therefore, are advised for quality control purposes. The combination of these analytical tests with traceability control is expected to provide more confidence in commercially treated bamboo poles, especially for structural use that requires consistent and trustworthy materials.

Chapter 4 - Development of alternative treatments for bamboo

In chapter 4, different alternatives for bamboo preservative treatment were explored. This part was divided into two independent studies, based on wood technologies: the in-situ polymerization of tannin/boron-based solutions for the decrease of boron leaching and improvement of overall properties of bamboo; chemical modification of bamboo with citric acid, also in combination with boron compounds, as a new possibility of treatment to improve dimensional and wettability behaviour. Both studies were conducted using local *D. asper* bamboo. Although already applied in wood, no previous studies of these two treatment possibilities for bamboo have been found in the literature. Therefore, physical, mechanical, thermal, chemical and degradation tests were applied to understand the main effects of the treatments on the properties of bamboo.

In the first part, bamboo strips were impregnated with tannin/hexamine/boron formulations through a vacuum/pressure process. The treated samples (tannin/hexamine, tannin/hexamine/boron, and DOT) did not cause considerable changes in water absorption and dimensional stability, with a small decrease in these properties for the tannin/hexamine/boron samples. In terms of boron leachability, although pure tannin/hexamine/boron formulation has the capacity to fix boron when applied to bamboo, it was not capable of avoiding boron loss after severe leaching cycles. This effect is assumed to be related to the balance between the chemicals used in the formulation and a possible effect of bamboo components on the polymerization process. However, fungi decay tests with white-rot and brown-rot fungi revealed that the tannin-based formulations could maintain fungicide activity even after leaching, being classified as durable and highly durable. The DOT-only treatment, on the other hand, although effective in protecting bamboo, completely lost the fungicide activity after leaching. In terms of the mechanical evaluation (through compression, interlaminar shear, and three-point bending), all the treatments caused a positive effect on the compression strength, modulus of rupture (MOR) and modulus of elasticity (MOE) in bending. The tannin-hexamine-boron treatment presented the highest values of MOR and MOE, 244.1 MPa and 23.36 GPa, respectively. The benign effects of DOT were also observed in this set of samples, as observed in chapter 3. Another important aspect explored in this study was the use of thermogravimetric analysis (TGA) under synthetic airflow to understand the real degradation behaviour at high

temperatures. It was demonstrated that the presence of boron in the treatment solutions improve the thermal stability of bamboo. Tannin/hexamine treatment also caused a mild increase in the char yield at 400 °C and had a positive effect on thermal degradation.

In the second study of this chapter, the chemical modification of bamboo with citric acid was assessed in details. The treatment process was performed through a vacuum/pressure impregnation of solutions composed of citric acid, citric acid/boron, and DOT and subsequently submitted to a curing process at 120 °C. The main effect of the modification was observed in the physical properties with a noticeable decrease in water absorption (up to 26%) and swelling (up to 43%) in comparison with the reference and DOT-treated samples. This effect was attributed to an esterification process, identified by FTIR analysis, with a considerable increase of the carbonyl (C=O) group. Despite the improved wettability behaviour, the combination of citric acid and boron compounds did not decrease boron leaching, that was equivalent to DOT treated samples. However, chemical modification increased the brittleness of bamboo, and although higher strengths in three-point bending and compression were observed, caution should be adopted for the bamboo treated with citric if it is subjected to tensile and shear forces. As observed in the previous study and in chapter 3, the set of samples treated only with DOT also presented an improvement on the overall mechanical properties. The effect of citric acid on the mechanical behaviour was explained by SEM analysis, where microcracks and detachment were identified around the parenchyma/fibre bundles in the modified samples. Additionally, through FT-IR and XRD analysis, it was possible to observe that citric acid resulted in some changes in cellulose structure, with the reduction of crystallinity index and possible hydrolysis of the amorphous phase, which might also explain the effects on the mechanical properties. Lastly, the treated samples were submitted to a thermogravimetric analysis under synthetic airflow, as performed in the previous study. Samples treated only with citric acid had higher weight losses upon heating than those of the reference samples, while the treatment only with DOT resulted in the best thermal stability, as previously observed. The combination of both citric acid and DOT was found to be an alternative to overcome this problem.

Since both treatment methods explored involve temperatures in the order of 100 °C, these methods are advised for bamboo strips and other non-round elements for treatment, since cracking of full-culm bamboos can be a problem. Additionally, milled materials have better solution absorption and balance the bamboo treatability problem.

This work provides insights into the use of non-hazardous chemicals as an alternative for bamboo-based materials treatment, opening new opportunities for the development of more durable products with improved stability. Nevertheless, more research is necessary to optimize the chemical modification reaction (using catalysts; different temperatures; inert atmosphere). The polymerization reaction of tannin-boron preservatives within the bamboo structure should also be further studied, exploring the use of different formulations and curing temperatures.

5.2. Proposals for future activities

Other results generated (under analysis and/or under testing) during this doctorate project are being used for the elaboration of additional studies as follow:

- Characterisation of P. edulis and D. asper bamboo treated with disodium octaborate tetrahydrate after field degradation tests:

Field degradation tests are currently being conducted in the laboratory of Construction and Ambience, USP. Samples of DOT treated and untreated full-culm bamboo, are being exposed to environmental conditions and in contact with the groud. Although boron treatment is not suitable for exterior applications, the main objective of this study is to evaluate if this treatment may increase the usage expectancy of bamboo culms in comparison with untreated material. The samples will be exposed to 18 to 24 months, and samples from the buried and above the ground parts will be evaluated through boron retention analysis, mechanical, physical and chemical characterizations. The degradation field is located in a controlled area with a meteorological station, measuring temperature, rainfall, and humidity throughout the entire test.

- Fungi decay of bamboo treated with citric acid and boron compounds:

In order to complement the results presented in section 4.3.2, additional chemical analysis by FT-IR and microstructural characterization are being performed to better explain the behaviour observed in the fungi decay tests. Additional samples modified with higher WPGs as a target are also planned to be tested and evaluated.

- On the influence of density and fibre bundle fraction and distribution on the mechanical properties of P.edulis and D. asper bamboo assessed by digital image correlation:

This paper will focus on the correlation of the data obtained through DIC analysis of *D. asper* and *P. edulis* bamboo and their macroscopic characteristics. Previous analyses showed that the fibre bundle fraction is not directly correlated to the density. For the same density, for example, *D. asper* has higher fibre bundle volume fraction than *P. edulis*. However, *P. edulis* presents the same specific strength in bending, which makes more efficient in terms of fibre use. This study also intends to correlate the fibre distribution with the experimental neutral zone under flexure loading and understand whether the density or fibre fraction is the main contributor.

- The effect of citric acid modification on the densification process of bamboo:

Preliminary tests with bamboo samples impregnated with citric acid subjected to a densification process (increase of density through thermal-mechanical modification) were performed. When untreated, the densification process may cause microcracks that are deleterious for dimensional stability (KADIVAR et al., 2019). The use of citric acid treatment in a specific condition, can overcome this problem by decreasing the pressure necessary for densification and, at the same time, chemically modify bamboo and improve its dimensional stability. Additionally, citric acid has the ability to act as a binder of lignocellulosic materials, possibly stabilizing the collapsed bamboo vessels after compression. Different citric acid impregnation loadings will be tested in combination with different densification temperatures. The resulted material will be characterized in terms of mechanical, physical and chemical properties.

- Chemical modification of wood and bamboo using citric acid in an inert atmosphere reaction:

The chemical modification intermediated by citric acid can be further improved and adapted for industrial production. This paper will focus on the use of a closed reactor with temperature control to chemically modify bamboo and wood in an inert atmosphere (nitrogen gas), with all treatment steps conducted in the same equipment. Previous tests with *D. asper* bamboo, pine and eucalyptus wood showed higher WPGs in comparison with the impregnation process used in chapter 4. Physical and chemical characterizations will be used to assess the treated materials, with special attention to treatment temperature and citric acid concentration.

REFERENCES

AKINBADE, Y.; HARRIES, K. A.; FLOWER, C. V.; NETTLESHIP, I.; PAPADOPOULOS, C.; PLATT, S. Through-culm wall mechanical behaviour of bamboo. **Construction and Building Materials**, v. 216, p. 485–495, 2019.

ALMEIDA, A. E. F. S.; TONOLI, G. H. D.; SANTOS, S. F.; SAVASTANO, H. Improved durability of vegetable fiber reinforced cement composite subject to accelerated carbonation at early age. **Cement and Concrete Composites**, v. 42, p. 49–58, 2013.

AMERICAN SOCIETY FOR TESTING AND MATERIALS. **D1037-12**: Standard Test Method for Evaluating Properties of Wood-Base Fiber and Particle Panel Materials. West Conshohoken, 2012.

ASTM. **D4761-13**: Standard Test Methods for Mechanical Properties of Lumber and Wood-Base Structural Material. West Conshohocken, 2013.

ASTM**. D143-14**: Standard test methods for small clear specimens of timber. West Conshohocken, 2014.

ASTM. **E1876-15**: Standard Test Method for Dynamic Young's Modulus, Shear Modulus, and Poisson's Ratio by Impulse Excitation of Vibration. West Conshohocken, 2015a.

ASTM. **D7264-15**: Standard Test Method for Flexural Properties of Polymer Matrix Composite MaterialsWest Conshohocken, 2015b.

ASTM. **D2395-17**: Standard Test Methods for Density and Specific Gravity (Relative Density) of Wood and Wood-Based MaterialsWest Conshohocken, 2017a.

ASTM. **D2915-17**: Standard Practice for Sampling and Data-Analysis for Structural Wood and Wood-Based ProductsWest Conshohocken, 2017b.

AMERICAN WOOD PROTECTION ASSOCIATION. **A65-15**: Standard method to determine the amount of boron in treated wood using azomethine-H or carminic acid. Birmingham, 2015.

AWPA. **E10-16**: Laboratory method for evaluating the decay resistance of wood-based materials against pure basidiomycete cultures: soil/block test. Birmingham, 2016.

ANUAR, S.; KRAUSE, A. Utilizing Malaysian bamboo for use in thermoplastic composites. **Journal of Cleaner Production**, v. 110, p. 16–24, 2016.

ANWAR, U.; HIZIROGLU, S.; HAMDAN, H.; LATIF, M. A. Effect of outdoor exposure on some properties of resin-treated plybamboo. **Crop Prod**., v. 33, n. 1, p. 140–145, 2011.

ARRUDA, L. M.; DEL MENEZZI, C. H. S.; TEIXEIRA, D. E.; DE ARAÚJO, P. C. Lignocellulosic composites from Brazilian giant bamboo (Guadua magna): Part 1: Properties of resin bonded particleboards. **Maderas. Ciencia y tecnología**, v. 13, n. 1, p. 49–58, 2011.

ASSOCIAÇÃO BRASILEIRA DE NORMAS TÉCNICAS. **NBR 7190**: Projeto de estruturas de madeira (Wood structures project). Rio de Janeiro, 1997.

ABNT. **NBR 6232**: Penetração e retenção de preservativos em madeira tratada sob pressão (Penetration and retention of preservatives in pressure-treated wood). Rio de Janeiro, 2013.

AWALLUDDIN, D.; MOHD ARIFFIN, M. A.; OSMAN, M. H.; HUSSIN, M. W.; A. ISMAIL, M.; LEE, H.-S.; ABDUL SHUKOR LIM, N. H. Mechanical properties of different bamboo species. **MATEC Web of Conferences**, v. 138, p. 1–10, 2017.

AZADEH, A. **The effect of heat on physical and mechanical properties of Dendrocalamus giganteus bamboo**. 2018. PhD Dissertation - PUC-Rio, Rio de Janeiro, 2018.

AZEREDO, H. M. C.; KONTOU-VRETTOU, C.; MOATES, G. K.; WELLNER, N.; CROSS, K.; PEREIRA, P. H. F.; WALDRON, K. W. Wheat straw hemicellulose films as affected by citric acid. **Food Hydrocolloids**, v. 50, p. 1–6, 2015.

BANIK, R. L. Morphology and Growth. In: LIESE, W.; KÖHL, M. (Ed.). **Bamboo: The plant and its uses**. Cham: Springer, 2015. p. 43–89.

BAYSAL, E.; ALTINOK, M.; COLAK, M.; KIYOKA OZAKI, S.; TOKER, H. Fire resistance of Douglas fir (Pseudotsuga menzieesi) treated with borates and natural extractives. **Bioresource Technology**, v. 98, n. 5, p. 1101–1105, 2007.

BAYSAL, E.; TOMAK, E. D.; TOPALOGLU, E.; PESMAN, E. Surface properties of bamboo and Scots pine impregnated with boron and copper based wood preservatives after accelerated weathering. **Maderas. Ciencia y tecnología**, v. 18, n. 2, p. 253–264, 2016.

BERALDO, A. L. Bamboo Housing – Evaluation of the Component ' s Decay After 17 Years of Exposure. In: **6th Amazon & Pacific Green Materials Congress and Sustainable Construction Materials LAT-RILEM Conference**, Cali, 2016.

BISWAS, D.; BOSE, S. K.; HOSSAIN, M. M. Physical and mechanical properties of urea formaldehyde-bonded particleboard made from bamboo waste Daisy. **International Journal of Adhesion**, v. 31, p. 84–87, 2011.

BRAGHIROLI, F. L.; AMARAL-LABAT, G.; BOSS, A. F. N.; LACOSTE, C.; PIZZI, A. Tannin gels and their carbon derivatives: A review. **Biomolecules**, v. 9, n. 10, 2019.

BUI, Q. B.; GRILLET, A. C.; TRAN, H. D. A bamboo treatment procedure: Effects on the durability and mechanical performance. **Sustainability (Switzerland)**, v. 9, n. 9, p. 1–11, 2017.

BUREAU OF INDIAN STANDARDS. **IS 401:2001**: Preservation of timber — Code of practice. New Delhi, 2001.

BIS. **IS 1902:2006**: Preservation of bamboo and cane for non-structural purposes - Code of practice. New Delhi, 2006a.

BIS. **IS 9096:2006**: Preservation of bamboo for structural purposes - Code of practice. New Delhi, 2006b.

CABI, C. I. **Invasive Species Compendium - Dinoderus minutus (bamboo borer)**. Available in: <https://www.cabi.org/isc/datasheet/19035.>.

CALDEIRA, F. Boron in Wood Preservation: A Review in its Physico-Chemical Aspects. **Silva Lusitana**, v. 18, n. 2, p. 179–196, 2010.

CANAVAN, S.; RICHARDSON, D. M.; VISSER, V.; ROUX, J. J. Le; VORONTSOVA, M. S.; WILSON, J. R. U. The global distribution of bamboos: assessing correlates of introduction and invasion. **AoB Plants**, v. 9, n. 1, p. plw078, 2016.

CAPELLE, R. Microdosage colorimetrique du bore en milieu aqueux, au moyen de reactifs a groupement azoique ou imine derives des acides H et K. **Analytica Chimica Acta**, v. 24, p. 555–572, 1961.

CARMO, C. A. F. de S. do; ARAÚJO, W. S. de; BERNARDI, A. C. de C.; SALDANHA, M. F. C. **Métodos de Análises de Tecidos Vegetais Utilizados na Embrapa Solos**. Rio de Janeiro: Embrapa Solos, 2000.

CHANG, F. C.; CHEN, K. S.; YANG, P. Y.; KO, C. H. Environmental benefit of utilizing bamboo material based on life cycle assessment. **Journal of Cleaner Production**, v. 204, p. 60–69, 2018.

CHAOWANA, P.; BARBU, M. C. Bamboo: Potential material for biocomposites. In: JAWAID, M.; MD TAHIR, P.; SABA, N. (Ed.). L**ignocellulosic Fibre and Biomass-Based Composite Materials: Processing, Properties and Applications**. Woodhead Publishing, 2017. p. 259–289.

CHAU, C. K.; HUI, W. K.; NG, W. Y.; POWELL, G. Assessment of CO_2 emissions reduction in high-rise concrete office buildings using different material use options. Resources, **Conservation and Recycling**, v. 61, p. 22–34, 2012.

CHEN, G.; LUO, H.; YANG, H.; ZHANG, T.; LI, S. Water effects on the deformation and fracture behaviors of the multi-scaled cellular fibrous bamboo. **Acta Biomaterialia**, v. 65, p. 203–215, 2018.

CHOW, A.; RAMAGE, M. H.; SHAH, D. U. Optimising ply orientation in structural laminated bamboo. **Construction and Building Materials**, v. 212, p. 541–548, 2019.

CHUNG, K. F.; YU, W. K. Mechanical properties of structural bamboo for bamboo scaffoldings**. Engineering Structures**, v. 24, n. 4, p. 429–442, 2002.

CHUNG, M. J.; WANG, S. Y. Mechanical properties of oriented bamboo scrimber boards made of Phyllostachys pubescens (moso bamboo) from Taiwan and China as a function of density. **Holzforschung**, v. 72, n. 2, p. 151–158, 2018.

CIRCABC. **Directive 98/8/EC concerning the placing biocidal products on the market. Assessment Report - Disodium octaborate tetrahydrate Product-type 8 (Wood preservative)**. Available in: <https://circabc.europa.eu/sd/a/6ba0bde3-b159-48f5-9c8a-931d31cc69e1/Draft assessment report DOT.pdf>.

CLARK, L. G.; LONDOÑO, X.; RUIZ-SANCHEZ, E. Bamboo Taxonomy and Habitat. In: LIESE, W.; KÖHL, M. (Ed.). **Bamboo: The plant and its uses**. Cham: Springer, 2015. p. 1–30.

COOK, J. et al. Consensus on consensus: a synthesis of consensus estimates on human-caused global warming. **Environmental Research Letters**, v. 11, n. 4, p. 048002, 1 abr. 2016.

CORREAL, J. F. Chapter 14: Bamboo design and construction. In: HARRIES, K. A.; SHARMA, B. (Ed.). **Nonconventional and Vernacular Construction Materials: Characterisation, Properties and Applications**. 1st. ed. Woodhead (Elsevier) Publishing, 2019.

CORREIA, V. C.; CURVELO, A. A. S.; MARABEZI, K.; ALMEIDA, A. E. F. S.; SAVASTANO, H. Bamboo cellulosic pulp produced by the ethanol/water process for reinforcement applications. **Ciencia Florestal**, v. 25, n. 1, p. 127–135, 2015.

CRUZ, M. L. S. **Caracterização fisica e mecânica de colmos inteiros do bambu da espécie phyllostachys aurea: comportamento à flambagem** [Physical and mechanical characterization of full-culm phyllostachys aurea bamboo: buckling behaviour]. 2002. Master Thesis – PUC-Rio, 2002.

DE ARAÚJO, P. C.; ARRUDA, L. M.; DEL MENEZZI, C. H. S.; TEIXEIRA, D. E.; DE SOUZA, M. R. Lignocellulosic composites from Brazilian giant bamboo (Guadua magna): Part 2: Properties of cement and gypsum bonded particleboards. **Maderas. Ciencia y tecnología**, v. 13, n. 3, p. 297–306, 2011

DE HOYOS-MARTÍNEZ, P. L.; MERLE, J.; LABIDI, J.; CHARRIER – EL BOUHTOURY, F. Tannins extraction: A key point for their valorization and cleaner production. **Journal of Cleaner Production**, v. 206, p. 1138–1155, 2019.

DEL MENEZZI, C.; AMIROU, S.; PIZZI, A.; XI, X.; DELMOTTE, L. Reactions with wood carbohydrates and lignin of citric acid as a bond promoter of wood veneer panels. **Polymers**, v. 10, n. 8, 2018.

DENG, J.; CHEN, F.; WANG, G.; ZHANG, W. Variation of Parallel-to-Grain Compression and Shearing Properties in Moso Bamboo Culm (Phyllostachys pubescens). **BioResources**, v. 11, n. 1, p. 1784–1795, 2016.

DESPOT, R.; HASAN, M.; JUG, M. Biological durability of wood modified by citric acid. **Drvna Industrija**, v. 59, n. 2, p. 55–59, 2008.

DIOUF, P. N.; STEVANOVIC, T.; CLOUTIER, A.; FANG, C. H.; BLANCHET, P.; KOUBAA, A.; MARIOTTI, N. Effects of thermo-hygro-mechanical densification on the surface characteristics of trembling aspen and hybrid poplar wood veneers. **Applied Surface Science**, v. 257, n. 8, p. 3558–3564, 2011.

DIXON, P. G.; AHVENAINEN, P.; AIJAZI, A. N.; CHEN, S. H.; LIN, S.; AUGUSCIAK, P. K.; BORREGA, M.; SVEDSTRÖM, K.; GIBSON, L. J. Comparison of the structure and flexural properties of Moso, Guadua and Tre Gai bamboo. **Construction and Building Materials**, v. 90, p. 11–17, 2015.

DIXON, P. G.; GIBSON, L. J. The structure and mechanics of Moso bamboo material. **Journal of the Royal Society Interface**, v. 11, n. 99, 2014.

DONMEZ CAVDAR, A.; MENGELOŁLU, F.; KARAKUS, K. Effect of boric acid and borax on mechanical, fire and thermal properties of wood flour filled high density polyethylene composites. **Measurement**, v. 60, p. 6–12, 2015.

DUBEY, M. K. **Improvements in statility, durability and mechanical properties of radiata pine wood after heat-treatment in a vegetable oil**. 2010. PhD Dissertation - University of Canterbury, Christchurch, 2010.

EBF. Environmental Bamboo Foundation, 2003. **Vertical Soak Diffusion for Bamboo**, 1st Ed. Linda Garland, Ubub, Bali, 26 p.

ESCAMILLA, E. Z.; HABERT, G.; DAZA, J. F. C.; ARCHILLA, H. F.; FERNÁNDEZ, J. S. E.; TRUJILLO, D. Industrial or traditional bamboo construction? Comparative life cycle assessment (LCA) of bamboo-based buildings. **Sustainability (Switzerland)**, v. 10, n. 9, p. 3096, 2018.

ESCAMILLA, E. Z.; HABERT, G. Environmental impacts of bamboo-based construction materials representing global production diversity. **Journal of Cleaner Production**, v. 69, p. 117–127, 2014.

ESPELHO, J. C. C. **Tratamento químico de colmos de bambu pelo método de boucherie modificado** [Chemical treatment of bamboo culms by modified boucherie method]. 2007. Master Thesis - Universidade Estadual de Campinas, Campinas, 2007.

ESPELHO, J. C. C.; BERALDO, A. L. Avaliação físico-mecânica de colmos de bambu tratados. **Revista Brasileira de Engenharia Agrícola e Ambiental**, v. 12, n. 6, p. 645–652, 2008.

ESSOUA, E. G. G.; BEAUREGARD, R.; AMOR, B.; BLANCHET, P.; LANDRY, V. Evaluation of environmental impacts of citric acid and glycerol outdoor softwood treatment: Case-study. **Journal of Cleaner Production**, v. 164, p. 1507–1518, 2017.

ESSOUA, G. G. E.; BLANCHET, P.; LANDRY, V.; BEAUREGARD, R. Pine wood treated with a citric acid and glycerol mixture: Biomaterial performance improved by a bio-byproduct. **BioResources**, v. 11, n. 2, p. 3049–3072, 2016.

EUROPEAN STANDARDS. **EN 350-1**: Durability of wood and wood-based products. Natural durability of solid wood. Part 1: Guide to the principles of testing and classification of natural durability of wood. Berlin, 1996.

ES. **EN 350-2**: Durability of wood and wood-based products. Natural durability of solid wood. Part 2: Guide to natural durability and treatability of selected wood species of importance in Europe. Berlin, 1997.

EVANS, P. D.; SCHMALZL, K. J.; FORSYTH, C. M.; FALLON, G. D.; SCHMID, S.; BENDIXEN, B.; HEIMDAL, S. Formation and Structure of Metal Complexes with the

Fungicides Tebuconazole and Propiconazole. **Journal of Wood Chemistry and Technology**, v. 27, n. 3–4, p. 243–256, 2007.

F.L. SUN, Y.Y. ZHOU, B.F. BAO, A.L. CHEN, C. G. Du. Influence of solvent treatment on mould resistance of bamboo. **BioResources**, v. 6, p. 2091–2100, 2011.

FAO. Food and agriculture organization of the United Nations. **Global Forest Resources Assessment 2010. Main Report**. FAO Forestry Paper 163, 2010. Available in: http://www.fao.org/3/i1757e/i1757e.pdf

FATRIASARI, W.; SYAFII, W.; WISTARA, N.; SYAMSU, K.; PRASETYA, B. Lignin and Cellulose Changes of Betung Bamboo (Dendrocalamus asper) pretreated Microwave Heating. **Int J Adv Sci Eng Inf Technol**, v. 6, n. 2, p. 187, 2016.

FENG, X.; XIAO, Z.; SUI, S.; WANG, Q.; XIE, Y. Esterification of wood with citric acid: The catalytic effects of sodium hypophosphite (SHP). **Holzforschung**, v. 68, n. 4, p. 427–433, 2014.

FILGUEIRAS, T. S.; GONÇALVES, A. P. S. A Checklist of the Basal Grasses and Bamboos in Brazil (POACEAE). **The Journal of the American Bamboo Society**, v. 18, n. 1, p. 7–18, 2004.

FIORELLI, J.; DONIZETTI, D.; BARRERO, N. G.; SAVASTANO, H.; MARIA, E.; AGNOLON, D. J.; JOHNSON, R. Particulate composite based on coconut fiber and castor oil polyurethane adhesive : An eco-efficient product. **Industrial Crops & Products**, v. 40, p. 69–75, 2012.

FREEMAN, M. H.; MCINTYRE, C. R.; JACKSON, D. A Critical and Comprehensive Review of Boron in Wood Preservation. **Proceedings of the American Wood Protection Assoc**., p. 279-294, 2009.

GARCI, A. A.; TADEO, J. L. Leaching of copper, chromium, and boron from treated timber during aboveground exposure. **Environmental Toxicology and Chemistry**, v. 25 (9), p. 2342–2348, 2006.

GARCIA, C. M.; MORRELL, J. J. Development of the Powderpost Beetle (Coleoptera: Bostrichidae) at Constant Temperatures. **Environmental Entomology**, v. 38, n. 2, p. 478–483, 2009.

GARCIA, R.; PIZZI, A. Polycondensation and autocondensation networks in polyflavonoid tannins. II. Polycondensation versus autocondensation. **Journal of Applied Polymer Science**, v. 70, n. 6, p. 1093–1109, 1998.

GATÓO, A.; SHARMA, B.; BOCK, M.; MULLIGAN, H.; RAMAGE, M. H. Sustainable structures : bamboo standards and building codes. **Proceedings of the ICE -Engineering Sustainability**, v. 167, n. ES5, p. 189–196, 2014.

GAUSS, C.; ARAUJO, V. De; GAVA, M.; CORTEZ-BARBOSA, J.; SAVASTANO JUNIOR, H. Bamboo particleboards: recent developments. **Pesquisa Agropecuária Tropical**, v. 49, p. 1–9, 2019.

GAUSS, C.; DOMINGUEZ, A. L. S.; SAVASTANO JR., H. Dimensional stability and water absorption of D. asper bamboo treated with citric acid and boron salts (In Portuguese). In: **3º Congresso Luso-Brasileiro Materiais de Construção Sustentáveis**, Coimbra, 2018.

GAUSS, C.; HARRIES, K. A.; KADIVAR, M.; AKINBADE, Y. A.; SAVASTANO, H.; Quality assessment and mechanical characterization of preservative-treated Moso bamboo (P. edulis). **European Journal of Wood and Wood Products**, 2020.

GAUSS, C.; KADIVAR, M.; SAVASTANO JR, H. Effect of disodium octaborate tetrahydrate on the mechanical properties of Dendrocalamus asper bamboo treated by vacuum/pressure method. **Journal of Wood Science**, v. 65, n. 27, 2019.

GAUSS, C.; SAVASTANO, H.; HARRIES, K. A. Use of ISO 22157 mechanical test methods and the characterisation of Brazilian P. edulis bamboo. **Construction and Building Materials**, v. 228, p. 116728, dez. 2019.

GÉRARDIN, P. New alternatives for wood preservation based on thermal and chemical modification of wood: a review. **Annals of Forest Science**, v. 73, n. 3, p. 559–570, 2016.

GEROTO, P. G. **Caracterização anatômica e física – por densitometria de raios X – de colmos de Dendrocalamus asper Backer, Dendrocalamus latiflorus Munro e Guadua angustifolia Kunth** [Anatomical and physical characterization - by X-ray densitometry - of Dendrocalamus asper Backer, Dendrocalamus latiflorus Munro and Guadua angustifolia Kunth culms]**.** 2014. Master Thesis - Universidade de São Paulo, Piracicaba, 2014.

GHAVAMI, K. **Bambu: Um material alternativo na Engenharia**. In: Revista do Instituto de Engenharia. São Paulo: Engenho Editora Técnica, 1992, n.192, 13-27 p.

GHAVAMI, K. Bamboo as reinforcement in structural concrete elements. **Cement and Concrete Composites**, v. 27, n. 6, p. 637–649, 2005.

GHAVAMI, K. Bamboo: Low cost and energy saving construction materials. XIAO, Y., INOUE, M., PAUDEL, S. K. (Eds.). In: **Modern Bamboo Structures**, Changsha: CRC Press, 2008. P. 5-21.

GHAVAMI, K.; MARINHO, A. B. Propriedades físicas e mecânicas do colmo inteiro do bambu da espécie Guadua angustifolia. **Revista Brasileira de Engenharia Agrícola e Ambiental**, v. 9, n. 1, p. 107–114, 2005.

GHAVAMI, K.; RODRIGUES, C. S.; PACIORNIK, S. Bamboo: Functionally graded composite material. **Asian Journal of Civil Engineering (Building and Housing)**, v. 4, n. 1, p. 1–10, 2003.

GHAVAMI, K.; TOLEDO FILHO, R. D.; BARBOSA, N. P. Behaviour of composite soil reinforced with natural fibres. **Cement and Concrete Composites**, v. 21, n. 1, p. 39–48, 1999.

GIBSON, L. J.; KUTNAR, A.; DIXON, P. G.; SMITH, G. D.; KAMKE, F. A.; SEMPLE, K. E. Comparison of the flexural behavior of natural and thermo-hydro-mechanically densified Moso bamboo. **European Journal of Wood and Wood Products**, v. 74, n. 5, p. 633–642, 2016.

HARRIES, K. A. In-the-Field Test Methods for Bamboo – The test-kit-in-a-backpack. In: **Proceedings 15th International Conference Non-conventional Materials and Technologies (NOCMAT 15)**, Winnipeg, Canada, 2015.

GOH, Y.; YAP, S. P.; TONG, T. Y. Bamboo: The Emerging Renewable Material for Sustainable Construction. In: **Reference Module in Materials Science and Materials Engineering**. Elsevier, 2019. p. 1-14.

GONZÁLEZ-LAREDO, R. F.; ROSALES-CASTRO, M.; ROCHA-GUZMÁN, N. E.; GALLEGOS-INFANTE, J. A.; MORENO-JIMÉNEZ, M. R.; KARCHESY, J. J. Wood preservation using natural products. **Madera y bosques**, v. 21, p. 127 p., 2015.

GOTTRON, J.; HARRIES, K. A.; XU, Q. Creep behaviour of bamboo. **Construction and Building Materials**, v. 66, p. 79–88, 2014.

GRANTA-DESIGN. **Material and Process Selection - The CES EduPAck Resource Booklet**. Cambridge University, 2010. Available in: <https://downloadfiles.grantadesign.com/pdf/teaching_resource_books/2-Materials-Charts-2010.pdf>.

GROSSER, D.; LIESE, W. On the anatomy of Asian bamboos, with special reference to their vascular bundles. **Wood Science and Technology**, v. 5, n. 4, p. 290–312, 1971.

GUJRATHI, A. M.; BABU, B. V. Environment friendly products from black wattle. **Energy Education Science and Technology**, v. 19, n. 1, p. 37–44, 2007.

GUO, J.; TANG, J.; WEN, Y.; ZHANG, J. L.; LI, Y. S. Development Status of Modern Bamboo Structure Building. **Applied Mechanics and Materials**, v. 351–352, p. 26–29, 2013.

GUO, W.; XIAO, Z.; WENTZEL, M.; EMMERICH, L.; XIE, Y.; MILITZ, H. Modification of Scots pine with activated glucose and citric acid: Physical and mechanical properties. **BioResources**, v. 14, n. 2, p. 3445–3458, 2019.

H. YAMAGUCHI, K. I. O. Chemically modified tannin and tannin-copper complexes as wood preservatives. **Holzforschung**, v. 52, p. 596–602, 1998.

HABIBI, M. K.; SAMAEI, A. T.; GHESHLAGHI, B.; LU, J.; LU, Y. Asymmetric flexural behavior from bamboo's functionally graded hierarchical structure: Underlying mechanisms. **Acta Biomaterialia**, v. 16, p. 178–186, 2015.

HARRIES, K. A.; BEN ALON, L.; SHARMA, B. Chapter 4: Codes and Standards Development for Nonconventional and Vernacular Materials. In: HARRIES, K. A.; SHARMA, B. (Ed.). **Nonconventional and Vernacular Construction Materials: Characterisation, Properties and Applications**. 2nd. ed. Woodhead (Elsevier) Publishing, 2019.

HARRIES, K. A.; SHARMA, B.; RICHARD, M. Structural Use of Full Culm Bamboo: The Path to Standardization. **International Journal of Architecture, Engineering and Construction**, v. 1, n. 2, p. 66–75, 2012.

HIDALDO-LÓPES, O. **Bamboo: The gift of the gods**. Bogota: D'Vinni Ltda, 2003.

HILL, C. **Wood modifications: Chemical, Thermal, and other Processes**. West Sussex: John Wiley and Sons, Ltd, 2006.

HOMAN, W. J.; JORISSEN, A. J. M. Wood modification developments. **Heron**, v. 49, n. 4, p. 361–386, 2004.

HU, J.; THEVENON, M. F.; PALANTI, S.; TONDI, G. Tannin-caprolactam and Tannin-PEG formulations as outdoor wood preservatives: biological properties. **Annals of Forest Science**, v. 74, n. 1, 2017.

HUANG, L.; KRIGSVOLL, G.; JOHANSEN, F.; LIU, Y.; ZHANG, X. Carbon emission of global construction sector. **Renewable and Sustainable Energy Reviews**, v. 81, n. November 2016, p. 1906–1916, 2018.

HUANG, X.; HSE, C.-Y.; SHUPE, T. F. Study of moso bamboo's permeability and mechanical properties. **Emerging Materials Research**, v. 4, n. 1, p. 130–138, 2015.

HUANG, Z.; SUN, Y.; MUSSO, F. Assessment of bamboo application in building envelope by comparison with reference timber. **Construction and Building Materials**, v. 156, p. 844–860, 2017a.

HUANG, Z.; SUN, Y.; MUSSO, F. Assessment on bamboo scrimber as a substitute for timber in building envelope in tropical and humid subtropical climate zones - Part 2 performance in

building envelope. **IOP Conference Series: Materials Science and Engineering**, v. 264, n. 1, 2017b.

IBACH, R. E. Chapter 19 - Specialty Treatments. In: **Wood Handbook - Wood as an engineering material**. Madison, Wisconsin: United States Department of Agriculture Forest Service, 2010. p. 1–16.

INBAR. An International Model Building Code for Bamboo. Beijing: The International Network on Bamboo and Rattan, 1999.

INTERNATIONAL ORGANIZATION FOR STANDARDIZATION. **CD 22156:2019** Bamboo – Structural Design. Geneva. [Committee Document: ongoing revisions to ISO 22156:2004, expected publication in 2021].

ISO **22157-1:2004**: Bamboo - Determination of physical and mechanical properties - Part 1: Requirements [withdrawn]. Geneva, 2004a.

ISO/TR **22157-2:2004**: Bamboo - Determination of physical and mechanical properties - Part 2: Laboratory manual [withdrawn]. Geneva, 2004b.

ISO **22156:2004**: Bamboo - Structural design. Geneva, 2004c.

ISO **19624:2018**: Bamboo structures - Grading of bamboo culms - Basic principles and procedures. Geneva, 2018.

ISO **22157:2019**: Bamboo structures – Determination of physical and mechanical properties of bamboo culms – Test methods. Geneva, 2019.

JAKOVLJEVIĆ, S.; LISJAK, D.; ALAR, Ž.; PENAVA, F. The influence of humidity on mechanical properties of bamboo for bicycles. **Construction and Building Materials**, v. 150, p. 35–48, 2017.

JANSSEN, J. J. A. **Bamboo in Building Structures**. 1981. PhD Dissertation - Eindhoven University of Technology, Eindhoven, 1981.

JANSSEN, J. J. A. Designing and Building with Bamboo. **International Network for Bamboo and Rattan**, 2000.

JAYANETTI, D. L.; FOLLETT, P. R. Bamboo in construction. XIAO, Y., INOUE, M., PAUDEL, S. K. (Eds.). In: **Modern Bamboo Structures**, Changsha: CRC Press, 2008. p. 23–32.

JIANG, F.; LI, T.; LI, Y.; ZHANG, Y.; GONG, A.; DAI, J.; HITZ, E.; LUO, W.; HU, L. Wood-Based Nanotechnologies toward Sustainability. **Advanced Materials**, v. 30, n. 1, p. 1–39, 2018.

JIANG, J.; LI, J.; GAO, Q. Effect of flame retardant treatment on dimensional stability and thermal degradation of wood. **Construction and Building Materials**, v. 75, p. 74–81, 2015.

JIT KAUR, P. Bamboo availability and utilization potential as a building material. **Forestry Research and Engineering: International Journal**, v. 2, n. 5, p. 240–242, 2018.

KADIVAR, M.; GAUSS, C.; MÁRMOL, G.; DOMINIQUE, A.; SÁ, D.; FIORONI, C.; GHAVAMI, K.; SAVASTANO, H. The influence of the initial moisture content on densification process of D . asper bamboo : Physical-chemical and bending characterization. **Construction and Building Materials**, v. 229, p. 116896, 2019.

KAMINSKI, S.; LAWRENCE A.; TRUJILLO D.; KING C. Structural use of bamboo. Part 2: durability and preservation. **The Structural Engineer**, v. 94(10), p. 38–43, 2016.

KAUR, P. J.; SATYA, S.; PANT, K. K.; NAIK, S. N. Eco-Friendly Preservation of Bamboo Species: Traditional to Modern Techniques. **BioResources**, v. 11, n. 4, p. 10604–10624, 2016.

KIM, T.; TANG, H.; LIESE, W. Pressure treatment of bamboo culms of three Vietnamese species with boron and CCB preservatives. **Journal of Bamboo and Rattan**, v. 10, n. 1&2, p. 63–76, 2011.

KRAUSE, J. Q.; DE ANDRADE SILVA, F.; GHAVAMI, K.; GOMES, O. da F. M.; FILHO, R. D. T. On the influence of Dendrocalamus giganteus bamboo microstructure on its mechanical behavior. **Construction and Building Materials**, v. 127, p. 199–209, 2016.

KRETSCHMANN, D. E. Chapter 5 - Mechanical Properties of Wood. In: **Wood Handbook - Wood as an engineering material**. Madison, Wisconsin: United States Department of Agriculture Forest Service, 2010. p. 1–46.

KUEHL, Y. Resources, Yield, and Volume of Bamboos. In: LIESE, W.; KÖHL, M. (Ed.). **Bamboo: The plant and its uses**. Cham: Springer, 2015. p. 91–111.

KUEHL, Y.; LI, Y.; HENLEY, G. Impacts of selective harvest on the carbon sequestration potential in Moso bamboo (Phyllostachys pubescens) plantations. **Forests Trees and Livelihoods**, v. 22, n. 1, p. 1–18, 2013.

KUMAR, S.; SHUKLA, K.; DEV, T.; DOBRIYAL, P. Bamboo preservation techniques: a review. **INBAR publication**, 1994.

LAHTELA, V.; HÄMÄLÄINEN, K.; KÄRKI, T. The effects of preservatives on the properties of wood after modification (Review paper). **Baltic Forestry**, v. 20, n. 1, p. 189–203, 2013.

LAKS, P. E.; MCKAIG, P. A.; HEMINGWAY, R. W.; MCKAIG, A. Flavonoid Biocides: Wood Preservatives Based on Condensed Tannins. **Holzforschung**, v. 42, n. 5, p. 299–306, 1988.

LEBOW, S. T. Chapter 15 - Wood preservation. In: **Wood Handbook - Wood as an engineering material**. Madison, Wisconsin: United States Department of Agriculture Forest Service, 2010. p. 1–28.

LEE, A. W. C.; CHEN, G.; TAINTER, F. H. Comparative treatability of Moso bamboo and Southern pine with CCA preservative using a commercial schedule. **Bioresource Technology**, v. 77, n. 1, p. 87–88, 2001.

LEE, C. H.; YANG, T. H.; CHENG, Y. W.; LEE, C. J. Effects of thermal modification on the surface and chemical properties of moso bamboo. **Construction and Building Materials**, v. 178, p. 59–71, 2018a.

LEE, S. H.; ASHAARI, Z.; LUM, W. C.; ABDUL HALIP, J.; ANG, A. F.; TAN, L. P.; CHIN, K. L.; MD TAHIR, P. Thermal treatment of wood using vegetable oils: A review. **Construction and Building Materials**, v. 181, p. 408–419, 2018b.

LEPAGE, E.; DE SALIS, A. G.; GUEDES, E. C. R. **Technology and protection of wood** (Portuguese). 1st. ed. São Paulo: Montana Química, 2017.

LEPAGE, E. S. **Informativo técnico divisão Osmose - Tratamento Preservativo do Bambu**. Disponível em: <https://www.montana.com.br/download/1187/file/InfTec_TraPre-Bambu.pdf>.

LEVAN, S. L.; JERROLD. E., W. Effects of fire-retardant treatments on wood strength: a review. **Wood and Fiber Science**, v. 22, n. 1, p. 113–131, 2007.

LI, J.; LI, B.; ZHANG, J.; ZHOU, X. Tannin Resins for Wood Preservatives: A Review. **Research and Application of Materials Science**, v. 1, n. 1, p. 45–48, 2019.

LI, M. Y.; FANG, B. S.; ZHAO, Y.; TONG, T.; HOU, X. H.; TONG, H. Investigation into the deterioration process of archaeological bamboo strips of China from four different periods by chemical and anatomical analysis. **Polymer Degradation and Stability**, v. 109, p. 71–78, 2014.

LI, T.; CHENG, D. li; WÅLINDER, M. E. P.; ZHOU, D. Wettability of oil heat-treated bamboo and bonding strength of laminated bamboo board. **Industrial Crops and Products**, v. 69, p. 15–20, 2015a.

LI, W.; WANG, H.; REN, D.; YU, Y.; YU, Y. Wood modification with furfuryl alcohol catalysed by a new composite acidic catalyst. **Wood Science and Technology**, v. 49, p. 1–12, 2015b.

LI, X.; SUN, C.; ZHOU, B.; HE, Y. Determination of Hemicellulose, Cellulose and Lignin in Moso Bamboo by Near Infrared Spectroscopy. **Nature Publishing Group**, v. 5, 2015c.

LI, X. B.; SHUPE, T. F.; PETER, G. F.; HSE, C. Y.; EBERHARDT, T. L. Chemical changes with maturation of the bamboo species Phyllostachys pubescens. **Journal of Tropical Forest Science**, v. 19, n. 1, p. 6–12, 2007.

LIESE, W., KUMAR, S. Bamboo Preservation compendium. **INBAR publication**, p. 32–55, 2003.

LIESE, W. Anatomy and properties of bamboo. **Bamboo Workshop Hangzhou**, p. 196–393, 1985.

LIESE, W. Research on bamboo. **Wood Science and Technology**, v. 21, n. 3, p. 189–209, 1987.

LIESE, W. **The Anatomy of Bamboo Culms**. Leiden: Brill, 1998.

LIESE, W. Preservation of a bamboo culm in relation to its structure. In: **Simposio Internacional de la Guadua**. Pereira, 2004.

LIESE, W.; TANG, T. K. H. Properties of the Bamboo Culm. In: LIESE, W.; KÖHL, M. (Ed.). **Bamboo: The plant and its uses**. Cham: Springer, 2015a. p. 227–256.

LIESE, W.; TANG, T. K. H. Preservation and Drying of Bamboo. In: LIESE, W.; KÖHL, M. (Ed.). **Bamboo: The plant and its uses**. Cham: Springer, 2015b. p. 257–297.

LIESE, W.; WEINER, G. Ageing of bamboo culms. A review. **Wood Science and Technology**, v. 30, n. 2, p. 77–89, 1996.

LIODAKIS, S.; TSAPARA, V.; AGIOVLASITIS, I. P.; VORISIS, D. Thermal analysis of Pinus sylvestris L. wood samples treated with a new gel-mineral mixture of short- and long-term fire retardants. **Thermochimica Acta**, v. 568, p. 156–160, 2013.

LIODAKIS, S.; ANTONOPOULOS, I.; KAKARDAKIS, T. Evaluating the use of minerals as forest fire retardants. **Fire Safety Journal**, v. 45, n. 2, p. 98–105, 2010.

LUGT, P. Van Der; VOGTLÄNDER, J.; BREZET, H. Bamboo, a Sustainable Solution for Western Europe Design Cases, LCAs and Land-use. Beijing: **INBAR publication**, 2009.

MAHDAVI, M.; CLOUSTON, P. L.; ARWADE, S. R. Development of Laminated Bamboo Lumber: Review of Processing, Performance, and Economical Considerations. **Journal of Materials in Civil Engineering**, v. 23, n. 7, p. 1036–1042, 2011.

MALANIT, P.; BARBU, M. C.; FRÜHWALD, A. Physical and mechanical properties of oriented strand lumber made from an Asian bamboo (Dendrocalamus asper Backer). **European Journal of Wood and Wood Products**, v. 69, n. 1, p. 27–36, 2011.

MANTANIS, G. I. Wood chemical modification. **BioResources**, v. 12, n. 2, p. 4478–4489, 2017.

MARÇAL, V. H. S. **Análise comparativa de normas técnicas internacionais para o emprego do bambu - colmo em estruturas prediais** [Comparative analysis of international technical

standards for the use of bamboo - culms in building structures]. 2018. Master Thesis - Universidade Nacional de Brasília, Brasília, 2018.

MATSUOKA, J. H. **Avaliação da eficiência do ácido pirolenhoso no tratamento preservativo de taliscas de bambu gigante contra a deterioração por fungos** [Evaluation of pyroligneous acid efficiency in preservative treatment of giant bamboo stalks against fungi decay]. 2011. Master Thesis – Universidade Estadual de Campinas, Campinas, 2011.

MATTONE, R. Sisal fibre reinforced soil with cement or cactus pulp in bahareque technique. **Cement and Concrete Composites**, v. 27, p. 611–616, 2005.

MENA, J.; VERA, S.; CORREAL, J. F.; LOPEZ, M. Assessment of fire reaction and fire resistance of Guadua angustifolia kunth bamboo. **Construction and Building Materials**, v. 27, n. 1, p. 60–65, 2012.

MENG, F.; YU, Y.; ZHANG, Y.; YU, W.; GAO, J. Surface chemical composition analysis of heat-treated bamboo. **Applied Surface Science**, v. 371, p. 383–390, 2016.

MITCH, D.; HARRIES, K. A.; SHARMA, B. Characterization of splitting behavior of bamboo culms. **Journal of Materials in Civil Engineering**, v. 22, n. 11, p. 1195–1199, 2010.

MOHAJERANI, A.; VAJNA, J.; ELLCOCK, R. Chromated copper arsenate timber : A review of products , leachate studies and recycling. **Journal of Cleaner Production**, v. 179, p. 292–307, 2018.

MOHAREB, A.; THÉVENON, M. F.; WOZNIAK, E.; GÉRARDIN, P. Effects of polyvinyl alcohol on leachability and efficacy of boron wood preservatives against fungal decay and termite attack. **Wood Science and Technology**, v. 45, n. 3, p. 407–417, 2011.

MONTEIRO, M. B. B. **Método alternativo de ensaio acelerado para avaliação da resistência natural de madeira ao ataque de fungos apodrecedores** [Alternative accelerated test method for assessing the natural resistance of wood to attack by rotting fungi]. 1997. Master Thesis - Universidade de São Paulo, São Paulo, 1997.

MORAIS, J. P. S.; ROSA, M. D. F.; MARCONCINI, J. M. Procedimentos para análise lignocelulósica. Campina Grande: **EMBRAPA Algodão**, 2010.

MOREIRA, L. E. **Desenvolvimento de estruturas treliçadas espaciais de bamboo** [Development of bamboo space trusses]. 1991. PhD Dissertation – PUC-Rio, Rio de Janeiro, 1991.

MORRELL, J. J. Protection of Wood-Based Materials. In: **Handbook of Environmental Degradation of Materials**. 3rd ed., Springer, 2018. p. 343–368

MORRIS, N. M.; CATALANO, E. A.; ANDREWS, B. A. K. FT-IR Determination of degree of esterification in polycarboxylic acid cross-link finishing of cotton. **Cellulose**, v. 2, p. 31–39, 1995.

NAM, S.; FRENCH, A. D.; CONDON, B. D.; CONCHA, M. Segal crystallinity index revisited by the simulation of X-ray diffraction patterns of cotton cellulose Iβ and cellulose II**. Carbohydrate Polymers**, v. 135, p. 1–9, 2016.

NGUYEN, C. T.; WAGENFÜHR, A.; PHUONG, L. X.; DAI, V. D.; BREMER, M.; FISCHER, S. The effects of thermal modification on the properties of two Vietnamese bamboo species, Part I: Effects on physical properties. **BioResources**, v. 7, n. 4, p. 5355–5366, 2012.

NISHIYAMA, Y.; SUGIYAMA, J.; CHANZY, H.; LANGAN, P. Crystal Structure and Hydrogen Bonding System in Cellulose Iα from Synchrotron X-ray and Neutron Fiber Diffraction. **Journal of the American Chemical Society**, v. 125, n. 47, p. 14300–14306, 2003.

NOGATA, F.; TAKAHASHI, H. Intelligent functionally graded material: Bamboo. **Composites Engineering**, v. 5, n. 7, p. 743–751, 1995.

OBANDA, D. N.; SHUPE, T. F.; BARNES, H. M. Reducing leaching of boron-based wood preservatives - A review of research. **Bioresource Technology**, v. 99, n. 15, p. 7312–7322, 2008.

ORTIZ, S. P. R. **Efecto de la impregnación con polimeros sobre las propriedades mecanicas de la Guadua** [Effect of impregnation with polymers on the mechanical properties of Guadua]. 2015. PhD Dissertation - Universidad Nacional de Colombia, Bogota, 2015.

OSORIO, L.; TRUJILLO, E.; LENS, F.; IVENS, J.; VERPOEST, I.; VAN VUURE, A. W. In-depth study of the microstructure of bamboo fibres and their relation to the mechanical properties. **Journal of Reinforced Plastics and Composites**, v. 37, n. 17, p. 1099–1113, 2018.

OUNJAIJOM, T.; MANEE-INTA, N.; PUNYACUM, W. Mechanical Properties of Five Species Dried Bamboo. **SWU Engineering Journal**, v. 12, n. 2, p. 8–14, 2017.

PANDEY, K. K.; PITMAN, A. J. FTIR studies of the changes in wood chemistry following decay by brown-rot and white-rot fungi. **International Biodeterioration and Biodegradation**, v. 52, n. 3, p. 151–160, 2003.

PAPADOPOULOS, a. N.; HILL, C. a S.; GKARAVELI, a.; NTALOS, G. a.; KARASTERGIOU, S. P. Bamboo chips (Bambusa vulgaris) as an alternative lignocellulosic raw material for particleboard manufacture. **Holz als Roh - und Werkstoff**, v. 62, n. 1, p. 36–39, 2004.

PARK, H. J.; WEN, M. Y.; CHEON, S. H.; KANG, C. W.; MATSUMURA, J. Fire retardant performance and thermal degradation of korean pine treated with fire retardant chemical. **Journal of the Faculty of Agriculture, Kyushu University**, v. 60, n. 1, p. 188–189, 2015.

PEÑA, C.; DE LA CABA, K.; RETEGI, A.; OCANDO, C.; LABIDI, J.; ECHEVERRIA, J. M.; MONDRAGON, I. Mimosa and chestnut tannin extracts reacted with hexamine in solution. **Journal of Thermal Analysis and Calorimetry**, v. 96, n. 2, p. 515–521, 2009.

PEREIRA, M. **Projeto bambu: introdução de espécies, manejo, caracterização e aplicações** [Bamboo project: species introduction, management, characterisation and applications]. Thesis – Universidade Estadual de São Paulo, Bauru, 2012.

PIZZI, A. Recent developments in eco-efficient bio-based adhesives for wood bonding: Opportunities and issues. **Journal of Adhesion Science and Technology**, v. 20, n. 8, p. 829–846, 2006.

PIZZI, A.; BAECKER, A. A new boron fixation mechanism for environment friendly wood preservatives. **Holzforschung**, v. 50, n. 6, p. 507–510, 1996.

PRININDYA, K. N. N.; ARDIANSYAH, L. The Effect of Chemical Substance and Immersion Time of Dendrocalamus asper as Chemical Preservation Treatment. **Int. Journal of Advances in Materials Science and Engineering**, v. 3, n. 1, p. 1–13, 2014.

RAMIREZ, D. O. S.; CARLETTO, R. A.; TONETTI, C.; GIACHET, F. T.; VARESANO, A.; VINEIS, C. Wool keratin film plasticized by citric acid for food packaging. **Food Packaging and Shelf Life**, v. 12, p. 100–106, 2017.

RAO, A. N.; RAO, V. R.; WILLIAMS, J. T.; DRANSFIELD, J.; WIDJAJA, E. Priority species of bamboo and rattan. **INBAR publication**, 1998.

RASBAND, W. S. ImageJ, U. S. National Institutes of Health. Available in: <https://imagej.nih.gov/ij>.

RATANOPHAT, C. **Sustainable management and utilization from bamboo. Final technical report.** Project: PD 56/59 Rev. 1(I) Promotion of the utilization of bamboo from sustainable sources in Thailand. Bangkok: Royal Forest Department and International Tropical Timber Organization, 2004.

RICHARD, M.; GOTTRON, J.; HARRIES, K. A.; GHAVAMI, K. Experimental Evaluation of Longitudinal Splitting of Bamboo Flexural Components. **ICE Structures and Buildings: Themed issue on bamboo in structures and buildings**, v. 170, n. 4, p. 265–274, 2017.

RICHARD, M. J.; HARRIES, K. A. **On Inherent Bending in Tension Tests of Bamboo. Wood Science and Technology**, v. 49, n. 1, p. 99–119, 2015.

ROMAINOR, A. N. B.; CHIN, S. F.; PANG, S. C.; BILUNG, L. M. Preparation and Characterization of Chitosan Nanoparticles-Doped Cellulose Films with Antimicrobial Property. **Journal of Nanomaterials**, v. 2014, p. 1–10, 2014.

ROWELL, R. Chemical modification of wood to produce stable and durable composites. **Cellulose Chemistry and Technology**, v. 46, n. 7–8, p. 443–448, 2012.

ROWELL, R. M. Chemical modification of wood. In: FAKIROV, S.; BHATTACHARYYA, D. **Handbook of Engineering Biopolymers: Homopolymers, Blends and Composites**. Munich: Hanser Publishers, 2007. p. 673–691.

SAIKIA, P.; DUTTA, D.; KALITA, D.; BORA, J. J.; GOSWAMI, T. Improvement of mechano-chemical properties of bamboo by bio-chemical treatment. **Construction and Building Materials**, v. 101, p. 1031–1036, 2015.

SALES-CAMPOS, C.; VIANEZ, B. F.; MENDONÇA, M. S. De. Estudo da variabilidade da retenção do preservante CCA tipo A na madeira de Brosimum rubescens Taub. Moraceae - (pau-rainha) uma espécie madeireira da região Amazônica [Study of the retention variability of CCA type A preservative in Brosimum rubescens Taub wood. Moraceae - (pau-rainha) a timber species from the Amazon region. **Revista Árvore**, v. 27, n. 6, p. 845–853, 2003.

SÁNCHEZ-RIVERA, M. M.; NÚÑEZ-SANTIAGO, M. del C.; BELLO-PÉREZ, L. A.; AGAMA-ACEVEDO, E.; ALVAREZ-RAMIREZ, J. Citric acid esterification of unripe plantain flour: Physicochemical properties and starch digestibility. **Starch/Staerke**, v. 69, n. 9–10, p. 1–7, 2017.

SANDBERG, D.; KUTNAR, A.; MANTANIS, G. Wood modification technologies - a review. **iForest - Biogeosciences and Forestry**, v. 10, n. 6, p. 895–908, 31 dez. 2017.

SARLO, H. B. **Influência das fases da lua, da época de corte e das espécies de bambus sobre o ataque de dinoderus minutus (fabr.) (coleoptera: bostrichidae)** [Influence of moon phases, cutting time and bamboo species on the attack of dinoderus minutus (fabr.) (Coleoptera: bostrichidae)]. 2000. Master Thesis - Universidade Federal de Viçosa, Viçosa, 2000.

SCHMIDT, O.; WEI, D. S.; LIESE, W.; WOLLENBERG, E. Fungal degradation of bamboo samples. **Holzforschung**, v. 65, n. 6, p. 883–888, 2011.

SCHORR, D.; BLANCHET, P.; ESSOUA ESSOUA, G. G. Glycerol and Citric Acid Treatment of Lodgepole Pine. **Journal of Wood Chemistry and Technology**, v. 38, n. 2, p. 123–136, 2018.

SCHULTZ, T. P., NICHOLAS, D. D., AND PRESTON, A. F. Perspective – A brief review of the past, present and future of wood preservation. **Pest Management Science**, v. 63(8), p. 784–788, 2007.

ŠEFC, B.; TRAJKOVIC, J.; HASAN, M.; KATOVIC, D.; VUKUSIC, S. B.; MARTINA, F. Dimensional stability of wood modified by citric acid using different catalysts. **Drvna industrija**, v. 60, n. 1, p. 23–26, 2009a.

ŠEFC, B.; HASAN, M.; TRAJKOVIĆ, J.; DESPOT, R.; JUG, M.; KATOVIĆ, D.; VUKUŠIĆ, S. B. Selected Properties of Beech Wood Modified by Citric Acid. **European Conference on Wood Modification**, p. 425–428, 2009b.

ŠEFC, B.; TRAJKOVIĆ, J.; SINKOVIĆ, T.; HASAN, M.; IŠTOK, I. Compression Strength of Fir and Beech Wood Modified by Citric Acid. **Drvna industrija**, v. 63, n. 1, p. 45–50, 2012.

SEN, S.; TASCIOGLU, C.; TIRAK, K. Fixation, leachability, and decay resistance of wood treated with some commercial extracts and wood preservative salts. **International Biodeterioration and Biodegradation**, v. 63, n. 2, p. 135–141, 2009.

SHAH, D. U.; SHARMA, B.; RAMAGE, M. H. Processing bamboo for structural composites: Influence of preservative treatments on surface and interface properties. **International Journal of Adhesion and Adhesives**, v. 85, n. May, p. 15–22, 2018.

SHARMA, B. **Performance Based Design of Bamboo Structures**. 2010. PhD Dissertation - University of Pittsburgh, Pittsburgh, 2010.

SHARMA, B.; GATÓO, A.; BOCK, M.; MULLIGAN, H.; RAMAGE, M. Engineered bamboo: state of the art. **Proceedings of the ICE - Construction Materials**, 2014.

SHARMA, B.; GATÓO, A.; BOCK, M.; RAMAGE, M. Engineered bamboo for structural applications. **Construction and Building Materials**, v. 81, p. 66–73, 2015a.

SHARMA, B.; HARRIES, K. a.; GHAVAMI, K. Methods of determining transverse mechanical properties of full-culm bamboo. **Construction and Building Materials**, v. 38, p. 627–637, 2013.

SHARMA, N. K.; VERMA, C. S.; CHARIAR, V. M.; PRASAD, R. Eco-friendly flame-retardant treatments for cellulosic green building materials. **Indoor and Built Environment**, v. 24, n. 3, p. 422–432, 2015b.

SHARMA, N. K.; CHARIAR, V. M.; PRASAD, R. Impact of fire on Dendrocalamus strictus - A natural green composite building material. **Indoor and Built Environment**, v. 24, n. 6, p. 740–745, 2015.

SHUKLA, S. R.; ZHANG, J.; KAMDEM, D. P. Pressure treatment of rubberwood (Heavea brasiliensis) with waterborne micronized copper azole: Effects on retention, copper leaching, decay resistance and mechanical properties. **Construction and Building Materials**, v. 216, p. 576–587, 2019.

SILVEIRA, A. G.; SANTINI, E. J.; KULCZYNSKI, S. M.; TREVISAN, R.; WASTOWSKI, A. D.; GATTO, D. A. Tannic extract potential as natural wood preservative of acacia mearnsii. **Anais da Academia Brasileira de Ciencias**, v. 89, n. 4, p. 3031–3038, 2017.

SINGHA, B. L.; BORAH, R. K. Traditional methods of post harvest bamboo treatment for durability enhancement. **International Journal of Scientific & Engineering Research**, v. 8, n. 1, p. 518–522, 2017.

SRIVARO, S.; JAKRANOD, W. Comparison of physical and mechanical properties of Dendrocalamus asper Backer specimens with and without nodes. **European Journal of Wood and Wood Products**, v. 74, n. 6, p. 893–899, 2016.

STUART, B. H. **Infrared Spectroscopy: Fundamentals and Applications**. West Sussex: John Wiley & Sons, Ltd, 2004.

SULAEMAN, A.; DUNGANI, R.; NURUDIN, N.; HARTATI, S.; KARLIATI, T.; ADITIAWATI, P.; HADIYANE, A.; SUHAYA, Y. Review on Quality Enhancement of Bamboo Utilization: Preservation, Modification and Applications. **Asian Journal of Plant Sciences**, v. 17, n. 1, p. 1–18, 2017.

SULAIMAN, O.; HASHIM, R.; WAHAB, R.; ISMAIL, Z. A.; SAMSI, H. W.; MOHAMED, A. Evaluation of shear strength of oil treated laminated bamboo. **Bioresource Technology**, v. 97, n. 18, p. 2466–2469, 2006.

SUMARDI, I.; ONO, K.; SUZUKI, S. Effect of board density and layer structure on the mechanical properties of bamboo oriented strandboard. **Journal of Wood Science**, v. 53, n. 6, p. 510–515, 2007.

SUPRAPTI, S. Decay Resistance of five Indonesian bamboo species against Fungi. **Journal of Tropical Forest Science**, v. 22, n. 223, p. 287–294, 2010.

TAN, T.; RAHBAR, N.; ALLAMEH, S. M.; KWOFIE, S.; DISSMORE, D.; GHAVAMI, K.; SOBOYEJO, W. O. Mechanical properties of functionally graded hierarchical bamboo structures. **Acta Biomaterialia**, v. 7, n. 10, p. 3796–3803, 2011.

TANG, T.; ZHANG, B.; LIU, X.; WANG, W.; CHEN, X.; FEI, B. Synergistic effects of tung oil and heat treatment on physicochemical properties of bamboo materials. **Scientific Reports**, v. 9, n. 1, p. 1–11, 2019a.

TANG, T.; CHEN, X.; ZHANG, B.; LIU, X.; FEI, B. Research on the Physico-Mechanical Properties of Moso Bamboo with Thermal Treatment in Tung Oil and Its Influencing Factors. **Materials**, v. 12, n. 4, p. 599, 2019b.

TANG, T. K. H. **Preservation and drying of commercial bamboo species of Vietnam**. 2013. PhD Dissertation - Hamburg University, Hamburg, 2013.

TANG, T. K. H.; SCHMIDT, O.; LIESE, W. Protection of bamboo against mould using environment-friendly chemicals. **Journal of Tropical Forest Science**, v. 24, n. 2, p. 285–290, 2012.

THÉVENON, M.-F.; TONDI, G.; PIZZI, A. Friendly Wood Preservative System Based on Polymerized Tannin Resin-Boric Acid for Outdoor Applications. **Maderas. Ciencia y tecnología**, v. 12, n. 3, p. 253–257, 2010.

THEVENON, M. F.; TONDI, G.; PIZZI, A. High performance tannin resin-boron wood preservatives for outdoor end-uses. **European Journal of Wood and Wood Products**, v. 67, n. 1, p. 89–93, 2009.

THEVENON MF, PIZZI A, H. J. One-step tannin fixation of non-toxic protein borates wood preservatives. **European Journal of Wood and Wood Products**, p. 56–90, 1998.

TIBURTINO, R. F.; PAES, J. B.; VIDAURRE, G. B.; BERALDO, A. L.; ARANTES, M. D. C. Resistência de duas espécies de bambu tratadas contra fungos xilófagos [Resistance of Two Bamboo Species Treated Against Xylophagous Fungi]. **Revista Árvore**, v. 39, n. 3, p. 567–574, 2015a.

TIBURTINO, R. F.; PAES, J. B.; BERALDO, A. L.; ARANTES, M. D. C.; BROCCO, V. F. Tratamento preservativo de duas espécies de bambu por imersão prolongada e boucherie modificado [Preservative treatment of two species of bamboo by long-term immersion and modified boucherie]. **Floresta e Ambiente**, v. 22, n. 1, p. 124–133, 2015b.

TIBURTINO, R. F.; PAES, J. B.; VIDAURRE, G. B.; ARANTES, M. D. C.; ROSA, R. A. Influência do diafragma no tratamento preservativo de duas espécies de bambu por substituição de seiva [Influence of diaphragm in the preservative treatment of two bamboo species by sap replacement method]. **Ciencia Florestal**, v. 26, n. 3, p. 925–938, 2016.

TOMAK, E. D.; ARICAN, F.; GONULTAS, O.; SAM PARMAK, E. D. Influence of tannin containing coatings on weathering resistance of wood: Water based transparent and opaque coatings. **Polymer Degradation and Stability**, v. 151, p. 152–159, 2018.

TONDI, G.; WIELAND, S.; LEMENAGER, N.; PETUTSCHNIGG, A.; PIZZI, A.; THEVENON, M. F. Efficacy of tannin in fixing boron in wood: Fungal and termite resistance**.** **BioResources**, v. 7, n. 1, p. 1238–1252, 2012a.

TONDI, G.; WIELAND, S.; WIMMER, T.; THEVENON, M. F.; PIZZI, A.; PETUTSCHNIGG, A. Tannin-boron preservatives for wood buildings: Mechanical and fire properties. **European Journal of Wood and Wood Products**, v. 70, n. 5, p. 689–696, 2012b.

TONDI, G.; PALANTI, S.; WIELAND, S.; THEVENON, M. F.; PETUTSCHNIGG, A.; SCHNABEL, T. Durability of tannin-boron-treated timber. **BioResources**, v. 7, n. 4, p. 5138–5151, 2012c.

TONDI, G.; THEVENON, M. F.; MIES, B.; STANDFEST, G.; PETUTSCHNIGG, A.; WIELAND, S. Impregnation of Scots pine and beech with tannin solutions: Effect of viscosity

and wood anatomy in wood infiltration. **Wood Science and Technology**, v. 47, n. 3, p. 615–626, 2013.

TONDI, G.; HU, J.; THEVENON, M. F. Advanced tannin-based wood preservatives. **Forest Products Journal**, v. 65, n. 3–4, p. S26–S32, 2015.

TRUJILLO, D.; JANGRA, S.; GIBSON, J. Flexural properties as a basis for bamboo strength grading. **ICE Structures and Buildings: Themed issue on bamboo in structures and buildings**, v. 170, n. 4, p. 284–294, 2017.

UNER, I. H.; DEVECI, I.; BAYSAL, E.; TURKOGLU, T.; TOKER, H.; PEKER, H. Thermal analysis of Oriental beech wood treated with some borates as fire retardants. **Maderas. Ciencia y tecnología**, v. 18, n. 2, p. 293-304, 2016.

VAN DER LUGT, P.; VOGTLÄNDER, J. G.; VEGTE, J. H. Van Der; BREZET, J. C. Environmental Assessment of Industrial Bamboo Products - Life Cycle Assessment and Carbon Sequestration. In: **10th World Bamboo Congress**, Korea, 2015.

VIDAL, J. M.; EVANGELISTA, W. V.; SILVA, J. C.; JANKOWSKY, I. P. Preservação de madeiras no Brasil: Histórico, cenário atual e tendências [Wood Preservation in Brazil: History, Current Scenario and Trends]. **Ciência Florestal**, v. 25, n. 1, p. 257–271, 2015.

VIRGO, J.; MORAN, R.; HARRIES, K. A.; GARCIA, J. J.; PLATT, S. Flat Ring Flexure Test for Full-Culm Bamboo. **Materials Research Proceedings**, v. 7, p. 349–358, 2018.

VOGTLÄNDER, J. G.; VAN DER VELDEN, N. M.; VAN DER LUGT, P. Carbon sequestration in LCA, a proposal for a new approach based on the global carbon cycle; cases on wood and on bamboo. The **International Journal of Life Cycle Assessment**, v. 19, n. 1, p. 13–23, 2014.

VOGTLÄNDER, J.; VAN DER LUGT, P.; BREZET, H. The sustainability of bamboo products for local and Western European applications. LCAs and land-use. **Journal of Cleaner Production**, v. 18, n. 13, p. 1260–1269, 2010.

VUKUSIC, S. B.; KATOVIC, D.; GRGAC, S. F.; TRAJKOVIC, J.; SEFC, B.; VONCINA, B. Study of the wood modification process with polycarboxylic acids and microwave treatment. **Wood Research**, v. 55, n. 3, p. 121–129, 2010.

WAHAB, R.; MOHAMAD, A.; SAMSI, H. W.; SULAIMAN, O. Effect of heat treatment using palm oil on properties and durability of Semantan bamboo. **Journal of Bamboo and Rattan**, v. 4, n. 3, p. 211–220, 2005.

WAHAB, R.; SALAM, M. A.; MOHAMED, A.; SAMSI, H. W.; RAHMAN, S.; MAT RASAT, M. S.; KHALID, I. Evauation on strength of chemically treated 2 and 4 year-old bamboo Bambusa vulgaris through pressurized treatment. R**esearch Journal of Pharmaceutical, Biological and Chemical Sciences**, v. 6, n. 1, p. 1282–1288, 2015.

WANG, F.; LIU, J.; LV, W. Thermal degradation and fire performance of wood treated with PMUF resin and boron compounds. **Fire and Materials**, v. 41, n. 8, p. 1051–1057, 2017.

WANG, Y.; ZHANG, Z.; FAN, H.; WANG, J. Wood carbonization as a protective treatment on resistance to wood destroying fungi. International Biodeterioration and Biodegradation, v. 129, n. June 2017, p. 42–49, 2018.

WATANABE, H.; YANASE, Y.; FUJII, Y. Evaluation of larval growth process and bamboo consumption of the bamboo powder-post beetle Dinoderus minutus using X-ray computed tomography. **Journal of Wood Science**, v. 61, n. 2, p. 171–177, 2015.

WEGST, U. G. K.; ASHBY, M. F. The mechanical efficiency of natural materials. **Philosophical Magazine**, v. 84, n. 21, p. 2167–2181, 2004.

WEI, D.; SCHMIDT, O.; LIESE, W. Durability test of bamboo against fungi according to EN standards. **European Journal of Wood and Wood Products**, v. 71, n. 5, p. 551–556, 2013b.

WIDSTEN, P.; DOOLEY, N.; PARR, R.; CAPRICHO, J.; SUCKLING, I. Citric acid crosslinking of paper products for improved high-humidity performance. **Carbohydrate Polymers**, v. 101, n. 1, p. 998–1004, 2014.

WIDYORINI, R.; PUSPA YUDHA, A.; ISNAN, R.; AWALUDDIN, A.; AGUS PRAYITNO, T.; NGADIANTO, A.; UMEMURA, K. Improving the Physico-Mechanical Properties of Eco-Friendly Composite Made from Bamboo. **Advanced Materials Research**, v. 896, p. 562–565, 2014.

WU, X.; BA, Y.; WANG, X.; NIU, M.; FANG, K. Evolved gas analysis and slow pyrolysis mechanism of bamboo by thermogravimetric analysis, Fourier transform infrared spectroscopy and gas chromatography-mass spectrometry. **Bioresource Technology**, v. 266, p. 407–412, 2018.

XIE, Y.; KRAUSE, A.; MILITZ, H.; TURKULIN, H.; RICHTER, K.; MAI, C. Effect of treatments with 1,3-dimethylol-4,5-dihydroxy- ethyleneurea (DMDHEU) on the tensile properties of wood. **Holzforschung**, v. 61, p. 43–50, 2007.

XU, G., WANG, L., LIU, J., AND HU, S. Decay resistance and thermal stability of bamboo preservatives prepared using camphor leaf extract. **International Biodeterioration & Biodegradation**, v. 78, p. 103–107, 2013.

XU, G.; WANG, L.; LIU, J.; WU, J. FTIR and XPS analysis of the changes in bamboo chemical structure decayed by white-rot and brown-rot fungi. **Applied Surface Science**, v. 280, p. 799–805, 2013.

XU, M.; CUI, Z.; CHEN, Z.; XIANG, J. The charring rate and charring depth of bamboo scrimber exposed to a standard fire. **Fire and Materials**, v. 42, n. 7, p. 750–759, 2018.

XU, Q.; HARRIES, K.; LI, X.; LIU, Q.; GOTTRON, J. Mechanical properties of structural bamboo following immersion in water. **Engineering Structures**, v. 81, p. 230–239, 2014.

YAMAGUCHI, H., YOSHINO, K., AND KIDO, A. Termite resistance and wood-penetrability of chemically modified tannin and tannin-copper complexes as wood preservatives. **Journal of Wood Science**, v. 48, n. 4, p. 331–337, 2002.

YAN, J.; ZHAO, T.; LIN, T.; LI, Y. Investigating multi-regional cross-industrial linkage based on sustainability assessment and sensitivity analysis: A case of construction industry in China. **Journal of Cleaner Production**, v. 142, p. 2911–2924, 2017.

YANG, T.; CAO, J.; MA, E. How does delignification influence the furfurylation of wood? **Industrial Crops and Products**, v. 135, p. 91–98, 2019.

YE, F.; FU, W. Physical and Mechanical Characterization of Fresh Bamboo for Infrastructure Projects. **Journal of Materials in Civil Engineering**, v. 30, n. 2, 2018.

YE, J.; LUO, S.; HUANG, A.; CHEN, J.; LIU, C.; MCCLEMENTS, D. J. Synthesis and characterization of citric acid esterified rice starch by reactive extrusion: A new method of producing resistant starch. **Food Hydrocolloids**, v. 92, p. 135–142, 2019.

YU, D.; TAN, H.; RUAN, Y. A future bamboo-structure residential building prototype in China: Life cycle assessment of energy use and carbon emission. **Energy and Buildings**, v. 43, n. 10, p. 2638–2646, 2011.

YU, H. Q.; JIANG, Z. H.; HSE, C. Y.; SHUPE, T. F. Selected physical and mechanical properties of moso bamboo (phyllostachys pubescens). **Journal of Tropical Forest Science**, v. 20, n. 4, p. 258–263, 2008.

YU, L.; CAI, J.; LI, H.; LU, F.; QIN, D.; FEI, B. Effects of boric acid and/or borax treatments on the fire resistance of bamboo filament. **BioResources**, v. 12, n. 3, p. 5296–5307, 2017.

YU, Y.; ZHU, R.; WU, B.; HU, Y.; YU, W. Fabrication, material properties, and application of bamboo scrimber. **Wood Science and Technology**, v. 49, n. 1, p. 83–98, 2015.

YUBOCHAI; LIU, J.; WANG, Z.; ZHAO, Y. Dimensional Stability and Mechanical Properties of Plantation Poplar Wood Esterified Using Acetic. **BioResources**, v. 12, n. 1, p. 912–922, 2017.

YUEN, J. Q.; FUNG, T.; ZIEGLER, A. D. Carbon stocks in bamboo ecosystems worldwide: Estimates and uncertainties. **Forest Ecology and Management**, v. 393, p. 113–138, 2017.

ZHANG, W.; YAO, X.; KHANAL, S.; XU, S. A novel surface treatment for bamboo flour and its effect on the dimensional stability and mechanical properties of high density polyethylene/bamboo flour composites. **Construction and Building Materials**, v. 186, p. 1220–1227, 2018.

ZHANG, Z. F.; HUANG, K.; GAO, J. S.; ZHANG, X. Research progress on the modification of bamboo. **Journal of Chemical and Pharmaceutical Research**, v. 6, n. 1, p. 237–239, 2014.

ZHOU, Z.; YAO, X.; DU, C.; YU, H.; HUANG, Q.; LIU, H. Effect of Hygroscopicity of fire retardant on hygroscopicity of fire retardant bamboo chips. **Wood Research**, v. 63, n. 3, p. 373–382, 2018.

ZHUANG, X.; WANG, J.; YANG, W.; PAN, X.; XU, M.; YU, H. Surface chemical changes analysis of UV-light irradiated Moso bamboo (Phyllostachys pubescens Mazel). **Royal Society Open Science**, v. 5, n. 6, p. 180110, 2018.

APPENDIX A – INDIVIDUAL TEST VALUES OF CHAPTER 3

This Appendix section gives the individual values of the mechanical tests data presented in chapter 3 with additional information regarding each tested sample. This section was divided into three main parts, referred to as each paper presented within this chapter. Additional details about testing procedures are also presented whenever necessary (if not provided in the related paper or in the complementary information section).

A1 - Section 3.1 (Effect of disodium octaborate tetrahydrate on the mechanical properties of Dendrocalamus asper bamboo treated by vacuum/pressure method)

A 1.1 - Excitation pulse non-destructive test

The dynamic elastic modulus (dMOE) was determined in an excitation pulse testing machine Sonelastic®, as per recommendations of the ASTM E1876-15 Standard, in the longitudinal and flexural modes. This technique is based on the sound wave speed obtained through a simple setup (Figure A1), where an actuator hits the sample, and a microphone is used to record the generated sound. The recorded frequency spectrum is then used to determine the fundamental flexural or longitudinal resonant frequency (directly related to density). The dynamic elastic modulus of a prismatic sample with rectangular or square cross-section can be calculated according to Equations A1 and A2, for flexural and longitudinal modes, respectively. The results are given directly in the equipment's software. The individual test results are presented in Table A1.

$$E = 0.9465 \left(\frac{m f_f^2}{2}\right)\left(\frac{L^3}{t^3}\right) T_1 \qquad \text{Eq A1}$$

$$E = 4 m f_l^2 \left(\frac{L}{btK}\right) \qquad \text{Eq A2}$$

Where:

E = Dynamic elastic modulus, Pa; m = mass of the sample, mm; b = width of the sample, mm; L = length of the sample, mm; t = thickness of the sample; f_f = fundamental resonant frequency of the sample in flexure, Hz; T_1 = correction factor for fundamental flexural mode to account for finite thickness of sample and Poisson's ratio; f_l = fundamental longitudinal frequency of the sample, Hz; K = correction factor for the fundamental longitudinal mode to account for the finite diameter-to-length ratio and Poisson's ratio.

Figure A1 – Setup used for excitation pulse measurements, a) flexural and b) longitudinal modes.

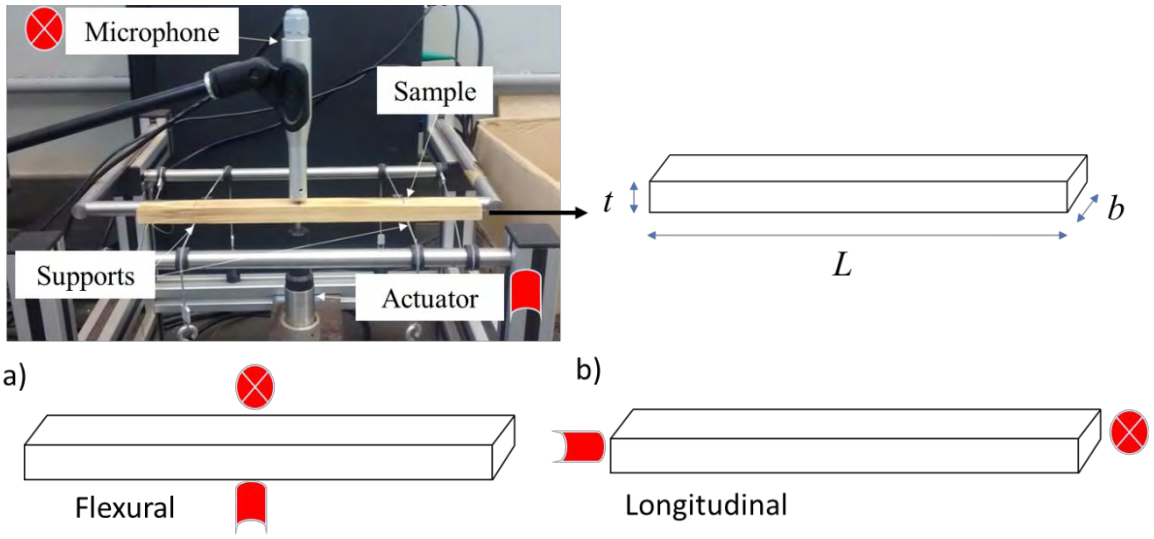

Table A1 – Individual values of excitation pulse non-destructive tests. Related to Table 3.4.

Sample ID	Treatment condition	Apparent density (g/cm^3)	Moisture content (%)	Flexural MOE (GPa)	Longitudinal MOE (GPa)	Specific Flexural MOE	Specific Longitudinal MOE
IntA1	Reference	0.692	11.61	21.70	23.07	31.36	33.34
IntA2		0.684	13.14	20.71	22.26	30.28	32.55
IntA3		0.643	12.25	20.33	20.48	31.64	31.87
IntB1		0.807	8.36	26.02	28.95	32.24	35.87
IntB2		0.791	10.21	26.16	28.58	33.08	36.14
IntB3		0.754	9.83	24.17	27.84	32.05	36.92
IntB4		0.783	12.47	22.38	26.64	28.60	34.04
IntB5		0.794	9.49	25.46	28.6	32.06	36.01
IntB6		0.775	9.16	23.25	27.35	30.00	35.29
Avg.		**0.747**	**10.72**	**23.35**	**25.97**	**31.26**	**34.67**
COV		**0.08**	**0.16**	**0.10**	**0.12**	**0.04**	**0.05**
IntA4	Water	0.689	10.50	24.14	24.34	35.06	35.35
IntA5		0.642	10.40	19.38	20.61	30.18	32.09
IntA6		0.639	11.73	20.81	21.91	32.57	34.29
IntB7		0.700	9.67	22.62	25.05	32.31	35.78
IntB8		0.766	8.28	31.67	28.14	41.33	36.73
IntB9		0.758	8.77	24.58	26.39	32.44	34.83
IntB10		0.769	7.85	23.67	26.6	30.77	34.58
IntB11		0.749	7.79	19.16	25.63	25.57	34.20
Avg.		**0.714**	**9.37**	**23.25**	**24.83**	**32.53**	**34.73**
COV		**0.08**	**0.15**	**0.17**	**0.10**	**0.14**	**0.04**
IntA7	5% DOT	0.649	11.65	18.10	20.21	27.90	31.15
IntA8		0.671	11.35	19.24	21.46	28.67	31.98
IntA9		0.599	12.63	20.31	19.95	33.93	33.33
IntB12		0.735	8.64	24.88	27.77	33.83	37.76
IntB13		0.738	8.61	27.20	29.63	36.85	40.14
IntB14		0.728	9.79	26.38	27.54	36.23	37.82
IntB15		0.755	8.95	27.26	28.64	36.13	37.95
IntB16		0.739	8.45	23.24	26.51	31.44	35.86
Avg.		**0.702**	**10.01**	**23.33**	**25.21**	**33.12**	**35.75**
COV		**0.08**	**0.16**	**0.16**	**0.16**	**0.10**	**0.09**
IntA10	8% DOT	0.729	10.69	25.88	26.08	35.48	35.76
IntA11		0.634	13.54	20.03	19.91	31.59	31.41
IntA12		0.684	11.58	21.18	24.01	30.97	35.11
IntB17		0.740	9.22	24.54	27.57	33.17	37.27
IntB18		0.735	9.56	24.19	27.02	32.91	36.76
IntB19		0.743	8.83	24.53	27.57	33.00	37.09
IntB20		0.751	9.44	24.27	26.93	32.32	35.86
IntB21		0.761	9.23	24.66	26.81	32.40	35.23
IntB22		0.751	9.99	26.34	28.06	35.06	37.35
Avg.		**0.725**	**10.23**	**23.96**	**26.00**	**32.99**	**35.76**
COV		**0.06**	**0.15**	**0.09**	**0.10**	**0.04**	**0.05**

A 1.2 - Three-point bending test

The static three-point bending tests were performed on the same samples used for the excitation pulse non-destructive test. The results of each tested specimen are given in Table A2.

Table A2 – Individual values of three-point bending tests. Related to Table 3.5.

Sample ID	Treatment condition	Apparent density (g/cm^3)	Moisture content (%)	MOE (GPa)	MOR (MPa)	Specific MOE*	Specific MOR*
IntA1	Reference	0.692	12.04	16.30	132.5	23.55	191.4
IntA2		0.684	12.94	16.23	132.1	23.72	193.1
IntA3		0.643	12.59	15.96	112.9	24.83	175.7
IntB1		0.807	8.80	16.09	194.5	19.93	241.0
IntB3		0.754	10.35	18.02	179.9	23.89	238.5
IntB4		0.783	11.22	15.65	148.8	20.00	190.2
IntB5		0.794	9.95	15.30	179.8	19.27	226.4
IntB6		0.775	9.74	15.91	169.4	20.53	218.6
Avg.		**0.741**	**10.95**	**16.18**	**156.2**	**21.97**	**209.4**
COV		**0.08**	**0.14**	**0.05**	**0.18**	**0.10**	**0.12**
IntA4	Water	0.689	11.03	17.00	147.6	24.69	214.3
IntA5		0.642	11.23	15.49	125.4	24.12	195.3
IntA6		0.639	11.79	17.91	123.4	28.03	193.2
IntB7		0.700	10.23	14.13	134.2	20.19	191.6
IntB8		0.766	9.04	16.88	172.8	22.02	225.5
IntB9		0.758	9.40	16.33	166.2	21.56	219.4
IntB10		0.769	8.58	13.37	164.5	17.38	213.9
IntB11		0.749	8.69	14.96	169.4	19.96	226.0
Avg.		**0.714**	**10.00**	**15.76**	**150.4**	**22.24**	**209.9**
COV		**0.08**	**0.12**	**0.10**	**0.14**	**0.15**	**0.07**
IntA7	5% DOT	0.649	12.23	14.70	127.3	22.66	196.2
IntA8		0.671	11.62	16.24	148.4	24.20	221.1
IntA9		0.599	12.84	16.13	128.8	26.94	215.1
IntB12		0.735	9.48	17.09	183.5	23.24	249.5
IntB13		0.738	9.41	18.21	189.5	24.67	256.7
IntB14		0.728	10.38	18.22	176.0	25.02	241.7
IntB15		0.755	9.54	17.53	176.9	23.23	234.5
IntB16		0.739	8.91	14.54	156.2	19.67	211.3
Avg.		**0.702**	**10.55**	**16.58**	**160.8**	**23.70**	**228.3**
COV		**0.08**	**0.14**	**0.09**	**0.15**	**0.09**	**0.09**
IntA10	8% DOT	0.729	11.36	17.47	188.8	23.95	258.9
IntA11		0.634	13.64	15.11	121.1	23.83	190.9
IntA12		0.684	12.00	16.83	179.4	24.62	262.4
IntB17		0.740	9.88	14.80	179.1	20.01	242.1
IntB19		0.743	9.50	15.11	164.8	20.33	221.8
IntB20		0.751	10.06	14.84	161.3	19.76	214.7
IntB21		0.761	9.63	16.50	179.9	21.68	236.3
IntB22		0.751	10.68	16.59	163.4	22.08	217.5
Avg.		**0.724**	**10.84**	**15.91**	**167.2**	**22.03**	**230.6**
COV		**0.06**	**0.13**	**0.07**	**0.13**	**0.09**	**0.10**

* - Specific values were determined by dividing the MOR or MOE by the apparent density.

A 1.3 - Compression parallel to the fibres test

Table A3 gives the individual values of the compression parallel to the fibres tests.

Table A3 – Individual values of axial compression tests. Related to Table 3.6.

Sample ID	Treatment condition	Apparent density (g/cm^3)	Moisture content (%)	f_c (MPa)	E_c (GPa)	Specific f_c^*	Specific E_c^*
IntA1	Reference	0.684	-	50.3	-	73.6	-
IntA2		0.690	10.39	55.5	18.03	80.4	26.14
IntA3		0.653	10.23	47.8	-	73.2	-
IntA4		0.613	10.04	47.6	19.20	77.7	31.31
IntB1		0.799	9.30	68.6	-	85.9	-
IntB2		0.799	8.15	66.8	36.17	83.6	45.26
IntB3		0.746	9.93	66.6	-	89.4	-
IntB4		0.745	-	69.2	30.09	92.9	40.37
IntB5		0.760	10.42	63.0	-	82.8	-
IntB6		0.766	-	61.8	27.91	80.7	36.44
IntB7		0.778	9.74	61.3	33.82	78.8	43.47
Avg.		**0.735**	**9.77**	**60.8**	**27.54**	**82.5**	**37.16**
COV		**0.09**	**0.08**	**0.13**	**0.27**	**0.07**	**0.20**
IntA5	Water	0.679	10.17	60.2	-	88.5	-
IntA6		0.677	9.37	63.5	16.07	93.8	23.72
IntA7		0.656	9.78	61.7	-	94.0	-
IntA8		0.626	9.27	61.4	20.56	98.0	32.84
IntA9		0.645	10.38	53.8	-	83.4	-
IntA10		0.643	9.96	58.2	17.50	90.5	27.20
IntB8		0.813	9.18	84.2	-	103.6	-
IntB9		0.748	8.55	72.8	22.70	97.4	30.35
IntB10		0.707	9.06	72.7	-	102.9	-
IntB11		0.660	8.77	73.3	22.24	111.0	33.69
IntB12		0.796	8.32	69.9	-	87.7	-
IntB13		0.741	7.67	73.2	28.39	98.8	38.31
IntB14		0.742	8.38	-	28.63	-	38.61
Avg.		**0.703**	**9.14**	**67.1**	**22.30**	**95.8**	**32.10**
COV		**0.09**	**0.09**	**0.13**	**0.22**	**0.08**	**0.17**
IntA11	5% DOT	0.676	10.37	71.9	-	106.4	-
IntA12		0.495	9.85	62.5	13.50	126.2	27.26
IntA13		0.659	10.86	71.2	-	108.1	-
IntA14		0.654	9.68	71.3	18.47	109.0	28.22
IntA15		0.616	9.96	66.6	-	108.1	-
IntA16		0.616	9.97	64.4	19.24	104.6	31.24
IntB15		0.741	9.44	81.6	-	110.2	-
IntB16		0.728	9.04	83.2	30.98	114.3	42.54
IntB17		0.752	10.00	80.3	-	106.7	-
IntB18		0.742	8.68	83.0	33.05	111.8	44.54
IntB19		0.744	9.36	76.5	-	102.8	-
IntB20		0.731	8.62	86.6	28.29	118.4	38.70
IntB21		0.771	9.36	86.5	-	112.2	-
IntB22		0.731	8.64	-	26.26	-	35.95
Avg.		**0.690**	**9.56**	**75.8**	**24.26**	**110.7**	**35.49**
COV		**0.11**	**0.07**	**0.11**	**0.30**	**0.06**	**0.19**

Table A3 – Continued.

Sample ID	Treatment condition	Apparent density (g/cm^3)	Moisture content (%)	f_c (MPa)	E_c (GPa)	Specific f_c^*	Specific E_c^*
IntA17	8% DOT	0.700	10.00	77.6	-	110.9	-
IntA18		0.695	8.82	82.3	23.19	118.3	33.35
IntA19		0.631	9.97	64.0	-	101.4	-
IntA20		0.632	9.65	62.1	18.12	98.4	28.68
IntA21		0.707	9.60	76.9	-	108.8	-
IntA22		0.691	9.07	77.2	19.74	111.7	28.57
IntB23		0.749	-	78.0	-	104.2	-
IntB24		0.735	8.79	72.7	31.76	98.8	43.20
IntB25		0.749	9.55	77.0	-	102.7	-
IntB26		0.705	8.74	78.6	27.05	111.5	38.35
IntB27		0.761	-	83.7	-	109.9	-
IntB28		0.741	7.78	78.1	27.12	105.3	36.60
IntB29		0.740	7.79	-	36.37	-	49.14
Avg.		**0.711**	**9.07**	**75.7**	**26.19**	**106.8**	**36.84**
COV		**0.06**	**0.09**	**0.09**	**0.25**	**0.06**	**0.20**

* - Specific values were determined by dividing the MOR or MOE by the apparent density.

A 2 - Section 3.2 (Quality assessment and mechanical characterization of preservative-treated Moso bamboo (*P. edulis*))

A 2.1 - Compression parallel to fibres test

The full-culm compression test values of each specimen are presented in Table A4. The dimensions of the samples are also provided.

Table A4 – Compression parallel to fibre test individual values. Related to Table 3.8.

Sample ID	Treatment condition	Node?	Avg. diameter (mm)	Avg. wall thickness (mm)	Avg. sample height (mm)	Apparent density (g/cm^3)	Moisture content (%)	f_c (MPa)	E_c (GPa)	LOP (MPa)
AD-1	A-DOT	No	80.07	8.31	83.13	0.813	10.06	57.9	17.13	47.0
AD-2		No	74.96	6.61	76.16	0.832	9.65	63.2	21.64	56.7
AD-3		No	74.52	6.65	74.04	0.827	9.89	66.1	22.47	62.1
AD-4		No	81.50	6.81	80.93	0.853	9.53	69.2	20.61	60.6
AD-5		No	83.17	7.97	81.54	0.808	9.79	62.0	20.88	55.6
AD-6		No	82.74	8.17	82.78	0.801	10.39	62.0	19.66	52.7
AD-7		No	85.69	8.75	83.10	0.726	10.11	52.6	20.68	40.0
AD-8		No	85.29	8.46	83.24	0.750	9.83	47.3	19.91	42.6
AD-9		No	75.11	8.42	74.01	0.821	10.42	57.9	17.62	46.1
AD-10		No	80.72	7.17	81.89	0.805	9.22	59.9	16.44	53.7
AD-11		No	76.13	7.70	68.53	0.889	-	64.2	18.00	53.6
AD-12		No	75.72	7.59	78.65	0.840	-	64.8	16.88	49.4
AD-13		No	76.96	7.34	77.42	0.817	9.96	56.4	18.36	52.9
AD-14		No	77.92	7.43	76.25	0.848	-	61.9	17.72	50.6
AD-15		No	82.06	8.16	81.21	0.703	9.30	51.3	16.57	45.4
AD-16		No	83.16	8.29	82.94	0.670	9.63	51.6	16.29	44.3
AD-17		Yes	80.51	8.32	81.73	-	10.26	60.4	21.67	43.3
AD-18		Yes	74.62	6.72	72.84	-	9.86	69.0	20.45	58.0
AD-19		Yes	81.28	7.03	83.12	-	9.85	64.9	20.44	59.2
AD-20		Yes	75.04	8.30	76.83	-	10.89	59.0	-	-
AD-21		Yes	81.72	7.40	80.74	-	10.03	59.8	19.31	49.1
AD-22		Yes	77.12	7.32	75.95	-	10.23	60.7	21.13	52.5
AD-23		Yes	79.01	7.60	75.93	-	9.84	62.1	19.73	51.0
AD-24		Yes	82.71	8.17	81.29	-	9.86	50.9	14.97	44.7
Avg.		**-**	**79.49**	**7.69**	**78.93**	**0.800**	**9.93**	**59.8**	**19.07**	**50.9**
COV		**-**	**0.04**	**0.08**	**0.05**	**0.07**	**0.04**	**0.10**	**0.11**	**0.12**
BD-1	B-DOT	No	79.98	7.84	78.88	0.790	10.66	58.5	19.60	48.1
BD-2		No	78.50	7.59	79.62	0.830	10.44	48.5	18.24	45.9
BD-3		No	78.05	7.38	78.41	0.838	10.44	56.6	21.54	52.2
BD-4		No	78.47	7.48	77.98	0.818	10.32	54.9	21.29	49.3
BD-5		No	75.52	6.49	71.02	0.811	10.15	53.3	20.61	42.3
BD-6		No	75.19	6.47	74.94	0.811	10.09	58.1	24.21	54.0
BD-7		No	74.61	6.39	75.39	0.798	10.11	53.4	20.98	49.7
BD-8		No	74.53	6.39	79.47	0.794	10.17	56.8	21.79	51.7
BD-9		No	74.21	6.33	76.69	0.797	10.25	54.0	21.18	52.6
BD-10		No	74.08	6.53	74.54	0.779	10.20	54.3	17.98	48.8
BD-11		No	79.87	7.15	77.51	0.795	9.87	51.9	20.25	50.0
BD-12		No	80.35	6.94	78.17	0.809	9.95	48.6	21.70	47.5
BD-13		No	80.65	6.97	78.08	0.811	9.96	56.3	21.79	47.5
BD-14		Yes	80.42	7.20	79.72	-	10.23	61.0	22.54	50.5
BD-15		Yes	75.02	6.57	76.70	-	10.44	57.2	24.55	46.0
Avg.		**-**	**77.30**	**6.91**	**77.14**	**0.806**	**10.22**	**54.9**	**21.22**	**49.1**
COV		**-**	**0.03**	**0.07**	**0.03**	**0.02**	**0.02**	**0.06**	**0.09**	**0.06**

Table A4 – Continued.

Sample ID	Treatment condition	Node?	Avg. diameter (mm)	Avg. wall thickness (mm)	Avg. sample height (mm)	Apparent density (g/cm^3)	Moisture content (%)	f_c (MPa)	E_c (GPa)	LOP (MPa)
BC-1	B-CCB	No	78.06	6.47	77.21	0.830	10.24	55.9	23.68	49.7
BC-2		No	76.40	6.48	76.63	0.827	10.48	59.8	20.26	54.0
BC-3		No	76.60	6.81	78.28	0.854	10.60	62.4	22.63	54.1
BC-4		No	77.06	6.94	76.61	0.839	10.64	62.2	21.13	58.9
BC-5		No	76.99	7.12	76.26	0.837	10.60	62.2	20.80	54.8
BC-6		No	77.51	7.01	75.03	0.808	10.40	50.8	20.10	44.0
BC-7		No	77.75	6.76	75.46	0.817	10.39	58.1	22.22	49.7
BC-8		No	78.16	6.63	76.99	0.825	10.30	53.2	21.12	46.9
BC-9		No	77.56	7.18	75.30	0.788	10.31	60.4	22.63	55.4
BC-10		No	77.27	6.79	78.96	0.809	10.30	60.6	20.42	56.0
BC-11		No	77.39	6.37	79.36	0.879	10.08	62.2	24.04	58.0
BC-12		No	77.41	6.66	76.41	0.847	10.10	54.8	21.11	53.7
BC-13		Yes	76.30	6.98	78.02	-	10.65	56.0	23.47	47.5
BC-14		Yes	77.07	7.02	76.87	-	10.82	61.6	22.60	56.0
BC-15		Yes	78.24	7.12	79.40	-	10.45	49.3	16.36	45.8
BC-16		Yes	77.61	6.95	76.95	-	10.41	60.4	21.15	49.0
Avg.		-	**77.33**	**6.83**	**77.11**	**0.830**	**10.42**	**58.1**	**21.48**	**52.1**
COV		-	**0.01**	**0.04**	**0.02**	**0.03**	**0.02**	**0.07**	**0.09**	**0.09**

A 2.2 - Shear parallel to fibres test

The full-culm shear parallel to fibre test results of each specimen are presented in Table A5. The dimensions of the samples are also provided.

Table A5 – Shear parallel to fibres test individual values. Related to Table 3.8.

Sample ID	Treatment condition	Node?	Avg. diameter (mm)	Avg. wall thickness (mm)	Avg. sample height (mm)	Apparent density (g/cm^3)	Moisture content (%)	f_v (MPa)	G (GPa)	LOP (MPa)
AD-1	A-DOT	No	79.87	8.12	79.88	0.828	10.76	16.6	2.70	12.7
AD-2		No	75.74	6.94	76.66	0.808	10.56	18.5	2.45	11.1
AD-3		No	74.81	6.87	75.87	0.817	10.41	18.1	2.46	13.3
AD-4		No	80.28	6.95	79.93	0.845	10.59	18.1	2.87	12.3
AD-5		No	80.33	6.72	78.21	0.858	10.55	19.3	3.01	13.3
AD-6		No	82.72	8.26	80.60	0.802	10.79	16.1	2.49	12.1
AD-7		No	85.14	8.35	81.00	0.742	10.45	16.6	3.02	11.5
AD-8		No	74.34	8.20	75.63	0.832	10.82	19.5	-	-
AD-9		No	74.68	8.27	73.72	0.810	11.05	17.9	2.74	11.9
AD-10		No	82.70	7.42	80.56	0.788	10.25	17.2	2.95	11.5
AD-11		No	82.76	7.77	80.27	0.762	10.30	14.8	-	-
AD-12		No	75.53	7.73	75.12	0.829	10.27	17.0	3.01	12.9
AD-13		No	77.10	7.20	77.88	0.854	10.44	18.6	2.96	12.8
AD-14		No	77.47	7.25	77.40	0.845	10.53	15.9	2.58	11.1
AD-15		No	77.78	7.24	75.10	0.868	10.18	18.9	2.97	13.6
AD-16		No	77.94	7.54	76.81	0.848	10.20	16.0	2.64	13.6
AD-17		No	82.27	7.85	81.31	0.707	10.29	15.7	2.08	10.5
AD-18		Yes	81.30	8.33	80.32	-	11.00	18.3	2.38	11.2
AD-19		Yes	79.95	8.07	80.00	-	11.07	17.7	2.74	10.9
AD-20		Yes	75.06	7.04	74.26	-	10.74	19.4	2.88	13.1
AD-21		Yes	83.07	8.22	81.19	-	10.83	18.8	2.87	12.3
AD-22		Yes	85.28	8.55	83.38	-	10.76	16.4	2.98	11.0
AD-23		Yes	77.61	7.46	78.10	-	10.70	16.8	2.69	13.1
AD-24		Yes	78.42	7.57	73.70	-	10.32	18.6	2.47	14.7
AD-25		Yes	81.46	7.90	81.13	-	10.56	15.6	2.29	10.6
Avg.		**-**	**79.34**	**7.67**	**78.32**	**0.814**	**10.58**	**17.5**	**2.71**	**12.2**
COV		**-**	**0.04**	**0.07**	**0.04**	**0.05**	**0.03**	**0.08**	**0.10**	**0.09**
BD-1	B-CCB	No	77.78	7.27	78.29	0.836	-	19.34	3.64	12.72
BD-2		No	77.73	7.51	78.07	0.829	9.71	20.50	3.09	12.44
BD-3		No	75.20	6.42	75.79	0.817	9.68	21.02	3.21	12.64
BD-4		No	75.62	6.91	77.08	0.765	9.84	17.47	2.84	10.71
BD-5		No	75.52	6.76	73.84	0.772	9.57	18.90	2.87	10.57
BD-6		No	75.45	6.50	73.48	0.796	-	19.52	2.70	12.01
BD-7		No	75.49	6.54	73.42	0.793	-	19.76	2.92	11.65
BD-8		No	76.00	6.43	74.77	0.796	9.79	20.23	2.88	12.09
BD-9		Yes	76.93	6.98	74.46	-	-	19.81	2.75	13.75
BC-10		No	77.77	6.74	79.03	0.865	-	17.2	2.96	14.1
BC-11		No	77.82	6.76	76.84	0.845	9.96	18.6	2.94	12.4
Avg.		**-**	**77.24**	**6.88**	**76.61**	**0.824**	**9.97**	**18.0**	**2.88**	**12.4**
COV		**-**	**0.01**	**0.03**	**0.03**	**0.03**	**0.02**	**0.07**	**0.09**	**0.12**

Table A5 – Continued

Sample ID	Treatment condition	Node?	Avg. diameter (mm)	Avg. wall thickness (mm)	Avg. sample height (mm)	Apparent density (g/cm^3)	Moisture content (%)	f_v (MPa)	G (GPa)	LOP (MPa)
BC-1	B-CCB	No	76.32	6.78	78.38	0.801	-	17.6	-	11.3
BC-2		No	77.41	6.55	71.52	0.809	9.99	16.3	2.65	9.2
BC-3		No	76.74	7.17	76.03	0.852	10.06	17.3	3.27	13.4
BC-4		No	77.20	7.19	76.91	0.832	10.23	19.6	3.08	14.2
BC-5		No	76.69	6.95	75.78	0.860	10.19	19.8	3.03	13.4
BC-6		No	77.67	6.72	76.51	0.801	9.51	18.1	2.86	11.7
BC-7		No	77.54	6.78	77.92	0.805	9.85	19.4	2.89	12.2
BC-8		No	77.11	7.02	78.15	0.801	9.85	17.0	2.84	13.1
BC-9		No	77.39	6.98	75.71	0.793	10.06	17.2	2.87	11.2
BC-10		No	77.77	6.74	79.03	0.865	-	17.2	2.96	14.1
BC-11		No	77.82	6.76	76.84	0.845	9.96	18.6	2.94	12.4
BC-12		Yes	76.75	6.68	76.07	-	10.23	18.4	2.96	11.1
BC-13		Yes	78.24	7.53	75.82	-	10.03	18.4	3.23	11.3
BC-14		Yes	77.45	6.96	77.13	-	9.67	17.6	2.81	12.2
BC-15		Yes	77.68	6.74	77.20	-	-	19.6	3.18	13.1
Avg.		-	**77.32**	**6.90**	**76.60**	**0.824**	**9.97**	**18.1**	**2.97**	**12.3**
COV		-	**0.01**	**0.04**	**0.02**	**0.03**	**0.02**	**0.06**	**0.06**	**0.11**

A 2.3 - Tension parallel to fibres test

The results of all the samples submitted to the tension parallel to fibres test are presented in Table A6.

Table A6 – Tension parallel to fibres individual values. Related to Table 3.8.

Sample ID	Treatment condition	Node?	Avg. width (mm)	Avg. thickness (mm)	Avg.reduced section thickness (mm)	Apparent density (g/cm^3)	Moisture content * (%)	ft (MPa)	Et (GPa)
AD-1	A-DOT	No	6.73	2.74	1.05	0.82	6.80	244.2	18.27
AD-2		No	6.73	2.66	1.05	0.85		259.1	16.19
AD-3		No	6.74	2.67	0.78	0.84		281.6	17.55
AD-4		No	6.66	2.67	1.07	0.82		220.0	16.25
AD-5		No	8.00	3.45	1.17	0.77		260.1	-
AD-7		No	7.62	3.28	1.04	0.77		257.5	16.09
AD-8		No	8.25	2.79	1.09	0.73		257.7	18.16
AD-9		No	8.26	3.39	0.90	0.72		234.8	14.71
AD-10		No	7.72	3.19	1.07	0.74		234.2	14.93
AD-11		No	7.80	3.30	0.75	0.77		200.8	16.20
AD-12		No	7.76	3.07	1.11	0.82		279.1	15.38
AD-13		No	7.82	2.94	1.03	0.78		257.1	15.13
AD-14		No	7.82	3.27	1.12	0.78		257.5	14.52
AD-15		No	7.44	3.32	1.27	0.81		249.5	15.71
AD-16		No	7.54	3.21	1.25	0.79		258.4	17.17
AD-17		No	7.76	3.40	0.89	0.80		241.1	14.83
AD-18		No	7.67	3.01	1.25	0.78		208.9	15.46
AD-19		No	7.56	2.82	0.95	0.83		249.2	13.37
AD-20		No	7.67	3.10	1.18	0.81		253.1	15.1
AD-21		No	7.94	3.27	1.02	0.82		237.0	15.71
Avg.		-	**7.57**	**3.08**	**1.05**	**0.79**	**6.80**	**247.0**	**15.83**
COV		-	**0.06**	**0.09**	**0.14**	**0.05**	-	**0.08**	**0.08**
BD-1	B-DOT	No	6.38	2.45	1.01	0.71	6.85	282.9	17.41
BD-2		No	6.07	2.33	0.91	0.77		266.4	18.10
BD-3		No	6.09	2.69	1.34	0.79		280.1	18.41
BD-4		No	6.56	2.28	0.80	0.78		300.3	17.04
BD-5		No	7.35	2.38	0.66	0.81		260.4	18.5
BD-6		No	6.04	2.54	1.07	0.87		296.5	19.23
BD-7		No	7.40	2.68	1.08	0.76		271.2	18.36
BD-8		No	7.48	2.94	1.45	0.76		279.1	18.28
BD-9		No	7.29	3.07	1.20	0.79		310.7	18.1
BD-10		No	7.49	2.85	1.14	0.78		276.3	17.55
BD-11		No	7.63	3.17	1.13	0.81		279.8	17.88
BD-12		No	7.49	2.93	1.30	0.83		273.5	18.55
BD-13		No	6.75	2.52	1.07	0.79		274.2	17.87
BD-14		No	6.07	2.16	1.02	0.84		320.1	19.95
BD-15		No	5.93	2.18	1.03	0.88		322.5	19.34
BD-17		No	6.88	2.85	1.32	0.78		262.7	18.00
BD-18		No	6.56	2.69	1.10	0.79		256.3	18.72
BD-19		No	6.61	2.92	0.82	0.77		288.6	18.37
Avg.		-	**6.78**	**2.65**	**1.08**	**0.79**	**6.85**	**283.4**	**18.31**
COV		-	**0.09**	**0.12**	**0.19**	**0.05**	-	**0.07**	**0.04**

Table A6 – Continued

Sample ID	Treatment condition	Node?	Avg. width (mm)	Avg. thickness (mm)	Avg.reduced section thickness (mm)	Apparent density (g/cm^3)	Moisture content * (%)	ft (MPa)	Et (GPa)
BC-1	B-CCB	No	6.06	2.48	0.94	0.79	6.84	287.0	17.34
BC-2		No	7.14	2.95	1.05	0.80		296.1	18.86
BC-3		No	7.76	2.85	1.34	0.74		263.3	-
BC-4		No	7.23	2.87	1.19	0.76		291.8	18.25
BC-5		No	7.45	2.58	1.14	0.77		278.6	17.32
BC-6		No	6.62	2.86	0.79	0.76		284.9	18.67
BC-7		No	6.82	2.19	1.01	0.76		328.5	20.23
BC-8		No	6.77	3.01	1.09	0.78		302.5	18.41
BC-9		No	6.69	2.40	1.00	0.80		314.7	18.17
BC-10		No	7.83	2.78	1.07	0.80		263.1	18.65
BC-11		No	8.02	2.94	1.21	0.77		277.6	16.91
BC-12		No	7.72	2.54	0.80	0.83		271.3	18.57
BC-13		No	6.10	2.43	0.91	0.84		288.7	18.68
BC-14		No	6.66	2.02	0.75	0.85		326.1	18.86
BC-15		No	6.55	2.60	0.97	0.84		289.5	17.55
BC-16		No	6.54	2.86	1.07	0.85		303.8	18.87
BC-17		No	6.32	2.90	1.07	0.84		300.2	19.52
BC-18		No	6.10	2.44	1.04	0.83		290.8	18.24
Avg.		**-**	**6.91**	**2.65**	**1.02**	**0.80**	**6.84**	**292.1**	**18.42**
COV		**-**	**0.09**	**0.11**	**0.15**	**0.04**	**-**	**0.06**	**0.04**

* The moisture content was determined with the sum of the weight of all the samples (not individual values).

A 2.4 - Three-point small coupon bending test

The results of all the samples submitted to three-point bending test are given in Table A7.

Table A7 – Three-point bending test individual values. Related to Table 3.8.

Sample ID	Treatment condition	Node?	Avg. width (mm)	Avg. wall thickness (mm)	Apparent density (g/cm3)	Moisture content (%)	MOR (MPa)	MOE (GPa)	LOP (MPa)
AD-1	A-DOT	No	10.31	6.33	0.796	7.14	224.4	17.29	118.9
AD-2		No	10.36	6.39	0.776	7.22	216.9	16.36	114.1
AD-3		No	9.31	5.96	0.804	7.14	227.8	17.51	112.6
AD-4		No	9.75	7.35	0.726	7.07	190.8	16.40	126.6
AD-5		No	9.99	6.47	0.781	8.42	199.7	17.53	122.8
AD-6		No	11.02	7.06	0.737	7.34	184.8	15.48	127.1
AD-7		No	10.61	7.22	0.774	7.08	209.6	15.89	127.7
AD-8		No	10.00	7.55	0.791	7.96	202.3	15.92	127.4
AD-9		No	10.23	7.38	0.801	7.89	210.5	16.81	130.8
AD-10		No	10.23	7.18	0.833	7.62	195.5	15.08	110.6
AD-11		No	9.89	7.00	0.797	-	199.0	15.67	122.3
AD-12		No	9.73	7.30	0.793	6.86	192.8	15.09	122.5
AD-13		No	10.78	7.02	0.796	7.92	185.7	15.20	120.8
AD-14		No	10.17	7.36	0.782	8.16	186.9	14.94	115.5
AD-15		No	10.44	7.53	0.801	8.77	177.3	13.79	106.7
AD-16		No	10.72	6.96	0.772	7.21	209.1	17.50	133.8
AD-17		No	9.94	6.95	0.750	-	216.9	18.00	138.6
AD-18		No	10.10	7.14	0.760	7.62	211.7	17.27	130.3
Avg.		**-**	**10.20**	**7.01**	**0.782**	**7.59**	**202.3**	**16.21**	**122.7**
COV		**-**	**0.04**	**0.06**	**0.03**	**0.07**	**0.07**	**0.07**	**0.07**
BD-1	B-DOT	No	9.87	7.81	0.756	-	205.5	15.76	130.3
BD-2		No	9.80	7.86	0.757	6.19	207.3	16.20	132.6
BD-3		No	9.33	7.64	0.760	6.52	208.7	16.16	125.6
BD-4		No	9.77	7.92	0.763	7.14	196.1	15.39	121.4
BD-5		No	10.80	8.27	0.800	6.96	208.8	16.65	126.3
BD-6		No	9.82	7.70	0.830	6.80	216.9	17.46	136.4
BD-7		No	9.48	7.66	0.806	7.22	205.1	16.42	125.1
BD-8		No	10.83	8.15	0.795	6.25	216.2	17.32	130.0
BD-9		No	8.67	6.82	0.848	7.41	234.9	18.75	135.4
BD-10		No	10.17	7.51	0.827	-	219.6	17.24	132.8
BD-11		No	10.30	7.45	0.846	7.14	217.9	17.66	126.8
BD-12		No	8.88	7.05	0.781	7.41	207.3	16.37	124.2
BD-13		No	9.07	7.27	0.785	5.75	189.5	15.62	107.4
BD-14		No	9.37	7.34	0.799	6.59	203.7	16.62	120.0
BD-15		No	9.78	7.35	0.757	6.82	186.3	15.33	113.2
BD-16		No	9.99	6.94	0.768	-	204.1	16.03	128.9
BD-17		No	9.49	7.31	0.759	6.98	218.6	16.80	120.1
BD-18		No	9.21	7.19	0.768	7.14	206.8	16.18	120.2
Avg.		**-**	**9.70**	**7.51**	**0.789**	**6.82**	**208.5**	**16.55**	**125.4**
COV		**-**	**0.06**	**0.05**	**0.04**	**0.07**	**0.05**	**0.05**	**0.06**

Table A7 – Continued.

Sample ID	Treatment condition	Node?	Avg. width (mm)	Avg. wall thickness (mm)	Apparent density (g/cm^3)	Moisture content (%)	MOR (MPa)	MOE (GPa)	LOP (MPa)
BC-1	B-CCB	No	11.07	8.63	0.805	7.44	197.1	16.29	127.1
BC-2		No	11.18	8.65	0.804	7.32	199.4	16.14	123.4
BC-3		No	11.37	8.55	0.805	6.45	201.4	16.57	120.1
BC-4		No	10.64	8.36	0.814	7.76	204.7	16.28	127.2
BC-5		No	10.13	8.06	0.760	7.84	202.1	15.94	129.9
BC-6		No	10.67	8.43	0.757	7.21	198.5	16.54	123.9
BC-7		No	10.48	7.75	0.762	-	201.0	16.21	118.7
BC-8		No	10.51	7.72	0.820	7.69	205.3	15.32	123.6
BC-9		No	10.11	7.43	0.881	7.92	211.8	17.40	126.3
BC-10		No	9.62	7.21	0.855	8.70	216.2	16.93	130.8
BC-11		No	10.22	7.67	0.767	-	207.6	15.79	124.8
BC-12		No	9.67	7.54	0.772	8.79	210.0	16.76	117.1
BC-13		No	9.02	7.51	0.760	6.82	197.2	15.69	113.7
BC-14		No	9.68	7.45	0.784	7.69	196.9	15.82	138.9
BC-15		No	10.24	7.47	0.821	7.22	210.0	16.81	119.7
BC-16		No	10.35	7.41	0.798	7.45	201.0	16.34	140.9
BC-17		No	10.59	7.55	0.804	7.07	198.6	15.60	126.8
BC-18		No	10.37	7.49	0.800	7.37	199.0	15.47	112.5
Avg.		-	**10.33**	**7.83**	**0.798**	**7.55**	**203.2**	**16.21**	**124.7**
COV		-	**0.06**	**0.06**	**0.04**	**0.08**	**0.03**	**0.03**	**0.06**

A 2.5 - Flat ring flexure test

The flat ring flexure test was conducted in a four-point bending setup (Figure A2). In the symmetric specimen, only circumferential stresses are present. The modulus of rupture was then calculated according to Equation A3 (VIRGO et al., 2018). Only samples that failed in and close the constant moment region (L and CMR respectively) were considered as valid results. The CMR region is represented as the dimension "c" in Figure A2 and examples of failure modes can be seen in Figure A3, where A are the samples failed outside the CMR region. The individual test values are given in Table A8.

$$f_r = \frac{3.F_r.a}{(t_N+t_S).L^2} \qquad \text{Eq A3}$$

Where,

Fr – Total load applied to the specimen
a – Shear span
t_N and t_S – Culm wall thicknesses at failure locations on either side of the culm
L – Length of culm section

Figure A2 – Configuration and sample dimensions used for the flat ring flexure test.

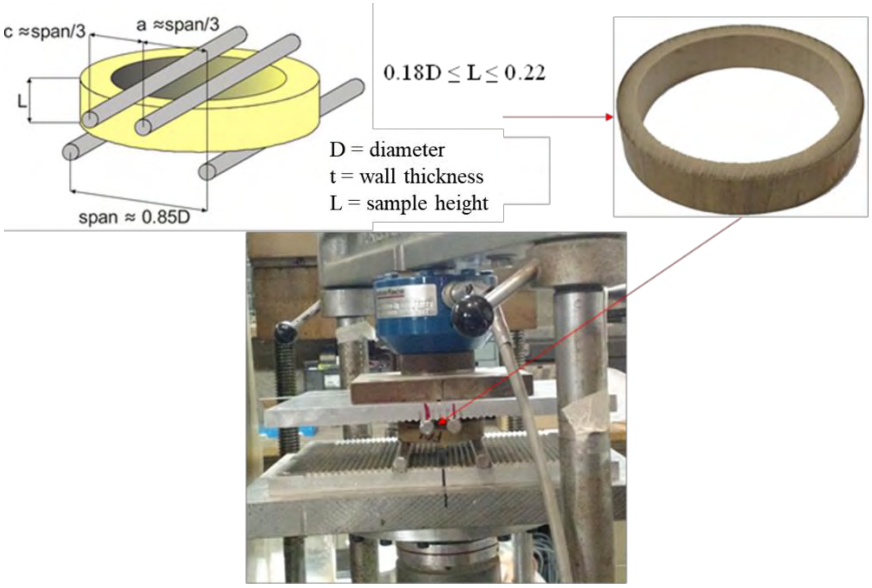

Figure A3 – The different types of failures observed in the flat ring flexure test.

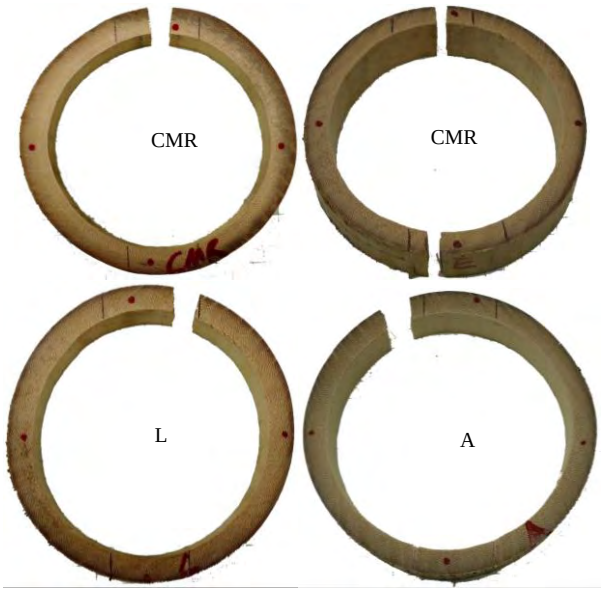

Table A8 – Flat ring flexure test individual values. Related to Table 3.8.

Sample ID	Treatment condition	D/t	L/D	a/L	Apparent density (g/cm^3)	Moisture content (%)	f_r (MPa)	Failure mode
AD-1	A-DOT	10.48	0.19	1.28	0.701	9.60	8.9	CMR
AD-2		10.38	0.20	1.23	0.690	9.24	8.0	CMR
AD-3		10.28	0.20	1.25	0.678	9.50	7.4	L
AD-4		9.84	0.20	1.26	0.703	9.55	7.7	L
AD-5		10.04	0.20	1.22	0.676	9.14	7.4	CMR
AD-6		10.14	0.20	1.24	0.791	10.48	14.0	CMR
AD-7		10.03	0.19	1.32	0.794	-	10.2	CMR
AD-8		9.78	0.20	1.24	0.772	9.91	11.3	CMR
AD-9		9.73	0.19	1.29	0.782	9.80	14.5	CMR
AD-10		10.62	0.20	1.15	0.733	9.17	14.9	CMR
AD-11		10.57	0.19	1.22	0.736	8.80	9.9	L
AD-12		10.34	0.19	1.25	0.730	9.00	14.4	CMR
AD-13		10.48	0.20	1.18	0.741	9.33	10.4	CMR
Avg.		**10.21**	**0.20**	**1.24**	**0.73**	**9.46**	**10.69**	**-**
COV		**0.03**	**0.03**	**0.04**	**0.06**	**0.05**	**0.27**	**-**
BD-1	B-DOT	10.47	0.22	1.15	0.730	9.84	12.3	CMR
BD-2		11.44	0.20	1.30	0.781	-	12.0	CMR
BD-3		11.62	0.19	1.37	0.796	9.68	12.8	CMR
BD-4		11.54	0.21	1.22	0.790	9.77	13.8	CMR
BD-5		11.70	0.20	1.28	0.796	9.64	12.7	L
BD-6		11.61	0.20	1.28	0.782	9.70	13.5	CMR
BD-7		11.62	0.20	1.30	0.786	-	16.1	CMR
Avg.		**11.43**	**0.20**	**1.27**	**0.78**	**9.73**	**13.31**	**-**
COV		**0.04**	**0.05**	**0.06**	**0.03**	**0.01**	**0.10**	**-**
BC-1	B-CCB	11.81	0.19	1.38	0.793	9.40	15.1	CMR
BC-2		11.78	0.18	1.43	0.798	9.72	12.7	L
BC-3		11.82	0.19	1.36	0.801	10.00	13.1	CMR
BC-4		12.02	0.20	1.37	0.841	9.27	9.3	L
BC-5		11.51	0.19	1.43	0.813	10.34	14.4	CMR
BC-6		11.50	0.20	1.35	0.807	9.87	10.4	CMR
BC-7		11.43	0.20	1.39	0.820	9.66	12.8	L
BC-8		11.57	0.20	1.36	0.827	9.46	18.5	CMR
Avg.		**11.68**	**0.19**	**1.38**	**0.81**	**9.71**	**13.29**	**-**
COV		**0.02**	**0.03**	**0.02**	**0.02**	**0.04**	**0.21**	**-**

A 3 - Section 3.3. (Use of ISO 22157 mechanical test methods and the characterisation of Brazilian *P. edulis* bamboo)

A 3.1 - Compression parallel to fibres test

The full-culm compression test values of each specimen are presented in Table A9. The dimensions of the samples are also provided.

Table A9 - Compression parallel to fibre test individual values. Related to Table 3.9

Sample ID	Node?	Avg. diameter (mm)	Avg. wall thickness (mm)	Avg. sample height (mm)	Apparent density (g/cm^3)	Moisture content (%)	f_c (MPa)	E_c (GPa)	LOP (MPa)
AD-1	No	80.07	8.31	83.13	0.813	10.06	57.9	17.13	47.0
AD-2	No	74.96	6.61	76.16	0.832	9.65	63.2	21.64	56.7
AD-3	No	74.52	6.65	74.04	0.827	9.89	66.1	22.47	62.1
AD-4	No	81.50	6.81	80.93	0.853	9.53	69.2	20.61	60.6
AD-5	No	83.17	7.97	81.54	0.808	9.79	62.0	20.88	55.6
AD-6	No	82.74	8.17	82.78	0.801	10.39	62.0	19.66	52.7
AD-7	No	85.69	8.75	83.10	0.726	10.11	52.6	20.68	40.0
AD-8	No	85.29	8.46	83.24	0.750	9.83	47.3	19.91	42.6
AD-9	No	75.11	8.42	74.01	0.821	10.42	57.9	17.62	46.1
AD-10	No	80.72	7.17	81.89	0.805	9.22	59.9	16.44	53.7
AD-11	No	76.13	7.70	68.53	0.889	-	64.2	18.00	53.6
AD-12	No	75.72	7.59	78.65	0.840	-	64.8	16.88	49.4
AD-13	No	76.96	7.34	77.42	0.817	9.96	56.4	18.36	52.9
AD-14	No	77.92	7.43	76.25	0.848	-	61.9	17.72	50.6
AD-15	No	82.06	8.16	81.21	0.703	9.30	51.3	16.57	45.4
AD-16	No	83.16	8.29	82.94	0.670	9.63	51.6	16.29	44.3
BD-1	No	79.98	7.84	78.88	0.790	10.66	58.5	19.60	48.1
BD-2	No	78.50	7.59	79.62	0.830	10.44	48.5	18.24	45.9
BD-3	No	78.05	7.38	78.41	0.838	10.44	56.6	21.54	52.2
BD-4	No	78.47	7.48	77.98	0.818	10.32	54.9	21.29	49.3
BD-5	No	75.52	6.49	71.02	0.811	10.15	53.3	20.61	42.3
BD-6	No	75.19	6.47	74.94	0.811	10.09	58.1	24.21	54.0
BD-7	No	74.61	6.39	75.39	0.798	10.11	53.4	20.98	49.7
BD-8	No	74.53	6.39	79.47	0.794	10.17	56.8	21.79	51.7
BD-9	No	74.21	6.33	76.69	0.797	10.25	54.0	21.18	52.6
BD-10	No	74.08	6.53	74.54	0.779	10.20	54.3	17.98	48.8
BD-11	No	79.87	7.15	77.51	0.795	9.87	51.9	20.25	50.0
BD-12	No	80.35	6.94	78.17	0.809	9.95	48.6	21.70	47.5
BD-13	No	80.65	6.97	78.08	0.811	9.96	56.3	21.79	47.5
BC-1	No	78.06	6.47	77.21	0.830	10.24	55.9	23.68	49.7
BC-2	No	76.40	6.48	76.63	0.827	10.48	59.8	20.26	54.0

Table A9 – Continued.

Sample ID	Node?	Avg. diameter (mm)	Avg. wall thickness (mm)	Avg. sample height (mm)	Apparent density (g/cm^3)	Moisture content (%)	f_c (MPa)	E_c (GPa)	LOP (MPa)
BC-3	No	76.60	6.81	78.28	0.854	10.60	62.4	22.63	54.1
BC-4	No	77.06	6.94	76.61	0.839	10.64	62.2	21.13	58.9
BC-5	No	76.99	7.12	76.26	0.837	10.60	62.2	20.80	54.8
BC-6	No	77.51	7.01	75.03	0.808	10.40	50.8	20.10	44.0
BC-7	No	77.75	6.76	75.46	0.817	10.39	58.1	22.22	49.7
BC-8	No	78.16	6.63	76.99	0.825	10.30	53.2	21.12	46.9
BC-9	No	77.56	7.18	75.30	0.788	10.31	60.4	22.63	55.4
BC-10	No	77.27	6.79	78.96	0.809	10.30	60.6	20.42	56.0
BC-11	No	77.39	6.37	79.36	0.879	10.08	62.2	24.04	58.0
BC-12	No	77.41	6.66	76.41	0.847	10.10	54.8	21.11	53.7
Avg.		**78.24**	**7.19**	**77.78**	**0.81**	**10.13**	**57.46**	**20.30**	**50.93**
COV		**0.04**	**0.10**	**0.04**	**0.05**	**0.03**	**0.09**	**0.10**	**0.10**
BC-13	Yes	76.30	6.98	78.02	-	10.65	56.0	23.47	47.5
BC-14	Yes	77.07	7.02	76.87	-	10.82	61.6	22.60	56.0
BC-15	Yes	78.24	7.12	79.40	-	10.45	-	16.36	45.8
BC-16	Yes	77.61	6.95	76.95	-	10.41	60.4	21.15	49.0
AD-17	Yes	80.51	8.32	81.73	-	10.26	60.4	21.67	43.3
AD-18	Yes	74.62	6.72	72.84	-	9.86	-	20.45	58.0
AD-19	Yes	81.28	7.03	83.12	-	9.85	64.9	20.44	59.2
AD-20	Yes	75.04	8.30	76.83	-	10.89	59.0	-	-
AD-21	Yes	81.72	7.40	80.74	-	10.03	59.8	19.31	49.1
AD-22	Yes	77.12	7.32	75.95	-	10.23	60.7	21.13	52.5
AD-23	Yes	79.01	7.60	75.93	-	9.84	62.1	19.73	51.0
AD-24	Yes	82.71	8.17	81.29	-	9.86	50.9	14.97	44.7
BD-14	Yes	80.42	7.20	79.72	-	10.23	61.0	22.54	50.5
BD-15	Yes	75.02	6.57	76.70	-	10.44	57.2	24.55	44.7
Avg.		**78.33**	**7.33**	**78.29**	**-**	**10.27**	**59.51**	**20.64**	**50.10**
COV		**0.03**	**0.08**	**0.04**	**-**	**0.04**	**0.06**	**0.13**	**0.10**
All specimens									
Avg.		**78.26**	**7.23**	**77.91**	**-**	**10.17**	**57.93**	**20.38**	**50.73**
COV		**0.04**	**0.09**	**0.04**	**-**	**0.03**	**0.08**	**0.11**	**0.10**

A 3.2 - Shear parallel to fibres test

The full-culm shear parallel to fibre test results of each specimen are presented in Table A10. The dimensions of the samples are also provided.

Table A10 - Shear parallel to fibres individual values. Related to Table 3.10.

Sample ID	Node?	Avg. diameter (mm)	Avg. wall thickness (mm)	Avg. sample height (mm)	Apparent density (g/cm^3)	Moisture content (%)	f_v (MPa)	G (GPa)	LOP (MPa)
AD-1	No	76.32	6.78	78.38	0.801	-	17.56	-	11.26
AD-2	No	77.41	6.55	71.52	0.809	9.99	16.33	2.65	9.23
AD-3	No	76.74	7.17	76.03	0.852	10.06	17.27	3.27	13.37
AD-4	No	77.20	7.19	76.91	0.832	10.23	19.55	3.08	14.17
AD-5	No	76.69	6.95	75.78	0.860	10.19	19.83	3.03	13.38
AD-6	No	77.67	6.72	76.51	0.801	9.51	18.14	2.86	11.72
AD-7	No	77.54	6.78	77.92	0.805	9.85	19.39	2.89	12.20
AD-8	No	77.11	7.02	78.15	0.801	9.85	17.02	2.84	13.10
AD-9	No	77.39	6.98	75.71	0.793	10.06	17.24	2.87	11.24
AD-10	No	77.77	6.74	79.03	0.865	-	17.20	2.96	14.13
AD-11	No	77.82	6.76	76.84	0.845	9.96	18.58	2.94	12.38
AD-12	No	77.78	7.27	78.29	0.836	-	19.34	3.64	12.72
AD-13	No	77.73	7.51	78.07	0.829	-	20.50	3.09	12.44
AD-14	No	75.20	6.42	75.79	0.817	9.68	21.02	3.21	12.64
AD-15	No	75.62	6.91	77.08	0.765	9.84	17.47	2.84	10.71
AD-16	No	75.52	6.76	73.84	0.772	9.57	18.90	2.87	10.57
AD-17	No	75.45	6.50	73.48	0.796	-	19.52	2.70	12.01
BD-1	No	75.49	6.54	73.42	0.793	-	19.76	2.92	11.65
BD-2	No	76.00	6.43	74.77	0.796	9.79	20.23	2.88	12.09
BD-3	No	79.87	8.12	79.88	0.828	10.76	16.63	2.70	12.70
BD-4	No	75.74	6.94	76.66	0.808	10.56	18.52	2.45	11.14
BD-5	No	74.81	6.87	75.87	0.817	10.41	18.14	2.46	13.33
BD-6	No	80.28	6.95	79.93	0.845	10.59	18.11	2.87	12.34
BD-7	No	80.33	6.72	78.21	0.858	10.55	19.35	3.01	13.31
BD-8	No	82.72	8.26	80.60	0.802	10.79	16.12	2.49	12.06
BC-10	No	85.14	8.35	81.00	0.742	10.45	16.57	3.02	11.52
BC-11	No	74.34	8.20	75.63	0.832	10.82	19.51	-	-
BC-1	No	74.68	8.27	73.72	0.810	11.05	17.86	2.74	11.92
BC-2	No	82.70	7.42	80.56	0.788	10.25	17.18	2.95	11.45
BC-3	No	82.76	7.77	80.27	0.762	10.30	14.78	-	-
BC-4	No	75.53	7.73	75.12	0.829	10.27	16.96	3.01	12.92
BC-5	No	77.10	7.20	77.88	0.854	10.44	18.56	2.96	12.84
BC-6	No	77.47	7.25	77.40	0.845	10.53	15.90	2.58	11.08
BC-7	No	77.78	7.24	75.10	0.868	10.18	18.85	2.97	13.62
BC-8	No	77.94	7.54	76.81	0.848	10.20	15.99	2.64	13.56
BC-9	No	82.27	7.85	81.31	0.707	10.06	15.71	2.08	10.47
Avg.		**77.77**	**7.18**	**77.04**	**0.814**	**10.23**	**18.04**	**2.86**	**12.21**
COV		**0.03**	**0.08**	**0.03**	**0.04**	**0.04**	**0.08**	**0.10**	**0.09**

Table A10 - Continued

Sample ID	Node?	Avg. diameter (mm)	Avg. wall thickness (mm)	Avg. sample height (mm)	Apparent density (g/cm^3)	Moisture content (%)	f_v (MPa)	G (GPa)	LOP (MPa)
BC-12	Yes	76.75	6.68	76.07	-	10.23	18.40	2.96	11.11
BC-13	Yes	78.24	7.53	75.82	-	10.03	18.40	3.23	11.33
BC-14	Yes	77.45	6.96	77.13	-	9.67	17.60	2.81	12.19
BC-15	Yes	77.68	6.74	77.20	-	-	19.60	3.18	13.14
AD-18	Yes	81.30	8.33	80.32	-	11.00	18.30	2.38	13.75
AD-19	Yes	79.95	8.07	80.00	-	11.07	17.70	2.74	11.19
AD-20	Yes	75.06	7.04	74.26	-	10.74	19.40	2.88	10.90
AD-21	Yes	83.07	8.22	81.19	-	10.83	18.80	2.87	13.05
AD-22	Yes	85.28	8.55	83.38	-	10.76	16.40	2.98	12.31
AD-23	Yes	77.61	7.46	78.10	-	10.70	16.80	2.69	11.03
AD-24	Yes	78.42	7.57	73.70	-	10.32	18.60	2.47	13.13
AD-25	Yes	81.46	7.90	81.13	-	10.56	15.60	2.29	14.70
BD-9	Yes	76.93	6.98	74.46	-	-	19.81	2.75	10.59
Avg.		**79.17**	**7.54**	**77.90**	**-**	**10.54**	**18.11**	**2.79**	**12.19**
COV		**0.04**	**0.08**	**0.04**	**-**	**0.04**	**0.07**	**0.10**	**0.11**
All specimens									
Avg.		**78.14**	**7.28**	**77.27**	**-**	**10.31**	**18.06**	**2.84**	**12.21**
COV		**0.04**	**0.08**	**0.03**	**-**	**0.04**	**0.08**	**0.10**	**0.09**

A 3.3 - Tension parallel to fibres test

The results of all the samples submitted to the tension parallel to fibres test are presented in Table A11.

Table A11 - Tension parallel to fibres individual values. Related to Table 3.11.

Sample ID	Node?	Avg. width (mm)	Avg. thickness (mm)	Avg.reduced section thickness (mm)	Apparent density (g/cm^3)	Moisture content * (%)	ft (MPa)	Et (GPa)
AD-1	No	6.73	2.74	1.05	0.82	6.80	244.2	18.27
AD-2	No	6.73	2.66	1.05	0.85		259.1	16.19
AD-3	No	6.74	2.67	0.78	0.84		281.6	17.55
AD-4	No	6.66	2.67	1.07	0.82		220.0	16.25
AD-5	No	8.00	3.45	1.17	0.77		260.1	-
AD-7	No	7.62	3.28	1.04	0.77		257.5	16.09
AD-8	No	8.25	2.79	1.09	0.73		257.7	18.16
AD-9	No	8.26	3.39	0.90	0.72		234.8	14.71
AD-10	No	7.72	3.19	1.07	0.74		234.2	14.93
AD-11	No	7.80	3.30	0.75	0.77		200.8	16.20
AD-12	No	7.76	3.07	1.11	0.82		279.1	15.38
AD-13	No	7.82	2.94	1.03	0.78		257.1	15.13
AD-14	No	7.82	3.27	1.12	0.78		257.5	14.52
AD-15	No	7.44	3.32	1.27	0.81		249.5	15.71
AD-16	No	7.54	3.21	1.25	0.79		258.4	17.17
AD-17	No	7.76	3.40	0.89	0.80		241.1	14.83
AD-18	No	7.67	3.01	1.25	0.78		208.9	15.46
AD-19	No	7.56	2.82	0.95	0.83		249.2	13.37
AD-20	No	7.67	3.10	1.18	0.81		253.1	15.1
AD-21	No	7.94	3.27	1.02	0.82		237.0	15.71
BD-1	No	6.38	2.45	1.01	0.71	6.85	282.9	17.41
BD-2	No	6.07	2.33	0.91	0.77		266.4	18.10
BD-3	No	6.09	2.69	1.34	0.79		280.1	18.41
BD-4	No	6.56	2.28	0.80	0.78		300.3	17.04
BD-5	No	7.35	2.38	0.66	0.81		260.4	18.5
BD-6	No	6.04	2.54	1.07	0.87		296.5	19.23
BD-7	No	7.40	2.68	1.08	0.76		271.2	18.36
BD-8	No	7.48	2.94	1.45	0.76		279.1	18.28
BD-9	No	7.29	3.07	1.20	0.79		310.7	18.1
BD-10	No	7.49	2.85	1.14	0.78		276.3	17.55
BD-11	No	7.63	3.17	1.13	0.81		279.8	17.88
BD-12	No	7.49	2.93	1.30	0.83		273.5	18.55
BD-13	No	6.75	2.52	1.07	0.79		274.2	17.87
BD-14	No	6.07	2.16	1.02	0.84		320.1	19.95
BD-15	No	5.93	2.18	1.03	0.88		322.5	19.34
BD-16	No	6.08	2.29	1.00	0.86		349.0	-
BD-17	No	6.88	2.85	1.32	0.78		262.7	18.00
BD-18	No	6.56	2.69	1.10	0.79		256.3	18.72
BD-19	No	6.61	2.92	0.82	0.77	6.84	288.6	18.37
BC-1	No	6.06	2.48	0.94	0.79		287.0	17.34
BC-2	No	7.14	2.95	1.05	0.80		296.1	18.86
BC-3	No	7.76	2.85	1.34	0.74		263.3	-
BC-4	No	7.23	2.87	1.19	0.76		291.8	18.25

Table A11 - Continued

Sample ID	Node?	Avg. width (mm)	Avg. thickness (mm)	Avg.reduced section thickness (mm)	Apparent density (g/cm^3)	Moisture content * (%)	ft (MPa)	Et (GPa)
BC-5	No	7.45	2.58	1.14	0.77	6.84	278.6	17.32
BC-6	No	6.62	2.86	0.79	0.76		284.9	18.67
BC-7	No	6.82	2.19	1.01	0.76		328.5	20.23
BC-8	No	6.77	3.01	1.09	0.78		302.5	18.41
BC-9	No	6.69	2.40	1.00	0.80		314.7	18.17
BC-10	No	7.83	2.78	1.07	0.80		263.1	18.65
BC-11	No	8.02	2.94	1.21	0.77		277.6	16.91
BC-12	No	7.72	2.54	0.80	0.83		271.3	18.57
BC-13	No	6.10	2.43	0.91	0.84		288.7	18.68
BC-14	No	6.66	2.02	0.75	0.85		326.1	18.86
BC-15	No	6.55	2.60	0.97	0.84		289.5	17.55
BC-16	No	6.54	2.86	1.07	0.85		303.8	18.87
BC-17	No	6.32	2.90	1.07	0.84		300.2	19.52
BC-18	No	6.10	2.44	1.04	0.83		290.8	18.24
Avg.	**-**	**7.09**	**2.79**	**1.05**	**0.80**	**6.83**	**274.6**	**17.47**
COV	**-**	**0.10**	**0.13**	**0.16**	**0.05**	**-**	**0.11**	**0.09**
BC-19	Yes	7.40	2.10	-	0.77	6.80	110.7	11.45
BC-20	Yes	7.33	2.97	-	0.76		94.6	14.87
BC-21	Yes	7.58	2.02	-	0.75		74.2	-
BC-22	Yes	6.83	3.04	-	0.77		94.5	-
BD-20	Yes	6.30	2.53	-	0.73	6.90	102.0	9.14
BD-21	Yes	6.34	2.08	-	0.73		105.1	11.22
BD-22	Yes	5.90	1.85	-	0.74		149.0	-
BD-23	Yes	6.19	2.76	-	0.74		106.8	12.66
BD-24	Yes	6.15	2.05	-	0.87		106.8	-
BD-25	Yes	6.35	2.36	-	0.82		124.6	12.31
BD-26	Yes	6.04	1.49	-	0.83		112.0	-
BD-27	Yes	6.16	1.66	-	0.77		132.8	-
BD-28	Yes	6.98	2.21	-	0.78		96.2	12.31
BD-29	Yes	6.72	2.70	-	0.80		106.8	9.86
BD-30	Yes	6.78	2.50	-	0.77		103.2	12.14
BD-31	Yes	6.71	2.37	-	0.78		118.9	14.52
AD-22	Yes	7.26	2.06	-	0.77	6.80	67.3	9.22
AD-23	Yes	8.14	1.97	-	0.76		62.7	7.1
AD-24	Yes	7.98	1.95	-	0.78		94.4	-
AD-25	Yes	7.69	2.64	-	0.75		67.9	-
AD-26	Yes	6.82	2.01	-	0.84		96.2	10.35
AD-27	Yes	6.45	2.15	-	0.86		70.8	9.39
AD-28	Yes	6.88	2.49	-	-		102.6	13.49
AD-29	Yes	7.66	2.77	-	0.83		115.6	12.24
AD-30	Yes	7.95	3.06	-	0.78		96.2	9.07
AD-31	Yes	7.85	3.40	-	0.81		103.2	12.13
AD-32	Yes	7.83	2.97	-	0.79		83.6	9.07
Avg.	**-**	**6.97**	**2.38**	**-**	**0.78**	**6.83**	**99.94**	**11.19**
COV	**-**	**0.10**	**0.20**	**-**	**0.05**	**-**	**0.20**	**0.18**

* The moisture content was determined with the sum of the weight of all the samples (not individual values).

A 3.4 - Three-point small coupon bending test

The results of all the samples submitted to three-point bending test are given in Table A12.

Table A12 - Three-point bending test individual values. Related to Table 3.12.

Sample ID	Node?	Orient. *	Avg. width (mm)	Avg. wall thickness (mm)	Apparent density (g/cm^3)	Moisture content (%)	MOR (MPa)	MOE (GPa)	LOP (MPa)	SE (kJ/m2)
AD-1	No	OC	10.31	6.33	0.796	7.14	224.4	17.29	118.9	52.28
AD-2	No	OC	10.36	6.39	0.776	7.22	216.9	16.36	114.1	51.18
AD-3	No	OC	9.31	5.96	0.804	7.14	227.8	17.51	112.6	61.39
AD-4	No	OC	9.75	7.35	0.726	7.07	190.8	16.40	126.6	33.06
AD-5	No	OC	9.99	6.47	0.781	8.42	199.7	17.53	122.8	36.06
AD-6	No	OC	11.02	7.06	0.737	7.34	184.8	15.48	127.1	32.16
AD-7	No	OC	10.61	7.22	0.774	7.08	209.6	15.89	127.7	44.64
AD-8	No	OC	10.00	7.55	0.791	7.96	202.3	15.92	127.4	39.40
AD-9	No	OC	10.23	7.38	0.801	7.89	210.5	16.81	130.8	40.19
AD-10	No	OC	10.23	7.18	0.833	7.62	195.5	15.08	110.6	37.49
AD-11	No	OC	9.89	7.00	0.797	-	199.0	15.67	122.3	41.66
AD-12	No	OC	9.73	7.30	0.793	6.86	192.8	15.09	122.5	36.90
AD-13	No	OC	10.78	7.02	0.796	7.92	185.7	15.20	120.8	30.97
AD-14	No	OC	10.17	7.36	0.782	8.16	186.9	14.94	115.5	35.13
AD-15	No	OC	10.44	7.53	0.801	8.77	177.3	13.79	106.7	36.96
AD-16	No	OC	10.72	6.96	0.772	7.21	209.1	17.50	133.8	36.53
AD-17	No	OC	9.94	6.95	0.750	-	216.9	18.00	138.6	40.29
AD-18	No	OC	10.10	7.14	0.760	7.62	211.7	17.27	130.3	41.36
BD-1	No	OC	9.87	7.81	0.756	-	205.5	15.76	130.3	37.49
BD-2	No	OC	9.80	7.86	0.757	6.19	207.3	16.20	132.6	34.13
BD-3	No	OC	9.33	7.64	0.760	6.52	208.7	16.16	125.6	37.79
BD-4	No	OC	9.77	7.92	0.763	7.14	196.1	15.39	121.4	34.14
BD-5	No	OC	10.80	8.27	0.800	6.96	208.8	16.65	126.3	40.39
BD-6	No	OC	9.82	7.70	0.830	6.80	216.9	17.46	136.4	37.60
BD-7	No	OC	9.48	7.66	0.806	7.22	205.1	16.42	125.1	41.28
BD-8	No	OC	10.83	8.15	0.795	6.25	216.2	17.32	130.0	44.22
BD-9	No	OC	8.67	6.82	0.848	7.41	234.9	18.75	135.4	44.98
BD-10	No	OC	10.17	7.51	0.827	-	219.6	17.24	132.8	41.25
BD-11	No	OC	10.30	7.45	0.846	7.14	217.9	17.66	126.8	41.27
BD-12	No	OC	8.88	7.05	0.781	7.41	207.3	16.37	124.2	39.33
BD-13	No	OC	9.07	7.27	0.785	5.75	189.5	15.62	107.4	34.15
BD-14	No	OC	9.37	7.34	0.799	6.59	203.7	16.62	120.0	37.05
BD-15	No	OC	9.78	7.35	0.757	6.82	186.3	15.33	113.2	30.83
BD-16	No	OC	9.99	6.94	0.768	-	204.1	16.03	128.9	36.53
BD-17	No	OC	9.49	7.31	0.759	6.98	218.6	16.80	120.1	42.41
BD-18	No	OC	9.21	7.19	0.768	7.14	206.8	16.18	120.2	37.23
BC-1	No	OC	11.07	8.63	0.805	7.44	197.1	16.29	127.1	36.77
BC-2	No	OC	11.18	8.65	0.804	7.32	199.4	16.14	123.4	38.75
BC-3	No	OC	11.37	8.55	0.805	6.45	201.4	16.57	120.1	36.92

Table A12 – Continued.

Sample ID	Node?	Orient. *	Avg. width (mm)	Avg. wall thickness (mm)	Apparent density (g/cm^3)	Moisture content (%)	MOR (MPa)	MOE (GPa)	LOP (MPa)	SE (kJ/m2)
BC-4	No	OC	10.64	8.36	0.814	7.76	204.7	16.28	127.2	40.57
BC-5	No	OC	10.13	8.06	0.760	7.84	202.1	15.94	129.9	38.16
BC-6	No	OC	10.67	8.43	0.757	7.21	198.5	16.54	123.9	38.76
BC-7	No	OC	10.48	7.75	0.762	-	201.0	16.21	118.7	42.65
BC-8	No	OC	10.51	7.72	0.820	7.69	205.3	15.32	123.6	40.87
BC-9	No	OC	10.11	7.43	0.881	7.92	211.8	17.40	126.3	40.46
BC-10	No	OC	9.62	7.21	0.855	8.70	216.2	16.93	130.8	45.20
BC-11	No	OC	10.22	7.67	0.767	-	207.6	15.79	124.8	43.61
BC-12	No	OC	9.67	7.54	0.772	8.79	210.0	16.76	117.1	42.41
BC-13	No	OC	9.02	7.51	0.760	6.82	197.2	15.69	113.7	42.47
BC-14	No	OC	9.68	7.45	0.784	7.69	196.9	15.82	138.9	35.07
BC-15	No	OC	10.24	7.47	0.821	7.22	210.0	16.81	119.7	40.04
BC-16	No	OC	10.35	7.41	0.798	7.45	201.0	16.34	140.9	34.59
BC-17	No	OC	10.59	7.55	0.804	7.07	198.6	15.60	126.8	35.20
BC-18	No	OC	10.37	7.49	0.800	7.37	199.0	15.47	112.5	40.89
Avg.	-	-	**10.08**	**7.45**	**0.79**	**7.33**	**204.68**	**16.32**	**124.28**	**39.50**
COV	-	-	**0.06**	**0.07**	**0.04**	**0.09**	**0.06**	**0.06**	**0.06**	**0.13**
AD-31	No	OT	10.06	6.51	0.801	8.16	200.1	17.11	69.0	97.29
AD-32	No	OT	10.21	7.33	0.720	7.84	147.0	14.73	57.5	53.46
AD-33	No	OT	10.25	7.41	0.793	-	188.7	16.20	69.9	77.45
AD-34	No	OT	9.74	7.19	0.777	7.14	172.8	14.92	62.0	80.64
AD-35	No	OT	10.84	7.63	0.807	7.32	177.1	14.16	64.7	75.65
AD-36	No	OT	10.59	7.47	0.725	6.09	178.5	15.65	60.2	78.25
BD-27	No	OT	9.85	5.80	0.824	6.74	189.9	13.41	92.7	57.19
BD-28	No	OT	8.95	5.99	0.792	-	188.5	16.53	63.8	71.60
BC-23	No	OT	10.29	6.48	0.794	-	198.0	16.29	71.9	115.95
BC-24	No	OT	8.41	6.30	0.835	8.43	187.4	16.73	58.5	77.07
Avg.	-	-	**9.92**	**6.81**	**0.79**	**7.39**	**182.79**	**15.57**	**67.00**	**78.46**
COV	-	-	**0.07**	**0.10**	**0.05**	**0.11**	**0.08**	**0.08**	**0.15**	**0.23**

Table A12 – Continued.

Sample ID	Node?	Orient. *	Avg. width (mm)	Avg. wall thickness (mm)	Apparent density (g/cm^3)	Moisture content (%)	MOR (MPa)	MOE (GPa)	LOP (MPa)	SE (kJ/m2)
AD-19	Yes	OC	9.35	5.84	0.826	7.14	154.8	16.39	94.2	17.59
AD-20	Yes	OC	9.36	6.31	0.788	6.90	119.2	14.36	78.0	11.26
AD-21	Yes	OC	9.14	6.19	0.806	7.06	135.9	15.74	79.4	15.23
AD-22	Yes	OC	9.07	6.27	0.801	8.33	129.7	15.47	78.6	12.56
AD-23	Yes	OC	10.35	7.04	0.804	7.41	124.0	14.33	89.5	15.82
AD-24	Yes	OC	10.24	7.07	0.800	6.48	126.7	14.88	89.2	13.75
AD-25	Yes	OC	10.70	6.82	0.808	7.34	131.1	14.80	85.4	20.19
AD-26	Yes	OC	9.91	7.08	0.806	7.69	129.9	14.63	89.8	14.26
AD-27	Yes	OC	8.85	7.37	0.741	7.78	123.6	14.47	86.4	18.32
AD-28	Yes	OC	9.72	7.04	0.750	7.29	116.3	13.95	95.1	11.97
AD-29	Yes	OC	10.21	7.12	0.774	6.60	141.3	16.60	91.9	13.56
AD-30	Yes	OC	10.11	7.12	0.789	-	139.0	15.55	98.4	16.12
BD-19	Yes	OC	9.82	5.69	0.828	5.68	134.2	16.13	96.7	13.25
BD-20	Yes	OC	9.51	5.58	0.832	5.95	128.3	16.55	91.1	13.81
BD-21	Yes	OC	9.96	6.23	0.800	6.38	131.5	15.88	104.2	13.46
BD-22	Yes	OC	10.89	6.22	0.806	-	130.7	15.30	95.4	13.88
BD-23	Yes	OC	8.95	6.17	0.797	7.41	114.6	15.52	87.4	10.46
BD-24	Yes	OC	8.47	5.87	0.803	6.76	124.0	14.56	85.9	11.47
BD-25	Yes	OC	9.94	6.12	0.757	7.06	99.9	13.36	59.5	8.36
BD-26	Yes	OC	9.89	6.22	0.757	-	94.8	12.74	70.9	7.90
BC-19	Yes	OC	9.56	6.84	0.762	7.53	128.3	14.93	82.9	12.93
BC-20	Yes	OC	9.97	5.71	0.780	7.23	152.3	16.18	80.3	17.52
BC-21	Yes	OC	10.00	6.69	0.740	-	101.3	13.71	72.9	8.40
BC-22	Yes	OC	10.05	6.73	0.767	7.22	134.7	15.14	94.3	13.88
Avg.	**-**	**-**	**9.75**	**6.47**	**0.788**	**7.06**	**126.9**	**15.05**	**86.6**	**13.58**
COV	-	-	**0.06**	**0.08**	**0.034**	**0.09**	**0.1**	**0.07**	**0.1**	**0.23**

* Orientation of the specimen during the test, where OC = outer layer in compression and OT = outer layer in tension.

APPENDIX B – INDIVIDUAL TEST VALUES OF CHAPTER 4

This Appendix section gives the individual values of the physical and mechanical tests data presented in chapter 4 with additional information regarding each tested sample. This section was divided into two main parts, referred to each paper presented within this chapter.

B 1 – Section 4.1 (Assessment of *Dendrocalamus asper* bamboo treated with tannin-boron preservatives)

B 1.1 - Water absorption, swelling and leaching

The individual values of the physical properties (water absorption, swelling and weight loss) obtained for each tested specimen during the leaching process are presented in Table B1. The leached samples were used for the fungi decay tests.

Table B1 – Individual values of water absorption, thickness and width swelling, and weight loss after leaching (WL). Related to Tables 4.6 and 4.7.

Condition	Sample ID	Water absorption (%)			Thickness swelling (%)			Width swelling (%)			WL* (%)
		12h	24h	288h	12h	24 h	288 h	12h	24 h	288 h	
Ref.	1	30.15	42.11	71.27	7.42	11.11	14.59	4.70	6.31	8.16	7.40
	2	29.32	39.84	64.55	6.98	10.27	12.39	3.72	4.85	5.87	6.57
	3	28.96	39.05	63.58	6.56	9.89	12.06	3.29	4.54	5.75	6.43
	4	29.34	39.86	70.30	6.57	9.61	12.58	3.81	6.14	6.96	6.32
	5	30.80	43.23	72.62	7.55	11.85	14.69	4.89	6.70	8.14	7.69
	6	31.27	41.79	71.02	7.79	10.63	13.16	4.61	5.74	6.97	6.56
	7	27.31	37.38	64.58	6.29	9.63	12.88	3.50	5.10	6.45	6.55
	8	26.54	37.19	63.20	5.94	9.01	12.18	2.91	4.53	6.51	6.21
	9	27.48	37.73	66.47	5.47	8.34	11.49	3.43	5.24	7.06	6.11
	10	31.89	43.15	71.92	8.12	11.71	14.68	4.84	6.35	7.78	7.26
	11	26.21	36.62	62.51	6.20	9.60	13.04	3.68	5.21	6.74	6.36
	12	29.26	39.65	68.98	7.32	10.85	14.69	4.46	6.06	7.56	7.08
	13	29.78	40.28	70.35	6.28	9.37	12.21	3.80	4.99	6.28	6.20
	14	27.16	38.20	62.73	6.79	10.00	13.10	3.43	4.30	7.03	6.37
Avg.		**28.96**	**39.72**	**67.43**	**6.81**	**10.13**	**13.12**	**3.93**	**5.43**	**6.95**	**6.65**
COV		**0.06**	**0.06**	**0.06**	**0.11**	**0.10**	**0.08**	**0.16**	**0.14**	**0.11**	**0.07**
B5	1	31.15	40.56	64.32	7.71	10.29	13.76	4.33	5.57	6.91	6.75
	2	28.60	37.65	61.62	5.91	8.48	11.01	3.90	4.96	6.62	6.12
	3	21.07	29.12	52.08	5.06	7.94	11.93	2.98	4.44	7.01	6.92
	4	29.26	37.64	62.50	5.92	8.53	10.84	4.31	5.75	7.07	6.24
	5	31.15	40.43	64.53	7.01	9.69	12.98	4.43	5.77	7.34	7.88
	6	32.77	40.97	61.64	9.11	11.91	14.49	4.61	5.63	7.04	7.27
	7	26.87	35.26	55.58	6.55	8.52	11.58	4.22	5.43	7.33	6.09
	8	24.30	33.44	56.40	5.89	7.78	14.27	3.88	5.51	7.57	8.19
	9	26.38	33.80	55.91	5.52	8.41	10.44	3.83	5.13	6.58	6.17
	10	28.99	37.22	63.54	4.99	7.16	8.93	3.29	4.32	5.92	6.34
	11	28.91	37.34	61.17	5.93	8.26	9.97	4.11	5.09	6.76	5.99
	12	29.58	38.22	62.21	5.42	7.69	9.49	3.66	4.75	5.58	6.38
	13	30.22	38.33	62.32	6.27	8.04	9.41	3.81	4.89	5.93	5.80
	14	22.17	30.18	54.07	4.80	7.33	9.77	3.03	4.50	6.61	6.47
	15	29.58	37.15	57.59	6.50	8.33	9.56	4.95	5.39	6.80	6.30
	16	21.78	30.16	51.37	4.88	7.57	10.68	3.40	4.82	7.00	7.10
Avg.		**27.36**	**35.66**	**58.64**	**5.99**	**8.37**	**11.02**	**3.89**	**5.10**	**6.75**	**6.65**
COV		**0.14**	**0.11**	**0.08**	**0.19**	**0.14**	**0.16**	**0.15**	**0.10**	**0.09**	**0.11**

Table B1 – Continued.

Condition	Sample ID	Water absorption (%)			Thickness swelling (%)			Width swelling (%)			WL* (%)
		12h	24h	288h	12h	24 h	288 h	12h	24 h	288 h	
TH10B5	1	29.66	37.32	57.70	6.09	8.45	9.78	3.56	4.38	5.26	6.50
	2	25.85	34.97	58.72	5.49	8.50	12.08	3.44	4.47	5.96	6.83
	3	31.38	38.37	58.32	6.82	9.28	11.38	3.79	4.67	5.62	7.41
	4	28.09	35.56	57.96	5.41	7.38	9.34	3.40	4.27	5.51	5.76
	5	28.66	38.15	59.00	6.00	9.03	12.05	3.35	4.40	5.56	7.81
	6	33.19	41.84	64.77	7.19	9.85	12.57	4.51	5.27	6.13	7.02
	7	31.15	41.24	66.15	7.07	10.16	13.46	3.98	5.56	6.69	7.48
	8	28.13	36.25	56.80	5.65	7.51	9.98	3.58	4.50	5.70	7.15
	9	25.85	33.71	57.08	4.72	6.49	8.46	3.35	4.57	5.74	5.50
	10	29.07	36.41	56.06	5.19	7.02	8.64	3.53	4.39	5.10	6.64
	11	26.52	34.25	56.17	4.89	6.79	8.66	3.99	4.55	5.54	5.59
	12	27.86	36.47	56.47	5.05	7.40	9.29	3.40	4.28	5.19	6.43
	13	30.58	37.73	57.92	5.68	7.34	8.89	3.56	4.43	5.43	6.94
	14	28.86	36.84	58.21	5.29	7.03	8.68	3.21	3.28	4.91	6.81
	15	31.26	40.48	66.38	6.38	8.47	11.17	3.91	4.77	6.23	7.24
	16	33.84	42.23	66.20	6.78	8.99	11.20	4.10	4.89	6.21	7.12
Avg.		**29.60**	**37.82**	**59.82**	**5.87**	**8.05**	**10.27**	**3.69**	**4.56**	**5.68**	**6.78**
COV		**0.08**	**0.07**	**0.07**	**0.14**	**0.15**	**0.16**	**0.10**	**0.11**	**0.09**	**0.11**
TH10	1	30.67	37.82	59.74	5.47	7.68	9.57	4.78	5.61	6.62	4.97
	2	33.53	41.45	63.52	6.19	8.14	9.42	4.05	4.39	4.75	5.84
	3	28.72	38.15	63.38	6.40	8.93	11.74	3.80	5.51	6.68	5.70
	4	30.24	38.13	59.97	6.27	8.83	10.80	5.22	6.17	7.48	5.77
	5	32.72	39.33	61.63	6.44	7.98	9.56	3.80	4.84	5.95	4.87
	6	32.18	41.67	66.98	7.16	9.50	11.40	4.22	4.98	6.13	6.28
	7	30.59	38.71	62.65	6.45	8.38	10.45	3.78	4.51	5.40	5.44
	8	29.54	39.68	63.35	6.70	9.50	12.39	3.49	4.68	6.25	5.91
	9	30.33	39.02	62.61	5.48	6.98	8.71	3.43	4.23	5.22	5.94
	10	28.12	35.86	57.97	5.05	6.99	8.29	3.70	4.61	5.34	5.51
	11	30.73	38.86	63.24	6.15	7.24	8.62	3.72	4.68	6.01	5.19
	12	29.06	37.40	60.74	5.17	7.23	8.57	3.18	3.95	4.93	6.12
	13	28.41	36.83	59.87	5.21	7.07	8.28	3.67	4.55	5.64	6.00
	14	29.70	38.12	61.55	5.38	7.05	8.67	2.97	3.73	4.55	6.32
	15	28.89	37.41	62.16	5.91	7.58	8.98	3.95	4.95	6.21	5.00
Avg.		**30.20**	**38.62**	**62.11**	**6.00**	**7.96**	**9.71**	**3.78**	**4.70**	**5.75**	**5.71**
COV		**0.05**	**0.04**	**0.03**	**0.11**	**0.12**	**0.14**	**0.14**	**0.13**	**0.14**	**0.08**

B 1.2 – Fungi decay test

The individual values obtained for the fungi decay tests of both Brown-rot and White-rot fungi are given in Table B2.

Table B2 – Fungi decay test results of all tested samples. Related to 4.8.

Sample	Reference		B5		TH10		TH10B5	
	Unleached	Leached	Unleached	Leached	Unleached	Leached	Unleached	Leached
Gloeophyllum trabeum - Brown-rot								
1	5.52	1.19	2.14	20.65	4.20	3.57	-	1.03
2	5.18	14.64	4.13	24.89	6.16	2.79	-	0.37
3	5.88	-	5.57	7.72	5.59	3.24	2.96	-
4	6.93	18.88	5.93	8.69	4.06	1.37	4.00	0.96
5	6.39	6.35	2.83	16.56	3.12	1.57	5.97	1.49
6	5.61	10.03	2.96	12.16	2.82	6.92	5.86	2.84
7	6.83	11.44	1.86	10.42	4.21	4.33	5.48	0.43
8	6.69	6.71	2.23	10.03	3.36	1.92	3.59	-
9	4.99	3.12	2.51	13.31	2.82	6.75	-	-
10	5.06	9.07	2.75	28.82	4.10	-	-	0.28
11	6.05	29.17	5.37	4.56	2.55	7.64	4.16	0.61
12	6.48	-	4.58	0.56	4.27	4.82	4.13	4.02
13	5.63	7.57	2.88	14.62	4.30	2.93	4.05	2.26
14	6.64	9.73	3.07	13.60	2.87	0.84	5.23	0.54
15	6.15	8.22	2.62	11.18	2.52	2.34	4.29	-
16	6.28	11.18	2.50	16.08	3.97	1.23	3.90	-
Avg.	**6.02**	**10.52**	**3.37**	**13.37**	**3.81**	**3.48**	**4.47**	**1.35**
COV	**0.11**	**0.66**	**0.39**	**0.53**	**0.27**	**0.63**	**0.21**	**0.90**
Pycnoporus sanguineus - White-rot								
1	7.98	16.54	6.82	14.84	10.26	12.68	6.76	2.82
2	7.51	11.11	4.10	14.76	8.37	14.75	6.25	3.71
3	10.76	17.74	3.78	4.41	8.36	1.73	6.49	3.35
4	9.67	17.13	4.37	5.56	8.23	3.46	6.04	2.42
5	6.83	13.18	8.04	8.81	6.21	6.14	3.05	10.00
6	16.08	9.99	3.65	16.72	4.30	5.81	4.75	21.91
7	8.77	11.45	4.38	16.12	3.72	14.68	7.00	10.01
8	9.87	11.70	3.80	18.40	7.76	15.95	3.75	15.00
9	7.70	13.94	4.27	6.51	6.66	17.24	6.86	1.92
10	7.80	18.12	3.99	4.52	9.49	14.89	5.39	1.37
11	10.60	20.63	3.77	3.63	7.05	3.51	5.80	2.24
12	9.18	19.38	3.68	4.97	4.70	2.58	3.57	2.93
13	7.55	11.43	4.91	6.52	6.49	3.79	4.41	16.12
14	8.72	13.68	5.14	11.26	6.77	3.80	2.95	16.85
15	9.10	17.46	3.82	17.19	6.25	16.65	-	2.32
16	9.96	17.02	3.46	13.91	7.05	18.91	6.13	8.29
Avg.	**9.26**	**15.03**	**4.50**	**10.51**	**6.98**	**9.79**	**5.28**	**7.58**
COV	**0.23**	**0.22**	**0.28**	**0.51**	**0.26**	**0.65**	**0.27**	**0.88**

B 1.3 – Compression parallel to fibres test

The small coupon compression test results of each sample are presented in Table B3.

Table B3 – Individual values of compression parallel to fibres test. Related to Table 4.8.

Condition	Sample ID	Avg. width (mm)	Avg. wall thickness (mm)	Avg. sample height (mm)	Apparent density (g/cm^3)	Moisture content * (%)	f_c (MPa)
Ref.	D1-1	10.61	10.71	43.7	0.85	7.61	101.4
	D1-2	10.94	10.78	43.9	0.85		103.7
	A19-1	10.38	10.72	44.1	0.92		105.0
	A19-2	10.94	10.61	44.1	0.90		103.7
	C5-1	9.69	9.09	39.6	0.83		95.9
	C5-2	9.47	9.03	39.5	0.83		96.8
	F1-2	9.06	9.22	37.1	0.84		114.2
	F1-1	9.47	9.18	37.5	0.83		104.5
	E1-1	8.78	8.96	35.3	0.86		108.5
	E1-2	9.17	9.13	35.4	0.84		108.5
	B2-1	8.29	8.20	33.0	0.98		112.8
	B2-2	8.39	8.30	33.1	0.95		108.2
Avg.		**9.60**	**9.49**	**38.85**	**0.87**	**-**	**105.3**
COV		**0.10**	**0.10**	**0.11**	**0.06**	**-**	**0.05**
B5	D6-1	10.35	10.36	46.2	0.89	7.28	129.9
	D6-2	10.47	10.66	46.3	0.87		127.4
	A10-1	8.96	8.88	43.4	0.96		129.3
	A10-2	10.19	9.45	43.6	0.98		135.3
	F7-1	9.43	9.02	40.8	0.92		135.3
	F7-2	9.41	9.11	40.6	0.92		131.5
	C10-1	9.11	8.78	36.9	0.81		120.0
	C10-2	9.11	8.62	36.8	0.83		126.3
	B6-1	8.62	8.37	36.9	0.94		129.3
	B6-2	8.48	8.08	36.7	0.96		131.6
	E9-1	9.42	8.70	38.5	0.92		133.8
	E9-2	8.53	8.16	38.7	0.93		139.0
Avg.		**9.34**	**9.01**	**40.43**	**0.91**	**-**	**130.7**
COV		**0.07**	**0.09**	**0.09**	**0.06**	**-**	**0.04**

Table B3 – Continued.

Condition	Sample ID	Avg. width (mm)	Avg. wall thickness (mm)	Avg. sample height (mm)	Apparent density (g/cm^3)	Moisture content (%)	f_c (MPa)
TH10	D11-1	10.85	11.76	46.5	0.86	6.89	112.2
	D11-2	10.88	10.90	46.4	0.85		113.3
	F12-1	9.55	9.93	41.0	0.87		114.7
	F12-2	9.87	9.75	40.8	0.89		114.8
	E11-1	9.34	9.16	38.1	0.86		113.9
	E11-2	9.32	9.33	38.0	0.88		114.0
	A14-1	10.48	10.06	41.5	0.98		119.4
	A14-2	10.81	10.22	41.6	0.98		121.6
	B13-1	9.06	8.73	37.8	1.01		119.2
	B13-2	8.89	8.47	38.4	1.00		121.0
	C14-1	8.32	8.72	35.3	0.86		117.5
	C14-2	8.90	8.85	35.3	0.86		114.7
Avg.		**9.69**	**9.65**	**40.06**	**0.91**	-	**116.3**
COV		**0.09**	**0.10**	**0.09**	**0.07**	-	**0.03**
TH10B5	C20-1	9.82	9.17	38.7	0.83	8.22	120.2
	C20-2	9.16	8.53	38.8	0.83		121.4
	B19-1	10.07	9.77	43.6	0.96		124.4
	B19-2	10.16	9.42	43.4	0.99		127.8
	D16-1	11.11	10.00	44.2	0.94		131.3
	D16-2	10.89	10.48	44.5	0.91		127.0
	A4-1	9.73	9.25	39.0	1.00		123.5
	A4-2	9.64	9.37	39.2	1.02		122.4
	E17-1	9.93	9.71	41.7	0.87		124.5
	E17-2	9.91	9.54	41.6	0.87		123.7
	F20-1	9.61	9.30	38.7	0.87		128.0
	F20-2	9.36	8.66	38.6	0.90		128.6
Avg.		**9.95**	**9.43**	**40.99**	**0.91**	**-**	**125.2**
COV		**0.06**	**0.06**	**0.06**	**0.07**	**-**	**0.03**

* The moisture content was determined with the sum of the weight of all the samples (not individual values).

B 1.4 – Interlaminar shear test

The interlaminar shear tests were performed on coupon specimens scored halfway through their depth perpendicular to the loading direction at two locations resulting in a shear plane having an area $A = L_s \times t$ (Figure B1). The shear strength is calculated using the maximum load at failure divided by the shear area A. The obtained results of each sample are given in Table B4.

Figure B1 - Specimen layout used for interlaminar shear tests.

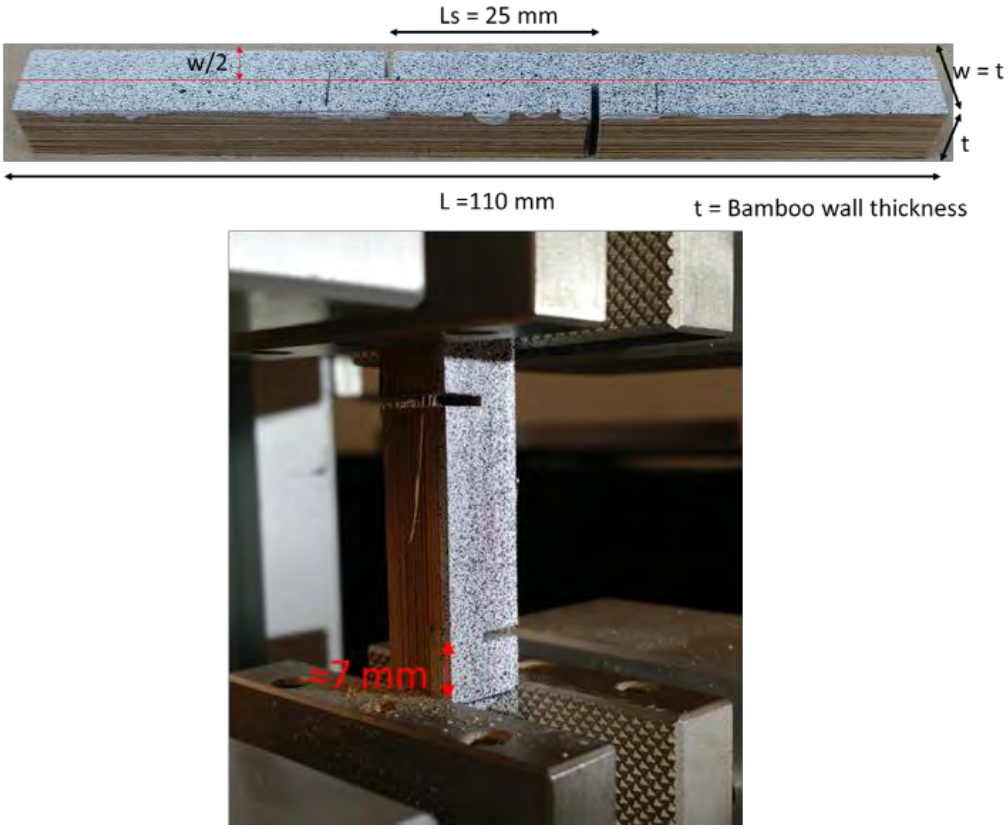

Table B4 – Individual values of interlaminar shear test. Related to Table 4.8.

Condition	Sample ID	Avg. wall thickness (mm)	Avg. width (mm)	Shear plane length (mm)	Apparent density (g/cm^3)	Moisture content (%)	f_v (MPa)
Ref.	D1-2	11.42	10.81	22.2	0.84	7.77	8.24
	D1-1	11.36	10.20	21.0	0.84	7.22	9.68
	F1-2	9.34	9.98	23.5	0.85	7.59	8.16
	F1-1	9.27	9.73	20.9	0.84	6.33	8.71
	B2-2	8.41	9.13	22.7	0.95	6.67	7.87
	C5-2	9.08	9.04	21.9	0.82	-	8.83
	E1-1	9.60	9.69	23.1	0.85	8.97	9.45
	E1-2	9.49	8.92	22.2	0.85	6.94	6.86
	C5-1	9.25	8.78	23.9	0.82	5.80	7.23
	A19-1	10.64	9.81	23.3	0.91	7.23	9.03
Avg.		**9.79**	**9.61**	**22.48**	**0.86**	**7.17**	**8.4**
COV		**0.10**	**0.07**	**0.05**	**0.05**	**0.13**	**0.11**
B5	A10-1	9.61	9.72	23.9	0.98	6.38	8.84
	B6-2	8.66	8.94	23.9	0.97	7.69	8.32
	F7-1	9.91	9.76	23.5	0.88	-	8.47
	F7-2	9.66	9.93	23.9	0.90	6.59	7.51
	A10-2	9.75	10.10	23.9	1.00	6.86	7.88
	E9-1	8.91	9.45	23.9	0.92	6.25	10.51
	D6-1	11.44	11.45	23.6	0.85	6.90	7.02
	C10-1	9.54	9.45	23.9	0.81	8.00	7.92
	E9-2	9.52	9.86	23.9	0.89	6.98	9.99
	B6-1	8.57	8.68	24.0	0.98	7.59	8.41
Avg.		**9.56**	**9.73**	**23.83**	**0.92**	**7.0**	**8.5**
COV		**0.08**	**0.08**	**0.01**	**0.07**	**0.1**	**0.13**
TH10	E11-1	9.33	9.60	23.9	0.88	6.17	7.15
	F12-1	9.70	9.02	24.0	0.87	6.33	6.81
	A14-2	9.97	10.14	23.9	0.98	6.93	9.41
	C14-1	9.24	8.62	23.9	0.86	7.14	7.33
	B13-1	8.71	8.65	23.9	0.97	-	7.83
	B13-2	8.58	9.02	24.0	0.98	6.41	7.43
	A14-1	9.87	8.74	23.9	0.95	7.06	9.21
	D11-2	12.15	11.72	23.7	0.84	6.45	9.39
	C14-2	8.59	8.46	23.8	0.85	7.81	7.96
	E11-2	9.29	9.78	23.8	0.86	6.17	6.56
Avg.		**9.54**	**9.37**	**23.85**	**0.90**	**6.7**	**7.9**
COV		**0.11**	**0.11**	**0.00**	**0.06**	**0.1**	**0.14**

Table B4 – Continued.

Condition	Sample ID	Avg. width (mm)	Avg. wall thickness (mm)	Shear plane length (mm)	Apparent density (g/cm^3)	Moisture content (%)	f_v (MPa)
TH10B5	A4-1	9.56	10.11	24.3	0.99	6.12	8.77
	C20-2	8.82	9.21	23.8	0.83	7.25	7.33
	A4-2	9.85	10.15	24.5	0.97	6.00	8.82
	B19-2	9.52	10.10	24.6	0.98	6.25	9.39
	F20-2	10.14	10.08	23.6	0.86	6.59	7.24
	C20-1	9.02	9.23	24.2	0.82	7.04	6.83
	E17-1	9.56	10.02	23.7	0.84	7.32	7.16
	B19-1	9.52	9.95	23.8	0.98	-	7.34
	E17-2	9.51	9.33	24.5	0.85	5.13	6.97
	D16-2	10.17	10.09	24.5	0.91	7.53	7.92
	F20-1	9.78	-	24.5	-	7.41	7.64
Avg.		**9.58**	**9.83**	**24.16**	**0.90**	**6.66**	**7.8**
COV		**0.04**	**0.04**	**0.02**	**0.08**	**0.12**	**0.11**

B 1.4 – Three-point bending small coupon bending test

The results of all the samples submitted to three-point bending test are given in Table B5.

Table B5 – Three-point bending test individual values. Related to Table 4.8

Condition	Sample ID	Avg. width (mm)	Avg. wall thickness (mm)	Apparent density (g/cm^3)	Moisture content (%)	MOR (MPa)	MOE (GPa)
Ref.	D2-1	10.38	11.10	0.85	-	192.5	20.80
	A2-1	10.34	10.09	0.93	-	222.4	22.42
	B5-1	10.16	8.54	0.99	7.50	222.5	22.13
	E3-1	10.44	9.27	0.86	-	218.5	21.84
	C3-1	10.19	8.61	0.81	7.58	181.4	20.06
	A2-2	10.57	9.74	0.93	7.91	222.5	-
	F4-1	10.29	10.01	0.85	7.32	199.3	20.76
	A1-1	9.80	9.06	0.99	-	240.7	-
	B1-1	9.41	9.17	0.98	7.64	246.8	21.96
	C3-2	10.19	8.33	0.80	7.03	178.7	-
	E3-2	10.46	9.42	0.85	6.96	213.3	-
	B5-2	9.69	8.90	0.98	8.33	216.3	-
	F4-2	10.36	9.77	0.85	7.45	207.5	-
	A1-2	8.89	8.90	0.96	7.75	227.2	21.60
	B1-2	10.04	8.90	0.98	7.98	239.7	-
Avg.		**10.08**	**9.32**	**0.91**	**7.59**	**215.3**	**21.45**
COV		**0.05**	**0.08**	**0.08**	**0.05**	**0.10**	**0.04**
B5	B10-1	10.84	9.66	0.98	7.85	263.6	22.42
	B10-2	9.91	9.29	0.96	-	256.9	-
	E6-1	10.04	8.72	0.88	7.69	232.8	24.65
	A9-1	10.29	10.17	0.97	-	243.6	22.86
	C6-1	10.34	8.77	0.91	7.84	255.2	24.25
	E6-2	10.30	9.21	0.87	-	221.9	-
	D10-1	10.02	10.50	0.90	7.34	207.8	24.39
	B8-1	10.02	8.56	0.99	-	274.1	-
	A8-1	10.11	9.33	0.99	8.05	257.7	-
	D10-2	10.46	10.22	0.92	7.65	222.9	-
	B8-2	10.75	8.21	1.00	7.93	287.5	24.11
	F8-1	10.57	9.90	0.85	7.88	212.2	22.24
	C6-2	10.57	9.49	0.86	7.45	231.2	-
	F8-2	10.41	9.78	0.86	7.36	220.6	-
	A8-2	9.87	9.19	0.98	7.83	236.7	21.78
	A9-2	10.17	9.81	0.97	7.73	256.7	-
Avg.		**10.29**	**9.43**	**0.93**	**7.72**	**242.6**	**23.34**
COV		**0.03**	**0.07**	**0.06**	**0.03**	**0.09**	**0.05**

Table B5 – Continued.

Condition	Sample ID	Avg. width (mm)	Avg. wall thickness (mm)	Apparent density (g/cm^3)	Moisture content (%)	MOR (MPa)	MOE (GPa)
TH10	A15-1	9.78	8.95	0.99	-	242.7	-
	A12-1	10.10	10.35	0.97	-	209.1	20.34
	A12-2	10.59	10.12	0.98	8.21	217.9	-
	F13-1	10.73	8.89	0.87	-	231.0	22.63
	B14-1	10.07	8.44	1.00	7.59	239.8	22.83
	D12-1	10.59	11.61	0.82	7.41	163.2	-
	B14-2	10.37	8.80	0.96	7.98	234.3	-
	C13-1	10.07	9.33	0.84	-	195.4	21.96
	B15-1	10.76	9.02	0.97	7.39	239.5	-
	D12-2	11.03	11.51	0.82	7.73	171.1	20.56
	F13-2	9.84	9.34	0.87	8.11	223.6	-
	A15-2	9.98	8.88	1.01	7.78	252.5	22.93
	E15-1	10.56	8.88	0.88	7.84	264.9	23.03
	C13-2	10.57	9.52	0.85	7.55	200.6	-
	B15-2	10.17	8.90	0.98	7.83	232.2	21.78
	E15-2	10.70	9.23	0.87	7.50	243.1	-
Avg.		**10.37**	**9.49**	**0.92**	**7.74**	**222.5**	**22.01**
COV		**0.04**	**0.10**	**0.08**	**0.03**	**0.13**	**0.05**
TH10B5	B20-1	10.49	8.88	0.97	-	256.0	22.52
	D19-1	10.38	10.88	0.88	-	215.8	24.04
	E17-1	10.04	8.99	0.99	7.19	272.8	24.54
	F16-1	9.59	9.26	0.88	7.53	242.7	23.89
	C17-1	10.48	9.45	0.85	6.96	202.6	21.92
	D19-2	9.82	10.91	0.89	6.70	221.7	-
	E18-1	9.21	8.85	0.90	7.30	258.8	-
	E18-2	9.97	8.38	0.92	-	275.8	-
	B17-1	10.60	8.80	0.99	6.94	269.5	24.44
	A5-1	9.86	9.08	1.01	7.06	265.5	23.09
	A16-1	10.41	8.98	1.00	7.47	236.7	-
	A16-2	10.16	9.72	1.00	7.57	248.0	22.41
	C11-1	9.73	9.68	0.87	7.19	228.7	-
	B20-2	10.09	8.82	0.97	7.41	256.7	-
	C17-2	10.40	9.85	0.85	6.75	204.8	-
	A5-2	10.06	9.11	0.98	7.74	250.3	-
Avg.		**10.08**	**9.35**	**0.93**	**7.22**	**244.1**	**23.36**
COV		**0.04**	**0.08**	**0.07**	**0.04**	**0.10**	**0.04**

B 2 – Section 4.2 (Chemical modification of Dendrocalamus asper bamboo with citric acid: effects on the physical-chemical, mechanical and thermal properties)

B 2.1 – Water absorption, swelling, and leaching

The individual values of the physical properties (water absorption, swelling and weight loss) obtained for each tested specimen during the leaching process are presented in Table B6.

Table B6 – Individual values of water absorption, thickness and width swelling, and weight loss after leaching (WL). Related to Tables 4.15 and 4.16.

Condition	Sample ID	Water absorption (%)			Thickness swelling (%)			Width swelling (%)			WL (%)
		12h	24h	288h	12h	24 h	288 h	12h	24 h	288 h	
Ref.	1	32.11	45.47	84.83	6.98	10.33	12.97	4.16	6.20	6.45	5.48
	2	28.86	40.87	82.53	5.35	8.55	10.92	3.17	4.42	5.26	5.55
	3	26.68	39.02	74.85	4.46	7.19	9.89	3.12	3.87	4.74	5.39
	4	29.14	42.10	83.18	5.66	7.58	9.50	3.24	3.11	4.30	5.81
	5	31.06	43.72	82.06	5.78	7.99	9.92	2.30	3.13	3.30	6.46
	6	29.26	42.05	81.96	6.08	9.25	11.83	3.51	4.86	5.19	5.87
	7	30.79	43.58	83.79	5.87	9.51	11.75	4.08	5.25	6.05	5.48
	8	23.69	34.89	72.43	3.75	6.41	9.25	3.08	4.22	5.86	4.86
	9	27.32	38.94	77.96	5.47	8.06	10.65	3.21	4.66	4.88	5.38
	10	30.14	42.22	81.28	4.94	7.27	9.08	2.96	3.49	3.74	6.04
	11	30.78	43.23	80.36	6.00	9.05	11.21	4.14	5.22	5.97	5.41
	12	28.42	40.03	78.34	5.15	8.05	10.62	3.67	5.02	5.53	5.58
	13	30.54	43.08	81.26	5.75	8.87	11.05	3.90	4.90	5.77	5.43
	14	28.82	40.16	79.68	5.09	7.15	9.06	2.86	3.57	3.98	5.90
	15	26.28	38.24	73.59	4.24	6.61	9.10	3.24	4.45	5.49	5.15
Avg.		**28.93**	**41.17**	**79.87**	**5.37**	**8.12**	**10.45**	**3.37**	**4.42**	**5.10**	**5.59**
COV		**0.08**	**0.07**	**0.05**	**0.15**	**0.14**	**0.11**	**0.16**	**0.20**	**0.18**	**0.07**
B5	1	31.86	44.79	83.42	4.93	6.89	8.98	3.25	3.81	4.24	6.13
	2	34.79	47.05	85.81	5.45	7.54	9.84	3.83	4.34	5.53	5.99
	3	27.81	39.09	73.96	5.10	7.85	11.94	3.39	4.47	5.59	6.52
	4	25.99	36.88	70.07	3.79	6.64	10.09	3.03	4.29	5.71	6.43
	5	26.98	37.64	71.46	4.64	7.34	10.73	2.64	3.83	4.72	6.99
	6	43.16	55.41	98.84	7.93	10.37	13.12	4.29	4.78	5.77	6.89
	7	40.03	52.76	98.95	5.98	7.94	9.91	2.43	3.43	4.03	7.00
	8	27.10	38.81	73.02	4.75	7.81	11.62	2.96	4.31	5.74	6.27
	9	27.93	38.91	71.81	4.66	7.63	10.11	3.27	3.99	4.98	7.37
	10	41.30	50.89	92.97	5.63	7.06	8.32	3.34	4.09	4.51	8.07
	11	39.77	50.83	94.36	5.77	7.07	8.72	2.95	3.60	4.17	7.95
	12	33.84	43.59	74.39	5.88	8.06	9.64	3.25	4.20	4.56	7.50
	13	30.39	40.68	69.37	4.51	7.29	8.43	3.42	4.21	4.90	7.04
	14	33.79	45.57	85.54	4.84	6.36	7.62	3.46	3.24	4.48	7.24
	15	32.33	43.46	83.47	4.53	6.48	8.39	2.36	3.45	4.18	7.04
	16	28.27	40.18	69.59	4.45	7.38	8.67	2.91	4.16	5.03	7.00
Avg.		**32.83**	**44.16**	**81.06**	**5.18**	**7.48**	**9.76**	**3.17**	**4.01**	**4.88**	**6.96**
COV		**0.17**	**0.13**	**0.13**	**0.18**	**0.12**	**0.15**	**0.15**	**0.10**	**0.13**	**0.09**

Table B6 – Continued.

Condition	Sample ID	Water absorption (%)			Thickness swelling (%)			Width swelling (%)			WL (%)
		12h	24h	288h	12h	24 h	288 h	12h	24 h	288 h	
CA10	1	18.85	26.63	56.87	3.15	4.74	6.17	1.73	2.87	3.56	4.70
	2	24.35	30.94	62.00	3.93	5.23	6.36	2.73	3.01	3.19	4.71
	3	18.64	26.16	53.80	3.34	5.01	6.89	2.87	3.67	4.08	4.95
	4	25.94	31.73	64.14	4.05	5.43	6.55	2.41	2.82	3.05	4.44
	5	22.41	29.45	58.38	3.69	4.45	5.71	2.78	3.03	3.40	5.62
	6	24.14	30.40	64.30	3.58	4.66	5.41	2.56	2.91	3.23	4.89
	7	24.01	30.86	58.86	3.78	4.74	5.61	3.05	3.05	3.13	5.12
	8	21.28	28.63	55.01	4.15	5.08	6.33	2.22	1.21	3.31	5.12
	9	19.13	26.18	53.67	3.08	4.51	5.86	2.44	3.10	3.67	5.09
	10	19.07	25.97	55.19	3.02	4.67	6.07	2.56	2.90	3.92	5.00
	11	23.02	29.56	62.41	3.31	4.20	5.12	2.89	3.29	3.62	5.57
	12	20.41	26.72	54.03	3.49	4.80	5.96	2.79	3.15	3.59	5.03
	13	27.80	33.76	64.89	4.01	5.34	6.10	2.97	3.03	3.62	5.13
	14	24.26	30.44	63.64	3.21	4.12	4.78	2.52	2.90	2.47	5.38
	15	20.29	26.39	55.52	3.64	4.90	5.89	2.41	3.11	3.44	4.75
	16	28.68	34.40	62.82	4.60	5.40	5.97	2.84	2.97	3.25	5.18
Avg.		**22.64**	**29.26**	**59.10**	**3.63**	**4.83**	**5.92**	**2.61**	**2.94**	**3.41**	**5.04**
COV		**0.14**	**0.09**	**0.07**	**0.12**	**0.08**	**0.09**	**0.13**	**0.17**	**0.11**	**0.06**
CA10B5	1	23.64	32.41	64.21	3.97	5.91	6.84	2.70	3.02	3.79	8.54
	2	27.87	36.49	79.30	4.02	5.48	6.01	2.65	2.79	3.31	9.65
	3	23.08	30.74	64.34	3.07	4.35	5.11	2.38	2.91	4.01	8.71
	4	24.29	33.03	66.33	3.91	5.21	5.71	3.37	4.30	4.16	9.14
	5	26.95	34.24	62.93	4.73	6.21	6.86	3.04	3.65	4.35	8.59
	6	23.06	31.25	64.27	3.00	4.48	5.04	2.44	3.36	3.95	8.84
	7	29.54	38.10	78.41	4.47	5.77	6.21	1.65	2.04	2.33	9.43
	8	24.01	32.22	63.64	3.81	5.25	5.65	2.79	3.66	4.86	9.39
	9	23.03	31.21	64.54	3.49	4.89	5.54	2.45	3.19	3.44	8.90
	10	22.94	31.66	63.82	3.92	5.84	6.86	2.85	3.31	3.82	8.46
	11	27.33	37.18	79.42	4.07	5.69	6.10	2.76	3.14	3.32	9.57
	12	25.99	35.65	73.06	3.65	5.65	6.06	2.30	3.61	3.47	10.93
	13	21.78	30.29	59.98	3.89	6.38	7.45	2.87	3.48	4.09	9.40
	14	24.56	32.87	61.39	4.07	4.98	5.66	2.69	3.24	4.00	9.85
	15	24.57	33.02	65.76	3.73	4.86	5.67	3.54	3.77	4.17	10.08
	16	22.27	30.43	60.00	3.67	5.06	5.79	2.49	3.03	3.38	9.32
Avg.		**24.68**	**33.17**	**66.96**	**3.84**	**5.38**	**6.03**	**2.69**	**3.28**	**3.78**	**9.30**
COV		**0.09**	**0.07**	**0.10**	**0.11**	**0.11**	**0.11**	**0.16**	**0.15**	**0.15**	**0.07**

B 2.2 – Compression parallel to fibres test

The small coupon compression test results of each sample are presented in Table B7.

Table B7 – Individual values of compression parallel to fibres test. Related to Table 4.17.

Condition	Sample ID	Avg. width (mm)	Avg. wall thickness (mm)	Avg. sample height (mm)	Apparent density (g/cm^3)	Moisture content (%)	f_c (MPa)	E_c (GPa)
Ref.	B6-1	11.40	11.30	45.5	0.77	6.29	103.7	22.35
	B6-2	11.38	11.15	45.6	0.76		102.9	19.41
	C11-1	10.76	10.79	45.0	0.77		95.2	22.64
	C11-2	10.57	10.79	44.8	0.73		95.1	20.41
	D22-1	10.68	10.58	41.9	0.78		97.4	20.98
	D22-2	10.55	10.45	42.3	0.77		100.6	22.61
	A5-1	12.35	13.05	53.1	0.72		93.9	22.15
	A5-2	12.80	13.02	53.9	0.68		81.4	18.29
	E19-1	10.66	10.11	39.3	0.76		99.6	23.51
	E19-2	10.45	10.00	39.5	0.78		105.4	23.31
	F18-1	8.99	9.72	40.0	0.74		98.7	21.60
	F18-2	9.49	9.74	39.8	0.73		96.0	19.54
Avg.		**10.84**	**10.89**	**44.21**	**0.75**	**-**	**97.5**	**21.40**
COV		**0.10**	**0.10**	**0.11**	**0.04**	**-**	**0.06**	**0.08**
B5	D17-1	10.01	9.69	38.3	0.81	7.30	122.9	27.74
	D17-2	9.69	9.58	38.3	0.82		123.2	33.25
	B2-1	10.13	10.56	44.9	0.73		104.9	-
	B2-2	11.41	11.09	45.2	0.73		103.1	20.05
	A8-1	11.30	11.73	46.8	0.72		105.4	-
	A8-2	11.16	11.27	47.1	0.74		110.0	23.29
	F15-1	10.08	10.52	43.8	0.80		117.4	27.89
	F15-2	10.21	10.67	43.8	0.78		115.2	-
	C6-1	9.33	9.36	38.1	0.75		111.4	24.84
	C6-2	9.40	9.42	38.0	0.74		109.8	24.11
	E20-1	8.68	9.45	38.4	0.83		116.3	27.33
	E20-2	8.44	9.29	38.8	0.82		121.7	25.53
Avg.		**9.98**	**10.22**	**41.78**	**0.77**	**-**	**113.4**	**26.00**
COV		**0.10**	**0.08**	**0.09**	**0.05**	**-**	**0.06**	**0.14**
CA10	A7-1	11.09	11.30	44.9	0.76	4.65	110.7	25.72
	A7-2	10.98	11.34	45.3	0.75		110.9	23.51
	F6-1	9.92	9.63	40.2	0.81		124.5	24.38
	F6-2	9.91	9.49	40.4	0.79		121.3	24.27
	C14-1	10.71	10.58	42.6	0.81		119.9	26.14
	C14-2	10.42	10.42	42.2	0.81		115.3	27.47
	D7-1	10.03	10.01	41.6	0.79		120.4	28.36
	D7-2	10.10	10.04	41.9	0.80		117.1	26.49
	B15-1	10.29	10.34	42.2	0.71		104.0	21.61
	B15-2	9.86	9.76	42.4	0.71		98.6	-
	E10-1	9.47	9.28	40.5	0.81		119.0	26.05
	E10-2	9.72	9.67	40.7	0.78		118.3	24.79
Avg.		**10.21**	**10.15**	**42.08**	**0.78**	**-**	**115.0**	**25.34**
COV		**0.05**	**0.07**	**0.04**	**0.05**	**-**	**0.07**	**0.07**

Table B7 – Continued.

Condition	Sample ID	Avg. width (mm)	Avg. wall thickness (mm)	Avg. sample height (mm)	Apparent density (g/cm^3)	Moisture content (%)	f_c (MPa)	E_c (GPa)
CA10B5	A21-1	11.76	12.62	47.0	0.75	5.23	104.8	23.28
	A21-2	11.76	12.31	47.3	0.73		104.2	20.66
	C7-1	11.78	12.02	48.7	0.75		95.4	19.83
	C7-2	11.03	11.76	48.7	0.71		97.9	23.51
	B13-1	10.75	11.72	48.4	0.72		96.7	21.50
	B13-2	9.73	10.92	48.0	0.67		85.3	18.71
	F13-1	10.23	9.97	44.4	0.73		98.7	19.41
	F13-2	9.94	9.88	43.9	0.74		103.7	23.21
	D2-1	9.49	9.70	37.6	0.72		91.7	-
	D2-2	9.33	9.38	37.3	0.70		100.3	20.96
	E4-1	9.60	9.44	39.8	0.75		97.2	19.65
	E4-2	9.48	9.72	39.8	0.74		104.3	25.82
Avg.		**10.40**	**10.78**	**44.24**	**0.73**	**-**	**98.3**	**21.50**
COV		**0.09**	**0.11**	**0.10**	**0.03**	**-**	**0.06**	**0.10**

B 2.3 – Interlaminar shear test

The interlaminar shear test results of each specimen are given in Table B8.

Table B8 - Individual values of interlaminar shear test. Related to Table 4.17.

Condition	Sample ID	Avg. wall thickness (mm)	Avg. width (mm)	Shear plane length (mm)	Apparent density (g/cm^3)	Moisture content (%)	f_v (MPa)
Ref.	B22-2	10.60	10.47	25.0	0.74	5.88	5.70
	A5-1	12.89	11.45	25.0	0.72	5.41	6.37
	A5-2	12.74	11.32	26.2	0.68	5.94	5.17
	F18-2	9.64	9.39	23.2	0.73	5.88	6.04
	E19-1	10.65	11.15	25.3	0.78	6.32	6.47
	D22-1	10.44	10.43	24.6	0.75	-	5.54
	F18-1	9.53	9.32	24.6	0.75	5.80	5.29
	C11-2	10.71	10.14	25.3	0.72	6.25	5.52
	B6-1	10.76	10.33	25.6	0.75	5.81	6.14
	C11-1	10.80	10.55	25.5	0.75	5.68	6.34
Avg.		**10.87**	**10.45**	**25.03**	**0.74**	**5.89**	**5.86**
COV		**0.10**	**0.07**	**0.03**	**0.04**	**0.05**	**0.08**
B5	F15-1	10.12	9.35	24.3	0.78	6.58	6.32
	F15-2	9.68	10.15	25.0	0.79	6.41	6.17
	A8-2	11.43	10.65	25.8	0.72	6.67	6.17
	E2-2	9.83	9.80	24.9	0.78	6.49	6.84
	D7-2	10.53	10.35	23.9	0.76	7.06	6.30
	D7-1	10.25	9.90	25.7	0.77	6.25	6.02
	C6-2	10.04	9.59	24.2	0.75	6.76	6.81
	C6-1	10.00	8.99	24.5	0.74	-	5.59
	B2-1	10.89	10.01	25.0	0.75	4.82	5.77
Avg.		**10.31**	**9.86**	**24.80**	**0.76**	**6.38**	**6.22**
COV		**0.05**	**0.05**	**0.03**	**0.03**	**0.11**	**0.07**
CA10	E10-2	10.06	9.54	22.1	0.80	3.66	5.31
	A7-2	11.54	11.26	22.0	0.75	5.88	6.35
	D7-1	10.14	9.68	23.7	0.77	4.94	4.66
	D7-2	10.11	10.54	23.1	0.77	-	5.45
	C14-2	11.16	9.68	24.1	0.77	5.75	3.93
	F6-1	10.21	9.31	24.6	0.78	5.19	4.74
	B15-1	10.10	8.77	23.1	0.67	3.12	4.24
	B15-2	9.90	9.64	23.4	0.70	4.29	4.11
	C14-1	11.16	10.57	23.6	0.77	5.21	4.17
	E10-1	9.90	9.77	23.7	0.80	4.88	4.74
Avg.		**10.43**	**9.87**	**23.35**	**0.76**	**4.77**	**4.77**
CA10		**0.06**	**0.07**	**0.03**	**0.05**	**0.19**	**0.16**

Table B8 – Continued.

Condition	Sample ID	Avg. width (mm)	Avg. wall thickness (mm)	Shear plane length (mm)	Apparent density (g/cm^3)	Moisture content (%)	f_v (MPa)
CA10B5	D2-2	9.97	9.35	24.4	0.68	4.48	3.69
	B13-1	11.15	10.85	24.1	0.72	5.43	3.88
	A2-2	12.01	10.32	24.1	0.71	5.49	4.42
	D2-1	10.06	8.91	23.8	0.72	5.97	3.96
	F13-1	10.76	10.74	23.9	0.75	5.62	5.36
	F13-2	10.24	10.73	24.3	0.70	-	4.50
	C7-1	11.65	9.92	-	0.77	-	-
	C7-2	12.02	10.81	23.6	0.88	4.96	5.79
	B13-2	11.29	10.55	23.7	0.68	5.33	4.13
	A2-1	11.91	9.25	24.4	0.72	4.88	4.49
Avg.		**11.10**	**10.14**	**24.04**	**0.73**	**5.27**	**4.47**
COV		**0.07**	**0.07**	**0.01**	**0.08**	**0.09**	**0.16**

B 2.4 – Tension parallel to the fibres test

The results of each sample submitted to tension parallel to the fibres test are presented in Table B9.

Table B9 - Individual values of tension test parallel to the fibres. Related to Table 4.17.

Condition	Sample ID	Avg. width (mm)	Avg. thickness (mm)	Avg.reduced section thickness (mm)	Apparent density (g/cm^3)	Moisture content * (%)	f_t (MPa)	E_t (GPa)
Ref.	E2-1	10.48	2.96	1.04	0.77	5.58	249.1	24.42
	E11-1	10.06	2.87	0.74	0.78		291.4	22.64
	C8-1	11.72	3.72	1.10	0.72		255.1	21.7
	E11-2	9.76	3.40	0.99	0.76		302.3	-
	D11-1	10.99	2.65	0.93	0.72		269.4	23.21
	D11-2	11.00	3.44	1.05	0.71		236.9	22.54
	A1-1	12.54	3.69	1.14	0.70		242.9	23.07
	A1-2	12.24	3.68	1.10	0.71		298.9	24.36
	C8-2	12.44	3.84	1.15	0.77		227.1	23.66
	B17-1	11.15	3.42	1.01	0.73		274.2	23.95
	E2-2	10.21	3.00	1.02	0.78		281.4	-
	B17-2	10.89	3.97	1.12	0.75		304.6	25.04
Avg.		**11.12**	**3.39**	**1.03**	**0.74**	**-**	**269.4**	**23.46**
COV		**0.08**	**0.13**	**0.11**	**0.04**	-	**0.10**	**0.04**
B5	A16-1	11.89	2.99	0.85	0.74	5.37	306.3	25.67
	C9-1	10.85	3.00	0.88	0.75		299.7	24.17
	B1-1	10.77	3.20	0.83	0.75		262.4	28.54
	D10-1	10.93	2.99	0.80	0.77		253.5	24.38
	B1-2	10.77	3.12	1.01	0.77		287.2	26.24
	F7-1	9.33	3.00	0.95	0.77		338.3	25.49
	C9-2	10.46	2.75	0.87	0.73		303.2	25.43
	F7-2	9.45	3.09	0.88	0.77		344.4	28.33
	D10-2	10.66	3.00	0.95	0.79		320.4	25.72
	E20-1	10.15	2.20	0.66	0.80		302.1	25.46
	E20-2	10.34	2.15	0.91	0.76		258.5	25.08
	A16-2	10.95	2.71	0.93	0.75		299.1	26.35
	D10-3	10.98	3.02	0.78	0.75		280.1	-
Avg.		**10.58**	**2.86**	**0.87**	**0.76**	**-**	**296.6**	**25.91**
COV		**0.06**	**0.12**	**0.10**	**0.03**	-	**0.10**	**0.05**
CA10	C3-1	10.63	3.14	0.82	0.80	4.65	193.3	23.38
	E8-1	10.01	2.63	0.81	0.77		236.1	24.83
	F10-1	9.81	2.84	0.75	0.80		166.4	22.96
	D14-1	10.75	2.99	0.83	0.79		165.7	23.86
	B16-1	10.96	2.39	0.67	0.73		167.4	23.22
	B16-2	11.06	2.03	0.56	0.76		155.2	19.28
	A10-1	10.90	2.63	0.83	0.73		213.7	23.43
	C3-2	11.63	2.97	0.82	0.75		203.5	22.42
	D14-2	10.73	3.30	1.07	0.76		150.6	22.61
	A10-2	10.90	3.13	0.88	0.73		182.4	22.51
	E8-2	10.20	2.68	0.72	0.78		262.7	24.15
	F10-2	10.15	2.83	0.77	0.79		190.8	25.61
Avg.		**10.65**	**2.80**	**0.79**	**0.77**	**-**	**190.6**	**23.19**
COV		**0.05**	**0.13**	**0.15**	**0.04**	**-**	**0.18**	**0.07**

Table B9 – Continued.

Condition	Sample ID	Avg. width (mm)	Avg. thickness (mm)	Avg.reduced section thickness (mm)	Apparent density (g/cm^3)	Moisture content * (%)	f_t (MPa)	E_t (GPa)
CA10B5	F5-1	10.78	3.10	0.61	0.76	5.50	245.6	24.02
	D3-1	9.73	2.94	0.56	0.73		293.6	21.33
	F5-2	10.63	3.30	0.87	0.75		186.5	24.20
	B20-1	10.59	2.82	0.77	0.74		172.7	22.95
	E3-1	9.52	3.47	0.73	0.71		245.1	23.34
	A14-1	11.06	2.40	0.69	0.67		162.3	21.60
	B20-2	10.91	3.04	0.83	0.71		182.4	21.77
	D3-2	10.65	2.43	0.77	0.73		218.6	23.11
	C4-1	11.10	3.35	0.92	0.76		155.0	22.53
	C4-2	10.60	3.42	0.65	0.77		179.8	23.31
	A14-2	10.94	2.38	0.67	0.69		163.1	19.58
	E3-2	10.03	3.17	0.85	0.73		202.9	22.73
Avg.		**10.55**	**2.98**	**0.74**	**0.73**	**-**	**200.6**	**22.54**
COV		**0.05**	**0.13**	**0.15**	**0.04**	**-**	**0.21**	**0.06**

* The moisture content was determined with the sum of the weight of all the samples (not individual values).

B 2.5 – Three-point small coupon bending test

The results of all the samples submitted to three-point bending test are given in Table B10.

Table B10 – Three-point bending test individual values. Related to Table 4.18

Condition	Sample ID	Avg. width (mm)	Avg. wall thickness (mm)	Apparent density (g/cm^3)	Moisture content (%)	MOR (MPa)	MOE (GPa)	LOP (MPa)	SE (kJ/m^2)
Ref.	A15-2	10.03	11.06	0.72	6.00	184.1	18.9	114.9	31.73
	B3-2	11.00	10.94	0.74	6.59	193.8	20.5	119.2	33.54
	C16-1	10.10	10.59	0.70	6.38	181.4	17.4	113.0	29.90
	C16-2	10.73	9.91	0.72	6.25	192.6	19.8	127.5	30.30
	D1-1	10.06	9.09	0.70	6.61	179.3	19.0	112.1	23.57
	D1-2	10.62	10.04	0.71	6.29	182.2	18.0	122.2	25.78
	D13-1	10.76	11.11	0.79	6.18	211.0	22.6	122.8	33.55
	D13-2	11.00	10.97	0.76	6.36	201.4	20.7	147.7	29.02
	E11-1	10.88	9.53	0.79	-	214.1	22.2	149.9	32.40
	E11-2	10.48	9.82	0.80	6.45	215.2	23.5	146.8	28.52
	E15-1	10.59	8.38	0.74	-	196.8	21.9	128.6	25.41
	E15-2	10.93	9.40	0.74	6.29	178.7	20.5	126.1	26.40
	F4-1	9.69	9.59	0.76	6.82	184.0	20.4	109.0	28.18
	F4-2	10.54	9.22	0.77	-	200.4	23.2	139.5	28.94
Avg.		**10.53**	**9.97**	**0.75**	**6.38**	**193.9**	**20.6**	**127.1**	**29.09**
COV		**0.04**	**0.09**	**0.04**	**0.04**	**0.07**	**0.09**	**0.11**	**0.11**
B5	A12-1	9.05	10.97	0.75	6.34	204.5	22.6	154.3	29.37
	A12-2	8.01	10.25	0.74	-	189.5	21.1	144.2	26.34
	B5-1	9.89	10.75	0.77	6.49	207.8	22.1	142.7	32.43
	B5-2	9.73	10.91	0.78	6.41	220.6	22.5	142.0	35.97
	C18-1	8.57	10.17	0.78	6.35	214.6	22.9	150.7	34.76
	C18-2	8.77	10.29	0.76	6.20	230.6	23.1	157.7	36.28
	D5-2	8.98	9.92	0.78	6.06	230.4	23.2	153.3	35.65
	D5-1	10.05	10.67	0.79	6.25	243.8	23.9	167.3	39.62
	D16-1	9.33	10.23	0.75	5.93	215.1	21.8	140.2	36.62
	D16-2	8.89	10.97	0.76	6.43	211.8	22.2	147.8	31.98
	E1-1	8.67	9.69	0.79	-	233.2	23.6	166.7	33.96
	E1-2	9.64	9.80	0.78	6.43	226.5	22.9	153.7	35.25
	E12-1	10.20	10.42	0.78	-	187.0	21.1	158.5	21.82
	E12-2	9.77	10.37	0.80	6.58	222.1	22.0	162.7	29.74
	F8-1	10.17	9.07	0.79	6.57	241.8	23.9	172.3	37.74
	F8-2	9.39	8.94	0.80	6.30	248.3	24.4	177.8	41.08
Avg.		**9.32**	**10.21**	**0.77**	**6.33**	**220.5**	**22.7**	**155.7**	**33.66**
COV		**0.07**	**0.06**	**0.02**	**0.03**	**0.08**	**0.04**	**0.07**	**0.15**

Table B10 – Continued.

Condition	Sample ID	Avg. width (mm)	Avg. wall thickness (mm)	Apparent density (g/cm^3)	Moisture content (%)	MOR (MPa)	MOE (GPa)	LOP (MPa)	SE (kJ/m^2)
CA10	A20-1	8.45	10.67	0.69	5.04	147.1	18.6	132.7	16.67
	A20-2	10.06	10.31	0.70	4.32	156.2	18.8	146.4	16.11
	A22-1	9.92	11.12	0.75	4.40	196.2	20.6	142.9	26.68
	A22-2	9.55	10.97	0.77	5.19	206.4	21.9	152.2	29.74
	B7-1	9.88	10.17	0.77	4.76	192.5	21.6	164.8	21.66
	B7-2	8.94	9.59	0.76	4.84	191.2	21.8	157.5	20.54
	B19-1	9.19	10.18	0.76	-	193.4	21.4	158.1	22.29
	B19-2	8.27	10.18	0.75	4.96	201.4	22.7	149.6	27.46
	C12-1	10.04	10.89	0.77	4.97	200.6	22.7	160.2	24.27
	C12-2	9.93	10.52	0.74	4.73	173.5	19.8	137.5	21.92
	D4-1	9.72	9.40	0.83	-	258.0	26.4	168.3	33.98
	D4-2	10.15	9.60	0.77	4.86	220.9	22.6	162.3	31.62
	E16-1	9.94	8.60	0.79	4.65	212.4	22.8	181.0	24.77
	E16-2	9.90	8.89	0.78	5.34	204.2	21.9	160.4	26.12
	F17-1	10.24	9.35	0.76	-	187.4	23.0	141.6	26.97
	F17-2	9.43	9.38	0.78	4.55	197.5	23.7	149.9	21.40
Avg.		**9.60**	**9.99**	**0.76**	**4.82**	**196.2**	**21.89**	**154.09**	**24.51**
COV		**0.06**	**0.08**	**0.04**	**0.06**	**0.13**	**0.09**	**0.08**	**0.20**
CA10B5	A18-1	9.15	11.27	0.73	5.56	179.7	20.6	130.7	24.92
	A18-2	9.51	11.46	0.73	5.96	162.0	21.6	106.6	20.76
	B8-1	6.78	9.96	0.72	5.38	160.7	-	-	-
	B8-2	8.90	10.61	0.72	6.25	178.4	19.5	130.6	21.91
	B14-1	9.18	10.97	0.71	-	160.9	19.1	119.8	22.41
	C5-1	9.07	9.87	0.73	5.60	196.1	20.0	151.5	27.57
	C5-2	8.44	9.77	0.72	5.31	201.9	20.3	151.0	27.92
	D8-1	9.16	10.54	0.76	6.29	196.4	21.9	145.1	25.80
	D8-2	9.20	10.54	0.75	5.67	194.3	22.5	135.6	27.46
	E7-1	9.70	10.36	0.77	-	185.5	22.3	132.9	26.52
	E7-2	8.99	9.76	0.75	-	191.8	-	-	-
	F9-1	10.16	10.06	0.79	5.88	192.3	20.5	128.5	21.69
	F9-2	9.05	10.19	0.78	-	210.1	21.0	162.0	25.42
	F16-1	9.13	9.82	0.78	5.22	194.0	22.7	153.7	22.77
	F16-2	9.84	9.88	0.76	5.71	168.3	21.6	130.3	21.26
Avg.		**9.08**	**10.34**	**0.75**	**5.71**	**184.8**	**21.05**	**136.80**	**24.34**
COV		**0.08**	**0.05**	**0.04**	**0.06**	**0.09**	**0.05**	**0.11**	**0.11**